Characterisation of Chicken Interferon-inducible Transmembrane Proteins: Locus Architecture, Gene Expression and Viral Restriction

Thomas James Whitehead

Submitted for the degree of Doctor of Philosophy

University College London

June 2018

Preface

Declaration

I, Thomas Whitehead, confirm that the work presented in this thesis is my own. Where information has been derived from other sources, I confirm that this has been indicated in the thesis.

Signed…… Date…….

Thomas Whitehead

Published material

Bassano I, Ong SH, Lawless N, Whitehead T, Fife M, Kellam P. Accurate characterization of the IFITM locus using MiSeq and PacBio sequencing shows genetic variation in Galliformes. BMC Genomics. 2017; 18(1):419. Available from: DOI: 10.1186/s12864-017-3801-8

Whitehead T, James J, Gray A, Steyn A, Lawless N, Bassano I, Broadbent A, Shelton H, Kellam P, Fife M. Chicken Interferon-inducible Transmembrane (IFITM) Proteins Restrict Infection by Avian Influenza A Virus. *In Press*.

Abstract

Interferon-inducible transmembrane (IFITM) proteins are host cell derived restriction factors. Mammalian IFITM proteins have been shown to confer antiviral resistance when challenged with a diverse range of both enveloped and non-enveloped viruses. Little characterisation has been undertaken to date with the specific aim of elucidating their function and the antiviral properties of the chicken IFITM (*chIFITM*) gene family.

The *chIFITM* gene family contains four genes located within a 17kb region on *Gallus gallus* chromosome 5. Currently there is little information available about the sequence diversity of these genes, their expression profiles or the role that they may play in restricting avian viral pathogens. Data presented in this thesis outlines a novel DNA pull-down sequencing technique which has allowed for the generation of a high quality contiguous reference sequence, alongside targeted sequencing of chicken cell lines and *ex vivo* cell cultures. Studies in this thesis have established that the chIFITMs are interferon stimulated and have characterized their upregulation in response to viral challenge with influenza A virus (IAV) *in ovo*, *in vivo* and *in vitro,* alongside other avian viruses. Stably-overexpressing DF-1 (immortalized chick embryo fibroblast) cells that express chIFITM1, 2, 3 and 3^{MUT} (C71/71A) have been generated. These cell lines have been challenged with avian viruses including diverse strains of IAV and infectious bronchitis virus (IBV) and this data demonstrates that the chIFITMs are able to restrict avian viruses *in vitro*. Moreover, novel interactions have been identified which may help to uncover a possible mechanism of action.

Global food security and protection of livestock from infectious agents remains a key priority, both in the United Kingdom and Internationally. This study examines the role of chIFITM proteins during viral infections and highlights one potential method of safeguarding the poultry industry, ensuring continuity of global food security.

Impact Statement

The work undertaken in this thesis expands our current knowledge of chIFITM-mediated viral restriction, alongside the basic cellular mechanisms that results in their upregulation and activation. As part of this project, the communications team have provided updates of the project for a general audience through the Pirbright Institute website and social media. This has allowed for the dissemination of events such as publications, grant successes and award nominations such as the 'Young Innovator of the Year' award that was presented to me by Innovate Guildford in 2017. In addition, I am an active STEM ambassador, which creates opportunities to inspire young people and develop their creativity, problem-solving and employability skills through public engagement.

Using the data presented in this thesis, Dr Mark Fife (Supervisor) has been awarded a Livestock Vaccine innovation fund (LVIF) grant entitled "*chIFITM* knockdown/knockout technology for increased vaccine yields". This project aims to generate CRISPR/Cas9 edited cells that will have ablated *chIFITM* expression. It is hoped that this approach will overcome the rate limiting step in vaccine production, directly resulting in increased vaccine yields and improve the speed at which vaccines can be manufactured. The total value of vaccines (both human and animal health) manufactured in cell culture is around $11 billion (BCC Research, 2015). In particular, the total value of the leading animal heath vaccines produced in cell culture for diseases such as Marek's, IBV, Newcastle disease etc. is over $500 million. Higher yields can also result in lower initial capital investment costs if the same production capacity can be achieved within smaller cell culture volumes. All of these are important factors restraining vaccine production capacity in developing countries. It is hoped that this technology will benefit both developed and developing countries, making vaccines cheaper and more readily accessible.

Moreover, The Pirbright Institute has protected this invention through an international patent application (WO/2014/195692) which is now pending in multiple national jurisdictions (AU, BR, CA, CN, EP, IN, JP, KR, MX, TH, US, and ZA). As part of my studentship I have taken an active role in meeting with the knowledge exchange and commercialisation executives (The Pirbright Institute) alongside our external patent attorneys (D Young). This has resulted in considerable progress and the expectation of an awarded patent imminently. This will benefit the vaccine industry as this technology can then be licensed to smaller manufacturers in developing countries at a cost that is not prohibitive.

Acknowledgements

Firstly I would like to thank my supervisor Dr Mark Fife who believed in me enough to offer me the PhD studentship in the first place; I hope that I have made you proud! You have always been there, through the good times and those moments of self-doubt, without you I doubt I would have completed this. Alongside Mark there have been numerous members of both his own lab, and others that have contributed to my sanity. Although too many to name individually, I do want to say a heartfelt thank you to Dr Angela Steyn, Dr Holly Shelton, Dr Helena Maier, Dr Erica Bickerton, Sarah Keep, Karen Billington, Phoebe Stevenson-Leggett, Anabel Clements, Michael Oade and Kate Dulwich in particular. You have all contributed so much over the last 4 years and not only are you excellent work colleagues, but you are also incredible friends, thank you. I also have to mention the collective support of all of the students at the Pirbright Institute, both past and present. You are all such a lovely group of people and I wish you all the very best for your future endeavors.

I want to especially thank four people for their unwavering support, constant love and for their belief that anything is possible. My mum (Debra) and dad (Karl), my sister (Katy) and Nathan, for always believing in me and always being there, even if it's just for some much needed reassurance. Without their support I know that this journey would have been almost impossible and I am forever indebted to them.

Finally, I would like to thank The Pirbright Institute and the BBSRC for funding and supporting me throughout this PhD.

Table of Contents

List of Figures……..15

List of Tables……19

Abbreviations……21

Chapter 1……27

1.1 Poultry Industry and Avian Viral Diseases……28

1.2 Influenza A Virus……33

1.2.1 General overview……33

1.2.2 Maximising coding capacity of IAV……35

1.2.3 Influenza virion……35

1.2.4 Influenza cell entry……37

1.2.5 Replication and transcription of the viral genome……37

1.2 Infectious Bronchitis Virus……39

1.3.1 General overview……39

1.3.2 IBV virion……40

1.3.3 IBV cell entry……42

1.3.4 Replication, transcription and translation of the viral genome……42

1.4 Herpes Virus of Turkeys……47

1.5 Interferon Induction and Signalling……48

1.5.1 The interferons……48

1.5.2 Viral pathogen detection and interferon induction……49

1.5.3 Interferon signalling……50

1.5.4 Interferon induction and signalling in Galliformes……52

1.5.5 Viral evasion of the interferon response……54

1.6 Mammalian IFITMs……56

1.6.1 Early characterisation……56

1.6.2 Vertebrate orthologues of *IFITMs*……58

1.6.3 Conservation and post-translational modifications……59

1.6.4 Membrane topology and mechanism of action……60

1.6.5 Cellular localisation……61

1.6.6 Restriction of viral pathogens……62

1.7 Avian IFITMs……66

1.8 Aims and Objectives……70

Chapter 2……71

2.1 Materials……72

2.1.1 Suppliers of general reagents……72

2.1.2 Enzymes……73

2.1.3 Antibodies and dyes……73

2.1.4 Eukaryotic cell & bacterial culture medium……77

2.1.4.1 Eukaryotic cells……77

2.1.4.2 Eukaryotic cell culture……77

2.1.4.3 Bacterial culture……78

2.1.5 Western blotting……78

2.1.6 Immunofluorescence……79

2.1.7 Protein pulldown buffers……79

2.1.8 Agarose gel electrophoresis……79

2.1.9 Plasmids……80

2.1.10 Viruses……82

2.1.10.1 IAV……82

2.1.10.2 IBV……82

2.1.10.3 HVT……82

2.1.11 Oligonucleotides……82

2.1.12 Drugs……87

2.2 Methods……88

2.2.1 Ethics Statement……88

2.2.2 Recombinant DNA Techniques……89

2.2.2.1 DNA extraction from cells……89

2.2.2.1.1 BAC preparation for sequencing……89

2.2.2.2 Primers and DNA fragments……89

2.2.2.3 Polymerase chain reaction……89

2.2.2.4 Site-directed mutagenesis……90

2.2.2.5 Agarose gel electrophoresis……90

2.2.2.6 Restriction digests……90

2.2.2.7 Gel extraction/ PCR purification……90

2.2.2.8 Ligation……91

2.2.2.9 Transformation of *Escherichia coli*……91

2.2.2.10 Bacterial propagation……92

2.2.2.11 Plasmid DNA Miniprep……92

2.2.2.12 Plasmid DNA Maxiprep……..92

2.2.2.13 Sequencing……92

2.2.3 Cell Culture Methods……93

2.2.3.1 Eukaryotic cell culture media……93

2.2.3.2 General cell culture protocols……94

2.2.3.3 Cell counting……94

2.2.3.4 DNA transfection of primary and continuous cell cultures……95

2.2.3.5 Generation of stably-expressing DF-1 cell lines……..95

2.2.3.6 siRNA knockdown assays……95

2.2.3.7 Firefly and Renilla luciferase assays……96

2.2.3.8 Chicken interferon (IFNβ) and Mx reporter assays……96

2.2.4 Virological Methods……98

2.2.4.1 Virus propagation in embryonated hen's eggs……98

2.2.4.2 Virus infection……98

2.2.4.3 Titration of influenza viruses by plaque assay……98

2.2.4.4 Titration of infectious bronchitis viruses by plaque assay……99

2.2.5 Protein Methods……100

2.2.5.1 Cell lysis……100

2.2.5.2 SDS- polyacrylamide gel electrophoresis (PAGE)……100

2.2.5.3 Western blotting……100

2.2.5.4 Immunohistochemistry……101

2.2.5.5 Immunoprecipitation……..101

2.2.5.5.1 Cell Lysis……101

2.2.5.5.2 Immunoprecipitation of chIFITM-FLAG……102

2.2.5.6 Liquid Chromatography-Mass Spectrometry/MassSpectrometry….102

2.2.5.6.1 LC-MS/MS analysis……103

2.2.5.7 Co-Immunoprecipitation……104

2.2.6 Transcriptional Analysis……105

2.2.6.1 Total RNA extraction from tissues……105

2.2.6.2 Total RNA extraction from cells……105

2.2.6.3 Reverse transcription……105

2.2.6.4 Quantitative real-time PCR with SYBRgreen……105

2.2.6.5 Reference gene stability analysis by geNorm……106

2.2.6.6 Quantitative real-time PCR (TaqMan)……106

2.2.6.7 Real-time quantitative PCR data analysis……106

2.2.6.8 Extraction and sequencing of viral RNA (vRNA)……107

2.2.7 Bioinformatic and Statistical Analysis……108

2.2.7.1 chIFITM amino acid alignments……108

2.2.7.2 chIFITM DNA sequence alignments……108

2.2.7.3 Modelling chIFITM protein topology……108

2.2.7.4 Statistical analysis……109

Chapter 3……110

3.1 Introduction……111

3.2 chIFITM locus architecture……113

3.3 Re-sequencing the chIFITM locus……117

3.4 Basal expression of chIFITM transcripts in chicken tissues……122

3.5 Basal expression of chIFITM transcripts in chicken cell lines and ex vivo cell cultures……124

3.6 Multiple key residues are conserved among chIFITM sequences in Galliformes……130

3.7 Sequence variation within the chIFITM locus of commonly used chicken cell lines……134

3.8 Predicted structures of the chIFITM proteins and their corresponding membrane topologies……137

3.9 Cellular localisation of chIFITM1, 2 and 3 in vitro……142

3.10 Identifying proteins that interact with chIFITM1, 2 and 3……146

3.10.1 Mass spectrometry analysis of chIFITM-FLAG immunoprecipitations..146

3.10.2 Co-immunoprecipitations of interacting partners identified through mass spectrometry……150

3.11 Discussion……153

Chapter 4……157

4.1 Introduction……158

4.2 The modulation of chIFITM expression through type I and II interferons…..159

4.3 Treatment of chicken cells with lipopolysaccharide (LPS) does not induce chIFITM expression……166

4.4 Differential chIFITM expression when chicken cells are infected with a diverse range of avian viruses……170

4.4.1 Influenza A Virus (IAV) infection induces *chIFITM* expression in *ex vivo* cell cultures……170

4.4.2 Infectious bronchitis virus (IBV) infection induces chIFITM expression in ex vivo cell cultures……174

4.4.3 Assessing the effect of temperature and subsequent viral assembly and egress in modulating chIFITM expression……177

4.4.4 Herpesvirus of Turkeys (HVT) infection transiently upregulates chIFITM5 and Mx mRNA expression……180

4.4.5 *In ovo* Infection with H9N2 upregulates the expression of the chIFITMs……183

4.4.6 *In vivo* Infection of Rhode-Island Red chicks with H9N2 modulates chIFITM expression……189

4.5 Discussion……194

Chapter 5……202

5.1 Introduction……203

5.2 Transfection reagents are differentially toxic to cells……204

5.3 Transient overexpression results in chIFITM-mediated restriction of avian viruses……205

5.3.1 Transient overexpression of chIFITM1, 2, 3 and 5 in CEFs restricts H9N2……205

5.3.2 Transient overexpression of chIFITM1, 2, 3 and 5 in DF-1 cells differentially restricts H3N8, H5N3 or H9N2……209

5.3.3 Transient overexpression of chIFITM2 in DF-1 cells restricts IBV……213

5.4 Transient knockdown of *chIFITM* expression results in increased viral titres……217

5.4.1 Transient knockdown of *chIFITM1* renders CEFs more susceptible to IAV infection……217

5.4.2 Transient knockdown of *chIFITM1* and *3* renders DF-1 cells more susceptible to IAV infection……220

5.4.3 Transient knockdown of chIFITM2 renders DF-1s more susceptible to IBV infection……226

5.5 DF-1 cells stably-expressing chIFITM1, 2, 3 or 3MUT result in the restriction of avian viruses……232

5.5.1 DF-1 cells stably-expressing chIFITM1, 2, 3 or 3MUT differentially restrict H3N8, H5N3 or H9N2……232

5.5.2 Stably-expressing DF-1 cells differentially restrict IAV when infected at a high MOI……237

5.5.3 DF-1 cells stably-expressing chIFITM2 restrict IBV when cells are challenged at a high MOI……..241

5.6 Mutational analysis of chIFITM3 suggests that conserved domains may be important in determining antiviral activity against IAV……..243

5.7 Discussion……250

Chapter 6……..257

6.1 Concluding remarks……258

6.2 Future work and directions……259

Appendix……263

References……278

List of Figures

Chapter 1

Figure 1.1 Phylogenetic tree of the relationships among Galliformes……29

Figure 1.2 Karyotype of the female chicken……30

Figure 1.3 A schematic representation of an influenza A virion……36

Figure 1.4 A schematic representation of an IBV virion……41

Figure 1.5 A schematic representation of IBV transcription……44

Figure 1.6 A schematic representation of PAMP recognition and IFN induction……51

Figure 1.7 A schematic representation interferon signalling……53

Figure 1.8 A schematic representation of chicken interferon induction and signalling……55

Chapter 2

Figure 2.1 Mono and polyclonal chIFITM antibodies do not cross react with other chIFITM proteins……75

Chapter 3

Figure 3.1 The chIFITM locus architecture……115

Figure 3.2 Isolating the BAC clone for chIFITM locus re-sequencing……118

Figure 3.3 MiSeq and PacBio sequence analysis of the CH126-109H20 BAC clone……120

Figure 3.4 Endogenous levels of chIFITM expression in the tissues of Rhode Island Red (RIR) chickens……125

Figure 3.5 Endogenous levels of chIFITMs in avian cell lines……127

Figure 3.6 Multiple key residues are conserved among chIFITM sequences in Galliformes……132

Figure 3.7 Sequence variation within the chIFITM locus of commonly used chicken cell lines……136

Figure 3.8 Predicted structures of the chIFITM proteins and their corresponding membrane topologies……..139

Figure 3.9 Three models of IFITM protein transmembrane topology……141

Figure 3.10 Cellular localisation of transiently overexpressed chIFITM proteins in DF-1 and HD11 cells……...144

Figure 3.11 Immunoprecipitation of chicken cellular proteins after transient chIFITM-FLAG overexpression……...148

Figure 3.12 Co-Immunoprecipitation of interacting proteins with chIFITM1, 2 or 3……152

Chapter 4

Figure 4.1 Determining responsiveness of chicken cell lines to treatment with poly(I:C)…161

Figure 4.2 IFNβ quantification after stimulation of HD11s by IFN agonists……162

Figure 4.3 IFITM and Mx Induction in HD11s after stimulation with IFN agonists……163

Figure 4.4 IFITM, IL-6 and Mx Induction in DF-1 and HD11 cell after LPS treatment……167

Figure 4.5 Cellular distribution and protein abundance of P65 when DF-1 cells are stimulated with PMA, LPS and poly(I:C)……169

Figure 4.6 Infection of CEFs with H3N8, H5N3 and H9N2 upregulates the expression of the chIFITMs……171

Figure 4.7 Infection of CEFs with H9N2 upregulates the expression of the chIFITMs…….173

Figure 4.8 Infection of CK cells with BeauR, M41 and QX upregulates the expression of the chIFITMs……175

Figure 4.9 Infection of DF-1 cells with BeauR at 37°C and 41°C upregulates the expression of the chIFITMs……178

Figure 4.10 Infection of DF-1 cells with HVT transiently upregulates chIFITM5 and Mx expression……181

Figure 4.11 *Inovo*Infection with H9N2 upregulates the expression of the chIFITMs…….184

4.12 *In vivo* Infection with H9N2……190

Chapter 5

Figure 5.1 Determining the toxicity of transfection reagents in DF-1 cells……206

Figure 5.2 Transient overexpression of chIFITM1, 2, 3 and 5 in CEFs significantly reduces IAV viral titres……..208

Figure 5.3 Transient overexpression of chIFITM1, 2, 3 and 5 in DF-1 cells significantly reduces IAV viral titres……210

Figure 5.4 Transient overexpression of chIFITM2 in DF-1 cells significantly reduces IBV viral titres……..214

Figure 5.5 Transient knockdown of chIFITM1 renders CEFs more susceptible to IAV infection……218

Figure 5.6 Transient knockdown of chIFITM1 and 3 renders DF-1s more susceptible to IAV infection……221

Figure 5.7 Transient knockdown of chIFITM2 renders DF-1s more susceptible to IBV infection……228

Figure 5.8 DF-1 cells stably-overexpressing chIFITM1, 2, 3 and 3^{MUT} restrict IAV infection……233

Figure 5.9 DF-1 cells stably-overexpressing chIFITM1, 2, 3 and 3^{MUT} restrict IAV infection……238

Figure 5.10 DF-1 cells stably-overexpressing chIFITM2 restrict IBV infection……242

Figure 5.11 Mutational analysis of chIFITM3 suggests that certain domains may be important in determining antiviral activity against IAV……247

List of Tables

Chapter 1

Table 1.1 Members of the *Gallus* genus and their geographical distribution……..31

Table 1.2 Core proteins of IAV that are conserved and essential for replication……..34

Table 1.3 The size and function of the non-structural proteins (nsps) in IBV……43

Table 1.4 The size and function of the structural and accessory protein of IBV……46

Chapter 2

Table 2.1 List of antibodies used for western blot and immunofluorescence……74

Table 2.2 List of secondary antibodies used for western blot and immunofluorescence……76

Table 2.3 List of fluorescent dyes……76

Table 2.4 List of plasmids……..80

Table 2.5 Primers for pGEM_chIFITM cloning……83

Table 2.6 Primers for chIFITM_FLAG cloning……83

Table 2.7 Primers and probes for house-keeping genes (RT-qPCR)……84

Table 2.8 Primers and probes for targets of interest (RT-qPCR)……85

Table 2.9 Primers and probes for viral quantification (RT-qPCR)……86

Table 2.10 Sequencing primers……86

Table 2.11 Reagent concentrations for Lysogeny broth……91

Table 2.12 Components of cell culture medium……93

Table 2.12 siRNAs used to knockdown chIFITM expression……96

Chapter 3

Table 3.1: Percentage (%) identity between human and chicken IFITM DNA sequences….114

Table 3.2: Percentage (%) identity between human and chicken IFITM amino acid sequences……114

Table 3.3 Function and localisation of proteins classified as significant interacting partners for chIFITM1, 2 and/or 3……151

Appendix

Table 7.1: Cellular proteins identified through LC-MS/MS that significantly interact with chIFITM1-FLAG……..264

Table 7.2: Cellular proteins identified through LC-MS/MS that significantly interact with chIFITM2-FLAG……..270

Table 7.3: Cellular proteins identified through LC-MS/MS that significantly interact with chIFITM3-FLAG……..275

Abbreviations

β2M – βeta-2-microglobulin

β-Actin – βeta actin

+ssRNA – positive-sense single-stranded RNA

-ssRNA – negative-sense single-stranded RNA

ANDV – Andes virus

ANOVA – analysis of variance

AP-1 – activator protein 1

ASLV – avian sarcoma and leucosis virus

ATMUV – avian Tembusu virus

BeauR – Beaudette recombinant

BES – N, N-bis(2-hydroxyethyl)-2-aminoethanesulfonic acid

BSA – bovine serum albumin

CARD – caspase activation and recruitment domain

cDNA – complementary DNA

CEFs – chicken embryonic fibroblasts

chIFITM – chicken interferon-inducible transmembrane proteins

CIL – cytoplasmic intracellular loop

CK Cells – chicken kidney cells

CoV – coronavirus

cRNA – complementary RNA

CS – chicken serum

CTD – C-terminal domain

DAPI – 4’,6-diamidino-2-phenylindole

DMEM – Dulbecco’s minimum essential medium

DMSO – dimethyl sulfoxide

dNTP – deoxyribosenucleotide triphosphate

DNA - deoxyribonucleic acid

Dpi – days post infection

dsDNA – double-stranded DNA

dsRNA – double-stranded RNA

DV – dengue virus

E – viral envelope protein

EBOV – ebola virus

E.coli – escherichia coli

EDTA - ethylenediaminetetraacetic acid

EMEM – Eagle's minimum essential medium

EPR –electron paramagnetic resonance

ER – endoplasmic reticulum

FCS – foetal calf serum

GAS – gamma-activated sequence

Gb - gigabase

gDNA – genomic DNA

GFP – green florescent protein

HA – hemagglutinin

HCV – hepatitis C virus

HIV – human immunodeficiency virus

HPAI – high pathogenicity avian influenza

HTNV - hantaan virus

huIFITM - human interferon-inducible transmembrane proteins

HVT – herpes virus of turkeys

IAV – influenza A virus

IBDV –infectious bursal disease virus

IBV – infectious bronchitis virus

IFITM – interferon-inducible transmembrane proteins

IFN – interferon

IFNAR – interferon receptor

IFNα – interferon-alpha

IFNβ – interferon-beta

IFNε – interferon- epsilon

IFNκ – interferon-kappa

IFNω – interferon-omega

IFNλ – interferon-lamda

IFNγ – interferon-gamma

IRES – internal ribosomal entry site

IKK – I kappa B kinase

IM – intramembrane

IP – immunoprecipitation

IRF 3/7 – interferon regulatory factor 3/7

ISG – interferon stimulated gene

ISGF3 – interferon stimulated gene factor 3

ISP-1 – interferon promoter stimulator-1

ISRE – IFN-stimulated response element

JAK – janus kinase

JEV – Japanese encephalitis virus

Kb – kilobases

kDa – kilodaltons

LACV – la crosse virus

LASV – lassa virus

LB – Luria-Bertani broth

LBV – Lagos bat virus

LC-MS/MS – liquid chromatography-mass spectrometry/mass spectrometry

LCMV – lymphocytic choriomeningitis virus

LGP2 – laboratory of genetics and physiology 2

LPAI - low pathogenic avian influenza

LPS – lipopolysaccharide

M1 - matrix protein 1

M2 - M2 proton channel

M41 – Massachusetts 41

M – viral M protein

MARV - Marburg virus

MAVS – mitochondrial antiviral signaling protein

MDA5 – melanoma differentiation-associated protein 5

MDCK – Madin-Darby canine kidney

MDV - marek's disease virus

MEFs – murine embryonic fibroblasts

MEM – minimum essential medium

MERS-CoV – Middle East respiratory syndrome coronavirus

MEXC – mex-3 RNA binding family member 3

MIQE – minimum information for the publication of quantitative real-time PCR experiments

MLV – murine leukemia virus

MOI – multiplicity of Infection

mRNA – messenger RNA

MS – mass spectrometry

Mx - myxovirus resistance protein 1

N – viral nucleocapsid protein

NA - neuraminidase

NEP - nuclear export protein

NF-κB – nuclear factor - kappa B

NGS – next generation sequencing

NMR – nuclear magnetic resonance

NP - nucleoprotein

NS1 – influenza A virus non-structural protein 1

Nsp – non-structural protein

NTD – N-terminal domain

ORF – open reading frame

PA - polymerase acidic protein

PAMP – pathogen-associated molecular pattern

PB1 - polymerase basic protein 1

PB2 - polymerase basic protein 2

PBS – phosphate buffered saline

PCR – polymerase chain reaction

PFU – plaque forming unit

PKR – protein kinase R

PLA2 – phospholipase A2 group IV A

PMA – phorbolmyristate acetate

Pol II – polymerase II

PolyI:C – polyinosinic:polycytidylic acid

pp1a/1ab – polyprotein 1a/1ab

PRR – pattern recognition receptor

PTM – post-translational modification

RABV – rabies virus

RdRp – RNA-dependent RNA polymerase

RIG-1 – retinoic acid-inducible gene I

RIPLET – rING finger protein leading to RIG-1 activation

RLR – RIG-1-like receptor

RLU – relative light units

RNA – ribonucleic Acid

RNP – ribonucleoprotein

RPL13 – ribosomal protein L13

RPLPO – ribosomal phosphoprotein PO

RPMI – Roswell Park Memorial Institute medium

RT – reverse transcription

RT-qPCR - reverse transcription quantitative polymerase chain reaction

RTC – replication-transcription complex

RVFV - Rift Valley fever virus

S – viral spike protein

SARS-CoV – severe acute respiratory syndrome coronavirus

SDS-PAGE – sodium dodecyl sulphate-polyacrylamide gel electrophoresis

SFV – Semliki forest virus

SNP – single nucleotide polymorphism

SPRY - SPla and the ryanodine Receptor

sgRNA – sub-genomic RNA

ssRNA – single stranded RNA

STAT1/3 – signal transducer and activator of transcription 1/3

TBK1 – TANK-binding kinase 1

TBP – TATA box binding protein

TNF – tumour necrosis factor

TMD – transmembrane domain

TPB – tryptose phosphate broth

TRIM25 – tripartite motif-containing protein 25

TRS – transcription regulatory sequence

TYK2 – tyrosine kinase 2

UTR – untranslated region

VISA - mitochondrial antiviral-signaling protein

VLP – virus like particle

VSV – vesicular stomatis virus

vRNA – viral RNA

vRNP - viral ribonucleoprotein

WNV – West Nile virus

WT – wild-type

Chapter 1

Introduction

1.1 Poultry Industry and Avian Viral Diseases

Domestic chickens (*Gallus gallus domestica*) belong to the order *Galliformes,* the family *Phasianidae* and genus *Gallus* (Figure 1.1). There are currently 281 recognized species of gamebirds distributed among 81 genera (Diamond, 1991;Hoyo et al., 1992;Roberts et al., 1985). In 2004, a consortium sequenced the genome of *Gallus gallus* (UCD 001) making it the first ancestral agricultural animal and the first of the aves to have its genome sequenced (Hillier et al., 2004). This came just a year after the completion of the human genome project (HGP) (International Human Genome Sequencing, 2004). The chicken genome is only 1.09Gb, less than half the size of the human genome (Warren et al., 2017) and consists of 40 autosomes and 2 sex chromosomes, Z and W. In chickens, the males are the homogametic sex (ZZ) and females are the heterogametic sex (ZW) (Figure 1.2). This is in contrast to humans where the females are homozygous (XX). In comparison to mammals, there is a large variation in the size of the chicken chromosomes which range from 200Mb (macro-chromosomes) to 5Mb (micro-chromosomes)(Romanov et al., 2009).

Chickens were first domesticated over 8,000 years ago in Southeast Asia, although one phylogenetic study suggests that divergence from the ancestral population occurred as early as 58,000 ± 16,000 years ago. While there are four ancestral members of genus *Gallus* (Table 1.1), phylogenetic analysis alongside biochemical and molecular techniques, have proposed a single common ancestor, the red junglefowl (Sawai et al., 2010;Kan et al., 2010). Charles Darwin first proposed the single-origin hypothesis in 1868 after observing that only red junglefowl could produce fertile F1 offspring when mated with chickens (Murray, 2016). This finding was later confirmed by mitochondrial sequencing (Fumihito et al., 1996). The natural dissemination of chickens is unlikely as they are not a migratory species and they lack the ability to fly and swim for long distances. Therefore, their global distribution is directly attributed to human movement. The historical importance of the

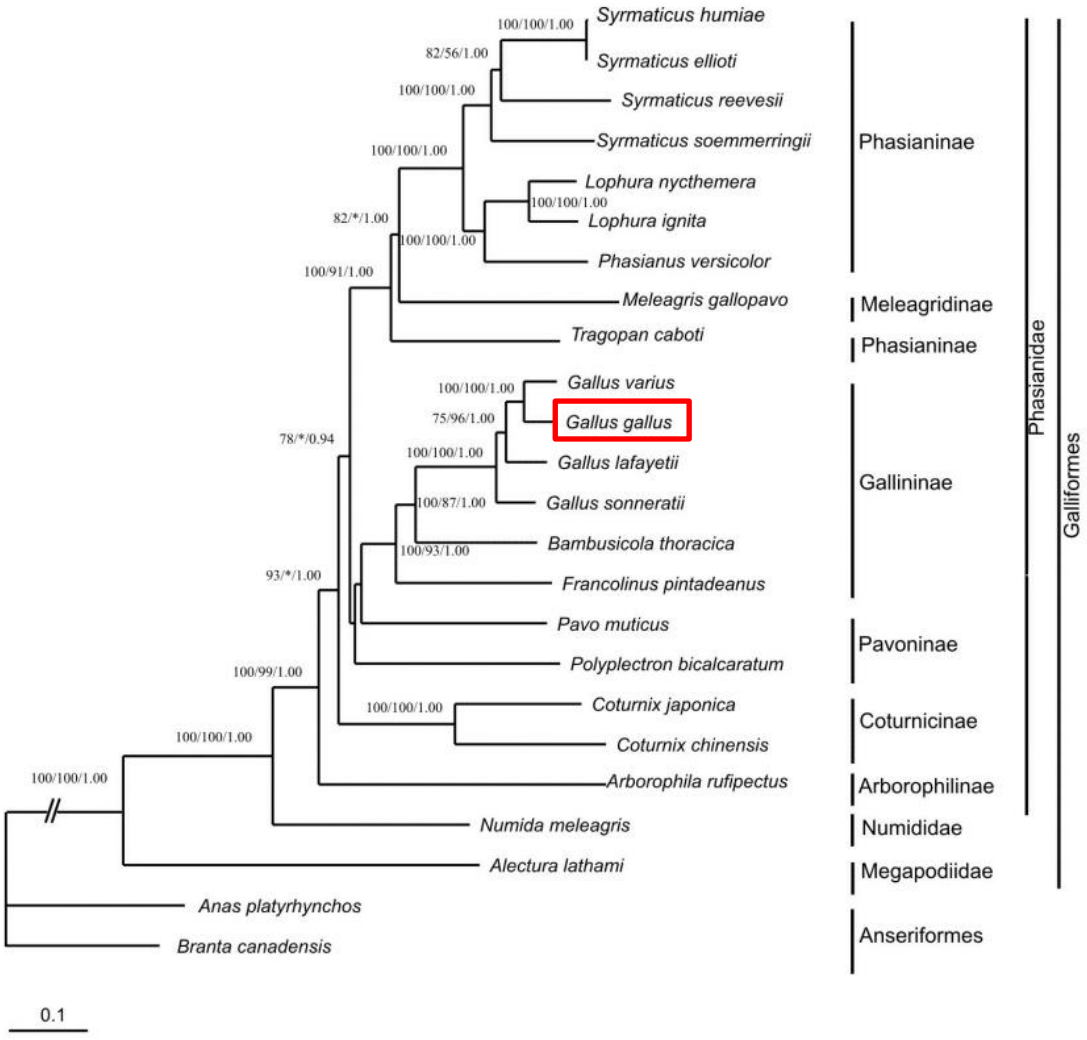

Figure 1.1 Phylogenetic tree of the relationships among Galliformes. Taxonomic relationships were determined by using a nucleotide dataset of 13 mitochondrial protein-coding genes. *Gallus gallus* (red junglefowl) is the last common ancestor of the domesticated chicken (*Gallus gallus domestica)* and is found in Southeast Asia. This tree demonstrates that ducks *(Anasplatyrhynchos)* and geese *(Brantacanadensis)* fall outside of the Galliforme order. Numbers beside the nodes specify bootstrap percentages from maximum likelihood (500 replicates) and maximum parsimony (1000 replicates), and posterior probabilities from Bayesian inference. [Taken from (Kan et al., 2010)]

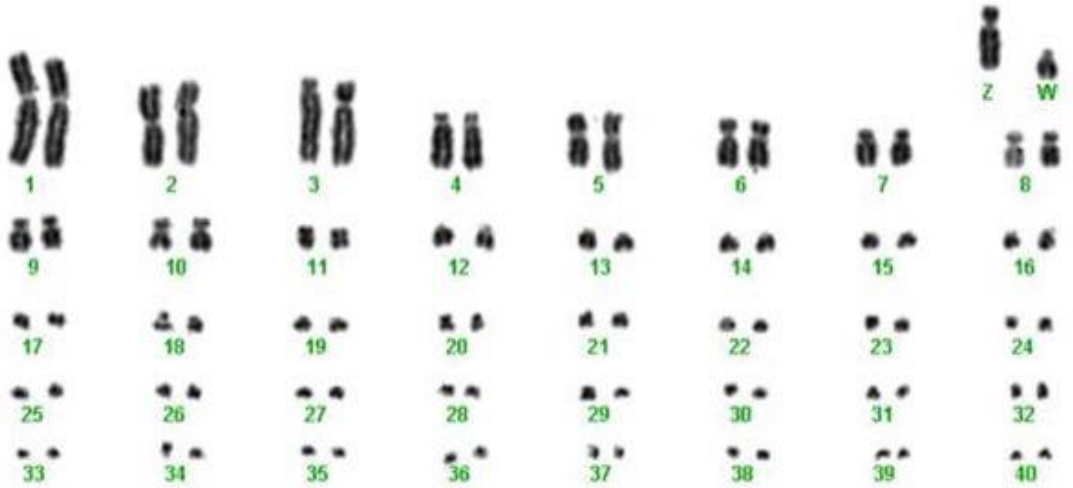

Figure 1.2 Karyotype of the female chicken. There are 40 autosomal pairs and 2 sex chromosomes (Z and W) in a standard diploid cell. The chromosomes are comprised of micro- and macrochromosomes with estimates suggesting that 95% of the DNA is within chromosomes 1 – 28, 32, Z and W. [Taken from (Romanov et al., 2009)]

Table 1.1 Members of the *Gallus* genus and their geographical distribution.

Binomial nomenclature	Common name	Geographic location
G. lafayettei	La Fayette's junglefowl	Sri Lanka
G. gallus	Red junglefowl	Extensive distribution throughout Southeast Asia
G. varius	Green junglefowl	Indonesia
G. sonnerati	Gray junglefowl	India

Abbrev. G = *Gallus*

chicken trade is evident due to their extensive distribution throughout the world (Sawai et al., 2010). The poultry industry is critical in ensuring that high quality protein remains available to a rapidly increasing population. The United Nations estimates a global population of 9.7bn people by the year 2050, an increase of over 32% in 32 years (United Nations, 2015). In the United Kingdom alone, there are over 2,500 poultry farms that collectively produce approximately 875 million chickens each year (British Poultry Council, 2016). Moreover, the volume of chicken being produced in the UK increased from 108,600 tonnes in March 2017 to 119,200 tonnes in March 2018, representing an annual increase of 9.8% (DEFRA, 2018). It is estimated that over 58bn chickens are produced annually worldwide (FAOSTAT, 2011). In comparison, only 269m cattle and 517m sheep are slaughtered each year. The significant increase in chicken production highlights the importance of poultry as a staple protein worldwide. Poultry meat is a good source of animal protein and is becoming more accessible around the world due to its relative affordability. The breeding efficiency of broiler chickens has increased over the years and currently, the average slaughter age is just 42 days (de Jonge and van Trijp, 2013). Other sources of animal protein, such as beef and pork, are prohibited in some regions due to local laws and customs that forbid its consumption. Furthermore, chickens have a high feed conversation ratio of just 1.7 in comparison to cattle and sheep (Salmon Farm Science, 2012) which require over 10kgs of feed for 1kg of meat. These factors, taken together with versatile models of production, make poultry a readily available protein.

Avian viruses present a current and persistent threat to both human health and global food security. Infections with endemic pathogens such as infectious bronchitis virus (IBV) and emerging viral pathogens such as Influenza A viruses (IAVs) decrease productivity through morbidity and increased mortality (Lv et al., 2015;Yunis et al., 2002). An incursion of avian influenza into the United Kingdom from the wild bird population remains a constant threat that could severely damage the poultry industry. In addition to protecting global food

security, controlling cross-species transmission events between birds, pigs and humans, as was seen in the 1997 Influenza outbreak (H5N1) which originated in Hong Kong (Bui et al., 2017), is also a major concern.

1.2 Influenza A Virus

1.2.1 General overview

Influenza viruses (IV) are comprised of four subtypes of influenza (A, B, C and D) grouped together depending on the genetic and antigenic properties of the virus (Ghebrehewet et al., 2016). Each genus belongs to the family *Orthomyxoviridae* and contains a single stranded, negative sense RNA (-ssRNA) genome (McGeoch et al., 1976). The number of segments, or molecules of RNA, is dependent on the subtype, although influenza A viruses (IAV) contain 8 segments with a total viral genome size of around 13.5kb (Ludwig et al., 1999). The genome encodes for 10 core proteins which are conserved across different strains of IAV and are essential for replication (Table 1.2). In addition to these core proteins, there are many other proteins, which are not essential for virus replication, that are encoded by some, but not all strains of IAV.

The natural host and reservoir of IAV are wild aquatic birds which are members of the orders Anseriformes and Charadriiformes and include species such as ducks and geese. In addition, IAV is able to infect a variety of avian and mammalian species, although for this to occur a number of host adaptations are required (Webster et al., 1992). Within the Influenza A genus, there are a number of different subtypes and these are grouped by the antigenicity of the surface glycoproteins, hemagglutinin (HA) and neuraminidase (NA). Currently, 16 HA subtypes and 9 NA subtypes have been described and all of these have been found in avian viruses, in the majority of the HA-NA combinations that are possible. In contrast, only H1, H2 and H3 subtype viruses have been confirmed to persist in humans to

Table 1.2 Core proteins of IAV that are conserved and essential for replication. Segment and protein sizes based on A/Puerto Rico/8/34 (H1N1). Adapted from: (Pleschka, 2013)

Segment	Segment length in nucleotides	Encoded Protein(s)	Protein length in amino acids	Protein function
1	2341	PB2	759	Polymerase subunit; mRNA cap recognition (Blaas et al., 1982)
2	2341	PB1	757	Polymerase subunit; RNA elongation (Braam et al., 1983)
3	2233	PA	716	Polymerase subunit (Dias et al., 2009)
4	1778	HA	550	Surface glycoprotein, involved in receptor binding and fusion (Skehel and Wiley, 2000)
5	1565	NP	498	RNA binding protein; required for polymerase activity (Portela and Digard, 2002)
6	1413	NA	454	Surface glycoprotein; sialidase activity, virus release (Shtyrya et al., 2009)
7	1027	M1	252	Matrix protein involved in RNA nuclear export regulation and viral budding (Gomez-Puertas et al., 2000)
		M2	97	Ion channel; which is required for virus uncoating and assembly (Pielak and Chou, 2011)
8	890	NS1	230	Interferon antagonist; regulation of host gene expression (Hale et al., 2008)
		NEP/NS2	121	Nuclear export of vRNA (O'Neill et al., 1998)

date, although infections with H5, H6, H7, H9 and H10 subtypes have been confirmed (Schrauwen and Fouchier, 2014). Two further subtypes of HA (H17 and H18) and NA (N10 and N11) have been described in bat isolates (Tong et al., 2012;Tong et al., 2013), although it is not currently known if these subtypes exist in any other host species.

1.2.2 Maximising coding capacity of IAV

IAV employs a number of different strategies for maximising its coding capacity, a process which is essential for viruses with limited genome sizes. Each segment contains one open reading frame (ORF) from which one or more protein products are produced. It is known that IAV utilises three main protein coding strategies; mRNA splicing in the case of segments 1, 7 and 8 (Yamayoshi et al., 2016;Lamb and Lai, 1980;Lamb and Choppin, 1981;Alonso-Caplen et al., 1992;Shih et al., 1998;O'Neill et al., 1998;Selman et al., 2012), ribosomal frame-shifting for the expression of PA-X which is translated from the +1 reading frame of PA mRNA on segment 3 (Firth et al., 2012;Jagger et al., 2012), and alternative translation initiation mechanisms such as downstream AUGs of the primary AUG on segment 2 that allow for the translation of PB1-F2 (Wise et al., 2011). A number of non-essential protein products are translated using these mechanisms.

1.2.3 Influenza virion

Influenza virions are pleomorphic with lab-adapted strains predominantly spheroidal with a typical diameter of 100nm (Figure 1.3). In contrast, clinical and field isolates are typically filamentous and are much larger, up to 20µm in length and 100nm in diameter (Mosley and Wyckoff, 1946;Harris et al., 2006). The virion is encased in a host cell-derived phospholipid bilayer which forms an envelope. This envelope is embedded with the two glycoproteins, HA and NA, which determine the viral subtype and antigenicity (Laver and Valentine, 1969). HA exists as a trimer, whilst NA is tetrameric. Beneath the envelope is a layer of

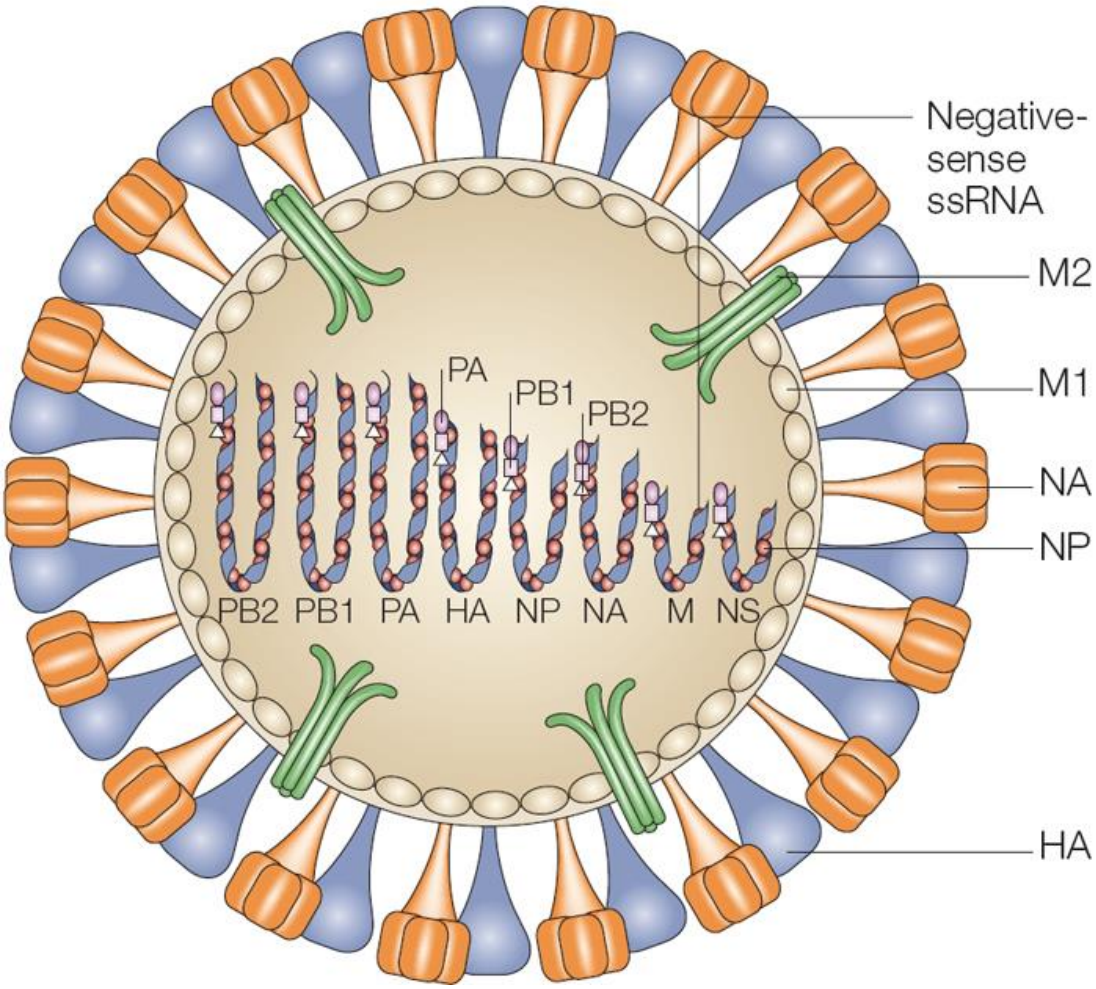

Figure 1.3 A schematic representation of an influenza A virion. Highlighted are the surface glycoproteins that determine the virus subtype (HA and NA), the matrix protein (M1), the ion pump (M2), the nucleoprotein that surrounds the viral RNA (NP) and the 8 segments of negative sense viral RNA. [Taken from: (Horimoto and Kawaoka, 2005)].

oligomerised M1 that provides the structural support for the virion. In addition, the lipid envelope also contains the homotetrameric integral membrane M2 proton channel (Zebedee and Lamb, 1988). The M2 ion channel is essential as it is a highly selective, pH-regulated, proton-conducting channel (H^+ ions) that mediates the acidification of the influenza virion and the release of the viral genome into the cytoplasm.

1.2.4 Influenza cell entry

IAV infection is initiated via the binding of the of virions HA protein to N-acetylneuraminic (sialic) acids which are located on the plasma membrane of the target host cell (Johnson et al., 1964). Spherical virions are internalised by clathrin-mediated endocytosis (Eierhoff et al., 2010) whilst filamentous virions enter via macropinocytosis (Rossman et al., 2012). Once the virus has been incorporated into host cell-derived endosomal compartments, a fusion event occurs which allows for the release of the virus into the cytoplasm. Following acidification of late endosomes, cleaved HA undergoes a pH-dependent conformational change (Jardetzky and Lamb, 2004). This process allows for the release of potential energy and results in the fusion of both the viral and endosomal membranes (Jardetzky and Lamb, 2004). H^+ ions are then pumped through the M2 proton channel acidifying the virion interior and disrupting the protein-protein interactions between M1 and the viral ribonucleoproteins (vRNPs) (Bui et al., 1996). The vRNPs that are no longer bound to M1 are then able to translocate into the cytoplasm of the cell.

1.2.5 Replication and transcription of the viral genome

Replication and transcription of the viral genome is undertaken by the trimeric RNA dependent RNA polymerase (RdRp) which is comprised of the polymerase basic 1 (PB1), polymerase basic 1 (PB2) and polymerase acidic (PA) subunits. Initiation of replication is primer-independent and is achieved through base pair complementarity of the 5’ and 3’

ends of the viral RNA (vRNA) which forms a pan handle structure (Luytjes et al., 1989). A positive sense copy of each vRNA segment is required for replication of the viral genome and this is mediated through the synthesis of an intermediate template termed complementary RNA (cRNA). This template is then used to produce further copies of vRNA, although the process is not yet fully understood (Deng et al., 2006;Flick et al., 1996;Fodor, 2013). Newly synthesised vRNA is encapsidated with nucleoprotein (NP), undergoes nuclear export, packaging and ultimately egress.

Transcription is mediated through the activities of cellular RNA polymerase II (Pol II) and the viral RdRp. During the initiation of cellular transcription, activation of the cellular cap synthesis complex is mediated through the phosphorylation of Serine 5 in the C-terminus of Pol II (Engelhardt et al., 2005). The mechanism of 'cap-snatching' involves the binding of host precursor mRNAs (pre-mRNAs) containing a 5' 7-methylguanosine cap (m7GpppXm) (Plotch et al., 1981). The PB2 subunit allows for the binding of the polymerase to the host's pre-mRNA 5' cap (Blaas et al., 1982). The PA subunit of the polymerase cleaves the 5' cap from the host pre-mRNA through its endonuclease activity (Hara et al., 2006;Dias et al., 2009;Yuan et al., 2009). The PB1 subunit of the RdRp complex mediates RNA elongation (Braam et al., 1983). Transcription is terminated at a 5 to 7 nucleotide long poly(uridine) (poly(U)) stretch located 15 to 17 nucleotides from the 5' end of the vRNA template (Robertson et al., 1981) The polymerase cannot move any further due to steric hindrance causing the active site to pause over the poly(U) tract (Moeller et al., 2012;Poon et al., 1998).

It is not clearly understood how the viral polymerase distinguishes between transcription and replication, since the same promoter is used during both processes. Two models have been proposed, but conflicting data suggests that further investigations are required (Fodor, 2013). One model suggests that the accumulation of viral proteins, such as

NS2/NEP, following translation, alters the function of the RdRp (Robb et al., 2009). The second model proposed by Moeller et al, states that the cRNA is produced when newly synthesised trans-acting polymerases associate with free 5' ends of vRNA. In parallel, the 3' end of the same vRNA is still associated with the original polymerase of the vRNP (Moeller et al., 2012).

1.3 Infectious Bronchitis Virus

1.3.1 General overview

The *coronavirinae* subfamily is split into four genera, alpha (α), beta (β), gamma (γ) and deltacoronaviruses (Δ). Each genus is assigned based solely on the sequence of the virus. Infectious bronchitis virus (IBV) belongs to the Nidovirales order, the *coronavirinae* subfamily and the gammacoronavirus genus. Other notable members of the *coronavirinae* include the β-*coronaviruses* Severe Acute Respiratory Syndrome (SARS) and Middle East Respiratory Syndrome (MERS)-CoV which infect mammalian species, including humans. Coronaviruses have among the largest RNA genomes found in nature, typically ranging from 26 – 32Kb in length. The genome is comprised of single-stranded positive-sense RNA (+ssRNA) and contains both a 5' methylated cap and 3' polyadenylated tail (Brian and Baric, 2005;Masters, 2006). This means that the viral genome of coronaviruses can act directly as mRNA. The genome of the prototypic gammacoronavirus, IBV, is 26.7Kb long and is expressed as six mRNAs during infection.

IBV establishes primary infection in the respiratory tract where it disseminates to the epithelial cells of the trachea and lung (Hofstad and Yoder, 1966;Ambali and Jones, 1990;Lee et al., 2002;Meir et al., 2004). Although IBV is primarily detected in the respiratory tissues, several emerging strains of IBV, such as QX, have been isolated from other organs such as the caecal tonsil and the kidneys (Benyeda et al., 2009;Terregino et al., 2008). A

reverse genetics system for avian coronaviruses was developed in 2001 and this resulted in the production of an apathogenic laboratory attenuated strain of IBV, Beaudette (BeauR) which was generated using the background sequence of Beau-CK (Casais et al., 2001). This strain of IBV is not able to disseminate from the site of inoculation (eyelids and beak) and has very mild clinical signs. Massachusetts 41 (M41) is a pathogenic field strain that has been found in the tissues of the respiratory tract but it does not disseminate to other organs unlike QX (Cook et al., 2012).

1.3.2 IBV virion

Coronaviruses, including IBV, are enveloped, spherical viruses with typical sizes ranging from 80 to 120nm. The virion is encased in a host cell-derived phospholipid bilayer which forms an envelope and contains three viral proteins: the spike (S) protein, the membrane protein (M) and the envelope protein (E) (Figure 1.4). The spike is necessary for mediating viral entry into the host cell as well determining host range (Enjuanes et al., 2006;Perlman and Netland, 2009). The S protein assembles as a trimer which gives coronaviruses the distinctive “corona”, or crown-like appearance. The E protein is a small 10KDa protein which is found embedded into the envelop at low densities (Yu et al., 1994). The E protein re-arranges secretary organelles which increases the efficiency of viral replication, thus propagating the production of new virions (Ruch and Machamer, 2011;Ruch and Machamer, 2012). The N protein of IBV is known to associate with the nascent gRNA to form the nucleocapsid that is incorporated into new virions (Klumperman et al., 1994). The M protein is a transmembrane protein that interacts with E and N proteins to assemble new virions during infection (Neuman et al., 2011;Narayanan et al., 2000;Corse and Machamer, 2003;Lim and Liu, 2001). Within the lipid envelope is the vRNP which is released upon virion binding and subsequent fusion with the cellular membranes.

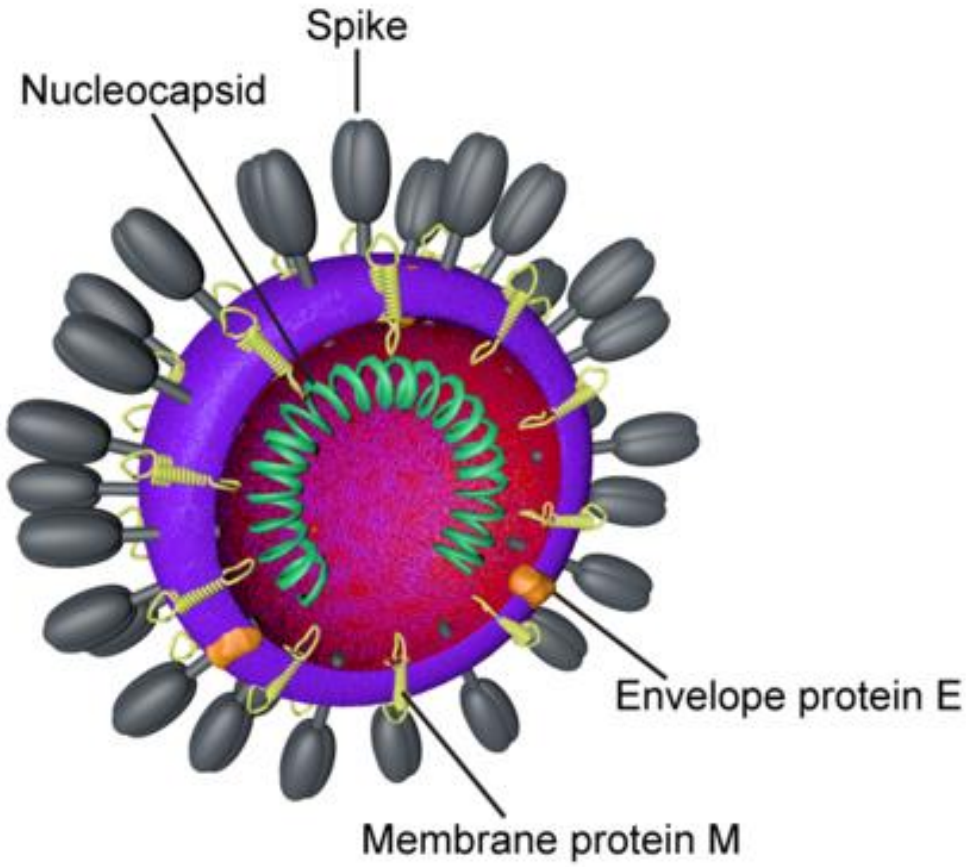

Figure 1.4 A schematic representation of an IBV virion. Highlighted is the surface glycoprotein spike (S), the membrane protein (M), the envelope protein (E), the nucleocapsid (N) that surrounds the viral RNA which is in the positive sense orientation. [Taken from: (Belouzard et al., 2012;Platanias, 2005)].

1.3.3 IBV cell entry

IBV utilises the S protein in order to gain entry into the host cell. The S protein is a large, type I transmembrane protein that is 1,160 amino acids in length. The S protein is split into two subunits, the N-terminal domain (S1) and the C-terminal domain (S2) which are cleaved by furin during infection (Yamada and Liu, 2009). The S1 domain mediates receptor binding and the S2 domain is responsible for fusion with the cell bilayer (Promkuntod et al., 2014). IBV attachment and entry is facilitated through the binding of the S protein to α-2,3-linked sialic acid, a ubiquitous cell surface molecule (Winter et al., 2006). Due to the restricted cellular tropism of IBV and the global distribution of sialic acid, it has been proposed that another unknown cell receptor is required for viral entry (Schultze et al., 1992;Winter et al., 2006). The exact mechanism of IBV entry is currently unknown, although clatherin-mediated endocytosis has been suggested (Yamada and Liu, 2009). It has been observed that IBV fusion is pH-dependent and the acidification of vesicular compartments mediates a conformational change in the S protein, revealing the fusion peptide within the S2 subunit. Release of the fusion peptide results in the fusion of the cellular and viral membranes, thereby releasing the vRNP into the cytoplasm (Bosch et al., 2003).

1.3.4 Replication, transcription and translation of the viral genome

Nidoviruses (which include coronaviruses) utilise complex methods of regulating replication and transcription of their polycistronic genomes (Snijder and Meulenberg, 1998;Lai and Cavanagh, 1997). As a positive sense RNA virus, viral genomic RNA acts directly as mRNA for the translation of the replicase polyproteins, pp1a and pp1ab, encoded by gene 1. The polyprotein pp1ab has an extended C-terminus and it is encoded for by two thirds of the viral genome. Translation of pp1ab occurs after a -1 frameshift which is found in the ORF of non-structural protein 11 (nsp11) (Brierley et al., 1987) and occurs when the ribosome encounters a slippery sequence when translating the coronavirus RNA.

Table 1.3 The size and function of the non-structural proteins (nsps) in IBV.

nsp	Alternative name	Protein length (aa)	Function
2	p87	673	Unknown function
3	PL-PRO	1594	Primarily a papain-like proteases, with many other functions (Lim and Liu, 1998)
4	Peptide HD2	514	Formation of DMVs (Oostra et al., 2007)
5	3C-like proteinase	307	Cysteine-like protease, polyprotein processing (Fang et al., 2010)
6	p34	293	Formation of DMVs, induces autophagy (Maier et al., 2013a)
7	p9	83	Unknown function
8	p24	210	Primase for the RNA polymerase (Tan et al., 2018)
9	p10	111	A protein of the Replicase complex (Chen et al., 2009)
10	p16	145	A protein of the Replicase complex (Fang et al., 2008)
11			Unknown
12	RNA-directed RNA polymerase	940	RNA-dependent RNA polymerase (RdRp) (Tan et al., 2018)
13	Helicase	600	Helicase (Seybert et al., 2005)
14	Exoribonuclease	521	3’ – 5’ exonuclease, RNA cap formation, methyltransferase (Xu et al., 2010)
15	Uridylate-specific endoribonuclease	338	Endonuclease (Bhardwaj et al., 2012)
16	Putative 2'-O-methyl transferase	302	RNA cap formation (Decroly et al., 2008)

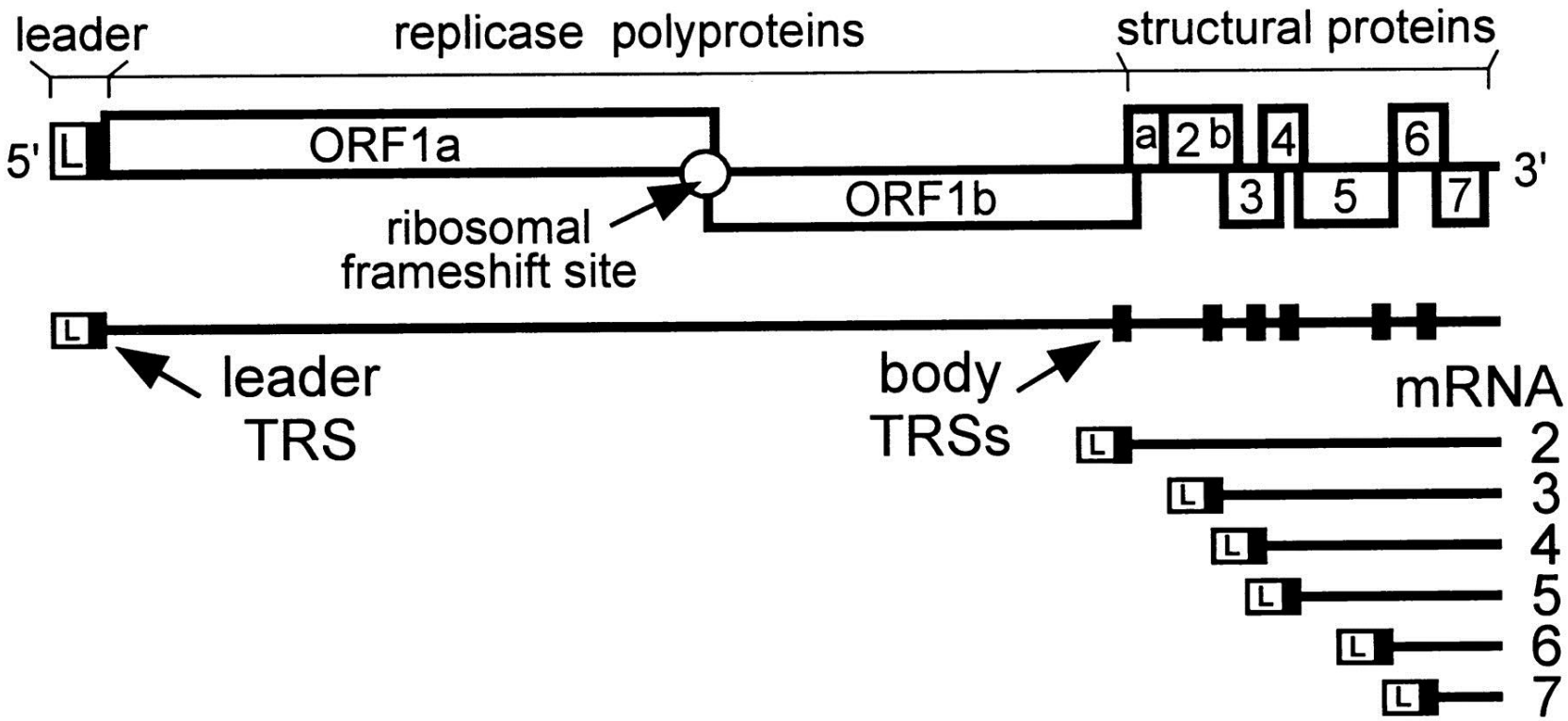

Figure 1.5 A schematic representation of coronavirus transcription. IBV utilises both continuous and discontinuous transcription of its genomic RNA. Continuous transcription is utilised by the virus for the creation of negative-sense full-length genome copies, which are then used as templates for new +ssRNA genomes. Discontinuous transcription creates a nested set of 5 negative-sense sgRNAs of varying lengths. These sgRNAs act as templates for the synthesis of positive-sense sgRNA, which are later translated into viral proteins. [Taken from: (van Marle et al., 1999)].

For the frameshift to arise, the ribosome must pause over the target sequence and this is achieved through secondary structure (pseudoknot) termed the stimulatory element. Once paused, the pseudoknot unwinds, allowing translation to reinitiate in the -1 orientation. The final product is the replicase polypeptide pp1ab (Brierley et al., 1987;Inglis et al., 1990). These polyproteins are cleaved by the virally encoded proteases: nsp3 and nsp5, into 15 individual nsps (Table 1.3). These nsps play a role in a multitude of functions, but are all associated with replication of the viral genome. A number of the nsps accumulate at the replication-transcription complex (RTC) and these are found in the cytoplasm of infected cells. (Ziebuhr et al., 2000).

Continuous transcription is utilised by the virus for the creation of negative-sense full-length genome copies, which are then used as templates for new +ssRNA genomes. To mediate expression of the structural and accessory proteins, IBV, and all viruses of the Nidovirales order, utilise a discontinuous method of RNA synthesis which produces sub-genomic RNA (sgRNA) (Figure 1.5) (Lai and Cavanagh, 1997). The structural and accessory genes are located downstream of the replicase gene (pp1ab), in the 3' third of the IBV genome. These genes are expressed from a set of at least five nested mRNAs and vary in length (Sawicki et al., 2007;van Vliet et al., 2002). A common leader sequence derived from the 5' terminus of the viral genome is found on each of the mRNAs (Vandermost et al., 1993). Together with the leader and coding sequences, the transcription regulating sequence (TRS) found at the 3' end of the leader sequence is critical for sgRNA synthesis (Makino et al., 1991). Each viral sgRNA is capped at the 5' end and polyadenylated at the 3' end. The functions of the structural and accessory proteins are summarised in Table 1.4.

Table 1.4 The size and function of the structural and accessory protein of IBV.

Protein	Protein length (aa)	Function
Spike (S)	1,162	Receptor binding (S1) and membrane fusion (S2) (Casais et al., 2003)
Envelope (E)	109	Modulates the secretory pathway, promotes viral replication (Ruch and Machamer, 2011)
3a	57	Supresses interferon expression (Kint et al., 2015)
3b	64	Supresses interferon expression (Kint et al., 2015)
Membrane (M)	225	Virion assembly (Narayanan et al., 2000)
5a	65	Unknown
5b	82	Host translational shut-off (Kint et al., 2016)
Nucleocapsid (N)	409	Chaperone for viral RNA (Zuniga et al., 2010)

1.4 Herpes Virus of Turkeys

Herpesvirus of Turkeys (HVT) is the third serotype within the Marek's disease virus (MDV) group. This group contains viruses that are genetically and antigenically related lymphotropic avian herpesviruses (Afonso et al., 2001). MDV1 is the etiologic agent which manifests itself as a lymphoma causing disease in chickens and is of considerable economic importance to the poultry industry (Prasad, 1979). In comparison, HVT is a non-pathogenic virus in chickens, and because of this and the associated immune response due to viremia, it has been used extensively as a vaccine candidate for viruses that infect poultry (Witter, 1972;Witter et al., 1970). Vaccine candidates have been produced for protection against: Newcastle disease virus (NDV) (El Khantour et al., 2017), infectious bursal disease virus (IBDV) (Darteil et al., 1995;Perozo et al., 2009), influenza A virus (IAV) (Kapczynski et al., 2016;Rauw et al., 2012) and MDV (Gimeno et al., 2016). HVT contains a large dsDNA genome of 159kb encoding 99 functional genes (Afonso et al., 2001). Research conducted on MDV (the etiological agent) found that cell-free MDV has only been detected in the epithelial cells of the feather follicle. The initial infection of chickens with MDV is through the inhalation of cell-free virus from the skin and associated feather follicle epithelium (Beasley et al., 1970;Addinger and Calnek, 1973;Calnek, 2001). Subsequent infection is mediated exclusively through cell-to-cell transmission (Churchill and Biggs, 1967). Once infection has been established, the next stage is the cytolytic phase in lymphoid organs followed by the establishment of latency in T cells, which ultimately results in the transformation of those T cells (Abdul-Careem et al., 2009).

1.5 Interferon Induction and Signalling

1.5.1 The interferons

Interferons (IFNs) are the molecules that protect cells from viral infection and were first discovered in 1957 by Isaacs and Lindenmann (Isaacs and Lindenmann, 1957). IFNs are soluble cytokines that have potent antiviral activities and are critical in controlling viral infection by activating a cell-intrinsic antiviral state (Stetson and Medzhitov, 2006;Foster, 1997). Following detection of a viral pathogen, cells secrete these cytokines which then bind to their cognate receptor, in an autocrine and paracrine fashion, resulting in the transcriptional activation and modulation of over 500 genes, collectively known as interferon stimulated genes (ISGs) (de Veer et al., 2001b;Santhakumar et al., 2017). Although the IFN response is robust, and in many cases will limit the severity of infection, it has been well established that viral pathogens have evolved various mechanisms to block the activation or effective signalling of IFNs (Randall and Goodbourn, 2008). There are three families of IFNs (type I, II and III) which are grouped according to their structure and function. Moreover, each family has its own specific receptor which allows for the propagation of an effective immune response (Platanias, 2005). In humans, type I IFNs include IFNα (13 different subtypes), IFNβ, IFNε, IFNκ, and IFNω (Platanias, 2005;Gibbert et al., 2013). The best characterised type I IFNs are IFNα and IFNβ, while the roles of IFNε, κ, and ω are less well understood. The type II IFN (IFNγ) is structurally different to the type I IFNs and is secreted by natural killer and activated T cells (Th1 CD4 and CD8 cytotoxic) (Farrar and Schreiber, 1993). IFNγ has an immunomodulatory role, not only protecting against intracellular pathogens, but also controlling tumour development (Schoenborn and Wilson, 2007). Type III IFNs include IFNλ1, IFNλ2, IFNλ3, and IFNλ4. It has been shown that type III IFNs are able to upregulate the expression of the same ISGs as type I IFNs, albeit at a lower level, in comparison to IFNα (Zhou et al., 2007). Moreover, it has been shown that

the expression of type III IFNs is restricted to mucosal epithelial cells which frequently encounter viral pathogens (Wack et al., 2015). Type I and type III IFNs are upregulated in direct response to viral infection and the binding of IFN to their cognate receptor results in the activation of the same downstream signalling molecules, such as those found in the canonical JAK/STAT pathway (Kotenko et al., 2003;Wack et al., 2015;Zhou et al., 2007). For the purposes of this thesis, I shall only make reference to IFNα and β (type I) and IFNγ (type II) and will not discuss any other subtypes or type III IFNs.

1.5.2 Viral pathogen detection and interferon induction

To detect invading viral pathogens, the immune system is equipped with specialised receptors known as pathogen recognition receptors (PRRs). These PRRs recognise a limited number of pathogen associated molecular patterns (PAMPs). One of the primary PAMPs that elicits IFN induction are non-host cell derived nucleic acids, such as dsRNA (Weber et al., 2006). However, other structures present on ssRNA viral genomes, such as 5' triphosphate groups, also elicit an IFN response (Hornung et al., 2006;Pichlmair et al., 2006). In mammals, the initial detection of virally-derived PAMPs is primarily mediated through Retinoic acid-inducible gene 1 (RIG-1) like receptors (RLRs) which are DExD/H box RNA helicases. There are three RLRs namely; retinoic acid-inducible gene 1 (RIG-1), melanoma differentiation-associated protein 5 (MDA5) and laboratory of genetics and physiology 2 (LGP2). All three RLRs contain an RNA helicase domain and a C-terminal regulatory domain (CTD), although only RIG-1 and MDA5 contain caspase activation and recruitment domains (CARD). LGP2 does not contain a CARD domain and has been implicated in regulating the function of RIG-1 and MDA5. During viral infection and upon the recognition of PAMPs, the CTD of RIG-1 and MDA5 binds to viral RNA, activating the CARD domains (Satoh et al., 2010;Yoneyama et al., 2005;Takahasi et al., 2008;Rehwinkel et al., 2010;Loo and Gale, 2011).

It is known that the primary PRR during IAV infection in humans is RIG-1, although the contribution of MDA5 has been shown to be important during *in vivo* infections (Graham et al., 2013;Benitez et al., 2015). For full activation, the CARD of RIG-1 is poly-ubiquitinated by either tripartite motif-containing protein 25 (TRIM25) (Gack et al., 2007), RING finger protein leading to RIG-1 activation (RIPLET) (Oshiumi et al., 2009), or Mex-3 RNA Binding Family Member C (MEXC) (Kuniyoshi et al., 2014). Poly-ubiquitination of the CARD domain results in the formation of a hetero-tetrameric complex of RIG-1 (with ubiquitin) which is essential for downstream signal transduction (Jiang et al., 2012). CARDs of RIG-1 then interact with the CARD of interferon promoter stimulator-1 (ISP-1) (also known as MAVS, VISA or Cardif) which acts as a signal adaptor molecule (Kawai and Akira, 2009). This results in the activation of I kappa B kinase (IKK) and TANK-binding kinase 1 (TBK1) (Loo and Gale, 2011). TBK1 and IKK then phosphorylate and activate the transcription factors interferon regulatory factor-3 (IRF3) and interferon regulatory factor-7 (IRF7) which dimerise and subsequently localise to the nucleus. This results in the activation and expression of type I IFNs. An overview of the process described above is illustrated in in Figure 1.6.

1.5.3 Interferon signalling

Once translated, IFN α/β is secreted from infected cells where it acts in an autocrine and paracrine manner, binding to the IFNα/β receptor (IFNAR) of the same, or neighbouring cells. The IFNAR receptor is a heterodimeric transmembrane receptor, which consists of the IFNα receptor 1 (IFNAR1) and IFNα receptor 2 (IFNAR2) subunits (Ivashkiv and Donlin, 2014). Binding of IFNα/β to the IFNAR activates a complex downstream signalling cascade which results in the synthesis and upregulation of ISGs with a number of antiviral and anti-proliferative functions (Schneider et al., 2014). Activation of innate immune pathways in uninfected cells 'prime' these cells, hindering viral infection. IFNα/β binding to IFNAR activates janus kinase 1 (JAK1) and tyrosine kinase 2 (TYK2), which results in the

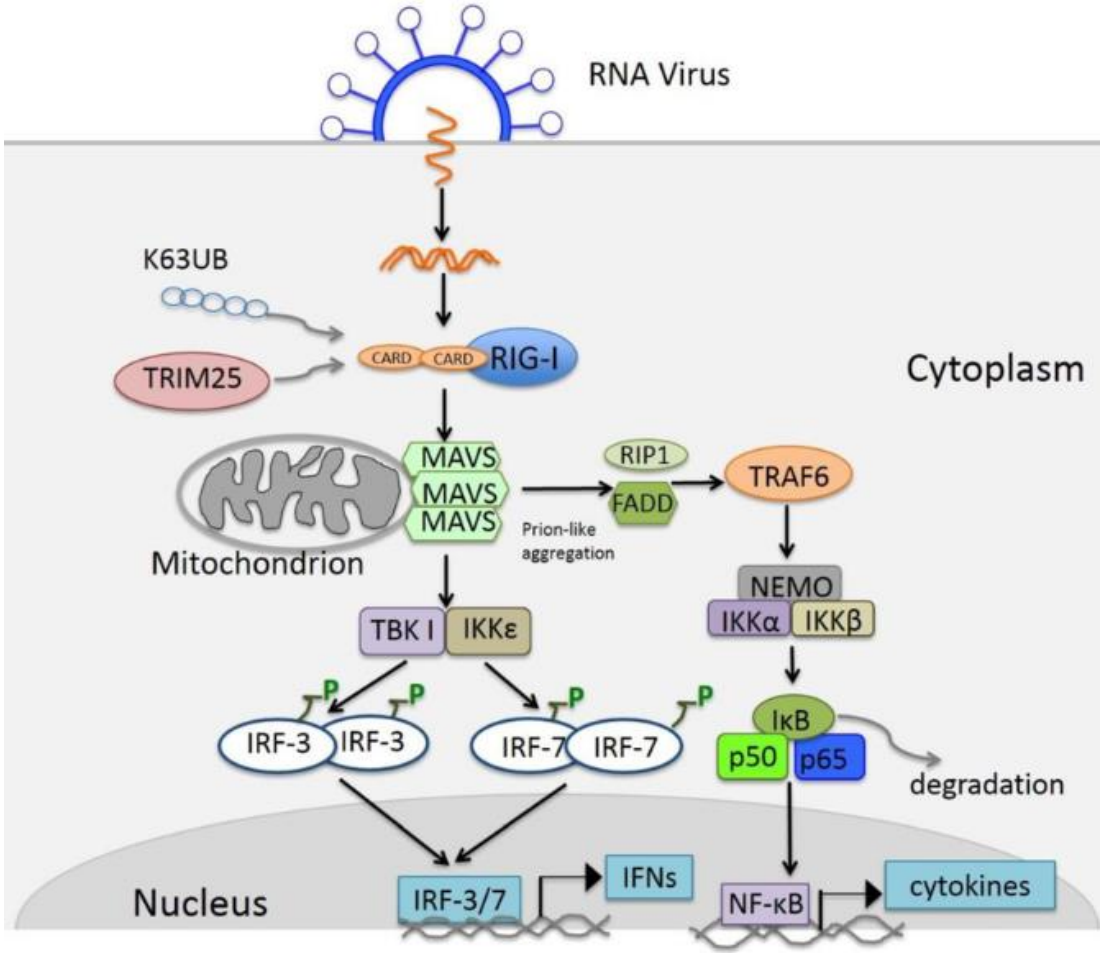

Figure 1.6 A schematic representation of PAMP recognition and IFN induction. The cytoplasmic dsRNA sensor RIG-1 is poly-ubiquitinated by TRIM25 which allows for the CARD of RIG-1 to interact with the CARD of ISP-1 (MAVS). This results in the activation of TBK I and IKKε which in turn phosphorylate and active the transcription factors IRF-3 and IRF-7. Homodimers then translocate into the nucleus and bind to the corresponding promoter sequences, inducing the expression of type I IFNs. [Taken from: (Nan et al., 2014)].

phosphorylation of signal transducer and activator of transcription 1 and 2 (STAT1 and STAT2) (Randall and Goodbourn, 2008). The phosphorylated STAT1/STAT2 heterodimer interacts with interferon regulatory factor 9 (IRF9) forming a complex called the interferon stimulated gene factor 3 (ISGF3) (Fu et al., 1990;Schindler et al., 1992). ISGF3 translocates to the nucleus and binds to IFN-stimulated response elements (ISREs) (Levy et al., 1986). ISREs are found in the promoter sequences of all ISGs which allows for the universal modulation of ISG expression through interferon signalling. This process also acts as a positive feedback mechanism, enhancing the type I IFN response. In contrast IFNγ binds to IFN-γ receptors 1 (IFNGR1) and 2 (IFNGR2) which results in the phosphorylation and homodimerization of STAT1 (Shuai et al., 1992). The activated STAT1 complex then undergoes nuclear translocation, and binds to the gamma-activated sequence (GAS) elements upstream of IFN-γ-induced genes (Decker et al., 1991). Interferon signalling is an essential process which allows for the modulation of ISG expression and protects the cell from invading viral pathogens. Figure 1.7 is a schematic illustrating interferon signalling in human cells.

1.5.4 Interferon induction and signalling in Galliformes

The general principals of interferon activation and signalling outlined in mammals are broadly transferable to chickens, although there are some notable exceptions. One of the most striking features of innate immunity in Galliformes is the absence of RIG-1 as a cytosolic sensor of virally-derived PAMPs (Karpala et al., 2011). However, this does not mean that chickens are unable to mount a potent innate immune response. It has been demonstrated that MDA5, which detects long dsRNAs in humans, is able to detect both short and long dsRNA's in chickens, suggesting some functional redundancy (Hayashi et al., 2014). In addition, chicken LGP2 has an MDA5-like helicase domain and a RIG-1-like C-terminal domain which is able to bind dsRNA (Uchikawa et al., 2016). It is currently

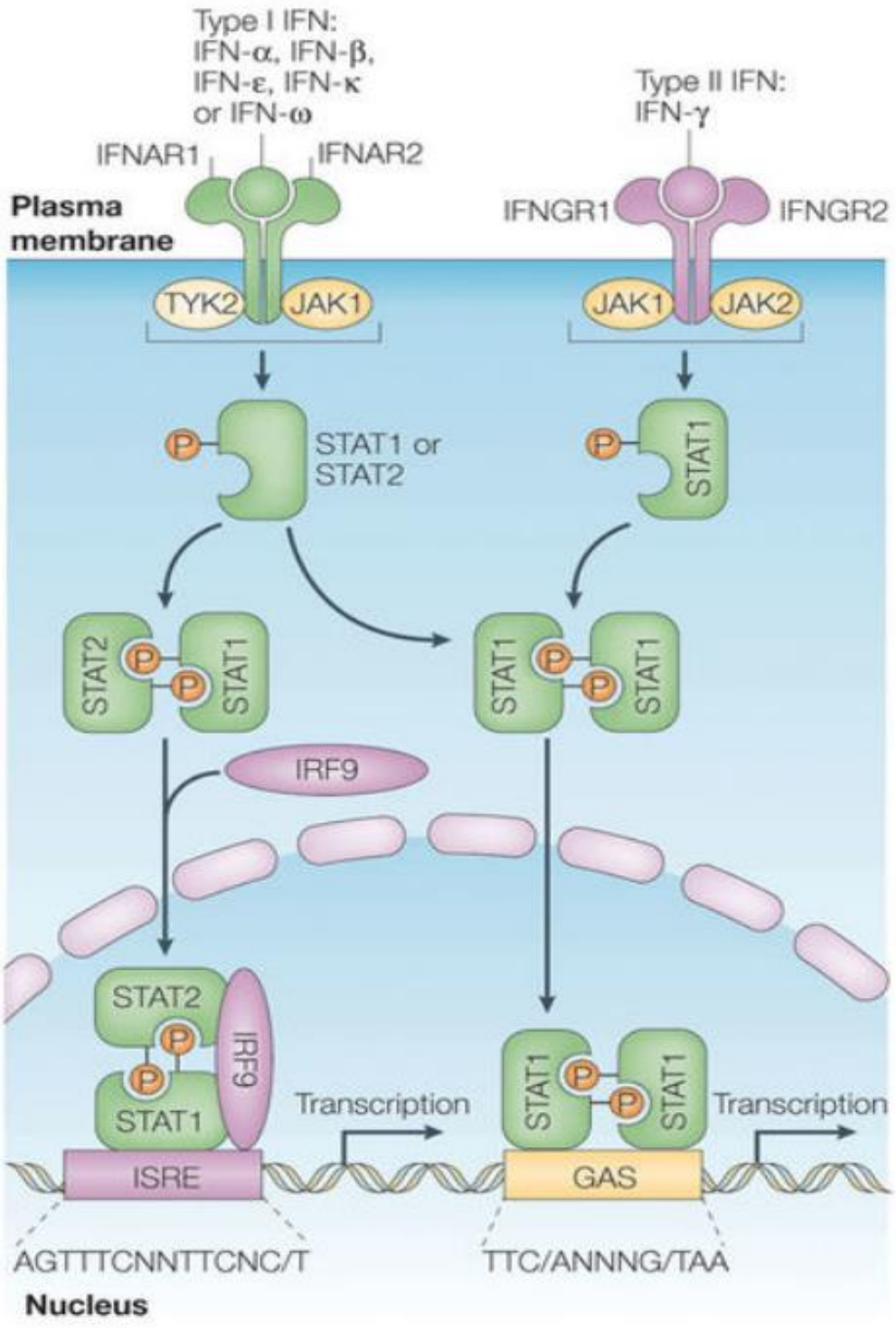

Figure 1.7 A schematic representation interferon signalling. IFNα/β bind to the IFNAR receptor which leads to the activation of TYK2/JAK1, activation and heterodimerisation of STAT1/2 and the formation of the ISGF3 complex through an interaction with IRF9. ISGF3 undergoes nuclear export where it binds to the ISRE promoter. In comparison IFNγ binds to the IFNGR receptor, leading to the activation of TYK2/JAK1, activation and homodimerisation of STAT1 which then binds to the GAS promoter. Both lead to the upregulation and modulation of ISGs. [Taken from: (Platanias, 2005)].

unknown if this plays a significant role in PAMP detection. In addition, comparative genomics suggest that IRF3 and IRF9 are absent from the chicken genome. IRF7 and IRF10 are the only members of the transcription factor family that have been identified in chickens to date (Santhakumar et al., 2017). Despite significant improvements over the past decades, the sequence and annotation of the chicken genome is still incomplete. Therefore, it is unclear if IRF3 and IRF9 are actually missing or whether they are yet to be identified. This is exemplified by a recent manuscript which claims to have found tumour necrosis factor-α (TNFα) in birds, a cytokine that was thought to be absent from the chicken genome (Rohde et al., 2018). In humans, there are 7 type I IFNs (IFNα, IFNβ, IFNε, IFNκ, IFNω, IFNδ, and IFNτ) whereas only 2 type I IFNs have been identified in chickens; IFNα and β. This highlights the vast difference between the innate immune systems of chickens and humans. For a complete overview, avian IFNs and innate immunity has been reviewed by Santhakumar et al, 2017 (Figure 1.8).

1.5.5 Viral evasion of the interferon response

Viral pathogens have evolved mechanisms to evade restriction by interferon and ISGs. The main interferon antagonist of IAV is the NS1 protein which utilises many mechanisms to evade the cellular innate immune responses. NS1 is able to bind to RIG-1 directly as well as to the E3 ligases TRIM25 and RIPLET, which are necessary for the poly-ubiquitination and activation of RIG-1 (Rajsbaum et al., 2012;Gack et al., 2009;Mibayashi et al., 2007). NS1 also inhibits the transcription factors AP-1, IRF3 and NF-κB (Talon et al., 2000;Wang et al., 2000;Ludwig et al., 2002). It has been observed that other IAV proteins, such as the RdRp and PA-X, are also able to reduce the effectiveness of the interferon response, by inducing host shut-off mediated by endonuclease events required for the translation of IAV-derived mRNAs. This is likely reduces the translation of host mRNAs which reduces the cells ability to increase expression of IFNs/ISGs (Bercovich-Kinori et al., 2016). It has also been shown

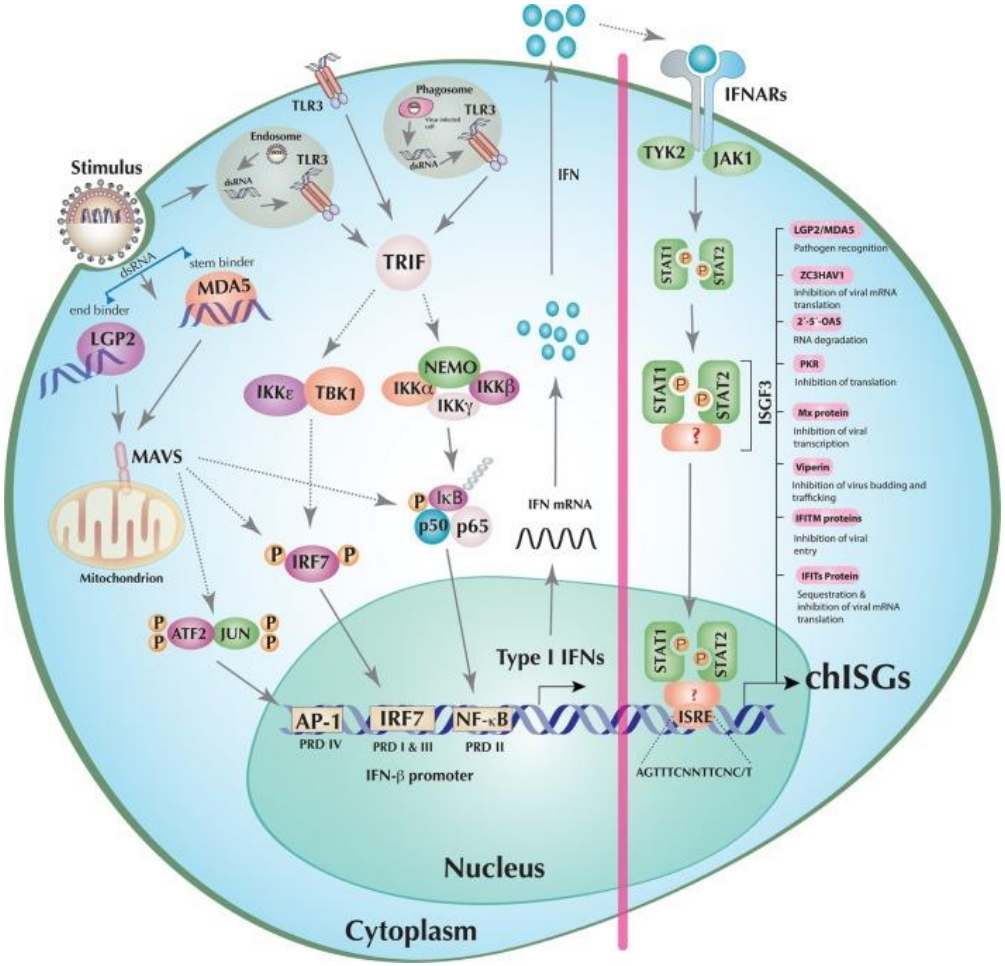

Figure 1.8 A schematic representation of chicken interferon induction and signalling. The pathways and proteins utilised in human and chicken cells for the activation of a cell-intrinsic antiviral state are broadly similar although some notable differences include a lack of RIG-1, IRF3 and IRF9. It is also unknown what molecule interacts with STAT1/STAT2 to form the ISGF3 complex. [Taken from: (Santhakumar et al., 2017)].

that HA of IAV is able to bind directly to the IFNAR receptor, inducing ubiquitination and therefore selecting them for degradation via the proteasome (Xia et al., 2016). A role has also been implicated for PB1-F2. It has been shown that PB1-F2's association with MAVS reduces the membrane potential across the mitochondria which interferes with IFN induction (Varga et al., 2012).The mechanisms employed by IBV to circumvent the interferon response are currently unknown. However, the mechanisms used by other coronaviruses have been investigated and includes the targeting of many of the same proteins as observed with IAV. For example, it has been observed that the N protein of SARS-CoV inhibits the ubiquitination of RIG-1 by binding to the SPRY domain of TRIM25 (Hu et al., 2017). In addition, the nsp1 of α and β-coronaviruses has been shown to induce host cell shut-off, selectively targeting host cell mRNAs for degradation and limiting the effectiveness of the interferon response (Kamitani et al., 2006).

1.6 Mammalian IFITMs

16.1 Early characterisation

The human IFITM proteins were discovered in 1984, making them amongst the first ISGs to be characterised (Friedman et al., 1984). The nomenclature was initially very different to what is used currently. They were originally named 9–27(IFITM1), 1-8D (IFITM2), and 1-8U (IFITM3). Further characterisation of these genes was undertaken in 1996 (Alber and Staeheli, 1996) where the authors noted that vesicular stomatis virus (VSV) could be inhibited by IFITM1, although the inhibition was less potent than with MxA. Moreover, when huIFITM1 was overexpressed in mouse cells, these cells were more refractory to infection with VSV than the wildtype controls. Interestingly, the authors noted that IAV was less potently inhibited by IFITM1 than VSV, a finding which is contradictory to the current literature (Huang et al., 2011). A further study examined the relationship between hepatitis C virus (HCV), IL-1 and 1-8U (IFITM3) and found that increased expression of 1-8U was

associated with a decrease in HCV mRNA, although no specific conclusions regarding antiviral activity were made from this study (Zhu and Liu, 2003).

In 2009, two separate IAV-targeting RNA interference studies identified huIFITM1, 2 and 3 as potential restriction factors against IAV (Brass et al., 2009;Shapira et al., 2009). In the study by Brass et al which aimed at selectively targeting *IFITM3* through siRNA treatment, they found that this targeted inhibition of *IFITM3* rescued H1N1 (A/PR/8/34) replication in U2OS cells that had been treated with IFNγ. Further characterisation was performed, and the authors observed that the overexpression of *IFITM1*, *IFITM2*, or *IFITM3* suppressed the replication of H1N1 (A/PR/8/34) and H3N2 (A/Udorn/72) in A549, U2OS, and MDCK cell lines as well as in chicken embryo fibroblasts (CEFs). They also found that murine leukemia virus (MLV) was not be restricted by the overexpression of these *IFITMs*, suggesting specificity in the viral pathogens that the IFITM proteins are able to target for restriction. In the same study, murine embryonic fibroblasts (MEFs), that lack the *ifitm* locus *(ifitm$^{-/-}$)*, were developed. When these cells were challenged with IAV or retroviruses pseudotyped with H1, H3, H5, and H7, viral replication was significantly restricted when compared to the wildtype controls. Moreover, West Nile Virus (WNV) and Dengue Virus (DV) were potently restricted in A549 or U2OS cells stably overexpressing *IFITM3*. Conversely, when *IFITM3* expression was knocked down via siRNA transfection, an increase in viral replication was observed, demonstrating that IFITM3 is a true restriction factor of IAV, WNV and DV. In contrast, there was no observed restriction of three arenaviruses, namely lymphocytic choriomeningitis virus (LCMV), Lassa virus (LASV) or Machupo virus (MACV), suggesting that there is some degree of specificity of IFITM restriction. The findings published in these studies prompted further research by many groups that sought to understand the mechanisms underpinning the antiviral activities of the mammalian IFITMs.

1.6.2 Vertebrate orthologues of *IFITMs*

Assigning vertebrate orthology is challenging due to the positive selection and divergence of innate immune genes, including the IFITM family (Zhang et al., 2012;Webb et al., 2015). There is a constant arms race between the virus and host which intensifies the process of positive selection of the innate immune genes (tenOever, 2016). Moreover, when one considers that chickens and humans diverged more than 300 million years ago (mya) it is not surprising that sequence homology is low and orthology is difficult to assign (Burt et al., 1999). There are 3 clades of *IFITM* genes, clade I contains *IFITM1, IFITM2 and IFITM3* (as well as murine Ifitm6 and Ifitm7), clades II and III contain just 1 gene, *IFITM5* and *IFITM10*, respectively. The identification of IFITM family members is through the conserved CD225 domain (Siegrist et al., 2011). The two terminal regions of the *IFITM* genes are hypervariable and this is thought to correlate with viral specificity (Compton et al., 2016). The majority of mammals have a locus containing at least the clade I *IFITM* genes, alongside birds (such as turkeys and chickens), fish (such as stickleback and zebra fish) and amphibians (frog) (Bailey et al., 2014;Zhang et al., 2012;Siegrist et al., 2011). Although syntenic, the *IFITM* locus is not always found on the same chromosome when comparing among species. For example, the *IFITM* locus is located on chromosome 11 in humans, chromosome 7 in the mouse and on chromosome 5 in the chicken. There are two conserved genes that flank the *IFITM* locus of all species ranging from mammals to amphibians (Smith et al., 2013), independent of the chromosome the locus is located on; the telomeric β-1,4-N-acetyl-galactosaminyl transferase 4 (B4GALNT4) and the centromeric acid trehalase-like 1 (ATHL1) gene. The identification of these two conserved genes makes the identification of the *IFITM* locus possible between species. A combination of BLAST searches and the use of synteny, led to the successful identification of the *chIFITM* locus by Smith et al., 2013 via bioinformatics analysis.

1.6.3 Conservation and post-translational modifications

IFITM proteins are small polypeptides of approximately 130 amino acids with a conserved CD225 domain, comprised of an intramembrane (IM) domain, a transmembrane domain (TMD) and a cytoplasmic intracellular loop (CIL). The CD225 domain is conserved both within paralogues and between orthologues from different species. The amino acids within the CD225 domain are subject to post-translational modifications (PTMs) such as palmitoylation, ubiquitination and methylation. These PTMs confer specific functions that are linked to restriction. The palmitoylation of two cysteine residues (Cys 71 and 72) situated within the IM domain are critical (especially Cys 72) for the restriction activity of huIFITM3 (Yount, 2012 and Yount 2010). Another Cys residue at position 105, located at the junction between the CIL and TMD, is also palmitoylated but the role of this poorly conserved residue does not seem essential for viral restriction. It is thought that the palmitoylation of these residues is important not only for restriction and IFITM subcellular localisation, but also for their association with lipid rafts. It has been shown that incremental mutagenesis of the Cys residues results in a reduction of antiviral activity (Yount et al., 2010;Yount et al., 2012). It is thought that ubiquitination enhances the stability of the proteins and mediates protein turnover. The ubiquitination of lysine residues located throughout the conserved domain (Lys24, Lys83, Lys88, and Lys104) of the IFITM proteins, has been shown to be unfavourable for IFITM restriction. However, studies on IFITM3 observed that a ubiquitinated IFITM3 is more stable and localises more consistently to the correct intracellular compartment (Yount et al., 2012). It has also been shown that Lys88 of IFITM3 can undergo monomethylation by set7 (Shan et al., 2013). Increased methylation at this position is correlated with a loss of restrictive function, whilst decreased methylation resulted in an enhanced restrictive phenotype (Chesarino et al., 2014b). Phosphorylation of Tyr20 is less conserved and is only present in huIFITM2 and 3 (and related orthologues) and regulates *IFITM* expression and sub-cellular localisation (Jia

et al., 2012). The hydrophobic N-terminal domains (NTDs) have a greater degree of heterogeneity in terms of length and sequence diversity, which could be critical in conferring specific antiviral function, and may explain potential differences in virus specificity (John et al, 2013).

1.6.4 Membrane topology and mechanism of action

Although the huIFITM proteins have been studied extensively, only a single study provides evidence that predicts the protein topology of huIFITM3 (Ling et al., 2016). Using nuclear magnetic resonance (NMR) and electron paramagnetic resonance (EPR) on huIFITM3 in detergent liquid micelles, Ling et al postulate the proposed type II transmembrane protein topology model for huIFITM3. Furthermore, PTMs of the NTD, particularly the ubiquitination of Lys24 and phosphorylation of Tyr20, suggest that the NTD resides intracellularly, as access to cytosolic enzymes such as ubiquitin ligases and protein kinases is essential (Jia et al., 2012;Yount et al., 2012). Evidence for the localisation of the C-terminal domain (CTD) is less definite, although additional studies assessing the PTMs in this region suggest that the CTD of murine ifitm1 could also reside intracellularly (Yount et al., 2012;Hach et al., 2013b). Conversely, models of murine ifitm3 and huIFITM1 suggest that the CTD resides extracellularly (Bailey et al., 2014;Weston et al., 2014).

The broad spectrum of viral restriction by IFITM proteins means that identifying the molecular mechanism(s) of specific viral restriction remains elusive. It is still not known why some viruses are insensitive to IFITM restriction whereas others are potently restricted. A study published in 2014 demonstrated that huIFITM3 interacts with Vesicle-membrane-protein-associated protein A (VAPA) which in turn prevents its association with oxysterol-binding protein (OSBP). This interaction disrupts cholesterol homeostasis and inhibits viral entry via cholesterol accumulation (Amini-Bavil-Olyaee et al., 2013). Two further studies found that host cell membranes underwent a loss of fluidity after an overexpression of

huIFITM1 which may be explained by the findings of Amini-Bavil-Olyaee et al (Li et al., 2013;Lin et al., 2013). In contrast, other studies suggest that IFITM-mediated viral restriction is independent on cholesterol and propose an alternate mechanism whereby IFITM3 has an ability to block fusion pore formation at a post-hemifusion stage. It is proposed that this process stabilises the cytoplasmic leaflet of endosomal membranes either directly or indirectly through proteins/lipid independently of cholesterol (Desai et al., 2014). In addition, further co-immunoprecipitation studies suggest that ZMPSTE24 can interact with members of the huIFITM protein family and the data implies that *ZMPSTE24* expression is essential for IFITM antiviral activity (Fu et al., 2017). These studies demonstrate the complexity of the mechanisms of IFITM-mediated restriction. It may also be possible that more than one mechanism is utilised during infection.

1.6.5 Cellular localisation

All of the huIFITMs are constitutively expressed (Everitt et al, 2013); however, type I IFN signalling enhances the expression of these genes. Human and mouse IFITM proteins have been extensively studied, and their localisation well characterised. Human IFITM1 has been shown to localise at the plasma membrane, with the C-terminal domain (CTD) available for cleavage by extracellular proteases (such as trypsin), which suggests that the CTD of huIFITM1 resides extracellularly (Weston et al., 2014). However, data generated by electron microscopy suggests that a fraction of huIFITM1 localises at intracellular compartments such as the golgi apparatus. Human IFITM3 has been shown to stain in consistent punctate structures at the early/late endosomes, co-localising with proteins such as Rab and Lamp1/2 (Weston et al., 2014;Narayana et al., 2015). A study has shown that localisation of huIFITM3 at the endosomes is important for the restriction of viruses such as IAV, which enter through the acidification of late endosomes (Yoshimura et al., 1982).

The localisation of huIFITM2 is more controversial. Some data suggests that it localises to similar compartments as huIFITM3, in punctate spots at the early/late endosomes (Narayana et al., 2015). Other groups report staining in punctate structures at the nucleus (Weston et al., 2014). Many studies have reported the possible implications of using tagged constructs, as the proteins may incorrectly localise and the function of the protein may be altered. At present, tagged constructs remain necessary because the antibodies against the different IFITM proteins cross-react (Zhao et al., 2014;Weston et al., 2014;Wrensch et al., 2015). In one study, it was observed that anti-IFITM1-NTD antibody detects both IFITM1 and IFITM3, whilst an anti-IFITM3-NTD antibody detects IFITM3 and IFITM2 (Weston et al., 2014).

1.6.6 Restriction of viral pathogens

Human IFITM proteins restrict the entry and replication of several highly pathogenic human viruses, including influenza A viruses (IAVs), flaviviruses (Dengue virus), filoviruses (Ebola virus and Marburg virus) and coronaviruses such as severe acute respiratory syndrome (SARS) and human immunodeficiency virus 1 (HIV-1) (Brass et al., 2009;Foster et al., 2016;Yu et al., 2015;Tartour et al., 2014;Lu et al., 2011;Compton et al., 2014;Chutiwitoonchai et al., 2013).

The evidence for IAV restriction is abundant and includes data generated from *in vitro* models and *in vivo* studies. Initial investigations using siRNA screens during IAV infection found that the IFITM proteins were able to potently restrict IAV (Brass et al., 2009). Since this time, IFITM3 has been found to be the most potent member of the IFITM family in restricting IAV, although IFITM2 and 1 do reduce IAV infectivity (Huang et al., 2011;Everitt et al., 2012). It has been shown that IAV is potently restricted by *ifitm3* in mice (Bailey et al., 2012). A mouse model with a disruptive insertion in exon 1 of *ifitm3* which abolishes gene function (Lange et al., 2008), (ifitm3-/-), found that a usually low pathogenicity H3N2 (A/X-

31) IAV resulted in weight loss of >25% and severe signs of clinical illness. Even though there are many different strains of IAV due to the many possible HA and NA combinations, there have been no reports of IAV escape from IFITM-mediated restriction (Bailey et al., 2014).

A wide range of other enveloped viruses are also restricted by the IFITM protein family. Flaviviruses, including DENV1 and DENV2, Japanese encephalitis virus (JEV), and WNV are all potently restricted (Brass et al., 2009;Huang et al., 2011;Jiang et al., 2010;John et al., 2013). It is believed that flaviviruses are restricted in the same manner as IAV because both viruses share a common method for viral entry; fusion with host cell membranes. In contrast, filoviruses (EBOV and MARV) and coronaviruses (SARS-CoV and MERS-CoV) require delayed proteolytic cleavage of the fusion peptide in order to enter the cytoplasm from the endosomes, therefore endosomal-viral fusion occurs much later on (Huang et al., 2006;Chandran et al., 2005). In general, these viruses are more sensitive to IFITM1 restriction than IAV (Huang et al., 2011). The bunyaviruses Andes virus (ANDV), Hantaan virus (HTNV), La Crosse virus (LACV) and Rift Valley fever virus (RVFV) are restricted by all of the IFITM proteins, with the notable exception of RVFV which is not restricted by huIFITM1 (Mudhasani et al., 2013).

The evidence regarding the restriction of HIV-1 by the IFITM proteins is not as clear as the data generated for the restriction of IAV. Initial work conducted by Brass et al (2009) failed to demonstrate that the overexpression of either *IFITM1, 2* or *3* restricted HIV-1 infection (Brass et al., 2009). However, subsequent work observed that the overexpression of *IFITM2* or *3* did in fact restrict HIV-1 infection. These results were verified by the ablation of *IFITM2* or *3* expression using shRNA (Schoggins et al., 2011). Moreover, further experiments focussing on the overexpression of *IFITM* genes, showed that *IFITM1*, *2* and *3* are able to decrease HIV-1 replication whilst the overexpression of *IFITM2* and *3*, but not *IFITM1*,

inhibit HIV-1 entry (Lu et al., 2011). As well as preventing replication and/or entry, IFITM proteins are also able to directly inhibit HIV-1 protein synthesis (Chutiwitoonchai et al., 2013). Promoter sequences with rev elements have been shown to be inhibited by the IFITMs, suggesting that they are able to selectively target RNA with specific secondary structure. HIV-1 can effectively mutate away from IFITM1-mediated restriction (Ding et al., 2014). As well as restricting intracellular infection, the IFITM proteins have been found in nascent HIV-1 virions and this is thought to reduce the infectivity of these particles as the infection spreads to neighbouring cells (Tartour et al., 2014;Compton et al., 2014).

In addition to restricting enveloped viruses, IFITMs are also able to restrict two strains of non-enveloped reoviruses (Anafu et al., 2013). Reoviruses enter the cytoplasm through the endosomal pathway and escape from these endosomes by perforating the membranes. Unlike IAV, reoviruses require acid-dependent cathepsins for the removal of the outer capsid, ensuring their genome is delivered into the cytoplasm for replication (Ebert et al., 2002). Interestingly, reoviruses are able to bypass IFITM3-mediated restriction through the production of subvirion particles which do not require endosomal proteolysis for entry (Chandran and Nibert, 1998;Anafu et al., 2013). Thus, restriction of reoviruses must occur in the endosomes.

Work has also been undertaken to understand the genetic predispositions within the huIFITM locus that result in differential susceptibility to disease. It has been proposed that the single nucleotide polymorphism (SNP) rs12252-C alters the splice acceptor site of huIFITM3, truncating the protein by 21 amino acids at the N-terminus. During the 2009-2011 pandemic of pH1N1/09, genetic analysis of *IFITM3* from patients hospitalised with either seasonal or pandemic influenza viruses, was conducted. In this study, it was found that a statistically significant number of patients had an enriched minor CC genotype (SNP rs12252-C in huIFITM3) although the mechanism of the risk phenotype was unclear (Everitt

et al., 2012). Moreover, the Han-Chinese population appear to have a greater frequency of this allele within the population in comparison to a similar European cohort. Data suggests that patients who are homozygous for the rs12252-C SNP are more likely to have a poor clinical outcome when infected with seasonal IAV. In another study, patients who were homozygous for this allele experienced a more severe disease phenotype after infection with H7N9 IAV when compared to either the heterozygote or rs12252-T/T patients (Wang et al., 2014b). Further associations between the CC minor allele (rs12252-C) and the outcome of clinical disease have been observed with coronary artery lesions (Bowles et al., 2014), HIV-1 (Zhang et al., 2015) and the onset of mild clinical disease with IAV infection (Mehrbod et al., 2017). However, the evidence linking the rs12252-C allele and its association with severe clinical outcomes is contradictory, with some reports suggesting that there is no such association (or cannot be proven with such small sample sizes and low frequencies within the population), while other studies question the antiviral activity of IFITM3$^{\Delta 21}$ *in vitro* (Williams et al., 2014;Lopez-Rodriguez et al., 2016;Mills et al., 2014). More recently, data obtained from RNA sequencing experiments suggest that truncated IFITM3 transcripts cannot be detected under mock conditions or during viral infection with pdm2009 H1N1 or non-replicative H7N1. However, full length IFITM3 mRNA transcripts are detected regardless of whether the individual was heterozygous, homozygous for the rs12252-C allele or have the wildtype IFITM genotype (Makvandi-Nejad et al., 2018). This work suggests that the association between the prevalence of the rs12252-C SNP (within huIFITM3) and the outcome of clinical disease is complex and may be difficult to conclusively demonstrate.

Up until 2016 it was thought that alphaviruses were not sensitive to IFITM restriction, however it has now been shown that Sindbis and Semliki Forest virus (SFV) are both sensitive to restriction by *IFITM3* and to a lesser extent *IFITM2*, but not *IFITM1* (Poddar et al., 2016;Weston et al., 2016). There are still a number of different viruses that are not

thought to be restricted by the IFITM proteins; namely murine leukemia virus (MLV) and every arenavirus tested, including LASV and MACV (Diamond and Farzan, 2013).

1.7 Avian IFITMs

In comparison to mammalian IFITMs, very little research has been conducted on avian IFITMs. Thus, big gaps exist in our knowledge of chIFITM-mediated restriction, their localisation and functional motifs/residues that are important in mediating this effect. Moreover, apart from chickens and ducks, there are no studies that investigate avian specific restriction of viruses and therefore our knowledge in this area is severely lacking. One of the problems facing researchers in this field is the incomplete genome build of many avian species, however, the IFITM locus in chickens has been resolved and there is now a contiguous sequence which will aid further research (Bassano et al., 2017).

Research has been conducted by two groups which aim to investigate the localisation of the chicken and duck IFITMs *in vitro.* In one study, Smith et al, (2013) showed that chIFITM1 and 2 localised at the plasma membrane, while chIFITM3 localised at the endosomes (Smith et al., 2013). The localisation of chIFITMs in this study was broadly similar to those reported for huIFITMs, with the notable exception of chIFITM2 that appears to localise at the plasma membrane and not at intracellular compartments. In the study focussing on the localisation of duck IFITMs (dIFITMs), Blyth et al (2016) observed that dIFITM1 and 3 localise to similar compartments as their mammalian counterparts, namely the plasma membrane and late endosomes, respectively. The localisation of dIFITM2 and 5 was less certain with only partial co-localisation observed at the endosomes. It is possible that the localisation of these two proteins has not been fully resolved and it would be useful to further investigate the localisation of avian IFITMs in other cell lines and tissues. In addition, there is currently no information available on the membrane topology or mechanism of restriction for the

chIFITMs. Moreover, it is known that the amino acid homology between human and chicken IFITMs is low, reaching only 36% for IFITM3. This makes inferring membrane topology and function difficult as it is not possible to simply use the huIFITMs for comparison. The CD225 domain within all IFITM sequences is well conserved across species and this could suggest that this region is essential for function.

Smith *et al.* conducted the very first experiments into chicken, indeed avian, IFITM-mediated viral restriction. In these experiments the authors examined the responsiveness of DF-1 cells to IFNα and γ and found that there was a modest induction in *chIFITM3* expression after treatment with IFNα (2.5 fold higher than control) with no induction observed with IFNγ treatment (Smith et al., 2013). Furthermore, they utilised a human cell line (A549) stably expressing *chIFITM2* or *3* alongside DF-1 cells either transiently overexpressing *chIFITM3* or treated with a siRNA against *chIFITM3* (which ablated endogenous expression). Using lentiviral vectors pseudotyped with the Lagos bat virus (LBV), rabies virus (RABV) or influenza (H1 [human], H5 [human], H7 [bird], or H10 [bird]) glycoproteins, they assessed percentage infection by FACS or viral titres by plaque assay titration (Smith et al., 2013). In brief, they found that cells stably expressing *chIFITM2* or *3* were resistant to infection with all of the pseudotyped viruses as measured by GFP expression. Moreover, DF-1 cells depleted of *chIFITM3* through siRNA transfection were more permissive to infection with WSN/33. In contrast, cells transiently overexpressing chIFITM3 were more refractory to infection with IAV (not pseudotyped). A second study primarily focussing on *chIFITM10* induction in CEF cells observed that after treatment with IFNα, there was an increase in *chIFITM2* (used as the positive control) expression but no significant upregulation in *chIFITM10* expression (Okuzaki et al., 2017). In addition, they found that *chIFITM10* was able to restrict both infection and fusion of VSV-G when overexpressed in HeLa cells. It has also been shown that chIFITM3 is able to restrict

pseudotyped VLPs that have the surface glycoproteins of either avian sarcoma and leukosis virus (ASLV), VSV or IAV. In these experiments the authors measure fusion via the BlaM assay (Desai et al., 2017). This work showed that *chIFITM3* was able to potently restrict all of these viruses *in vitro* and that the pH of fusion does not appear to have a significant effect on restriction. Work has also been performed examining the role of chIFITM-mediated restriction of the Avian Tembusu Virus (ATMUV) (Chen et al., 2017). In this study, they found that *chIFITM1, 2* and *3* were upregulated in DF-1 cells that were either pre-treated with IFNα or infected with ATMUV. Moreover, ablation of *chIFITM1* and *chIFITM3* expression promotes ATMUV replication in DF-1 cells as measured by $TCID_{50}$. Conversely, when *chIFITM1* and *3* were transiently overexpressed in DF-1 cells the authors noticed a significant decrease in viral titre and this could also be replicated using *dIFITM1* or *3*. Another study examined *chIFITM* and *dIFITM* expression in lung samples infected with a high pathogenicity avian influenza (HPAI) (H5N1) and found that the *chIFITMs* were only modestly upregulated in comparison with the corresponding *dIFITMs* (Smith et al., 2015). It is unclear whether the magnitude of upregulation plays a significant role in restriction or whether different strains of IAV may differentially upregulate both chicken and duck *IFITMs*. To date, there has only been one publication demonstrating the functional restriction of IAV by *dIFITM3* (Blyth et al., 2016) where they show that the overexpression of *dIFITM3*, but not *dIFITM1* or *2*, reduces the percentage of IAV-infected DF-1 cells *in vitro*. In contrast to mammalian *IFITM3*, neither *dIFITM1*, *2* or *3* are able to restrict rVSV-GFP-infected DF-1 cells *in vitro* (Brass et al., 2009;Weidner et al., 2010b;Jia et al., 2012;Jia et al., 2014;Amini-Bavil-Olyaee et al., 2013;Marini et al., 2014). The authors also found that the endosomal localisation motif (YEML) found in the N-terminus of *IFITM3* is dispensable in ducks for localisation and function. In contrast, a chimeric dIFITM1 containing the N-terminus of dIFITM3 was localised to the endosomes and its antiviral activities were

increased in comparison to the wildtype dIFITM1. This may suggest that the N-terminus of dIFITM3 is responsible for its antiviral activity.

1.8 Aims and Objectives

The main aims of this project were to investigate the architecture of the chIFITM locus, examine the expression of the *chIFITM* genes and to elucidate which viruses are restricted by *chIFITM* expression. A series of objectives were established to achieve this aim.

Objective 1

Re-sequence the chIFITM locus of the *Gallus gallus* reference alongside avian cell lines.

Objective 2

Examine the constitutive transcriptional profile and localisation of the *chIFITMs* in avian cells.

Objective 3

Investigate the transcriptional profile of the *chIFITMs* in response to a exogenous type I and II IFNs, poly(I:C) or viral infection.

Objective 4

Determine which avian viral pathogens are sensitive to chIFITM-mediated restriction.

Objective 5

Examine which regions or specific amino acids are necessary for the antiviral activity of chIFITM3.

Objective 6

The final objective was to utilise mass spectrometry to determine any cellular proteins that interact with chIFITM1, 2 or 3 that may allude to function.

Chapter 2

Materials and Methods

2.1 Materials

2.1.1 Suppliers of general reagents

General purpose reagents were supplied by Life Technologies, New England Biolabs, Fisher Scientific, Invitrogen and Sigma. The Pirbright Institute Central Services Unit (CSU) made and supplied phosphate buffered saline (PBS) and double distilled water (ddH_2O). Other reagents and their corresponding suppliers are listed below.

Agarose for electrophoresis	Invitrogen
Agar for plaque assay titration	Thermo Scientific
DNA blood and tissue extraction kit	Qiagen
DNA molecular weight markers	Invitrogen
DNA plasmid miniprep kit	Qiagen
DNA plasmid maxiprep kit	Qiagen
HiPerfect	Qiagen
Lipofectamine 2000	Invitrogen
Lipopolysacchride (LPS)	Sigma
Luciferase assays	Promega
PCR purification kit	Qiagen
Polyacrylamide gels	Bio-Rad
Polyinosinic:polycytidylic acid (poly I:C)	InVivoGen
Protein molecular weight markers	Bio-Rad
Quantitative RT-PCR system	Life Technologies
RNA extraction kit	Qiagen
Tris-acetate-EDTA	Thermo Fisher
Tris/Borate/EDTA (TBE) buffer	Thermo Fisher

Trizol Reagent	Invitrogen
Western blot transfer kit	Bio-Rad

2.1.2 Enzymes

The following enzymes were supplied by the stated suppliers, and were used according to manufacturer's instructions unless otherwise stated:

DNase	Qiagen
DNA restriction endonucleases	New England Biolabs.
Reverse transcriptase	Invitrogen
Taq DNA polymerase	Invitrogen
Taqman fast universal PCR master mix	Applied Biosystems
T4 DNA ligase	New England Biolabs.
L-1-tosylamide-2-phenylethyl chloromethyl ketone - (TPCK) – treated bovine pancreatic trypsin	Sigma
SYBR green PCR master mix	Primer Design

2.1.3 Antibodies and dyes

Unless stated otherwise, the following antibodies were purchased from Sigma, Abcam and Thermo Fisher (Table 2.1).

Table 2.1 List of antibodies used for Western blot and Immunofluorescence

Name	Target	Application	Dilution	Source
Monoclonal anti-FLAG M2 (Ms)	FLAG tag	WB	1:1000	Sigma
Monoclonal anti-FLAG M2 (Ms)	FLAG tag	IF	1:200	Sigma
Polyclonal anti-FLAG (Rb)	FLAG tag	WB	1:1000	Sigma
Polyclonal anti-FLAG (Rb)	FLAG tag	IF	1:200	Sigma
Monoclonal anti-Xpress (Ms)	Xpress epitope	WB	1:1000	Sigma
Polyclonal anti-c-Myc (Rb)	Myc tag	WB	1:1000	Sigma
Monoclonal anti-HA (Ms)	HA tag	WB	1:1000	Millipore
Polyclonal anti-Chicken Interferon Alpha (Rb)	IFNα	WB	1:250	AbD Serotec
Monoclonal anti-β-Actin (Ms)	β-Actin	WB	1:1000	Sigma
Polyclonal anti-β-Actin (Rb)	β-Actin	WB	1:1000	Invitrogen
Monoclonal anti-Pan cadherin (Ms)	Pan cadherin	IF	1:200	Abcam
Polyclonal anti-Rab7 (Rb)	Rab7	IF	1:200	Abcam
Polyclonal anti-Lamp1 (Rb)	Lamp1	IF	1:200	Abcam
Polyclonal anti-MBP-NP (2915) (Rb)	Nucleoprotein of IAV	IF	1:200	(Noton et al.,2007)
Polyclonal anti-chIFITM1 (Rb)	chIFITM1	WB	1:250	Custom made, Genscript
Polyclonal anti-chIFITM2 (Rb)	chIFITM2	WB	1:250	Custom made, Genscript
Monoclonal anti-chIFITM3 (Ms)	chIFITM3	WB	1:250	Custom made, Abmart
Polyclonal anti-chIFITM5 (Rb)	chIFITM5	WB	1:250	Custom made, Genscript

WB – western blot; IF – Immunofluoresence; Ms – mouse; Rb - rabbit

In order to ensure that the custom made chIFITM antibodies did not cross react with one another, western blots were performed on transiently overexpressed DF-1 cell lysates. Lysates were separated by SDS-PAGE, proteins were transferred to a nitrocellulose membrane and a western blot was performed using an antibody specific to each chIFITM or against the C-terminal tag (FLAG or HA). Cellular β-actin was used as a loading control.

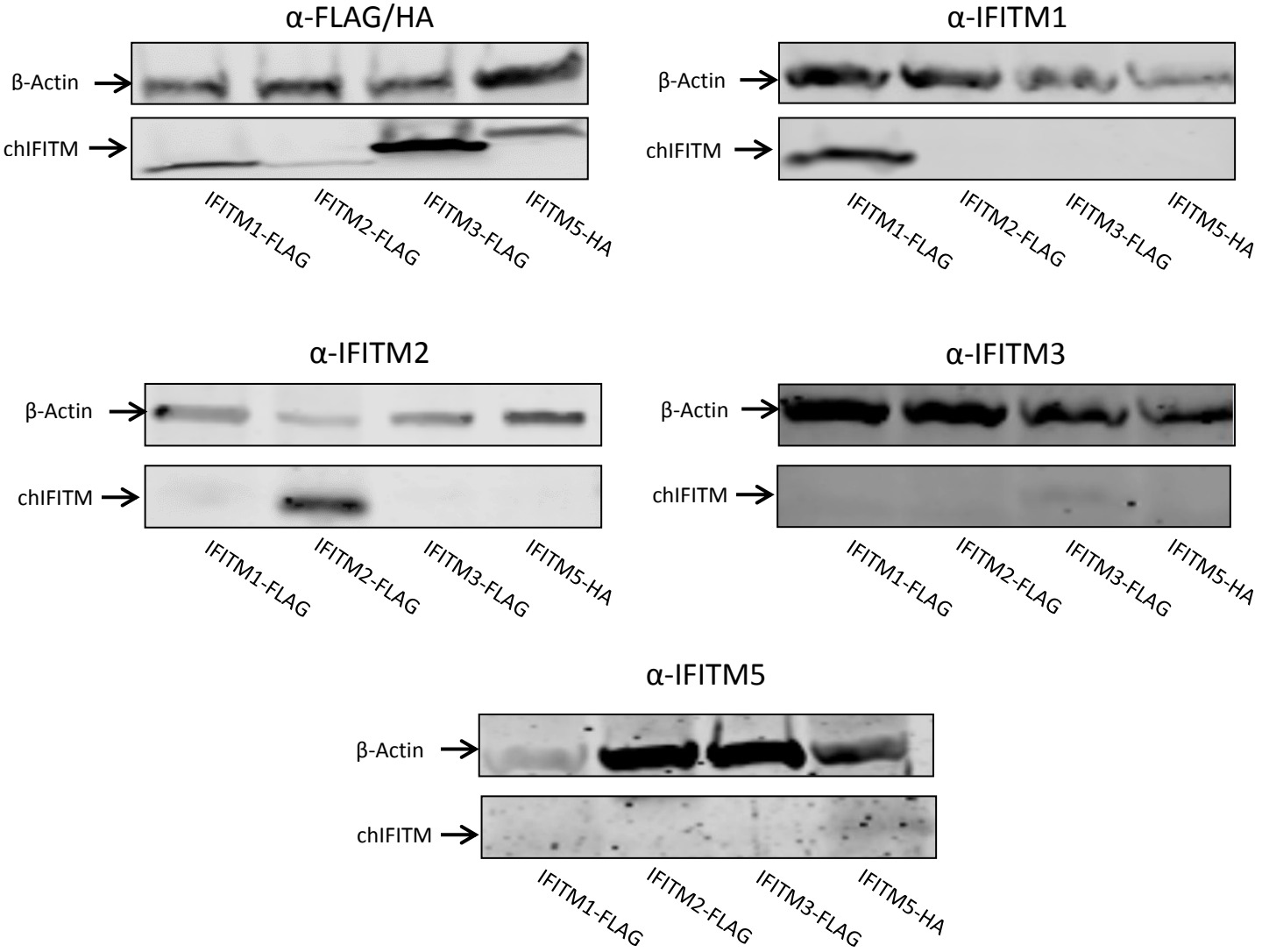
α-FLAG/HA
β-Actin
chIFITM
IFITM1-FLAG
IFITM2-FLAG
IFITM3-FLAG
IFITM5-HA
α-IFITM1
β-Actin
chIFITM
IFITM1-FLAG
IFITM2-FLAG
IFITM3-FLAG
IFITM5-HA
α-IFITM2
β-Actin
chIFITM
IFITM1-FLAG
IFITM2-FLAG
IFITM3-FLAG
IFITM5-HA
α-IFITM3
β-Actin
chIFITM
IFITM1-FLAG
IFITM2-FLAG
IFITM3-FLAG
IFITM5-HA
α-IFITM5
β-Actin
chIFITM
IFITM1-FLAG
IFITM2-FLAG
IFITM3-FLAG
IFITM5-HA

Figure 2.1 Mono and polyclonal chIFITM antibodies do not cross react with other chIFITM proteins. DF-1 cells were transfected with 1ug plasmid encoding chIFITM1, 2, 3 or 5 for 24 hours. Lysates were separated by SDS-PAGE and proteins were transferred to a nitrocellulose membrane and a western blot performed using an antibody specific to each chIFITM or against the C-terminal tag (FLAG or HA) as well as cellular β-actin.

Table 2.2 List of secondary antibodies used for western blot and Immunofluorescence

Antibody	Application	Dilution	Source
Donkey anti-Mouse IgG (H+L) Secondary Antibody, Alexa Fluor® 488 conjugate	IF	1:1000	Thermo Fisher
Donkey anti-Rabbit IgG (H+L) Secondary Antibody, Alexa Fluor® 488 conjugate	IF	1:1000	Thermo Fisher
Donkey anti-Mouse IgG (H+L) Secondary Antibody, Alexa Fluor® 568 conjugate	IF	1:1000	Thermo Fisher
Donkey anti-Rabbit IgG (H+L) Secondary Antibody, Alexa Fluor® 568 conjugate	IF	1:1000	Thermo Fisher
IRDye® 800CW Donkey anti-Rabbit IgG (H + L), 0.5 mg	WB	1:10000	Li-Cor
IRDye® 800CW Donkey anti-Mouse IgG (H + L)	WB	1:10000	Li-Cor
IRDye® 680LT Donkey anti-Mouse IgG (H + L)	WB	1:10000	Li-Cor
IRDye® 680LT Donkey anti-Rabbit IgG (H + L)	WB	1:10000	Li-Cor

WB – western blot; IF – Immunofluoresence; Ms – mouse; Rb - rabbit

Table 2.3 List of fluorescent dyes used for Immunofluorescence

Antibody	Application	Dilution	Source
4',6-Diamidino-2-Phenylindole, Dihydrochloride (DAPI)	IF	1:20000	Thermo Fisher

2.1.4 Eukaryotic cell & bacterial culture medium

2.1.4.1 Eukaryotic cells

Madin-Darby Canine Kidney Cells (MDCK)	ATCC
Human Embryonic Kidney 293T Cells (HEK 293T)	ATCC
HD11 cells	A kind gift from Prof Bernd Kaspers
DF-1 cells	ATCC
OU-2 cells	CSU

Chick Kidney (CK) cells: Primary chick cells derived from 3 week old Rhode Island Red (RIR) specific pathogen free (SPF) chicks. Briefly, the kidneys are extracted and trypsinised to release the cells, which are then are cultured.

Chicken Embryonic Fibroblasts (CEFs): Primary chick cells derived from 10 day old Rhode Island Red (RIR) specific pathogen free (SPF) embryonated hens eggs. Briefly, the embryo is decapitated, detached from the egg and the gastrointestinal tract is removed. The embryo is then homogenised and trypsinised and the resulting cells are cultured.

All primary chicken cells were prepared by the central services unit at The Pirbright Institute.

2.1.4.2 Eukaryotic cell culture

Media and additives used for culturing eukaryotic cells were purchased from the following suppliers:

Dulbecco’s Modified Eagle Medium (DMEM)	Life Technologies
Roswell Park Memorial Institute medium (RPMI-1640)	Life Technologies
Eagle's Minimum Essential Medium (EMEM)	Life Technologies

Fetal bovine serum (FBS)	Life Technologies
Chicken serum (CS)	Life Technologies
Penicillin/streptomycin	Life Technologies
Zeocin	Life Technologies
0.25% Trypsin-EDTA	Life Technologies
Opti-MEM	Life Technologies
Calcium/magnesium-free phosphate buffered saline	CSU
Tryptose phosphate broth (TPB)	Life Technologies

2.1.4.3 Bacterial culture

Media and additives used for culturing bacterial cells were purchased from the following suppliers:

Luria broth	Life Technologies
LB agar	CSU
Ampicillin sodium salt used at 100µg/µl	Sigma
Kanamycin sulfate salt used at 50µg/µl	Sigma

2.1.5 Western blotting

Lysis buffer (Laemmli's 2x sample buffer)	65.8mM Tris-HCL (pH 6.8), 26.3% (w/v) glycerol, 2.1% SDS, 0.01% bromophenol blue, 5% β-mercaptoethanol
SDS-PAGE running buffer	25mM Tris, 192mM glycine, 0.1% (w/v) SDS.
Tris-Glycine transfer buffer	25mM Tris, 192mM glycine, 20% (v/v) methanol

Blocking solution	PBS/5% (w/v) skimmed milk
Antibody binding solution	PBS/0.1% (v/v) Tween20, 5% (w/v) skimmed milk
Wash buffer	PBS/0.1% (v/v) Tween20

2.1.6 Immunofluorescence

Fixing solution	H_2O/4% (v/v) paraformaldehyde (PFA)
Permeabilisation solution	PBS/1% (w/v) saponin
Blocking solution	PBS/1% (w/v) bovine serum albumin (BSA)
Wash solution	PBS

2.1.7 Protein pulldown buffers

FLAG® Immunoprecipitation Kit (Sigma-Aldrich)

Lysis buffer	50mM Tris HCl, pH 7.4, with 150mM NaCl, 1mM EDTA, and 1% TRITON® X-100
10x wash buffer	0.5M Tris HCl, pH 7.4, with 1.5M NaCl

2.1.8 Agarose gel electrophoresis

TAE running buffer	40mM Tris, 20mM acetic acid, 1mM EDTA.
TBE running buffer	89mM Tris-borate and 2mM EDTA, pH 8.3
6x DNA loading dye	10mM Tris-HCl (pH 7.6) 0.03% bromophenol blue, 0.03% xylene cyanol FF, 60% glycerol 60mM EDTA.
SYBR™ Safe DNA Gel Stain	0.5X, 45mM Tris-borate, 1mM EDTA, pH ~8.3 (TBE) 1X, 40mM Tris-acetate, 1mM EDTA, pH ~8.3 (TAE)

2.1.9 Plasmids

Table 2.4 List of plasmids

Name	Description	Source
pEGFP-N1	Constitutively expresses eGFP under control of CMV promoter. MCS upstream allows opportunity to clone C-terminally tagged proteins.	Clontech
pcDNA3.1	Mammalian expression vector under the control of a CMV promoter for high level expression.	Invitrogen
pcDNA4myc/HIS B	Under the control of a CMV promoter with a zeocin selection marker suitable for the creation of stably-expressing cell lines.	Invitrogen
pGEM-T	Under the control of T7 and SP6 RNA polymerase promoters with a region encoding for β-galactosidase.	Promega
pFLAG-CMV-1	Mammalian expression vector under the control of a CMV promoter for high level expression.	Sigma
pGL3-P-chMx-luc	Firefly luciferase under control of chicken Mx promoter.	Gift from Prof Steve Goodbourn[a]
pGL3-P-chIFN-β-luc	Firefly luciferase under control of chicken IFNβ promoter.	Gift from Prof Steve Goodbourn[a]
pcDNA3-SHK-Mx1	Mx expression vector under the control of a CMV promoter.	Gift from Dr Laurence Tiley[b]
pGEM-chIFITM1	Untagged vector used for chIFITM1 standard curve in RT-qPCR.	
pGEM-chIFITM2	Untagged vector used for chIFITM2 standard curve in RT-qPCR.	
pGEM-chIFITM3	Untagged vector used for chIFITM3 standard curve in RT-qPCR.	
pGEM-chIFITM5	Untagged vector used for chIFITM5 standard curve in RT-qPCR.	
pBNHA-chIFITM5	Lentiviral vector with a C-terminal HA tag under the control of a SFFV promoter. For expression of chIFITM5	Gift from Dr Sarah Smith[c]
pFLAG-IFITM1	chIFITM1 expression vector under the control of a CMV promoter with a C-terminal FLAG tag.	
pFLAG-IFITM2	chIFITM2 expression vector under the control of a CMV promoter with a C-terminal FLAG tag.	
pFLAG-IFITM3	chIFITM3 expression vector under the control of a CMV promoter with a C-terminal FLAG tag.	
pFLAG-IFITM3.1	Alanine scanning mutant of the chIFITM3 expression vector under the control of a CMV promoter with a C-terminal FLAG tag.	

pFLAG-IFITM3.2	Alanine scanning mutant of the chIFITM3 expression vector under the control of a CMV promoter with a C-terminal FLAG tag.
pFLAG-IFITM3.3	Alanine scanning mutant of the chIFITM3 expression vector under the control of a CMV promoter with a C-terminal FLAG tag.
pFLA-IFITM3.4	Alanine scanning mutant of the chIFITM3 expression vector under the control of a CMV promoter with a C-terminal FLAG tag.
pFLAG-IFITM3.5	Alanine scanning mutant of the chIFITM3 expression vector under the control of a CMV promoter with a C-terminal FLAG tag.
pFLAG-IFITM3.6	Alanine scanning mutant of the chIFITM3 expression vector under the control of a CMV promoter with a C-terminal FLAG tag.
pFLAG-IFITM3.7	Alanine scanning mutant of the chIFITM3 expression vector under the control of a CMV promoter with a C-terminal FLAG tag.
pFLAG-IFITM3.8	Alanine scanning mutant of the chIFITM3 expression vector under the control of a CMV promoter with a C-terminal FLAG tag.
pFLAG-IFITM3.9	Alanine scanning mutant of the chIFITM3 expression vector under the control of a CMV promoter with a C-terminal FLAG tag.
pFLAG-IFITM3.10	Alanine scanning mutant of the chIFITM3 expression vector under the control of a CMV promoter with a C-terminal FLAG tag.
pFLAG-IFITM3.11	Alanine scanning mutant of the chIFITM3 expression vector under the control of a CMV promoter with a C-terminal FLAG tag.
pFLAG-IFITM3.12	Alanine scanning mutant of the chIFITM3 expression vector under the control of a CMV promoter with a C-terminal FLAG tag.
pFLAG-IFITM3.13	Alanine scanning mutant of the chIFITM3 expression vector under the control of a CMV promoter with a C-terminal FLAG tag.
pFLAG-IFITM3.14	Alanine scanning mutant of the chIFITM3 expression vector under the control of a CMV promoter with a C-terminal FLAG tag.
pFLAG-SCD-MYC	SCD expression vector under the control of a CMV promoter with a C-terminal MYC tag.
pFLAG-SOAT1-MYC	SOAT1 expression vector under the control of a CMV promoter with a C-terminal MYC tag.
pFLAG-STAT3-MYC	STAT3 expression vector under the control of a CMV promoter with a C-terminal MYC tag.

[a] St George's, University of London, Cranmer Terrace, London, SW17 0RE, UK.
[b] University of Cambridge, Department of Veterinary Medicine, Madingley Road, Cambridge CB3 0ES, UK.
[c] Wellcome Trust Sanger Institute, Hinxton, CB10 1SA, UK.

2.1.10 Viruses

2.1.10.1 IAV

A/Chicken/Pakistan/UDL-01/08 (H9N2)

A/duck/Ukraine/63 (H3N8)

A/duck/Sing-Q/119/97 (H5N3)

2.1.10.2 IBV

M41-CK: Pathogenic strain of IBV that has been adapted to grow in CK cell cultures.

Beau-R: The molecular clone of Beaudette-CK (Beau-CK) that has been adapted to grow in a range of cell types by serial passage in embryonated hen's eggs.

QX: D388, sourced from the Netherlands (GD Animal Health).

2.1.10.3 HVT

FC126: This virus was obtained from the Avian Disease and Oncology Laboratory (ADOL) East Lansing, MI, USA.

2.1.11 Oligonucleotides

DNA oligonucleotides were synthesised by and purchased from Sigma or invitrogen.

Table 2.5 Primers for pGEM-chIFITM cloning

Primer	Sequence (5' to 3')	Description
IFITM1 Forward	ACAGCTGCCCTCCAGCACCAT	Cloning of chIFITM1 into pGEM-T
IFITM1 Reverse	TAGAATGGGGAAGAAGCTTTA	
IFITM2 Forward	ATGAAGCCGCAACAGGCGGAGG	Cloning of chIFITM2 into pGEM-T
IFITM2 Reverse	CTATCTGCTGATCGCGGTGAT	
IFITM3 Forward	CACCGGGCTGCGGGGAAACGAA	Cloning of chIFITM3 into pGEM-T
IFITM3 Reverse	GTGGGACAAAAGTGAAAGATACC	
IFITM5 Forward	GCTGGGGGAAGGAGAAAC	Cloning of chIFITM5 into pGEM-T
IFITM5 Reverse	TTCGAGATGGGTGAGATGATTT	

Table 2.6 Primers for chIFITM-FLAG cloning

Primer	Sequence (5' to 3')	Description
IFITM1-FLAG Forward	CTCGGATCCATGCAGAGCTACCCCCA	Cloning of chIFITM1 into pFLAG_CMV1
IFITM1-FLAG Reverse	ATAAGCGGCCGCCTACTACTTGTCGTC ATCGTCTTTGTAGTCAGGCCGCACTGT GTACAGGGGC	
IFITM2-FLAG Forward	CTCGGATCCATGAAGCCCCAGCA	Cloning of chIFITM2 into pFLAG_CMV1
IFITM2-FLAG Reverse	ATAAGCGGCCGCCTACTACTTGTCGTC ATCGTCTTTGTAGTCTCTGCTGATGGC GGTGATGAAC	
IFITM3-FLAG Forward	CTCGGATCCATGGAAAGAGTGC	Cloning of chIFITM3 into pFLAG_CMV1
IFITM3-FLAG Reverse	ATAAGCGGCCGCCTACTACTTGTCGTC ATCGTCTTTGTAGTCTGTAGGTCCGAT GAACTCGGGG	
IFITM3^{MUT}-FLAG Forward	GCCAACGTCGCCTGCCTCGGCTTC	SDM of chIFITM3 (C71/72A)
IFITM3^{MUT}-FLAG Reverse	GAAGCCGAGGCAGGCGACGTTGGC	

Table 2.7 Primers and probes for house-keeping genes (RT-qPCR)

Gene	Full name	Forward Primer	Reverse Primer	Probe
β2M	Beta-2-microglobulin	AAGGAGCCCGCAGGTCTAC	CTTGCTCTTTGCCGTCATAC	(FAM)CCGGGATGAGCACGGTCTGAAGAAT(TAMRA)
β-Actin	Beta Actin	CAGGTCATCACCATTGGCAAT	GCATACAGATCCTTACGGATATCCA	(FAM) CACAGGACTCCATACCCAAGAAAGATGGC(TAMRA)
PLA2	Phospholipase A2 group IV A	GCACAAGACATTTGGCAGTTGT	TGTGACATTTGTGGCTTTCCTTA	(FAM)CAACACATTGTGGTGGAACACCAGTACTCA(TAMRA)
RPL13	Ribosomal protein L13	TCGTGCTGGCAGAGGATTC	TCGTCCGAGCAAACCTTTTG	(FAM)TAATGCCCGCCAGTTTAAGCTCTTCTAGGC(TAMRA)
RPLPO	Ribosomal phosphoprotein PO	TTGGGCATCACCACAAAGATT	CCCACTTTGTCTCCGGTCTTAA	(FAM)CATCACTCAGAATTTCAATGGTCCCTCGGG(TAMRA)
TBP	TATA box binding protein	CTTCGTGCCCGAAATGCT	GCGCAGTAGTAACGTGGTTCTCTT	(FAM)CTCATAATAACAGCAGCAAAACGCTTGGA(TAMRA)

Primers were used at a final concentration of 0.5µM and probes at 50nM.

Table 2.8 Primers and probes for targets of interest (RT-qPCR)

Gene	Full name	Forward Primer	Reverse Primer	Probe
IFITM1	Interferon-inducible transmembrane protein 1	TGTGCTCTCTCATACTCCATCA	TCTTCGCTGTCCTCCCATAG	(FAM)CCTACGAAGTCCTTGGCGATGATCCTATCC(MGB)
IFITM2	Interferon-inducible transmembrane protein 2	GCTTCGCTCTCGCCTACC	CAGTCGCGGGCCTTGAT	(FAM)TGCTTCTGCTTCCCCTCGCTCATCTT(MGB)
IFITM3	Interferon-inducible transmembrane protein 3	TCTTCTCCGTGAAGTCCAGG	GGCGATGATGAGGATGATGAG	(FAM)ATGGCTCCACTGCGAAGTACCTGAACA(MGB)
IFITM5	Interferon-inducible transmembrane protein 5	CACAAGCGGGACTCATCTCC	CCGGTCCCGTGCCTTGA	(FAM)CACCATCTACATGAACTTCTGCTGCCTCGG(MGB)
IFITM10	Interferon-inducible transmembrane protein 10	CAGGCAAGCGTACTCTTCCT	CTCCGTCTCTTTTCCTCCCAA	(FAM)ACCCTTTCCTACAGCAGCACGTACTGGTT(MGB)
Mx	Myxovirus Resistance	TTACTCGCTGTCCTCTGGAAC	TTCTTATTGCTTTCTTCACCTCTGA	(FAM)ACCCCTTTCCATTCCTGCGGAGCTGTC(MGB)
IL-6	Interleukin 6	AACATGCGTCAGCTCCTGAAT	TCTGCTAGGAACTTCTCCATTGAA	(FAM)AGCAGCACCTCCCTCAAGGCACC(TAMRA)

IL-6 primers were used at a final concentration of 0.5µM and probes at 50nM. The IFITM and Mx assays were designed by Primer Design and final concentrations are proprietary

Table 2.9 Primers and probes for viral quantification (RT-qPCR)

Gene	Full name	Forward Primer	Reverse Primer	Probe
M gene	Matrix gene of IAV	AGATGAGTCTTCTAACCGAGGTCG	TGCAAAAACATCTTCAAGTCTCTG	(FAM)TCAGGCCCCCTCAAAGCCGA(TAMRA)
N message	N message of IBV	GCTTTTGAGCCTAGCGTT	TTGTCCCGCGTGACCTCTC	(FAM)ACAAAGCAGGACAAGCA(TAMRA)

Table 2.10 Sequencing primers

Gene	Full name	Primer
CMV Forward	Cytomegalovirus	CGCAAATGGGCGGTAGGCGTG
T7 Forward	T7 RNA polymerase	TAATACGACTCACTATAGGG
PR8 Seq M Forward	PR8 M segment	ATGGTCTTCTAACCGACGTCG
PR8 Seq M Reverse	PR8 M segment	TAGTTTTTTACTCCAGCTCTATG

2.1.12 Drugs

Ampicillin sodium salt used at 100µg/µl	CSU
Kanamycin sulfate salt used at 50µg/µl	CSU
Chicken recombinant IFNα	AbD Serotec
Chicken IFNβ	Mohammad Munir (The Pirbright Institute)
Chicken IFNγ	Lonneke Vervelde (The Roslin Institute)
Polyinosinic-polycytidylic acid (PolyI:C)	Invivogen

2.2 Methods

2.2.1 Ethics Statement

All *in vivo* animal work was approved and regulated by the UK government Home Office under the project licence (PPL 30/2952). All personnel involved in the procedures were licensed by the UK Home Office under the 'Animals (scientific procedures) Act 1986'. Euthanasia of chickens was carried out by intravenous administration of sodium pentobarbital and confirmed through cervical dislocation.

2.2.2 Recombinant DNA Techniques

2.2.2.1 DNA extraction from cells

Cell were dissociated from the flask using a 0.25% trypsin-EDTA solution (life technologies), centrifuged at 1000rpm for 5 minutes and resuspended in 200µl of PBS containing proteinase K. Total DNA was extracted using the DNeasy® Blood & Tissue kit (Qiagen) according to the manufacturer's protocol. The DNA was eluted in 100µl of sterile DNase-free water and was stored at -20 °C. DNA quantified was performed using a Nanodrop Lite (ThermoFisher) and the 2200 TapeStation (Agilent).

2.2.2.1.1 BAC preparation for sequencing

The BAC clone was delivered as a stab culture and single colonies were isolated by streaking directly on Luria Broth (LB) agar (chloramphenicol 12.5 µg/mL). After incubating the plates overnight, single colonies were picked and the LB media was inoculated and then incubated overnight at the designated growth temperature. Plasmid DNA was then extracted and purified using a Qiagen Plasmid DNA kit and following the manufacturer's protocol. The resulting plasmid DNA (3µg) was sent to The Wellcome Trust Sanger Institute for sequencing using two NGS technology platforms, the Illumina MiSeq and PacBio RSII.

2.2.2.2 Primers and DNA fragments

The primers used for cloning are outlined in Tables 2.5 and 2.6. Where cloning primers are not listed, DNA fragments were synthesised by GeneArt (Invitrogen).

2.2.2.3 Polymerase chain reaction

End-point polymerase chain reaction (PCR) was performed using GoTaq DNA polymerase. Briefly, 1x GoTaq Reaction Buffer alongside 0.5µM of forward and reverse primers, 1.25U

GoTaq DNA polymerase and 0.2mM dNTPs (Promega) were added to a final volume of 20µl. The PCR was run according to the following cycling conditions: 95°C for 5 mins, 30 cycles of [95°C for 1 min, 50°C for 1 min, 72°C for 1 min/kb] then 75°C for 15 mins.

2.2.2.4 Site-directed mutagenesis

Site-directed mutagenesis (SDM) was performed using the QuikChange II Site-Directed Mutagenesis Kit (Agilent) as per the manufacturer's instructions. In brief, 125ng of each primer, 100mM of the dNTP mix, 50ng DNA template, 1x PfuUltra II reaction buffer and 1µl of PfuUltra II are added to a final volume of 50µl. The PCR was run according to the following cycling conditions: 95 °C for 30 sec, 16 cycles of [95 °C for 30 sec, 55 °C for 1 min, 68 °C for 1 min/kb] followed by 2 mins on ice. To digest methylated DNA, 1µl of the restriction enzyme DpnI (NEB) was added and the reaction was incubated at 37 °C for 2 hours.

2.2.2.5 Agarose gel electrophoresis

To visualise samples, 6x sample buffer was added to PCR products and these were loaded into wells alongside 5µl of 1 Kb DNA Ladder (Invitrogen). Gels were run on a 1% TBE/TAE containing SYBR safe (Invitrogen) at 50 V for approximately 1 hour. Gels were then visualised using a Gel Doc EZ Gel Documentation System (BIORAD).

2.2.2.6 Restriction digests

All PCR products and their corresponding vectors were digested using *Not1* and *BamH1* in buffer 3.1 at 37°C for 1 hour. Enzymes were deactivated by heating to 50°C for 10 minutes before ligation and transformation.

2.2.2.7 Gel extraction/ PCR purification

PCR products and digested DNA fragments were purified using the QIAquick PCR

Purification Kit (Qiagen). Quantification and purity of the PCR products was calculated using the Nanodrop Lite . For purification of DNA fragments from digested plasmids, DNA was separated by gel electrophoresis in a 1% TAE/TBE gel containing SYBR Safe (ThermoFisher). DNA was extracted from exercised gel segments using the QIAquick Gel Extraction Kit (Qiagen). DNA was eluted in 20µl of RNase-free water and quantified using the Nanodrop Lite .

2.2.2.8 Ligation

Ligations were performed using T4 Ligase (NEB) according to the manufacturer's protocol. An insert: vector molar ratio of 3:1 was used, and the reaction was performed at room temperature for 10 minutes.

2.2.2.9 Transformation of *Escherichia coli*

Turbo Competent E. coli (NEB) was used for routine cloning, whilst high efficiency XL1-Blue *E. coli* (Aglient) was used for site directed mutagenesis. For transformation, 3µl of the ligation mixture made in 2.2.2.8 was added to a 50µl aliquot of competent cells. Cells were incubated on ice for 30 mins, then heat shocked for 30 seconds at 42^{o}C, and then returned to ice for 5 mins. SOC media was added to the transformation mix and this was placed in the shaking incubator at 37^{o}C, 200 revolutions per minute (RPM) for 1 hour. After 1 hour, 350µl of the transformation mix was plated onto Lysogeny broth-agar (LB-agar) plates containing ampicillin (100µg/ml) or kanamycin (50µg/ml). The plates were incubated for 16 hours at 37 °C.

Table 2.11 Reagent concentrations for Lysogeny broth

Component	Final Concentration
Bacto tryptone	1% w/v
Yeast extract	0.5% w/v
NaCl	170 mM

2.2.2.10 Bacterial propagation

Appropriate volumes of liquid LB cultures, containing ampicillin (100µg/ml) or kanamycin (50µg/ml), were incubated while shaking at 200 RPM and 37^{O}C.

2.2.2.11 Plasmid DNA Miniprep

Bacterial cultures were placed in a 1ml eppendorf and centrifuged at 13,000 rpm for 5 minutes to pellet the bacteria. Plasmids were then purified using the Plasmid Miniprep Kit (Qiagen) according to manufacturer's instructions. Plasmids were eluted in 30µl of sterile RNase-free water. Plasmids were then sequenced by Sanger sequencing (Source Bioscience).

2.2.2.11 Plasmid DNA Maxiprep

After sequence conformation, 1ml of the plasmid positive LB culture was transferred to 100 ml of LB containing either ampicillin (100µg/ml) or kanamycin (50µg/ml) and incubated overnight in a shaker at 200 RPM and 37°C. Bacterial cultures were placed in 50 ml falcon tubes and centrifuged at 4,500 rpm for 1 hour to pellet the bacteria. Plasmids were then purified using the Plasmid Maxiprep Kit (Qiagen) according to manufacturer's instructions. Plasmids were eluted in 100µl of sterile RNase-free water. Plasmids were then sequenced by Sanger sequencing (Source Bioscience).

2.2.2.13 Sequencing

Plasmids were sent to Source Bioscience for sequencing by Sanger sequencing. Primers for sequencing of plasmids were provided by Source Bioscience. If custom primers were required, these were sent as per the sequencing specifications. The sequences of primers are shown in Table 2.9.

2.2.3 Cell Culture Methods

2.2.3.1 Eukaryotic cell culture media

All cell culture techniques were performed in a class II cabinet, unless otherwise stated.

Table 2.12 Components of cell culture medium

Name	Composition	Application
Complete Media	Dulbecco's Modified Eagle's Medium 10% heat inactivated Foetal Bovine Serum	Routine cell culture
Selection Media for Stably-Expressing DF-1 cells	Dulbecco's Modified Eagle's Medium 10% heat inactivated Foetal Bovine Serum 100µg/ml Zeocin	Culturing chIFITM stably-expressing DF-1 cells
CEF Media	Eagle's Minimum Essential Medium 0.35% Bovine Serum Albumin 1x Penicillin-Streptomycin 0.25µg/ml TPCK treated trypsin	Culturing CEFs
CKC Media	1x Eagle's Minimum Essential Medium 10% TPB 0.2% BSA 20mM N, N bis(2-hydroxemethyl)-2-aminoethanesulfonic acids (BES) (Sigma) 0.4% sodium bicarbonate 2mM L-Glutamine 250U Nystatin 100U Penicillin/Streptomycin	Culturing CKCs
HD11 Media	RPMI-1640 2.8% heat inactivated Foetal Bovine Serum 2.8% chicken serum 10% TPB	Culturing HD11 cells
OU-2 Media	EMEM	Culturing OU-2 cells

	6% heat inactivated Foetal Bovine Serum 2% chicken serum 12% TPB	
IAV Plaque Assay Overlay Media	0.6% agarose (Oxoid) Eagle's Minimum Essential Medium 0.21% Bovine Serum Albumin 1 mM L-Glutamate 0.15% Sodium Bicarbonate 10mM Hepes 1x Penicillin-Streptomycin 0.01% Dextran DEAE 2µg/ml TPCK treated trypsin	Titration of influenza virus by plaque assay
IBV Plaque Assay Overlay Media	2x Eagle's Minimum Essential Medium 20% TPB 0.4% BSA 40 mM N, N bis(2-hydroxemethyl)-2-aminoethanesulfonic acids (BES) (Sigma) 0.8% sodium bicarbonate 4mM L-Glutamine 500U Nystatin 200U Penicillin/Streptomycin	Titration of infectious bronchitis virus by plaque assay

2.2.3.2 General cell culture protocols

Chicken macrophage-like HD11 cells (CSU, The Pirbright Institute) were cultured at 41^{o}C and 5% CO_2 until confluent. Chicken embryonic fibroblast (CEF), chick kidney (CK), DF-1, canine Madin-Darby canine kidney (MDCK) (CCL-34, ATCC) and OU-2 cells (CSU, The Pirbright Institute) were cultured at 37^{o}C and 5% CO_2 until confluent. All primary, *ex vivo* cell cultures (CEF and CK cells) (Rhode Island Red) were generated at the Pirbright Institute. Continuous cell lines were routinely passaged twice weekly: cells were washed once with PBS and dissociated from the flask using a 0.25% trypsin-EDTA solution (life technologies). Cells were resuspended in complete DMEM and typically split 1 in 10. Primary cells were prepared every Friday and cells were not passaged.

2.2.3.3 Cell counting

Cells to be seeded were dissociated from the flask using a 0.25% trypsin-EDTA solution (life technologies). Cells were resuspended in complete DMEM and 10µl of the cell suspension was added into the chamber of a cell counting slide (BIORAD). The slide was inserted into the TC20 automated cell counter and the total cell population was calculated.

2.2.3.4 DNA transfection of primary and continuous cell cultures

Cells were transfected with lipofectamine 2000 reagent (Invitrogen) following the manufacturer's instructions. Transfection of primary cell cultures, namely CEFs, required a higher concentration of DNA than continuous cell cultures. The DNA:Lipofectamine ratio and volumes were scaled accordingly (4µl:1µg DNA) and the DNA:Lipofectamine complexes were diluted in Opti-MEM Reduced Serum Medium (Gibco) before being added dropwise onto the cell monolayer. Transfections were left for the time points indicated in the experimental protocol.

2.2.3.5 Generation of stably-expressing DF-1 cell lines

This work was done in collaboration with Dr Andrew Broadbent and Ms Alice Gray. Plasmids (Table 2.4) designed for stable incorporation of exogenous DNA were transfected into DF-1 cells (2.2.3.4). After 24 hours the media was aspirated from the cells, washed with PBS and replaced with complete media supplemented with 100µg/ml zeocin. Zeocin resistant DF-1 cells were further characterised.

2.2.3.6 siRNA knockdown assays

DF-1 cells were transfected with 20nM or 80nM small interfering RNA (siRNA) against *chIFITM1, 2, 3* and *5* or a non-specific siRNA (Table 2.12). Transfections were performed using HiPerFect (Qiagen) as per the manufacturer's protocol. The

siRNA:HiPerfect ratio and volumes were scaled accordingly (12µl:10nM siRNA) and the siRNA:HiPerfect complexes were diluted in Opti-MEM Reduced Serum Medium (Gibco) before being added dropwise onto the cell monolayer, 24 hours prior to infection.

Table 2.13 siRNAs used to knockdown *chIFITM* expression

Gene	siRNA	Sequence
IFITM1	1	UCAACUUUGUGCUGUGCAAUU
	2	CAGCGAAGAUCUUUAACAUUU
	3	GGAUCAUCGCCAAGGACUUUU
	4	GGGAUAGGAUCAUCGCCAAUU
IFITM2	1	GCCAAGGUGCUGAACAUCAUU
	2	GUGCUGAACAUCAUCUUCUUU
	3	CCAAGGUGCUGAACAUCAUUU
	4	GGGCCAAGGUGCUGAACAUUU
IFITM3	1	GCGAAGUACCUGAACAUCACG
IFITM5	1	UCAACACCAUCUACAUGAAUU
	2	ACACCAUCUACAUGAACUUUU
	3	GGUCCAUCUUCAACACCAUUU
	4	CCAGCGAUGACGAGGACAAUU
Negative Scramble	1	UUCUCCGAACGUGUCACGUGU

2.2.3.7 Firefly and Renilla luciferase assays

HD11 cells were transfected (2.2.2.4) and stimulated as per the experimental design. Cells were washed once with PBS and lysed in 100µl of 1 X passive lysis buffer (Promega). Plates were frozen for 30 min at -80 °C and defrosted before reading. 10µl of lysate was loaded onto a 96-well opaque white plate (Pierce) and analysed on a GloMax Multi plate reader (Promega) with 50µl of LARII and Stop and Glo reagents (Promega). Firefly luciferase signals were normalized to Renilla signals.

2.2.3.8 Chicken interferon (IFNβ) and Mx reporter assays

To determine chicken IFNβ and Mx promoter activities, pGL3 Luciferase (luc) reporter vectors containing the promoter regions from either IFNβ or Mx upstream of a Firefly luc gene, were used. In triplicate, cells were transfected with 250ng/well of pGL3-P-chIFN-β-luc or pGL3-P-chMx-luc and 100ng/well of a plasmid constitutively expressing Renilla luciferase using the method outlined in 2.2.2.4. After transfection, 2000U IFNα, 50µl of IFNβ or IFNγ cell supernatants from stably-expressing COS cells (The Pirbright and Roslin Institute's) or 500ng of HMW poly I:C were added passively to the cell culture media.

2.2.4 Virological Methods

2.2.4.1 Virus propagation in embryonated hen's eggs

Embryonated chicken eggs (VALO GmB) were incubated at 37°C, 40-50% humidity, for 10 days after which they were candled to check viability of the embryo prior to infection (this was done by animal services, The Pirbright Institute). Virus to be inoculated was diluted to 10^4 pfu/ml in PBS. The shell was sterilised with 70% (v/v) ethanol and a small hole was punctured in the egg shell just below the line of the air sac. The allantoic cavity was inoculated with 100µl of diluted virus stock and the hole was sealed using autoclave tape. The inoculated eggs were incubated at 37° C, 40-50% humidity, for 72 hours or until embryonic lethality. Eggs were culled using a schedule one method (chilling overnight at 4° C) and death was confirmed by decapitation. The allantoic fluid was harvested, centrifuged (4000 rpm, 10 min), and stored at -80°C.

2.2.4.2 Virus infection

Routinely, cells were seeded at 80-90% 1 day prior to infection. Once confluent, cells were washed once with sterile PBS to remove any residual serum. Influenza, infectious bronchitis virus or herpes virus of turkeys was diluted in an appropriate volume of serum-free media (Table 2.11). Cells were incubated at 37°C and 5% CO_2 for 1 hour, shaking every 20 minutes. The virus was removed by washing the monolayer twice with sterile PBS. An appropriate volume of maintenance media was added to the cells and infection was left for the time indicated. For multicycle infections, cells were overlaid with virus growth medium.

2.2.4.3 Titration of influenza viruses by plaque assay

Material to be assayed was 10-fold serially diluted in serum-free DMEM and used to infect MDCK cells in 12-well plates. After 1 hour of incubation, the inoculum was removed,

washed twice with sterile PBS and the cells were overlaid with the appropriate volume of overlay media containing 2% agar. After 3 days, the overlay was removed, and the cells were stained with crystal violet (Sigma) to determine the pfu/ml. All plaque assays were performed in a technical duplicate and biological triplicate, and samples re-titrated if the results were inconsistent.

2.2.4.4 Titration of infectious bronchitis viruses by plaque assay

Material to be assayed was 10-fold serially diluted in 1x BES and used to infect CK cells in 12-well plates. After 1 hour of incubation, the inoculum was removed, washed twice with sterile PBS and the cells were overlaid with the appropriate volume of 2x BES containing 2% agar. After 3 days, the overlay was removed, the cell fixed with 10% paraformaldehyde (in PBS) and the cells were stained with crystal violet to determine the pfu/ml. All plaque assays were performed in a technical duplicate and biological triplicate, and samples re-titrated if the results were inconsistent.

2.2.5 Protein Methods

2.2.5.1 Cell lysis

Cells were treated as per the experimental design. Cells were placed on ice and washed twice with ice cold PBS then lysed by adding an appropriate volume of 2x laemmli's sample buffer (containing 5% β-mercaptoethanol) or FLAG® Immunoprecipitation lysis buffer. The cells were incubated on ice for a minimum of 20 minutes to ensure complete cell lysis. Lysates were centrifuged at 13,000 rpm for 10 minutes at 4^{o}C and the supernatants were harvested and stored at -20^{o}C for future applications.

2.2.5.2 SDS- polyacrylamide gel electrophoresis (PAGE)

Cell lysates were denatured in 2x laemmli sample buffer (BIORAD) containing β-mercaptoethanol, sonicated and then heated to 100 °C for 10 minutes. Protein samples and standards were loaded into Mini-PROTEAN TGX™ Precast Gels (4-20%) (BIORAD) immersed in 1 x Tris/Glycine/SDS buffer (BIORAD). Gels were run at 80 V for approximately 90 minutes until resolved.

2.2.5.3 Western blotting

Proteins separated by SDS-PAGE were transferred to nitrocellulose membranes using the Transblot Turbo Transfer System (BIORAD). In brief, six sheets of filter paper were saturated in Semi-Dry Transfer Buffer, alongside a nitrocellulose membrane (0.2 µm) (BIORAD). The Transblot cassette was loaded as per the manufacturer's instructions, the unit sealed and run at 25 V/2.5 A for 3 min. Following transfer, membranes were incubated for 1 hour in 5% milk powder (Marvel) in PBS at R/T, then washed once in 0.1% Tween in PBS (PBS-T). The membrane was then incubated in PBS-T containing 5% milk powder and a specified amount of primary antibody (Table 2.1) for 1h at R/T and then washed 3x in PBS-T. The membrane

was then incubated in the dark in PBS-T containing 5% milk powder and an appropriate IRDye secondary antibody (Table 2.2) (LI-COR) for 1 h then rewashed as above. The membrane was finally washed once in PBS and imaged using an Odyssey CLx (LI-COR) imager. Densitometric analysis was performed using Image Studio™ Software (LI-COR), and the intensities were normalised to β-actin.

2.2.5.4 Immunohistochemistry

Cells were seeded at 1×10^5/well on coverslips in a 12-well plate 1 day prior to the experimental procedure. All steps were performer on a rocker. Cells were fixed with 500µl 4% paraformaldehyde for 10 minutes followed by permeabilisation with 0.1% saponin in PBS. Cells were blocked in 1% bovine serum albumin (BSA) for 30 minutes after which they were then incubated with a specified amount of primary antibody (Table 2.1) for 1h at R/T, and washed five times in PBS, followed by incubation with a secondary antibody conjugated to Alexa Fluor 568 or 488 (Table 2.2) (Life Technologies). After 1 hour the cells were washed five times with PBS. The nuclei of the cells were stained with DAPI (Table 2.3) and mounted onto slides with Vectashield Antifade Mounting Media (Vector Laboratories).

2.2.5.5 Immunoprecipitation

2.2.5.5.1 Cell Lysis

Cells were transfected as described in 2.2.3.4. Cells were washed twice with PBS and then 500µl of cell lysis buffer (2.1.7) containing protease inhibitor cocktail (Sigma) was added to each well of a 12 well plate. Cells were then Incubated for 15–30 minutes on a shaker to ensure complete lysis. The cell lysates were then harvested and centrifuged for 10 minutes at 13,000rpm. The supernatants were transferred to a chilled test tube and were stored at -20^{o}C if they were not being used immediately.

2.2.5.5.2 Immunoprecipitation of chIFITM-FLAG

The ANTI-FLAG M2 affinity gel was centrifuged at 5,000g for 30 seconds and was washed 3 times in IP wash buffer (2.2.5.5.1) before being incubated with the cell lysates overnight at 4 °C with regular agitation. Beads were washed three times with IP wash buffer (Table 2.1.7). Protein-antibody complexes were eluted using 100µl of 3x FLAG peptide in IP wash buffer (150ng/ml). Samples were stored at -20 °C until processing at the University of Liverpool.

2.2.5.6 Liquid Chromatography-Mass Spectrometry/Mass Spectrometry

Eluted samples were processed for LC-MS/MS analysis by Dr Stuart Armstrong (University of Liverpool) who supplied the following protocol. Samples were diluted 1:1 volume with 50mM ammonium bicarbonate (NH4HCO3). Proteins were reduced by the addition of dithiothreitol (Sigma) (3mM final) and heated at 60 °C for 10 minutes. The samples were returned to room temperature, and iodoacetamide (Sigma) (9mM final) added for 30 minutes in the dark to alkylate the proteins. Proteins were digested with 0.2µg of proteomic grade trypsin (Sigma) and left to incubate at 37 °C overnight. The resulting peptide samples were then acidified with trifluoroacetic acid (1% (v/v) final). Peptides were concentrated and desalted using C18 Stage tips (ThermoFisher Scientific) and then the samples were dried using a centrifugal vacuum concentrator (Eppendorf). Peptides were resuspended in 0.1% (v/v) trifluoroacetic acid and 5% (v/v) acetonitrile.

NanoLC MS ESI MS/MS analysis

Peptides were analysed by on-line nanoflow LC using the Ultimate 3000 nano system (Dionex/Thermo Fisher Scientific). Samples were loaded onto a trap column (Acclaim PepMap 100, 2 cm × 75 µm inner diameter, C18, 3 µm, 100 Å) at 5µl min−1 with an

aqueous solution containing 0.1%(v/v) TFA and 2%(v/v) acetonitrile. After 7 min, the trap column was set in-line an analytical column (Easy-Spray PepMap® RSLC 50 cm × 75µm inner diameter, C18, 2µm, 100Å) fused to a silica nano-electrospray emitter (Dionex). The column was operated at a constant temperature of 30°C and the LC system coupled to a Q-Exactive HF mass spectrometer (ThermoFisher). Chromatography was performed with a buffer system consisting of 0.1 % formic acid (buffer A) and 80% acetonitrile in 0.1% formic acid (buffer B). The peptides were separated by a linear gradient of 3.8 – 50% buffer B over 30 minutes at a flow rate of 300nl/min. The Q-Exactive HF was operated in data-dependent mode with survey scans acquired at a resolution of 60,000 and scan range 350-2000 m/z. Up to the top 10 most abundant isotope patterns with charge states +2 to +5 from the survey scan were selected with an isolation window of 2.0 Th and fragmented by higher energy collisional dissociation with normalized collision energies of 30. The maximum ion injection times for the survey scan and the MS/MS scans were 100 and 45ms respectively, and the ion target value was set to 3E6 for survey scans and 1E5 for the MS/MS scans. MS/MS events were acquired at a resolution of 30,000. Repetitive sequencing of peptides was minimized through dynamic exclusion of the sequenced peptides for 20s, (Tyanova et al., 2016;Cox et al., 2014).

2.2.5.6.1 LC-MS/MS analysis

MS spectra data was analysed by label-free quantification using the MaxQuant software (v 1.5.5.1, 1) and searched against a Gallus gallus protein database (Uniprot release-2017_03; 29,736 sequences) and the relevant bait protein sequences using the Andromeda search engine. The false discovery rate (FDR) was set to 0.01, and a decoy database was included in the search to help identify and remove false-positives. LFQ results were further processed with Perseus software (v 1.5.1.6, 2) to determine significance between FLAG alone compared to FLAG tagged chIFITM proteins. Statistical t-test analysis was used to

analyse intensity values. Proteins with a p-value <0.05 and a fold change >2 were considered statistically significant. Identification and statistical analysis of the mass spectrometry data were performed by Stuart Armstrong.

2.2.5.7 Co-Immunoprecipitation

Plasmids encoding the sequences of potential interacting partners were co-transfected into DF-1 cells according to section 2.2.3.4. After incubation for 24 h, cells were lysed in FLAG immunoprecipitation cell lysis buffer containing a protease inhibitor cocktail (Sigma). The cell lysates were then harvested and centrifuged for 10 minutes at 13,000rpm, after which the supernatant was collected and the cell pellet discarded. The ANTI-FLAG M2 affinity gel was centrifuged at 5,000g for 30 seconds and was washed 3 times in IP wash buffer before being incubated with the cell lysates (2.2.5.5.1) overnight at 4 °C with regular agitation. Beads were washed three times with IP wash buffer (Table 2.1.7). Protein-antibody complexes were eluted using 100µl of 3x FLAG peptide in IP was buffer (150ng/ml). Western blot analysis was then performed (2.2.5.2 – 2.2.5.3) using anti-FLAG and anti-MYC antibodies to assess possible protein-protein interactions.

2.2.6 Transcriptional Analysis

2.2.6.1 Total RNA extraction from tissues

In total, 19 tissues were removed from Rhode Island Red chickens at 3 weeks of age and immediately stored in RNA*later®* (ThermoFisher) at -80 °C. For tissue homogenisation, 100 mg of each tissue sample was placed into 350µl of RLT buffer (Qiagen) in a safelock tube containing a sterile metal bead (Qiagen). Tissues were disrupted in a bead beater until fully homogenised. Tissue debris was left to settle at room temperature for 5 mins before the liquid phase was transferred to a column from an RNeasy Mini Kit (Qiagen). The rest of the extraction was performed according to manufacturer's protocol. The RNA was eluted in 30µl RNase-free water and quantified on a NanoDrop Lite (ThermoFisher).

2.2.6.2 Total RNA extraction from cells

Cell were lysed in RLT buffer (Qiagen) containing 5% β-mercaptoethanol. Total RNA was extracted with the RNeasy Mini Kit (Qiagen) according to the manufacturer's protocol. RNAse free DNase (Qiagen) was also used according to the manufacturer's protocol. RNA was stored at -80 °C and quantified using a Nanodrop Lite (ThermoFisher).

2.2.6.3 Reverse transcription

Reverse transcription of 1µg total RNA was performed using the Superscript III Reverse Transcriptase kit (Invitrogen) according to the manufacturer's protocol using random primers (Promega). The cDNA was stored at -20°C.

2.2.6.4 Quantitative real-time PCR with SYBRgreen

Quantitative RT-PCR was performed using 2x PrecisionPlus Master Mix with ROX premixed with SYBRgreen (Primerdesign Ltd). The components for quantitative RT-PCR were added in

a 10µl reaction and the plate sealed. The thermal cycling conditions included an initial enzyme activation step at 95 °C for 2 minutes and 40 cycles at 95 °C for 5 seconds (denaturation) and 60 °C for 20 seconds (data collection step). A dissociation stage was also added for melt curve analysis.

2.2.6.5 Reference gene stability analysis by geNorm

The Ct values of each candidate reference gene across all of the samples were calculated using either the 7500 Fast Real-Time PCR Software version 2.3 (Life Technologies) or QuantStudio 5 Software v1.4.3. Raw Ct values were exported to Microsoft Excel for quality control and imported into the qbase+ real-time qPCR software version 3.0 (Biogazelle). The software, using the geNorm algorithm (Vandesompele et al., 2002), calculate the geNorm M value representing the stability of each reference genes and the geNorm V value which suggest the optimal reference gene number. All quantitative RT-PCR samples were run in technical triplicate.

2.2.6.6 Quantitative real-time PCR (TaqMan)

Quantitative RT-PCR was performed using TaqMan Universal Master Mix II, no UNG (Life Technologies). The components for quantitative RT-PCR were added in a 10µl reaction and the plate sealed. The thermal cycling conditions included an initial enzyme activation step at 95 °C for 10 minutes and 40 cycles at 95 °C for 15 seconds (denaturation) and 60 °C for 1 minute (data collection step).

2.2.6.7 Real-time quantitative PCR data analysis

The Ct values of each reference gene and gene(s) of interest, across all of the samples, were calculated using either the 7500 Fast Real-Time PCR Software version 2.3. (Life Technologies) or QuantStudio 5 Software v1.4.3. Raw Ct values were exported to Microsoft Excel for quality control and imported into the qbase+ real-time qPCR software version 3.0

(Biogazelle). Raw Ct values were normalised to those of the reference genes and the relative fold change in expression of each gene was calculated. Technical replicates were analysed, and where a difference of ≥ 0.5 cts was found, a value could be omitted from further analysis. All quantitative RT-PCR samples were run in technical triplicate.

2.2.6.8 Extraction and sequencing of viral RNA (vRNA)

Viral RNA (vRNA) was extracted from 140µl of allantoic fluid using the QIAamp Viral RNA Mini Kit (Qiagen) according to the manufacturer's instructions. Universal influenza primers and Superscript III (Invitrogen) were used to produce cDNA, according to the manufacturer's instructions (section 2.2.6.3). Segment specific primers were used in a PCR from cDNA using PfuUltra II (Aglient). PCR products were purified using agarose gel electrophoresis (section 2.2.2.5) followed by a QIAquick Gel purification Kit (Qiagen) (section 2.2.2.7). The resulting product was sequenced via Sanger sequencing (section 2.2..2.13).

2.2.7 Bioinformatic and Statistical Analysis

2.2.7.1 chIFITM amino acid alignments

The amino acid sequences of the avian IFITM proteins (1, 2, 3 and 5) were downloaded from Uniprot and saved in a word document in fasta format. Multiple sequence alignments were calculated using Clustal Omega (EMBL-EBI) using the default settings. The resulting alignment was formatted using Genedoc.

2.2.7.2 chIFITM DNA sequence alignments

Raw HiSeq DNA sequences in FastQ format were aligned to the Gallus gallus v5 reference genome using the Burrow Wheeler Aligner, BWA (v0.7.8) with the BWA-MEM alignment algorithm. Reads were then pre-processed with SAM tools v0.1.19 to convert the SAM files into BAM files and sorted. For local realignment and base quality score recalibration of the mapped reads, the tool Haplotype Caller from GATK (Genome Analysis Toolkit) v3.1 software package was applied. All tools were used with the recommended standard settings. This workflow is in accordance with the best practices from the Broad Institute. Variants were called with the tool UnifiedGenotyper from GATK. The resulting indexed BAM files were visualised using integrative genome viewer (IGV).

2.2.7.3 Modelling chIFITM protein topology

Amino acid sequences were imported into the Phyre2 software package (developed by Structural Bioinformatics Group, Imperial College, London) and protein structures were modelled using the intensive mode setting. Models are generated by PSI-BLAST searches against known homologues, secondary structure is modelled against Psi-pred and Diso-pred databases and from this data a hidden Markov model (HMM) is generated. Transmembrane helices and protein topology prediction is made by memsat-svm

2.2.7.4 Statistical analysis

All graphs were created and statistical analysis performed using GraphPad Prism 7/8 (GraphPad Software Inc). For each data set, the number of biological replicates and the type of data analysis, including the relevant key, is noted in the figure legend.

Chapter 3

Characterising the chIFITM locus

3.1 Introduction

The discovery of the human IFITM proteins occurred many decades ago, making them amongst the first ISGs to be characterised (Friedman et al., 1984). The nomenclature was initially very different to what is used currently and they were termed 9–27(IFITM1), 1-8D (IFITM2), and 1-8U (IFITM3). Further characterisation of these genes was undertaken in 1996 (Alber and Staeheli, 1996), 2003 (Zhu and Liu, 2003) and then in 2009. Two different IAV-targeting RNA interference studies identified huIFITM1, 2 and 3 as potential restriction factors against IAV (Brass et al., 2009;Shapira et al., 2009), with five similar studies published within weeks of one another. The findings published in these studies resulted in further experiments by many groups that sought to understand the mechanisms underpinning the antiviral activities of the mammalian IFITMs.

In addition, work has been undertaken to understand the genetic predispositions within the huIFITM locus that result in an increased susceptibility to disease. Specifically, the single nucleotide polymorphism (SNP) rs12252-C was proposed to alter the splice acceptor site, truncating huIFITM3 by 21 amino acids at the N-terminus. This variation has been associated with an increase in an individual's susceptibility of developing a severe Influenza A viral infection, specifically in the Han-Chinese population (Everitt et al., 2012;Zhang et al., 2013;Wang et al., 2014a;Yang et al., 2015;Pan et al., 2017;David et al., 2018). Further associations between the CC minor allele (rs12252-C) and the outcomes of clinical disease have been observed with coronary artery lesions (Bowles et al., 2014), HIV-1 (Zhang et al., 2015) and the onset of mild clinical disease with IAV infection (Mehrbod et al., 2017). However, the evidence linking the presence of the rs12252-C allele and its association with severe clinical outcomes is contradictory, with other reports suggesting that such an association does not exist (or cannot be proven with such small sample sizes and low frequencies within the population) with others questioning the antiviral activity of

IFITM3$^{\Delta 21}$ *in vitro* (Williams et al., 2014;Lopez-Rodriguez et al., 2016;Mills et al., 2014). More recently, data obtained from RNA sequencing experiments has suggested that truncated IFITM3 transcripts cannot be detected under mock conditions or during viral infection with H7N1 but full length IFITM3 mRNA transcripts are detected regardless of the genotype of the individual (Makvandi-Nejad et al., 2018). This work suggests that the association between the prevalence of the rs12252-C SNP (within IFITM3) and the outcome of clinical disease is a complex phenotype and may be difficult to conclusively demonstrate.

This level of genetic analysis has not been conducted in chickens because the chicken IFITM locus was only recently correctly annotated in the chicken genome (Bassano et al., 2017). To date, only one study has looked at basal *chIFITM* expression (excluding *chIFITM5*) in chicken tissues, highlighting variable expression between the tissues studied (Smith et al., 2013). Furthermore, work has not been undertaken to investigate the locus architecture, the variation within the locus, nor the possible interacting partners which modulate the *chIFITM* expression or its antiviral activity.

This chapter characterises the chIFITM locus and describes novel sequencing approaches of a BAC clone used in the sequencing of the reference Red Jungle fowl genome sequence, to generate an accurate, contiguous sequence for downstream applications. Constitutive levels of *chIFITM* expression were examined *in vivo* as well as in commonly used chicken cell lines. Aligning the avian IFITMs sequence against the Galgal 5 reference genome was performed in order to assess the level of sequence conservation and to identify conserved regions which may be important for viral restriction. Furthermore, the novel sequencing strategy developed by Bassano *et al.* (2017) was used to sequence three avian cell lines in order to identify genetic variation that may influence the cell line specific chIFITM-restriction. In addition, the cellular localisation of these proteins was characterised *in vitro* alongside any cellular interacting partners that may influence restriction or may control

how the genes are expressed under native conditions. Taken together, these data will allow for the characterisation of the chIFITM locus and may suggest the mechanisms underpinning chIFITM restriction.

3.2 chIFITM locus architecture

Prior to 2013, nothing was known about the chIFITM locus architecture or the gene content within this locus. Moreover, only chIFITM5 was partially annotated in the Galgal4 genome and this was because of the relatively high level of sequence homology between the chicken and human IFITM5 genes and amino acid sequences (Tables 3.1 and 3.2). The 310 million years of evolutionary distance between mammals and aves, and the constant arms race between virus and host, have resulted in low level sequence conservation between human and chicken IFITMs, with huIFITM3 and chIFITM3 sharing only 36% amino acid identity. This makes searching for orthologues difficult as they are not easily identifiable by performing BLAST searches, and this partially explains why a gap in *Gallus gallus* chromosome 5 existed for so many years. Moreover, this region is difficult to sequence using traditional sequencing methods, contributing to the lack of sequencing data available. In this chapter the chIFITM locus was characterised and further analysis was undertaken to understand the genetic diversity within the locus and the basic characteristics underpinning their mode of action.

As the IFITM genes were not annotated in the genome, bioinformatic analysis was conducted by researchers in the Genetics and Genomics group at the Pirbright Institute. The two genes flanking the putative IFITM locus in chickens are the telomeric β-1,4-N-acetyl-galactosaminyl transferase 4 (*B4GALNT4*) gene and the centromeric acid trehalase-like 1 (*ATHL1*) gene. Both of these genes are highly conserved between species, from mammals to amphibians (Smith et al., 2013). Once *B4GALNT4* and *ATHL1* had been identified on chromosome 5 of the *Gallus gallus* genome, the identification of the individual

Table 3.1: Percentage (%) identity between human and chicken IFITM DNA sequences.

	chIFITM1	chIFITM2	chIFITM3	chIFITM5
huIFITM1	47.3			
huIFITM2		41.9		
huIFITM3			50.9	
huIFITM5				67.2

Table 3.2: Percentage (%) identity between human and chicken IFITM amino acid sequences.

	chIFITM1	chIFITM2	chIFITM3	chIFITM5
huIFITM1	36.8			
huIFITM2		28		
huIFITM3			35.8	
huIFITM5				56.8

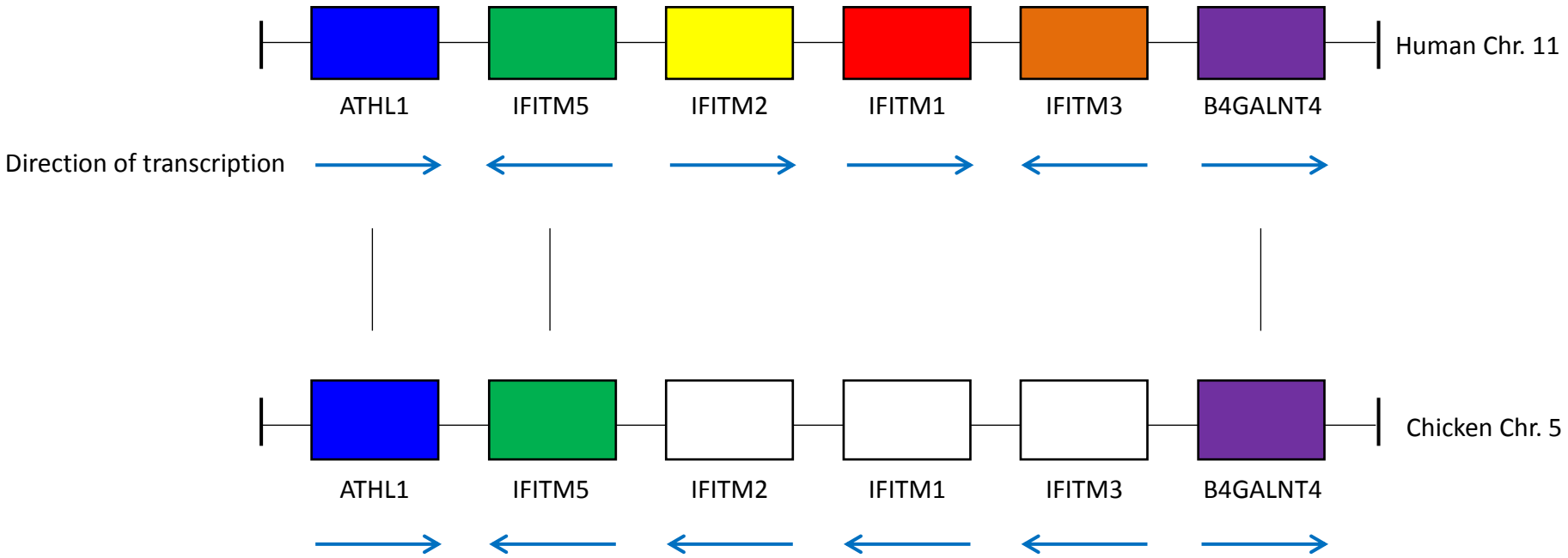

Figure 3.1 The chIFITM locus architecture. The IFITM locus on *Gallus gallus* chromosome 5 and the genes present are flanked by genes ATHL1 and B4GALNT4. This region is syntenic with the IFITM gene cluster on human chromosome 11. Note that the change in the direction of transcription of chIFITM2 and chIFITM1 makes the assignment of orthology difficult; therefore, the chicken genes are named by gene order and conservation of specific functionally defined amino acid residues. The coloured boxes and dashes denoted orthology as assigned by sequence similarity and conversation. [Taken from: (Smith et al., 2013)].

chIFITM genes were made based on the sequence conservation within the cytoplasmic intracellular loop (CIL). The sequence conservation in this region exists between the *chIFITM* genes which means that the nomenclature was predominantly based on synteny, rather than sequence data. Furthermore, due to the lack of functional data, it was not clear if the nomenclature was correct. However, without conclusive evidence demonstrating the function of the genes, this would have been entirely speculative to have altered the nomenclature and would not have added to our current understanding. The nomenclature used in this thesis represents the nomenclature presented in the schematic above (Figure 3.1) and the current annotation in NCBIv5.

The coloured blocks in the schematic denote genes annotated in the genome before 2013, and their corresponding positions within the locus, whether on the chicken or human chromosome. The gene blocks shown in white were not annotated in the genome and the names assigned to the blocks are based on synteny. The direction of transcription is in a different orientation for *chIFITM1* and *2*, indicating gene transversion, which further complicates the nomenclature and assigning orthology. In fact, it is still not clear if *chIFITM1, 2* and *3* are correctly named and this is primarily because of the low sequence identity between mammalian and avian genes. Drawing conclusions remains challenging and is further complicated by the 21 amino acid truncation of chIFITM2 which makes it similar to chIFITM1, in that both the YEML motif and phosphorylated Tyr20 are missing from this protein.

Taken together, assigning orthology remains challenging, and it is clear that this cannot be done based on sequence data alone. Studies focussing on the functionality of the chIFITM proteins will be essential as they may provide an insight into their restrictive profile, cellular localisation and regulation which may allow for a more systematic process of naming the genes.

3.3 Re-sequencing the chIFITM locus

Accurate assembly of the chIFITM locus is problematic due to the large gaps that exist in the genomic sequence (poor sequence coverage is not only a feature of the chIFITM locus, but has also been found across all species that have been sequenced to date, using NGS technologies). The chIFITM locus does not appear to be made up of a high percentage of repetitive sequences or have an unusually high GC content; characteristics that are known to affect sequencing coverage across a genome. Therefore, it remains unclear as to why this specific locus is difficult to sequence. The gaps in the sequencing data result from low confidence in the sequence and makes more comprehensive genetic analysis unfeasible. Moreover, it is difficult to design laboratory reagents without a contiguous, accurate sequence

To generate a contiguous sequence, the BAC clone (CHI261-109H20) from Red Jungle Fowl isolate inbred line (UCD001) covering the predicted IFITM locus (Figure 3.2) was purchased from BACPAC Resources Centre at the Children's Hospital Oakland Research Institute, United States (Bassano et al., 2017). The resulting plasmid DNA (3µg) was sent to The Wellcome Trust Sanger Institute for sequencing using two NGS technology platforms, the Illumina MiSeq and PacBio RSII. Quality control was conducted by The Wellcome Trust Sanger Institute's core sequencing facility. Once sequencing of the BAC clones was complete, Dr Irene Bassano (collaborator, Imperial College London) analysed the data and produced a contiguous sequence covering the entire chIFITM locus using *de novo* assembly (Bassano et al., 2017). In this study, it was essential to generate a contiguous sequence across the IFITM locus with a high degree of accuracy. It was known that the coverage across the chIFITM locus in v4 was poor and this resulted in gaps which could not be resolved without resequencing the locus using a different approach. The incorporation of the long PacBio sequencing reads has significantly improved the coverage across the

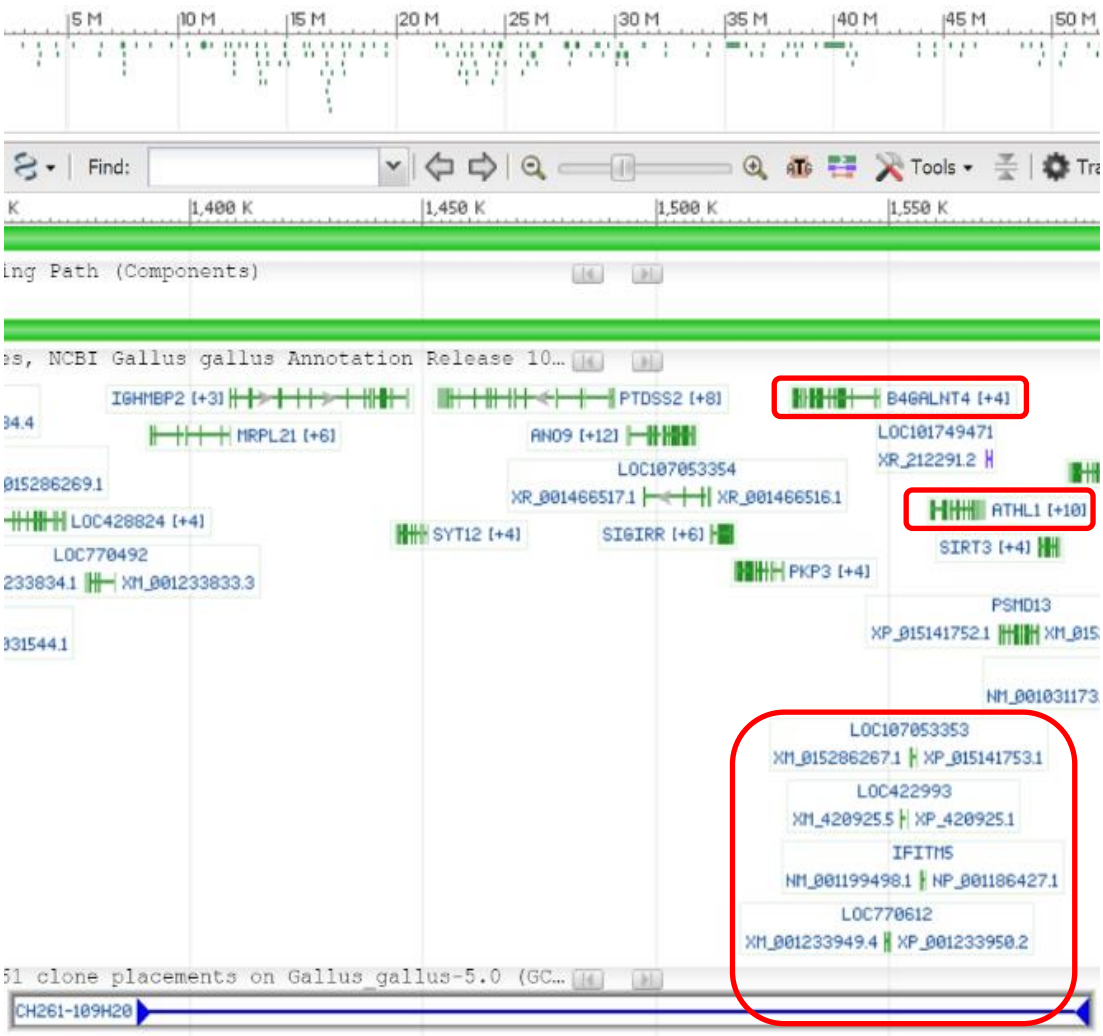

Figure 3.2 Isolating the BAC clone for chIFITM locus re-sequencing. The IFITM locus on *Gallus gallus* chromosome 5 is poorly annotated in the Galgal4 genome assembly. This region is flanked by genes *ATHL1* and *B4GALNT4* and this allowed for the identification of putative genes. Prior to 2013, only *chIFITM5* was already annotated in the genome. The BAC clone (CH261-109H20) was identified as covering the predicted chIFITM locus and was acquired from the Children's Hospital Oakland Research Institute (CHORI), United States. The BAC clone was streaked onto LB-agar, single colonies isolated and plasmid DNA extracted according to the manufacturers protocol. Regions highlighted included the chIFITM locus and the flanking genes *ATHL1* and *B4GALNT4*.

most recent version of the chicken genome (v5), including the IFITM locus. However, when aligning the MiSeq reads against v5 it is clear that gaps within the locus still exist (Figure 3.3B). When sequencing an entire genome, errors in assembly can occur due to gene duplication and paralogous gene families, both of which affect the accuracy of the alignment. The IFITM gene family is one of the most highly paralogous families known with multiple copies of the IFITM genes as well as pseudogenes (John et al., 2013;Smith et al., 2013).

To reduce error, only a relatively small region of chromosome 5 (203kb) containing the IFITM locus was sequenced at high coverage with both PacBio and Illumina MiSeq. Two different methods of sequencing were used to increase the sequence coverage across the IFITM locus and to minimize sequence gaps that may result from one single sequencing methodology. The average PacBio read length is >10kb but this is dependent on the activity of the polymerase (Eid et al., 2009;Au et al., 2012). Furthermore, it is accepted that raw PacBio reads have a higher error rate compared to other technologies (14% versus 0.1 to 1% for Illumina) but a high-quality consensus sequence can be obtained from overlapping reads. In contrast, the average read length on the Illumina MiSeq is 300bp which allows for enhanced coverage over the region of interest (Schirmer et al., 2015). Although the BAC clone (CH261- 109H20) does not include chIFITM10 because of its different chromosomal location, using a clone from the BAC library used to generate the original *Gallus gallus* genome allows for a more complete and robust assessment of the chIFITM locus when compared to the publically available genomes, namely v4 and v5. The sequencing results are summarised in a study published in BMC Genomics (Bassano et al., 2017). In brief, there was good coverage across the loci with both Miseq and PacBio Sequencing platforms. The differences in coverage were apparent when using the two most recent versions of the *Gallus gallus* genome assemblies as scaffolds. When aligning the MiSeq reads against the *Gallus gallus* v4 genome assembly (Figure 3.3A), it is clear that there are gaps within the

A

MiSeq aligned against *Gallus gallus* v4

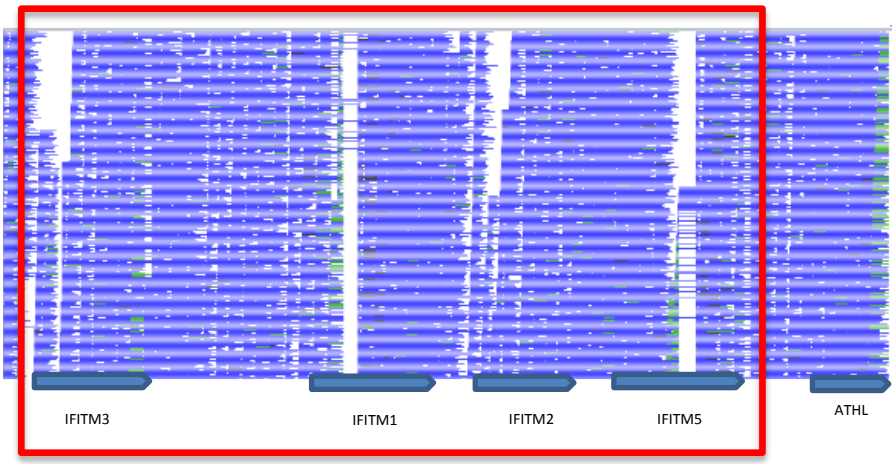

B

MiSeq aligned against *Gallus gallus* 5

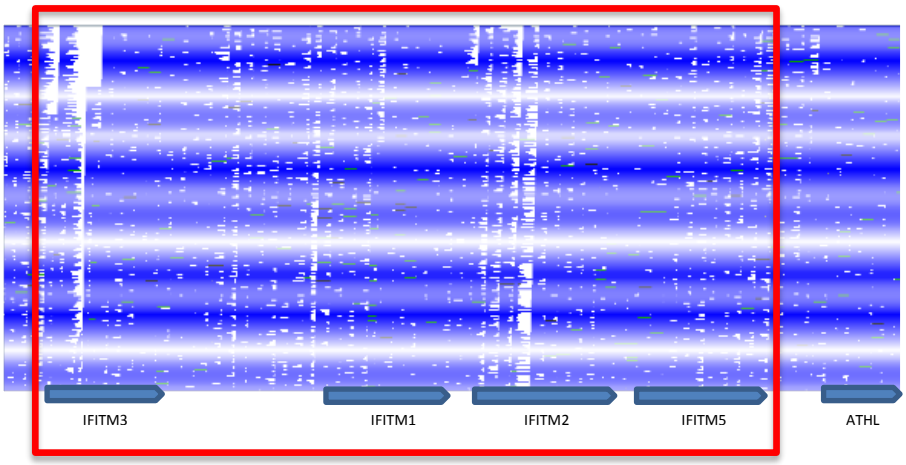

C

PacBio's RSII aligned against *Gallus gallus* 5

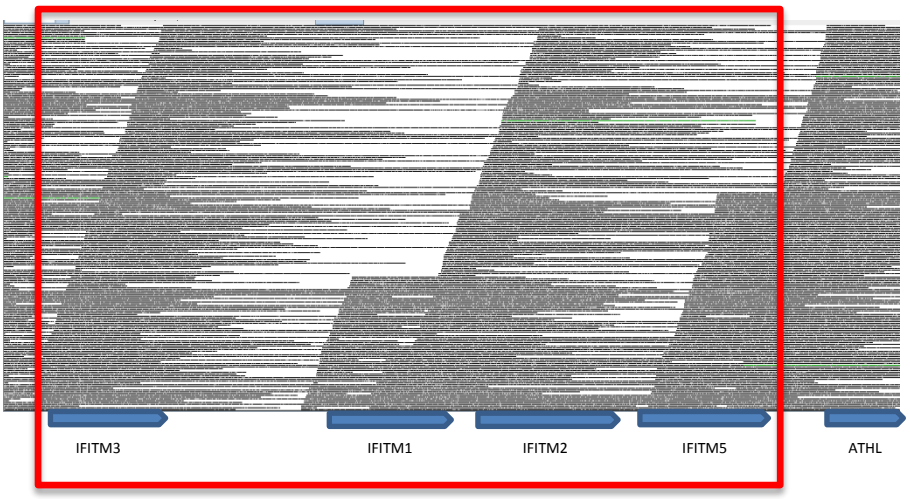

D

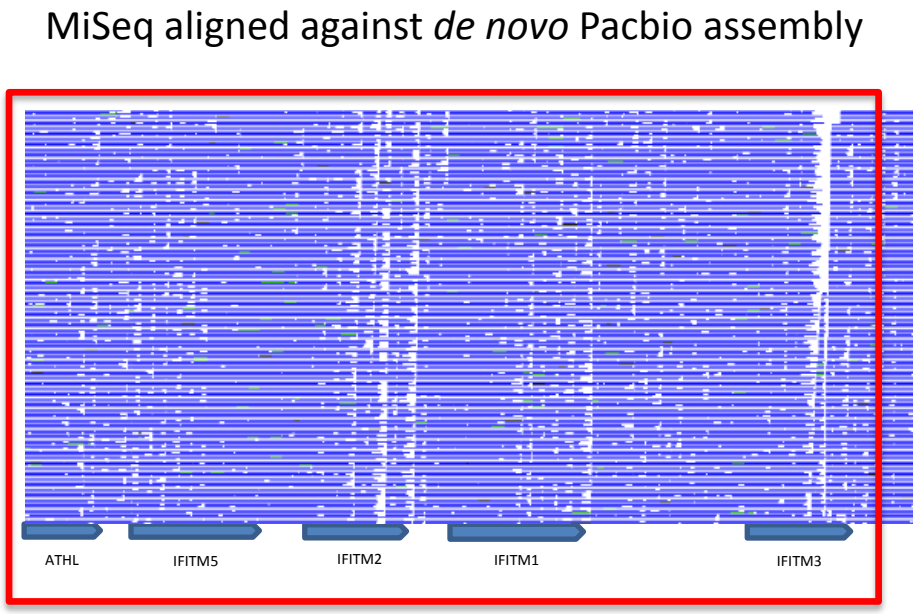

Figure 3.3 MiSeq and PacBio sequence analysis of the CH126-109H20 BAC clone. The BAC clone (CH126-109H20) was streaked onto LB-agar, single colonies isolated and plasmid DNA extracted according to the manufacturers protocol. The plasmid DNA was then sequenced at The Wellcome Trust Sanger Institute. (A) Sequence coverage over the chIFITM locus using MiSeq DNA sequencing. This reference was built using the annotation of *Gallus gallus* v4 as scaffold. (B) Sequence coverage over the chIFITM locus using MiSeq DNA sequencing. This reference was built using the annotation of *Gallus gallus* v5 as scaffold. (C) Sequence coverage over the chIFITM locus using PacBIO RSII DNA sequencing. This reference was built using the annotation of Gallus gallus v5 as scaffold. (D) Artemis coverage and stack view of Illumina MiSeq reads mapped against PacBio consensus sequence, producing a *de novo* assembly. The assembly is in the reverse orientation. Dr Irene Bassano (Imperial College London) prepared the figures and conducted DNA sequence analysis.

chIFITM locus and this highlights the substantial deficiencies to the v4 genome assembly. In contrast, the *Gallus gallus* v5 genome assembly which incorporates new PacBio sequencing in its assembly, is greatly improved over the previous assembly having fewer large sequence gaps. There is however, the addition of a small INDEL within the intronic region of chIFITM3 which is unlikely to have any significant effect although this has not been demonstrated (Figure 3.3B). The advantage of PacBio sequencing in this instance is that it generates read lengths of >10kb which are likely to reduce sequencing gaps within the regions that were poorly sequenced using MiSeq DNA sequencing. The sequencing data using this long read technology (Figure 3.3C) demonstrates that the coverage over the chIFITM locus increases dramatically in comparison to using MiSeq sequencing alone. Moreover, the coverage over the chIFITM coding regions is much better, even in comparison to other regions within the larger 203kb region.

These results demonstrate that the longer PacBio reads map well to the most current version of the reference chicken genome. In contrast, Illumina MiSeq raw reads are not sufficient to assemble this region *de novo* as there are a number of gaps within the locus that cannot be resolved. However, Illumina MiSeq raw reads do map accurately to the *de novo* PacBio reference (Figure 3.3D). Utilising two methods of sequencing has resulted in a contiguous, high coverage sequence across the chIFITM locus which can be used when designing new reagents and can act as the new reference sequence for further analysis.

3.4 Basal expression of chIFITM transcripts in chicken tissues

It has been established that the huIFITM proteins are present at basal levels (Zhao et al., 2014;Huang et al., 2011;Diamond and Farzan, 2013), however, the expression of IFITM mRNA and constitutive levels of protein differ between species, and therefore it was necessary to investigate the basal levels in chicken cells and tissues. Additionally, IFITM expression has also been found to be cell type or tissue specific (Tanaka et al., 2005;Lu et

al., 2017) and increases after the addition of exogenous type I interferons such as IFNα and IFNβ (Warren et al., 2014). The constitutive levels of chIFITM transcript abundance were assessed (Smith et al., 2013;Smith et al., 2015) and variable levels of *chIFITM1, 2* and *3* gene expression were observed, although *chIFITM5* was not investigated. To expand on the data already available, the current study focused on a wider range of tissues and included *chIFITM5*. In mammals, *IFITM5* is expressed only in the bone marrow and its function is restricted to bone mineralisation (Kasaai et al., 2013;Liu et al., 2012;Moffatt et al., 2008). There is little data suggesting a role of chIFITM5 in the chicken host. Constitutive levels of *chIFITM5* mRNA expression may provide insight into the functional role this IFITM may play in chickens.

In order to assess tissue-specific chIFITM gene expression, RNA was extracted from nineteen tissues from 3, 3-week-old Rhode Island Red (RIR) chickens. The tissues that were extracted include: brain, bursa of Fabricius, caeca, lower GIT (colon), Mid GIT, spleen, thymus, bone marrow, heart, liver, eye lid, trachea, pancreas, lung, skin, muscle (breast), gall bladder, caecal tonsil and kidney. These samples were chosen because they include a wide range of tissues, many of which show tissue tropism for one or more avian virus. For example, IBV is known to infect the trachea of chickens and this is a primary site of virus replication (Abdel-Moneim et al., 2009;Thiel, 2007). Understanding the constitutive levels of expression may give an insight into the immunocompetence of that tissue in response to infection. Tissue samples were harvested, homogenised using the TissueLyser, RNA was extracted and reverse transcribed into cDNA, which was used in relative quantitative RT-PCR. Copies of the chIFITMs were calculated from a standard curve using plasmids encoding the target sequence at known concentrations.

Expression of *chIFITM1* mRNA was largely variable across the different tissues analysed reaching the highest levels of expression in the bursa of Fabricius, the gastrointestinal tract,

and the caecal tonsil. Detectable levels of *chIFITM1* expression were also found in other tissues such as the trachea, lung and thymus but these were at much lower levels (approximately a 1 to 2 $\log_{10}$ decrease depending on the tissue being examined). In contrast, expression of *chIFITM2* and *3* mRNA was detected in all tissues, with expression, on average, higher than *chIFITM1* expression. Lower levels of *chIFITM2* and *3* expression were found in the brain, pancreas, muscle (breast) and brain. Finally, expression of *chIFITM5* mRNA was also variable with levels of expression higher in the gastrointestinal tract, brain, lung and caecal tonsil. Moreover, the levels of *chIFITM5* expression were consistently lower than expression of *chIFITM1, 2* or *3* in all tissues studied. However, it is interesting to note that although levels of expression are low, they are detectable. This is a marked difference in the data presented in the mammalian field and may suggest a different function for chIFITM5. It is unclear at the moment if enhanced distribution of expression necessarily results in a function that has yet to be described (Figure 3.4).

3.5 Basal expression of chIFITM transcripts in chicken cell lines and *ex vivo* cell cultures

The constitutive levels of *chIFITM* expression have been quantified in a range of different chicken tissues and this allows for a more robust assessment of quantitative RT-PCR data where relative fold change is used. It is important to put quantitative RT-PCR data into context as cells with a higher constitutive level of expression may have a lower relative fold change compared with cells expressing lower levels of chIFITM transcript abundance. Moreover, this data endorses chIFITMs as restriction factors insomuch that a basal level of expression is one of the classical definitions used to classify genes as host cell restriction factors. Avian cell lines are generally poorly characterised, especially in regard to endogenous *chIFITM* mRNA expression. To characterise *chIFITM* transcription *in vitro* without infection or stimulation, quantitative RT-PCR was performed on three chicken

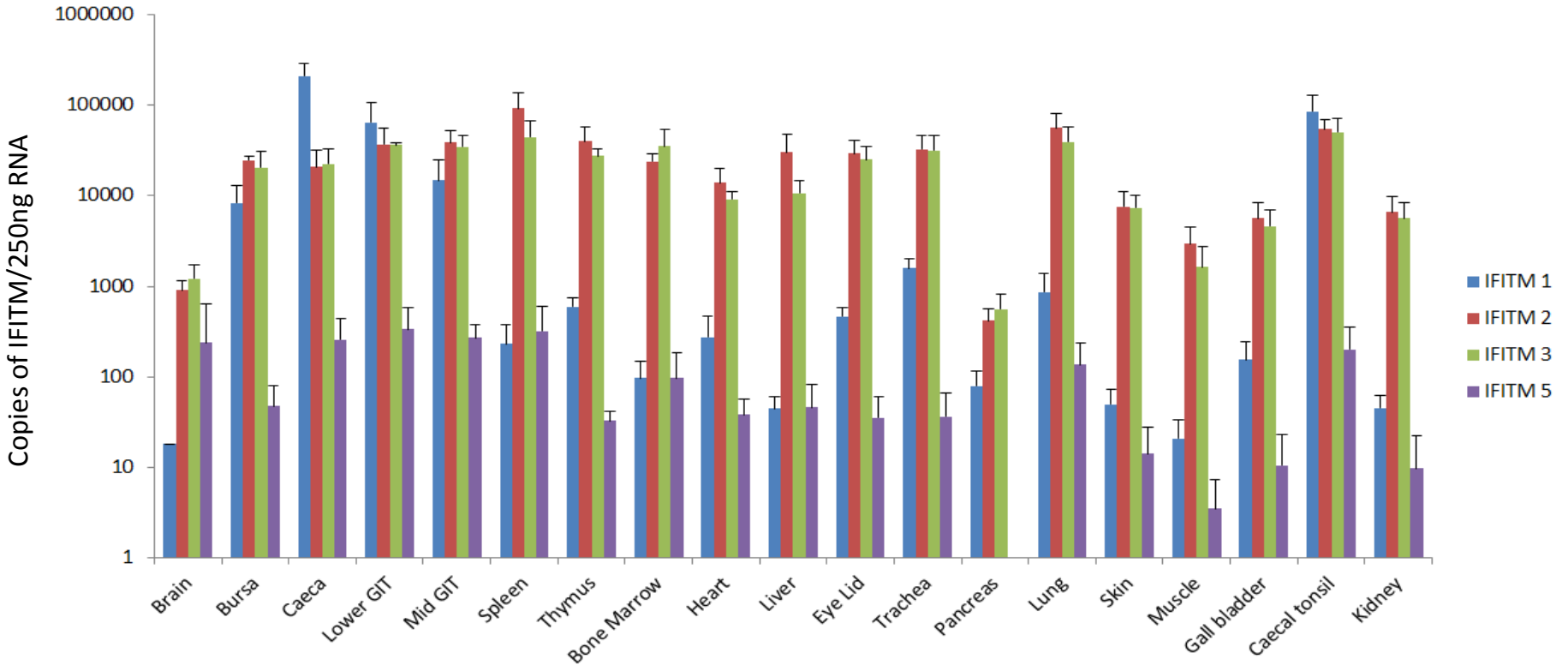

Figure 3.4 Endogenous levels of chIFITM expression in the tissues of Rhode Island Red (RIR) chickens. Nineteen tissues from 3 week old RIR chickens were removed, homogenised, the RNA extracted, reverse transcribed and the endogenous expression of *chIFITM1, 2, 3* and *5* was assessed by quantitative RT-PCR. Relative quantification of chIFITM transcripts was performed and copy numbers were determined from standard curves produced by using plasmids encoding the template at known concentrations. Error bars show standard deviations of the means from 3 chickens (*n* =3).

cell lines (DF-1, HD11 and OU-2) and two *ex vivo* cell cultures (CEF and CKC) routinely used for research purposes. Samples were harvested, cells were lysed, RNA extracted, reverse transcribed and *chIFITM*, β-*Actin* and *RPL13 mRNA* expression levels were measured by quantitative RT-PCR. Two reference genes, RPL13 and β-actin were used as endogenous controls and amplified well in all cell lines tested (Figure 3.52A and B). Interestingly, the amplification of β-actin in DF-1 cells, although stably expressed, was lower than in any of the other cell lines and the reason for this remains unclear. The amplification of the reference genes was otherwise comparable and stable across the cell lines and *ex vivo* cell cultures that were assayed. Amplification of *chIFITM1, 2, 3* and *5* cDNA was variable across the cell lines that were assayed (Figure 3.5C – F). OU-2 cells have the greatest level of basal *chIFITM* transcriptional expression, with average 40-CT values of 9.8, 17.8, 22 and 7.3, for *chIFITM1*, 2, 3 and 5, respectively. The transcriptional expression of the chIFITM genes in DF-1 and HD11 cells were broadly comparable to each other. As well as assessing continuous cell lines, the basal level of expression for chIFITMs in *ex vivo* cells including chicken embryonic fibroblasts (CEFs) and chick kidney (CK) was also examined. The average CT values of these two *ex vivo* cultures were also broadly similar to each other with the greatest variation seen in chIFITM5, with a difference of 4 CTs.

These data demonstrates that the chIFITMs are expressed at basal levels in all of the cell lines examined. It is also clear that a similar pattern of expression exists between the cell lines and the *in vivo* tissue samples that were examined. Expression of *chIFITM1* and 5 are lower and more variable across all of the samples. Conversely, *chIFITM2* and 3 are more highly expressed and the data suggests that there is less variation in expression, although some tissues and OU-2 cells do appear to have a generally higher level of expression. This may imply that *chIFITM2* and *3* are more tightly regulated in comparison to *chIFITM1* and *5*. Moreover, there is a large degree of variation in chIFITM expression in DF-1 cells and the reasons behind this are unclear. It is known that interferon expression and the

A

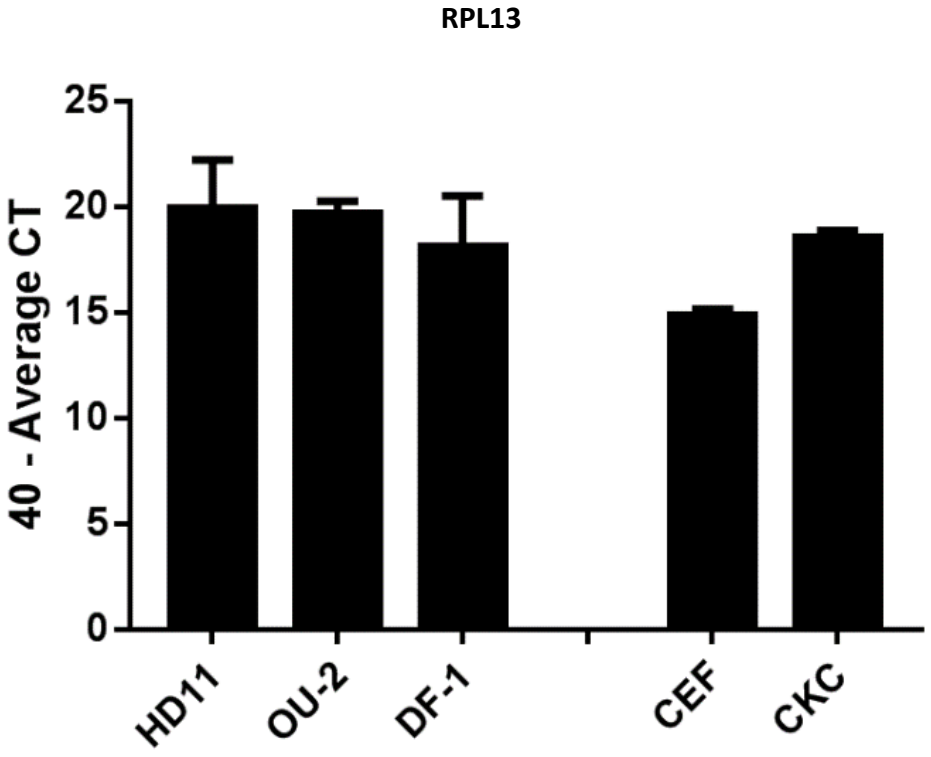
RPL13
40 - Average CT
25
20
15
10
5
0
HD11
OU-2
DF-1
CEF
CKC

B

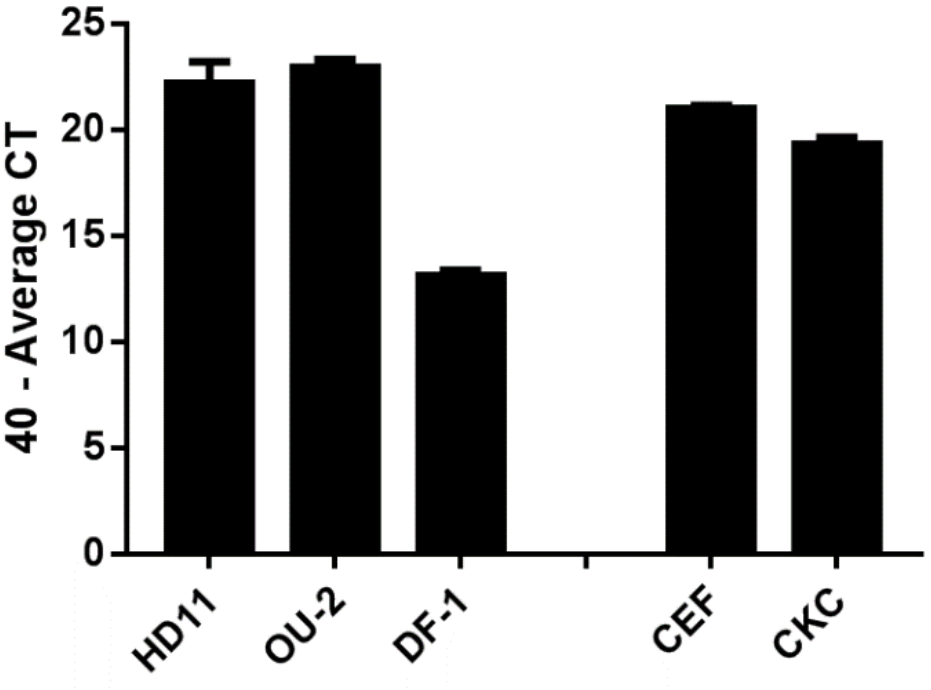
β-Actin
40 - Average CT
25
20
15
10
5
0
HD11
OU-2
DF-1
CEF
CKC

C

IFITM1

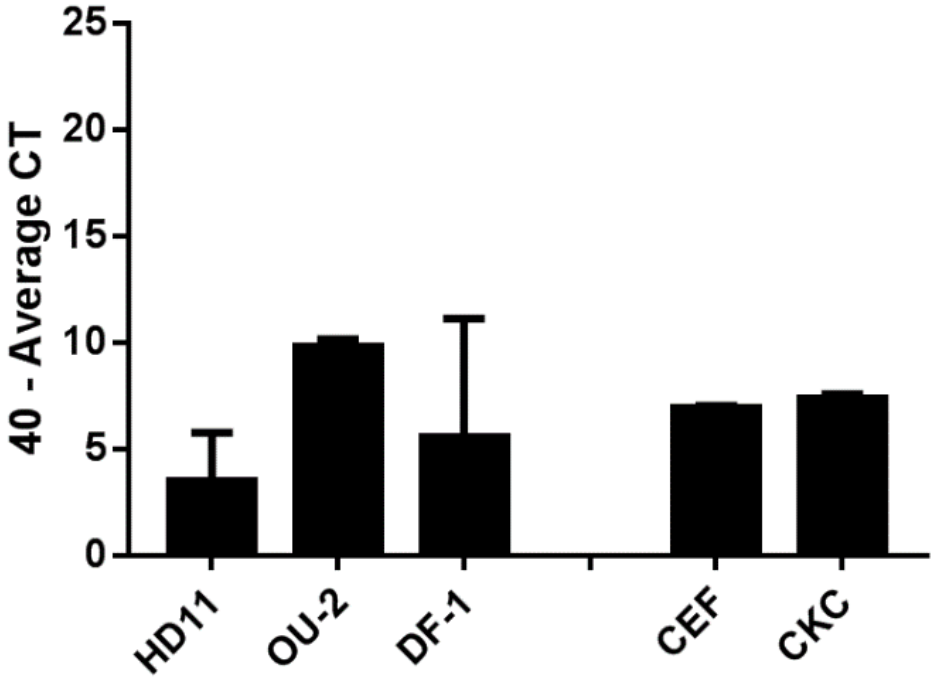

D

IFITM2

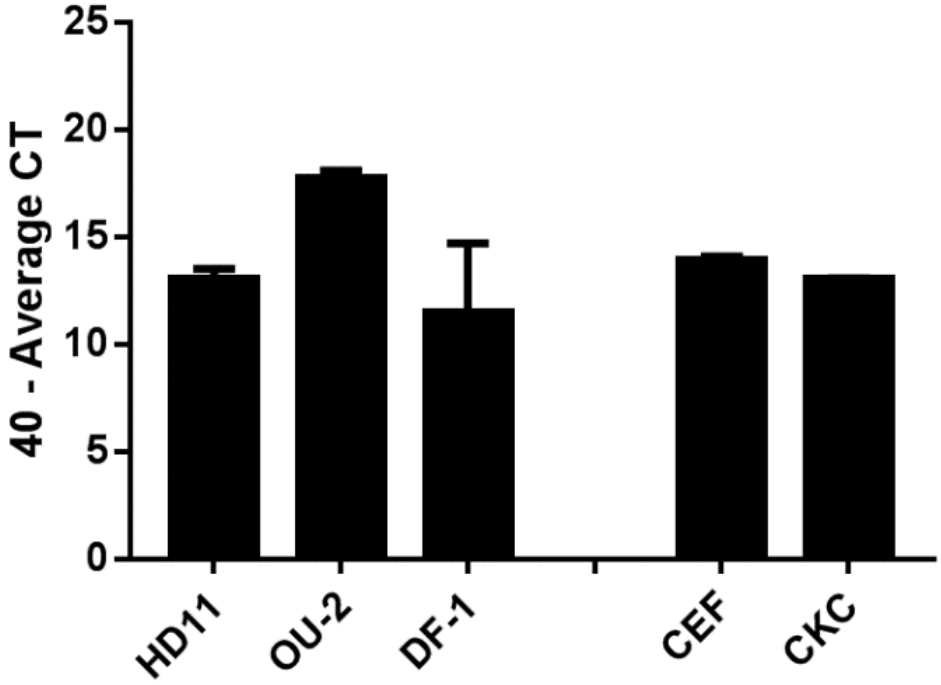

E

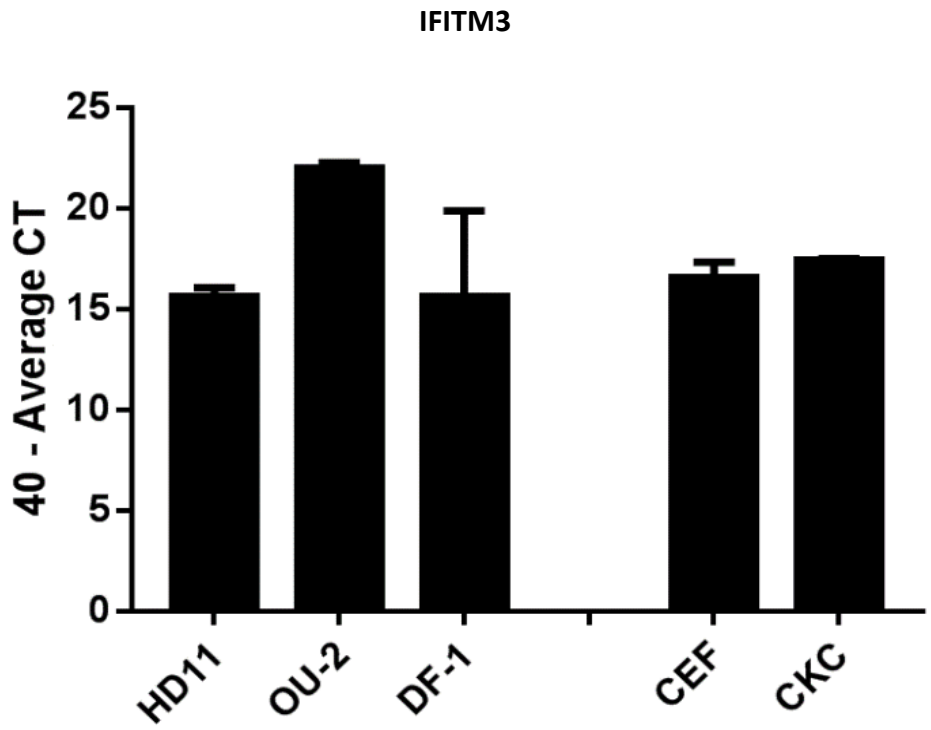

F

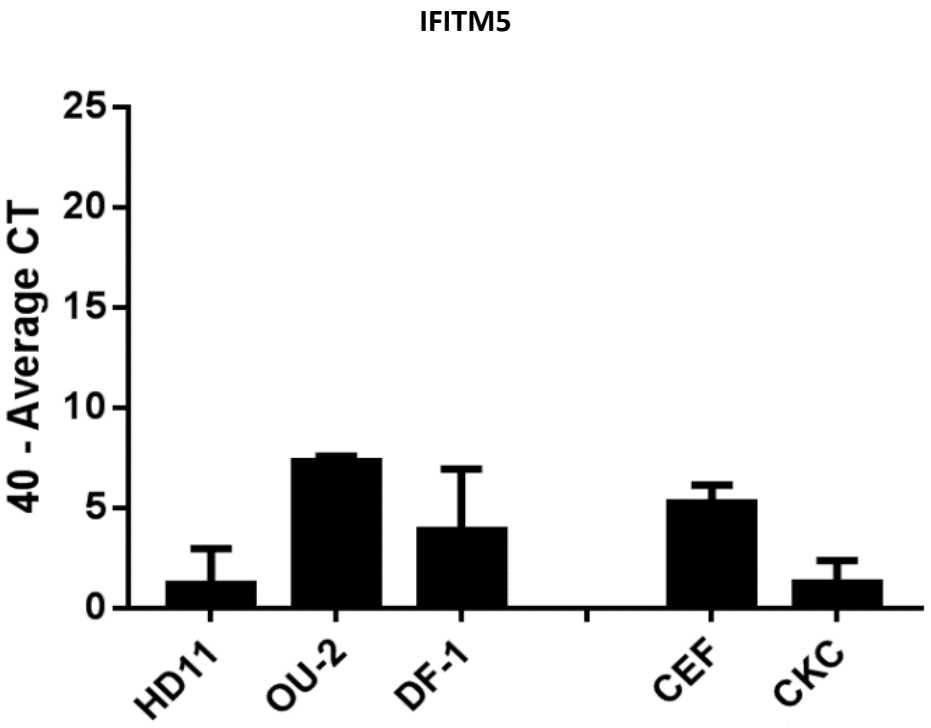

Figure 3.5 Endogenous levels of chIFITMs in avian cell lines. (A and B) Average CT value of two reference genes, RPL13 and β-actin were measured by quantitative RT-PCR and then subtracted from the number of cycles (40). (C-F) Average CT value of *chIFITM1, 2, 3* and *5* were measured by quantitative RT-PCR and then subtracted from the number of cycles (40). Input RNA was normalised to 1µg by Tapestation 2200 and then Nanodrop Lite. Error bars show standard deviations of the means of 3 biological replicates for the *ex vivo* cultures and 6 biological replicates of the continuous chicken cell lines.

upregulation of interferon is reduced in DF-1 cells and this has been attributed to a higher level of SOCS1 expression (Giotis et al., 2017). The suppression of innate immune responses in this cell line may contribute to the variation in expression, although other mechanisms may be mediating this effect.

3.6 Multiple key residues are conserved among chIFITM sequences in Galliformes

Using the recently published and most accurate genomic sequence for the IFITM locus for *Gallus gallus* (Bassano et al., 2017) it was possible to accurately compare avian and mammalian sequences for this gene family. To identify conserved domains, avian amino acid sequences were aligned against human and mouse IFITM sequences, identifying critical residues and regions that are known to modulate either the expression or antiviral activity of these mammalian proteins. For example, it is well documented that the cysteine residues at position 71 and 72 of huIFITM3 are critical in mediating viral restriction; if they are missing or mutated through site directed mutagenesis (SDM), the antiviral activity of huIFITM3 is diminished (Yount et al., 2010;Yount et al., 2012). Moreover, it has been shown that this effect is incremental and indirectly proportional to the number of mutated palmitoylated cysteine residues; the more mutated cysteine residues, the less antiviral activity is observed (Yount et al., 2010;Narayana et al., 2015). In addition to aligning the sequences based on the conservation of key resides, it is also known that the CD225 region is homologous between the sequences of different species and conservation within this region is high. The CD225 domain includes the IMD and CIL regions and is present in many prokaryotic and eukaryotic proteins. This domain is conserved between all species that have been studied thus far including mammals, aves and amphibians.

To examine sequence homology, all of the available avian IFITM amino acid sequences were aligned to ensure sufficient breadth to the investigation in conjunction with the most detailed analysis undertaken to date. Amino acid sequences of avian IFITM proteins were downloaded from UNIPROT and aligned in order to assess the degree to which previously published important residues/motifs (Bailey et al., 2014), identified in huIFITMs, are conserved in a number of divergent avian species (Figure 3.6). Many of the key residues are conserved between the avian species analysed, with specific emphasis on the palmitoylated Cys72, which is conserved in all but two species (hummingbird and medium ground finch) that were aligned, for the IFITM5 sequence. It has already been established that Cys72 is a critical residue in huIFITM3-mediated restriction of influenza and mutation causes it to mis-localise and attenuation of restriction is observed (Yount et al., 2012). Other residues such as Cys105 (also palmitoylated) and Lys24 are less well conserved, suggesting that only residues that are absolutely essential for function and viral restriction are conserved through evolutionary divergence. Strikingly, the alignment of chicken, mallard and turkey IFITM2 amino acids sequences reveals an N-terminal truncation which lacks the YEML motif (Y20). This motif interacts with the μ2 subunit of AP-2 complex and targets the protein for internalisation via clathrin-mediated endocytosis (Jia et al., 2014). For this reason, this truncation may impact the restrictive profile of chIFITM2, although at present there is limited information available to confidentially conclude. Currently the only functional data has been published by Smith et al (2013) who show that chIFITM2 is able to restrict lentiviral vectors at least as proficiently as chIFITM3. These results demonstrate that the avian species examined are missing the YEML motif which is essential for the localisation of the proteins to the endosomes (Jia et al., 2014). This may result in avian IFITM2 localising to different compartments which may impact restriction, although this has yet to be determined in chickens. In a study published in 2016, it was found through confocal microscopy that duck IFITM2 only partially localises with

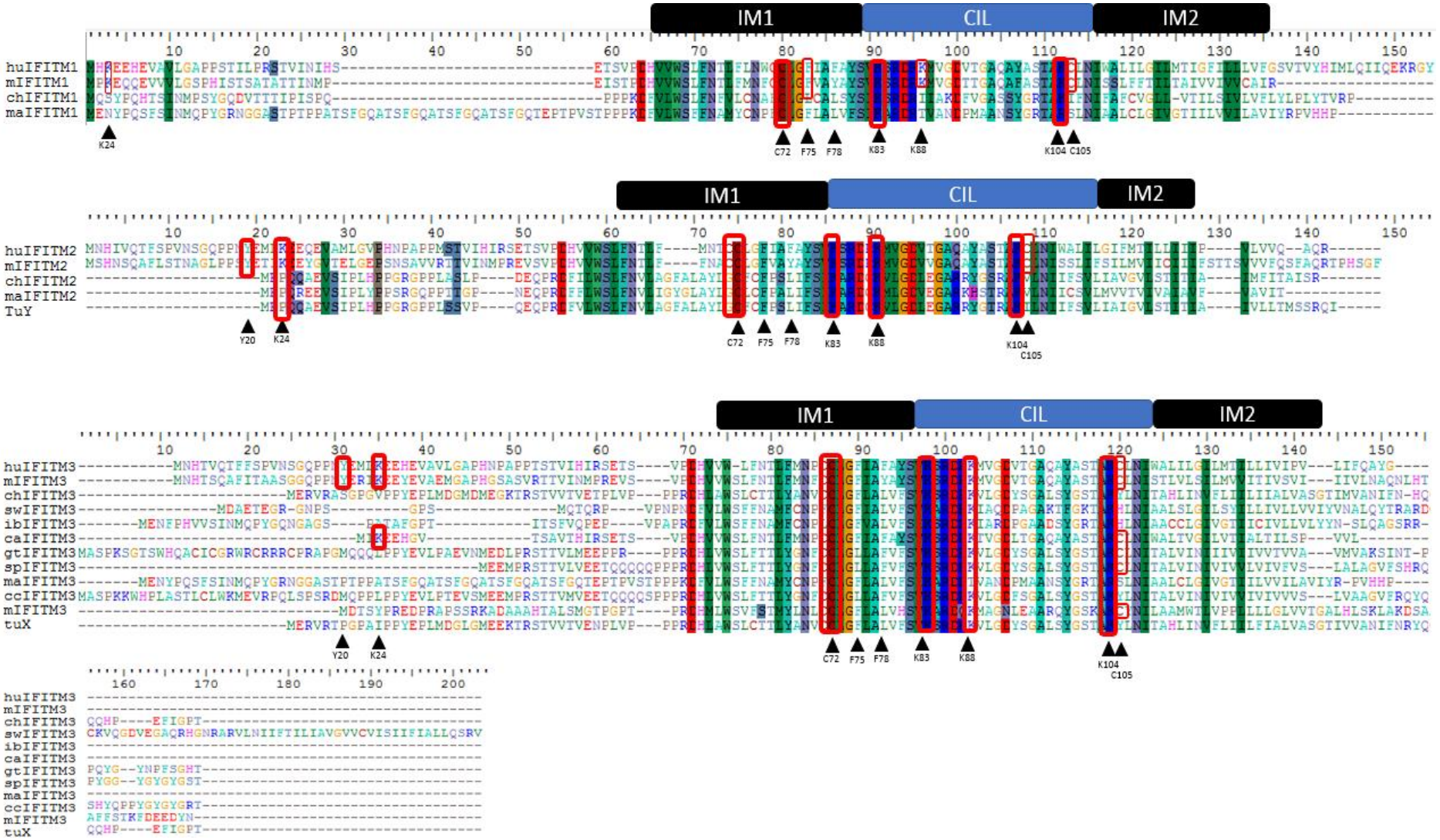
IM1
CIL
IM2
huIFITM1
mIFITM1
chIFITM1
maIFITM1
K24
C72
F75
F78
KB3
KB8
K104
C105
huIFITM2
mIFITM2
chIFITM2
maIFITM2
TuY
Y20
huIFITM3
mIFITM3
chIFITM3
swIFITM3
ibIFITM3
caIFITM3
gtIFITM3
spIFITM3
maIFITM3
ccIFITM3
tuX

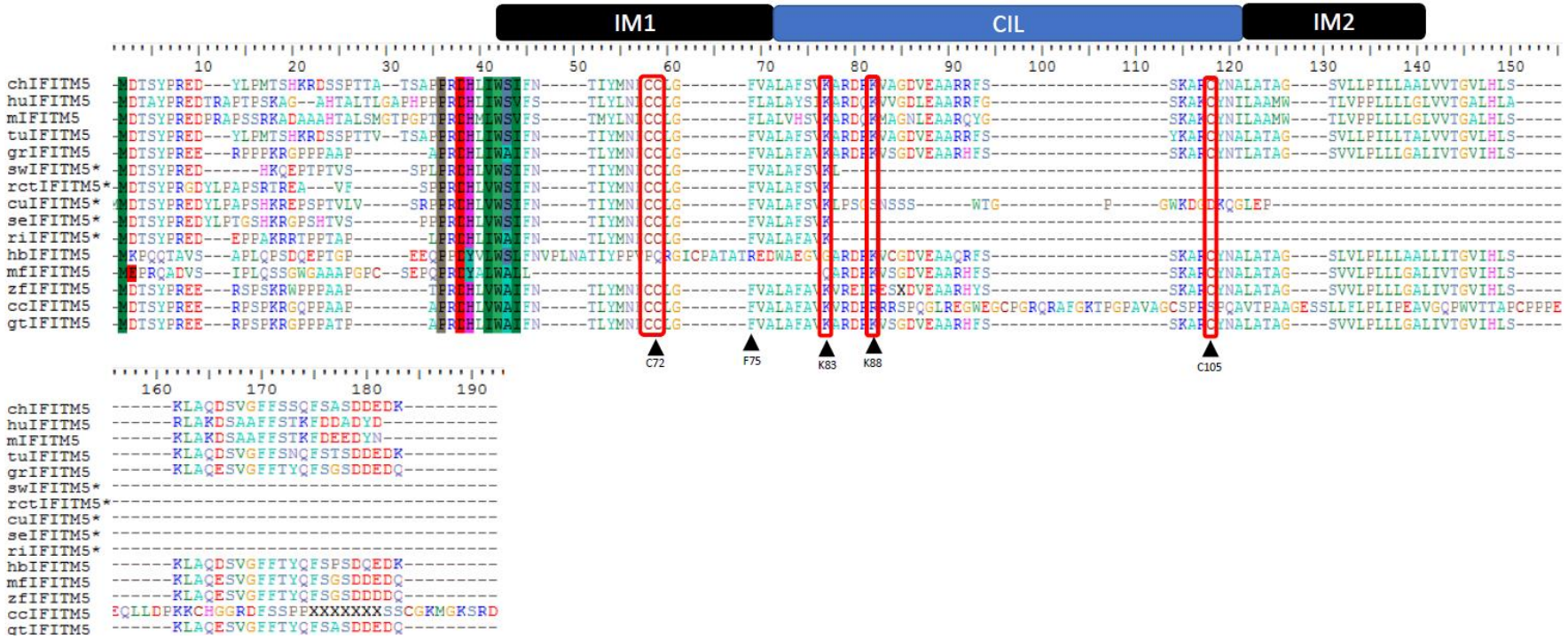

Figure 3.6 Multiple key residues are conserved among chIFITM sequences in Galliformes. The amino acid sequences of the avian IFITM proteins (1, 2, 3 and 5) were downloaded from Uniprot and saved in a word document in fasta format. Multiple sequence alignments were calculated using Clustal Omega (EMBL-EBI) using the default settings. The resulting alignment was formatted using Genedoc. The amino acid sequences of the chIFITM genes (1, 2, 3 and 5) were compared to various avian and mammalian homologs. The highlighted domains are N-terminal domain (NTD), intramembrane domain (IMD), conserved intracellular loop (CIL), transmembrane domain (TMD) and the C-terminal domain (CTD). Site specific similarities between amino acids are highlighted by the coloured letters. The YEML motif (red letters, Y20 arrow) promotes protein internalisation and localisation to the endosomes, ubiquitination of K24 and methylation of K88; F75 and F78 have been implicated in dimerization (blue) and palmitoylation of Cys71; Cys72 and Cys105 (red) have been shown to play a critical role in subcellular localisation and viral restriction. The species listed include: ch (chicken), hu (human), m (mouse), tu (turkey), sw (swift), Ib (ibis), ma (mallard), ba (little brown bat), ca (canary), gt (ground tit), sp (sparrow), cc (common canary), hb (hummingbird), mf (medium-ground finch), z (zebra finch), rct (red-crested turaco), cu (cuckoo roller), se (red-legged seriema), ri (rifleman).

Lysosomal-associated membrane protein 1 (LAMP1). The co-localisation was not as profound as the signal between duck IFITM3 and LAMP1 which may suggest differential localisation (Blyth et al., 2016). It is has also been observed that a number of residues are altered from chIFITM3, including Lys24, Phe78 and Cys105. At this time, it is unclear what impact this may have on chIFITM3-mediated restriction, although studies suggest that the impact may be minimal (Yount et al., 2012;Yount et al., 2010;Shan et al., 2013). Research published on huIFITM5 conclusively shows that the expression of this gene is restricted to the bone marrow and its primary function is involved in bone mineralisation. It has been shown that huIFITM5 does not function as an ISG (Farber et al., 2014;Moffatt et al., 2008;Tsukamoto et al., 2013). Interestingly, both chIFITM5 and huIFITM5 contain Cys71, Cys72 and Cys105 alongside Lys83 and Lys88 which are conserved between orthologues. We have established that chIFITM5 expression is not restricted to bone marrow (Figure 3.4), however, it is unclear if this is linked to its function and if *chIFITM5* is an ISG.

There is a large degree of heterogeneity between mammalian and avian IFITM protein sequences, although a greater degree of conservation is observed within the IM1, CIL and IM2 domains. Chicken, mallard and turkey IFITMs appear to share similar amino acids at these important positions which is in contrast with the consensus amino acid sequence which is derived from the huIFITM sequences. It is not yet known if functional residues at these positions are important, nor if the high degree of sequence homology indicates that IFITMs from different avian species act in a similar manner.

3.7 Sequence variation within the chIFITM locus of commonly used chicken cell lines

Now that a contiguous sequence has been generated, it is possible to interrogate the chIFITM locus in continuous avian cell lines that are routinely used in the laboratory. It is

unknown if these cell lines have an intact chIFITM locus or whether there are SNPs or other polymorphisms within the chIFITM locus compared to the *Gallus gallus* reference sequence. To answer this question sequencing was performed. This approach ensured that the reagents that have been developed (quantitative RT-PCR primers and probes, siRNAs and antibodies) were suitable across all of the cell lines that were used throughout the course of the project. Moreover, sequencing these cell lines allowed for the natural variation to be determined and may provide further insight into any observed differences in viral restriction between the cell lines. In order to sequence the chIFITM locus in three chicken cell lines, HD11, DF1 and OU-2 cells were cultured, the cells lysed and genomic DNA extracted. The quality and quantity of the DNA was analysed using both the Nanodrop and TapeStation 2200. The DNA was enriched using SureSelect pull down probes of the IFITM locus and sequenced using PacBio sequencing technology at the Wellcome Trust Sanger Institute. The DNA sequences were analysed for SNPs by Dr Angela Steyn (Genetics and Genomics group, The Pirbright Institute) but any further analysis regarding SNP location and/or possible putative function was conducted by myself.

There was relatively little sequence diversity within the chIFITM locus and only two mutations were found within the coding regions. These mutations were located within *chIFITM1* at position GGA5:1,552,864 and *chIFITM3* at position GGA5:1,550,177. As these were synonymous mutations, it is likely there will be no change in the antiviral properties of either protein. In total there were 27 single nucleotide polymorphisms (SNPs) within the chIFITM locus, and these were identified within the 5' untranslated region (UTR), the introns and in the 3' UTR. There was also a 3bp insertion into the 5' UTR of *chIFITM2* and two deletions (8 and 9bp) within the intronic region of *chIFITM3* (Figure 3.7). Variants within the introns can have profound effects on expression, splicing and gene regulation (Anna and Monika, 2018;Strobel and Abelson, 1986) . It is unknown if these variants impacted on the expression of the chIFITM genes or whether there were any effects on the

Gene: LOC422993	IFITM1	chr5							
1,552,649 - 1,554,227			HD-11		DF-1		OU-2		
SNP position	ref allele	variant allele	total counts	percentage of reads with variant (%)	total counts	percentage of reads with variant (%)	total counts	percentage of reads with variant (%)	Location
1,552,864	T	G	1619	99	1916	67	1375	74	Exon
1,552,976	G	C	1609	100	2063	68	1364	74	Intron
1,553,190	T	C	1505	99	2109	64	1368	73	Intron
1,553,342	G	A	1306	94	1786	59	1193	68	Intron
1,553,432	T	C	1299	99	1691	66	1106	70	Intron
1,553,439	G	A	13332	100	1719	66	1127	71	Intron
1,553,450	A	G	1376	100	1729	65	1167	69	Intron
1,553,812	T	C	1603	100	2230	64	1338	71	Intron
Gene: LOC107053353	IFITM2	chr5							
1,554,391-1,556,267			HD-11		DF-1		OU-2		
SNP position	ref allele	variant allele	total counts	percentage of reads with variant (%)	total counts	percentage of reads with variant (%)	total counts	percentage of reads with variant (%)	Location
1,554,400	C	T	1394	99	1889	63	1326	73	5' NCR
1,554,403 insertion	C TCC	T	1396	100	1876	63	1311	73	5'NCR
1,555,329	C	T	1348	99	1796	68	1237	77	Intron
1,555,390	C	T	1168	99	1539	69	1026	75	Intron
1,555,682	C	T	1203	100	1383	67	934	74	Intron
1,555,800	C	T	952	99	1362	65	810	77	Intron
1,555,801	C	G	957	99	1375	64	801	76	Intron
1,556,015	T	G	1417	99	1875	63	1325	73	3' NCR
1,556,059	T	C	1457	99	1844	62	1247	73	3' NCR
1,556,183	C	G	1406	99	1857	65	1316	74	3' NCR
1,556,196	G	C	1392	100	1860	65	1331	75	3' NCR
1,556,228	A	G	1466	99	1916	65	1371	74	3' NCR
Gene: LOC770612	IFITM3	chr5							
1,549,211 - 1,550,527			HD-11		DF-1		OU-2		
SNP position	ref allele	variant allele	total counts	percentage of reads with variant (%)	total counts	percentage of reads with variant (%)	total counts	percentage of reads with variant (%)	Location
1,549,516	T	G	387 (low coverage)	99	N/A	N/A	N/A	N/A	Intron
1,549,523 - 1,549,531			9bp deletion	>80					Intron
1,549,567 - 1,549,574			8bp deletion	>80					Intron
1,550,053	G	T	N/A	N/A	2251	64	1483	74	Intron
1,550,177	G	A	1521	100	N/A	N/A	N/A	N/A	Exon
IFITM5	IFITM5	chr5							
1,556,571 - 1,558,140			HD-11		DF-1		OU-2		
SNP position	ref allele	variant allele	total counts	percentage of reads with variant (%)	total counts	percentage of reads with variant (%)	total counts	percentage of reads with variant (%)	Location
1,556,674	A	G	1557	99	2072	63	1383	74	5' NCR
1,556,686	T	C	1570	99	2064	63	1404	74	5'NCR
1,556,705	A	C	1582	100	2116	62	1433	73	5' NCR
1,556,716	T	C	1598	99	2136	62	1434	73	5' NCR

Figure 3.7 Sequence variation within the chIFITM locus of commonly used chicken cell lines. HD11, DF1 and OU-2 cells were cultured, the cells lysed and DNA extracted using a Qiagen blood and cell culture mini kit, as per the manufacturer's instructions. The quality and quantity of the DNA was analysed using both the Nanodrop and TapeStation 2200. The DNA was enriched using SureSelect pull down probes of the IFITM locus and sequenced using PacBio sequencing technology. The DNA sequences were analysed by Dr Angela Steyn (Genetics and Genomics group, The Pirbright Institute).

resultant polypeptide, as studies have not focused on these regions and very little is understood regarding regulation of chIFITM expression. Interestingly, SNPs that have been identified are present in >90% of reads in HD11 cells which means that these SNPs can be called with confidence. In contrast, the same SNPs are present in ~60% and ~70% reads in DF-1 and OU-2 cells respectively. Although the SNPs in these two cell lines are present in fewer reads, it is likely that they are true SNPS, not a result of sequencing error, due to the concurrent presence of these SNPs in HD-11s. The SNP identified within *chIFITM3* at position GGA:1,550,053 has not been identified in HD11 cells and the percentage of reads with this variant in DF-1 cells is 64% and OU-2 cells is 74%. Therefore, it is difficult to confidently call whether this variant is a true SNP although it is present in more than one cell line.

Taken together, resequencing the chIFITM locus, aligning a diverse range of avian IFITM protein sequences and utilising new sequencing approaches to sequence commonly used chicken cell lines now allows for a comprehensive assessment of the chIFITM locus. This data provides information that allows for a greater understanding of this region and may provide insights into which regions are important for mediating restriction.

3.8 Predicted structures of the chIFITM proteins and their corresponding membrane topologies

Although the huIFITM proteins have been studied extensively, only a single report provides convincing evidence that predicts the protein topology of huIFITM3 (Ling et al., 2016). Even with new structural insights, the mechanism of restriction remains largely unknown. Using nuclear magnetic resonance (NMR) and electron paramagnetic resonance (EPR) on huIFITM3 in detergent liquid micelles, Ling et al proposed the type II transmembrane protein topology model for huIFITM3. Furthermore, PTMs of the NTD, particularly the

ubiquitination of Lys24 and phosphorylation of Tyr20, suggest that the NTD resides intracellularly, as access to cytosolic enzymes such as ubiquitin ligases and protein kinases, is essential (Yount et al., 2012;Jia et al., 2012). Evidence for the localisation of the C-terminal domain (CTD) is less definite, although additional studies assessing the PTMs in this region suggest that the CTD of murine ifitm1 could also reside intracellularly (Yount et al., 2012;Hach et al., 2013a). Conversely, models of ifitm3 and huIFITM1 suggest that the CTD resides extracellularly (Bailey et al., 2014;Weston et al., 2014). The conflicting data makes it difficult to determine the correct membrane topology of the human or extrapolate for the chicken IFITM proteins. It will not be until crystal structures of the proteins are generated that the structure will finally be determined. In the meantime, data collected though biochemical experiments and structural proteomic techniques will provide a more fundamental understanding of the protein topology and how this may influence viral restriction.

Amino acid sequences were imported into the Phyre2 software package (developed by Structural Bioinformatics Group, Imperial College, London) and protein structures were modelled using the intensive mode setting (Figure 3.8 A, C, E). In brief, models are generated by PSI-BLAST searches against known homologues, secondary structure is modelled against Psi-pred and Diso-pred databases and from this data a hidden Markov model (HMM) is generated. Intensive mode allows for further analysis as templates are selected to increase the coverage (Figure 3.8 B, D, F and H). Transmembrane helices and protein topology prediction is made by memsat-svm.

A

chIFITM1

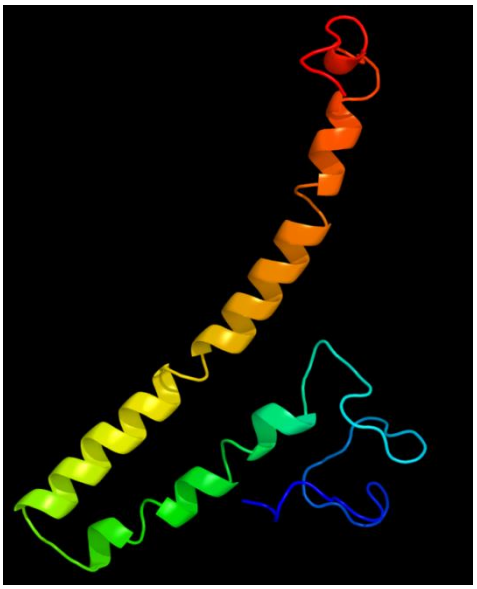

C

chIFITM2

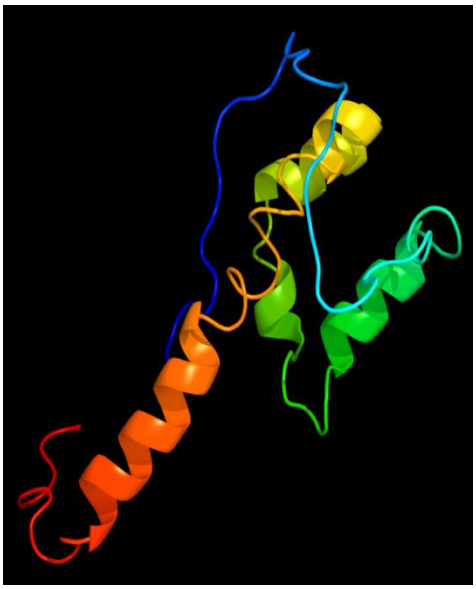

B

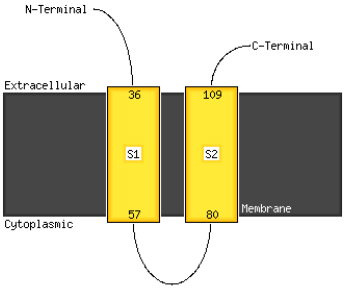

D

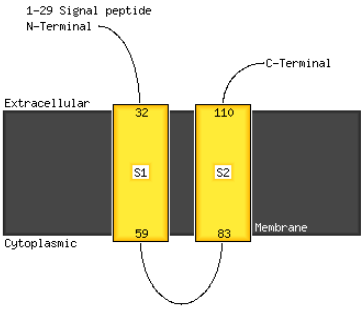

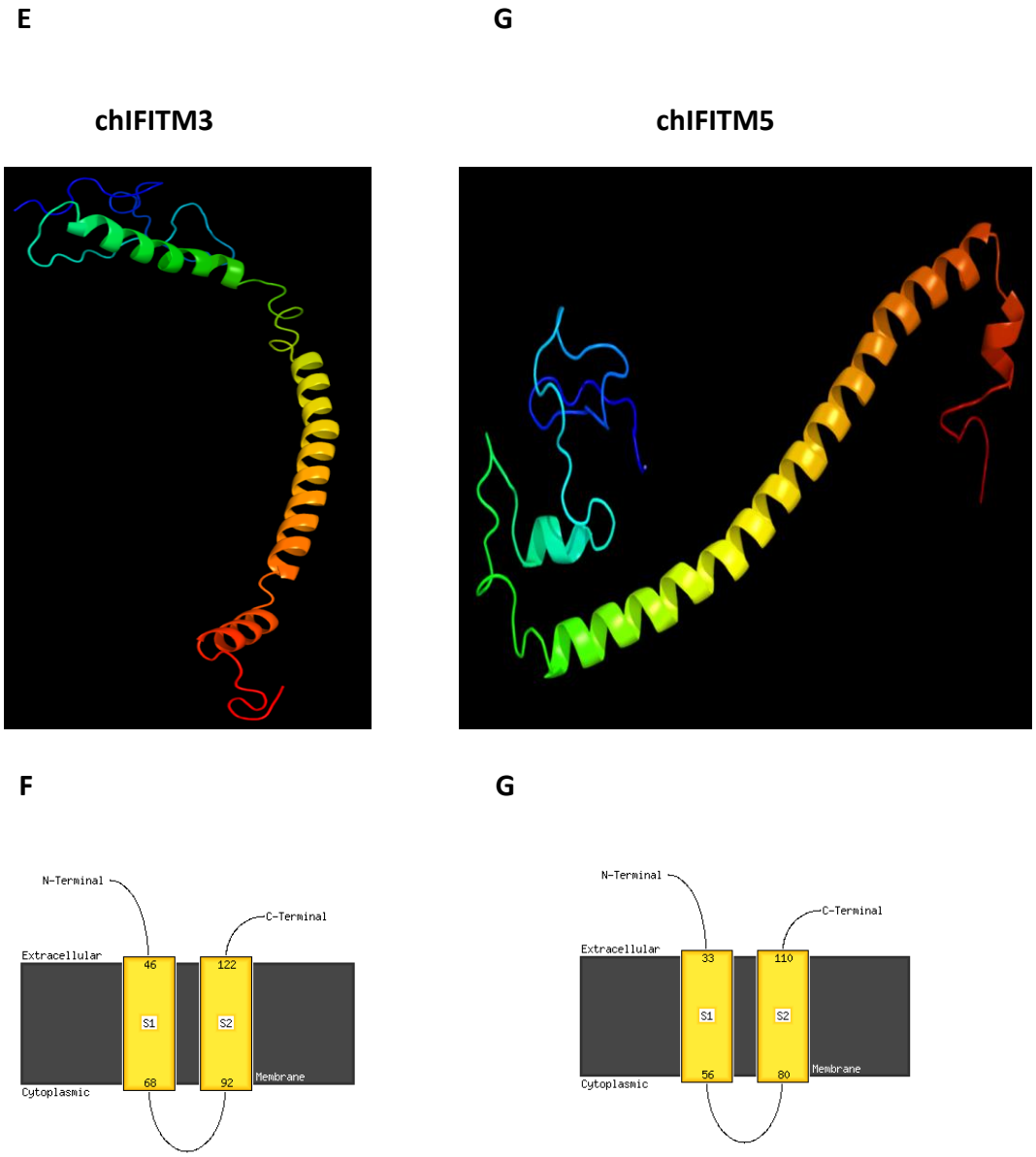

Figure 3.8 Predicted structures of the chIFITM proteins and their corresponding membrane topologies. (A, C, E and G) Amino acid sequences were inputted into the Phyre2 software package (developed by Structural Bioinformatics Group, Imperial College, London) and structures were modelled using the intensive mode setting. In brief, models are generated by PSI-BLAST searches against known homologues, secondary structure is modelled against Psi-pred and Diso-pred databases and from this data a hidden Markov model (HMM) model is generated. Intensive mode allows for further analysis as templates are selected to increase the coverage. (B, D, F, H) Transmembrane helix and topology prediction by memsat-svm.

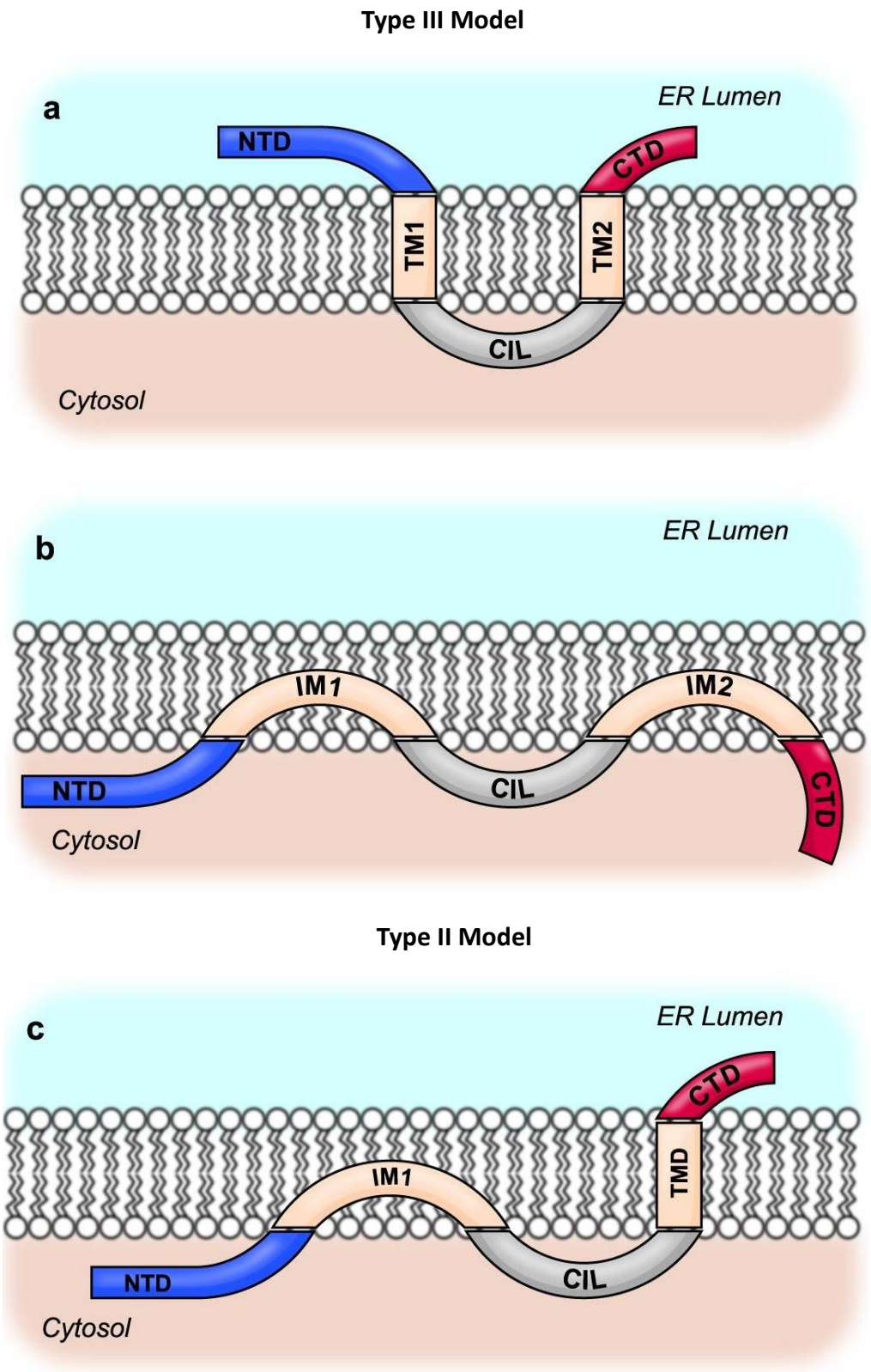

Figure 3.9 Three models of IFITM protein transmembrane topology. (A) A type III transmembrane topology model which has been proposed based on flow cytometry studies. (B) An intramembrane topology with both the N and CTD in the cytosol proposed on findings implicated through the availability of enzymes for PTMs. (C) A type II transmembrane topology model that has been proposed by Ling et al based on NMR and EPR studies of huIFITM3. Figure taken from (Bailey et al., 2014).

The protein modelling software generated 4 protein models alongside the membrane topologies that were expected given the structure generated (Figure 3.8A-H). The models are very similar between the different chIFITMs and suggest that each has a similar structure. In a review published in 2014 (Figure 3.9), Bailey et al show three different models that are proposed based on the different evidence that has been generated thus far. The models generated by Phyre2 most closely resemble a type III transmembrane topology and this has also been proposed by a number of other studies (Brass et al., 2009;Weidner et al., 2010a;Li et al., 2013;Bailey et al., 2013). This model stipulates that the NTD of IFITM1 or IFITM3 is located towards the exterior of the membrane in which the protein is located. The confidence key generated by the software package suggests that there is a high degree of confidence in the transmembrane domains but the N or CTDs have low confidence scores which means that it is not possible to draw confident conclusions on the locations of these on modelling alone. Further studies are required to strengthen the hypothesis that the chIFITM proteins fold in a manner similar to the type III transmembrane topology model as is being proposed.

3.9 Cellular localisation of chIFITM1, 2 and 3 *in vitro*

IFITM proteins are constitutively expressed (Smith et al., 2013;Everitt et al., 2013); however, IFITM expression can be further enhanced through type I IFN signalling. Human and mouse IFITM proteins have been extensively studied, and the localisation of these proteins has been well characterised although different groups still report different outcomes. Human IFITM1 has been shown to localise both at the plasma membrane and at intracellular compartments such as the Golgi apparatus (Weston et al., 2014). Human IFITM3 has been shown to consistently form punctate structures at the early/late endosomes, co-localising with Rab and Lamp1/2 proteins (Weston et al., 2014;Narayana et al., 2015). The localisation of huIFITM2 is more controversial. Some data suggests that

huIFITM2 localises to similar compartments as huIFITM3, in puncta at the early/late endosomes (Narayana et al., 2015). Other groups report staining in punctate structures within the nucleus (Weston et al., 2014). Many studies have reported the possible implications of using tagged constructs, although at present tagged constructs remain important as antibodies against IFITMs have been reported to cross-react (Zhao et al., 2014;Weston et al., 2014;Wrensch et al., 2015). In one study it was found that Anti-IFITM1-NTD antibody detects both IFITM1 and IFITM3, whilst an Anti-IFITM3-NTD antibody detects IFITM3 and IFITM2 (Weston et al., 2014). In chickens, the localisation of the chIFITM proteins remains largely understudied and the available antibodies are poor. Smith et al, 2013 showed that chIFITM1 and 2 localised at the plasma membrane, while chIFITM3 localised at the endosomes (Smith et al., 2013). The only other avian IFITM proteins to have been investigated are the duck IFITMs (dIFITMs) (Blyth et al., 2016). In this study it was found that dIFITM1 and 3 localise to similar compartments as their mammalian counterparts, namely the plasma membrane and late endosomes, respectively. The localisation of dIFITM2 and 5 was far less convincing with only partial co-localisation of staining observed at the endosomes. It is likely that the localisation and their function is linked to the restrictive profile of the IFITM proteins.

To assess the subcellular localisation of chIFITM1, 2 and 3, DF-1 cells were transiently transfected with separate expression plasmids containing the chIFITM gene sequences with a C-terminal FLAG-tag. DF-1 cells were transfected with 1µg of a plasmid encoding chIFITM1, 2 or 3 for 24 hours. Cells were fixed with 4% paraformaldehyde for 10 minutes and permeabilised with 0.1% saponin in PBS. Cells were blocked in 1% bovine serum albumin (BSA) for 30 minutes. The FLAG epitope was targeted by an anti-FLAG M2 antibody, followed by incubation with a secondary antibody conjugated to Alexa Fluor 594. The plasma membrane was stained with a Pan-Cadherin antibody plasma membrane) and

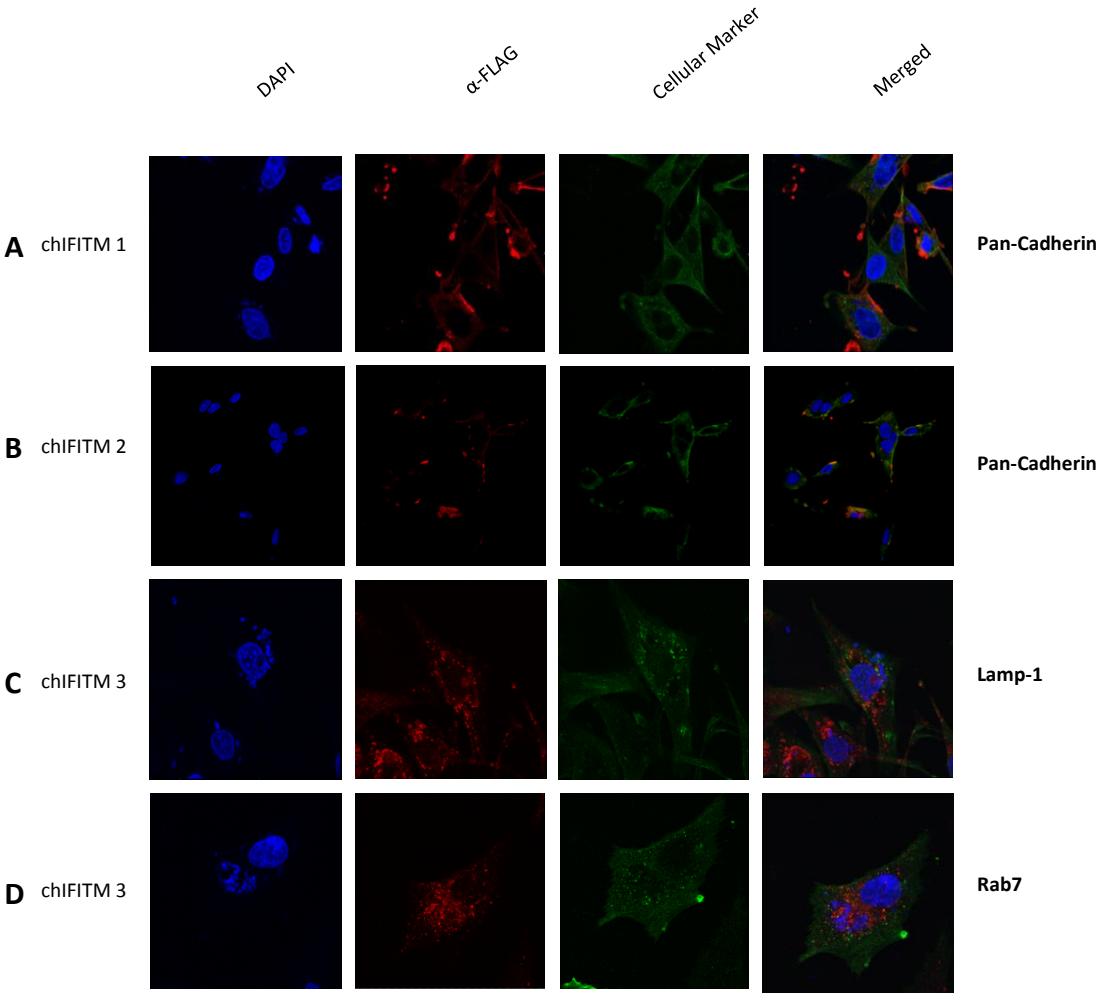

Figure 3.10 Cellular localisation of transiently overexpressed chIFITM proteins in DF-1 and HD11 cells. (A-D) Confocal microscopy in DF-1 cells transfected with plasmids expressing chIFITM1, 2 and 3. Panels show nuclei stained with DAPI (4', 6-diamidino-2-phenylindole [blue]), chIFITM protein stained with an antibody against the FLAG-tag epitope (red) and the intracellular compartments stained with Pan-Cadherin, Rab-7 or Lamp-1 (green) and then merged.

the (endosomes were visualized by a Rab7 antibody (late endosomes), and Lamp1 antibody (lysosomes) followed by incubation with a secondary antibody conjugated to Alexa Fluor 488. In DF-1 cells, chIFITM1 did not localise with any particular marker whilst CHIFITM2 predominantly localised with the plasma membrane, with chIFITM2 co-localising with pan-cadherin (Figure 3.10A and B). In contrast, there was a perinuclear localisation for chIFITM3, consistent with that of huIFITM3 (Figure 3.10C and D).

The localisation of huIFITM1, 2 and 3 has been postulated to have an impact on their restrictive profile, with huIFITM3 localising at the endosomes and restricting viruses such as IAV, which enter through the acidification of late endosomes (Yoshimura et al., 1982). In this part of the chapter, the localisation of transiently overexpressed FLAG-tagged chIFITM1, 2 and 3 was examined in DF-1 cells. The data suggests that both chIFITM1 and 2 predominately localise at the plasma membrane, whereas chIFITM3 failed to localises with Rab7, a marker for the late endosomes, or any other marker that was assessed (data not shown). Previous data has shown that huIFITM1 has been shown to localise at the plasma membrane, whereas huIFITM2 was shown to localise at internal membrane compartments, distinct from the observation of chIFITM2 in avian cells. Alignment of the human and chicken IFITM2 amino acids sequences reveals that chIFITM2 has an N-terminal truncation, lacking the YEML motif (Figure 3.10) and this truncation may explain why chIFITM2 resides primarily at the plasma membrane and may impact the restrictive profile of chIFITM2.

3.10 Identifying proteins that interact with chIFITM1, 2 and 3

3.10.1 Mass spectrometry analysis of chIFITM-FLAG immunoprecipitations

Interacting partners have been identified through a variety of experimental methods such as immunoprecipitations, yeast-2-hybrids and biochemical assays. This has resulted in a range of cellular factors that have been implicated in binding to the huIFITM proteins and it has been hypothesised that these interactions modulate the antiviral phenotype of the IFITM proteins. A study published in 2013 demonstrated that huIFITM3 interacts with Vesicle-membrane-protein-associated protein A (VAPA) which in turn prevents its association with oxysterol-binding protein (OSBP). This interaction disrupts cholesterol homeostasis and inhibits viral entry via cholesterol accumulation (Amini-Bavil-Olyaee et al., 2013). Two further studies found that host cell membranes underwent a loss of fluidity after overexpression of huIFITM1 which may be explained by the findings of Amini-Bavil-Olyaee et al (Li et al., 2013;Lin et al., 2013). In contrast, other studies suggest that IFITM-mediated viral restriction is not dependent on cholesterol and propose a mechanism whereby IFITM3 has an ability to block fusion pore formation at a post-hemifusion stage. It is proposed that this process stabilises the cytoplasmic leaflet of endosomal membranes either directly or indirectly through proteins/lipid independently of cholesterol (Desai et al., 2014). In addition, further co-immunoprecipitation studies suggest that ZMPSTE24 can interact with members of the huIFITM protein family and the data implies that ZMPSTE24 expression is essential for IFITM antiviral activity (Fu et al., 2017). These studies demonstrate the uncertainty regarding the mechanism of IFITM-mediated restriction, although it is possible that more than one mechanism is utilised during infection.

Mass spectrometry was utilised to identify any interacting partners for chIFITM1, 2 or 3, that may help to determine the mechanism of restriction utilised by the chIFITM proteins alongside any additional functions that are, as of now, unknown. DF-1 cells were

transfected with 1µg chIFITM-FLAG or pFLAG-CMV1 control expression vectors. After 24 hours, cells were lysed and chIFITM-FLAG or FLAG immunoprecipitation was performed using a FLAG Immunoprecipitation Kit (Sigma Aldrich). This assay was completed in triplicate for each plasmid, performed on different days. Eluate samples were analysed by western blot to confirm successful immunoprecipitation of chIFITM-FLAG (Figure 3.11A).

Eluates were then sent to the University of Liverpool and were analysed by liquid chromatography mass spec/mass spec (LC-MS/MS) by Dr Stuart Armstrong. In total 269, 230 and 142 proteins were identified in significantly higher levels in the chIFITM1, 2 or 3-FLAG eluate respectively, compared to the FLAG only control (Appendix, Table 7.1, 7.2 and 7.3). Proteins were identified by comparing unique peptides to a database of chicken proteins. As the chicken genome contains regions of poor coverage, thus poor annotation, some sequences were manually mined in order to identify the peptide of interest. In order to reduce the chance of misidentification of interacting proteins, proteins where only a single unique peptide was identified were removed. For each protein identified, the fold-change (Log2) in relative abundance was calculated by comparing chIFITM1, 2 or 3-FLAG to the FLAG control. The p-value, as determined by two-way ANOVA, was calculated from the three independent biological replicates. A p-value above one (-Log10) along with a fold-change (Log2) above two were considered significant interactions and had the highest chance of interacting with one of the chIFITM proteins. For each protein, the confidence score (-Log2) was calculated, which is the cumulative value of p; the probability of the identified peptide sequence occurring randomly, for each unique peptide identified.

To reduce the number of significant hits that were identified, further analysis was conducted by myself with the aim of isolating peptides that may be involved in chIFITM-mediated restriction. To prioritise the proteins that were identified, proteins that are

A

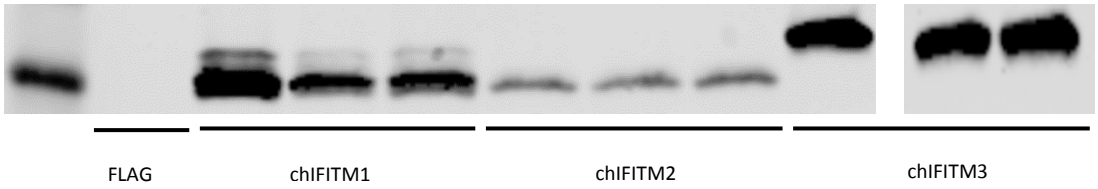
FLAG
chIFITM1
chIFITM2
chIFITM3

B

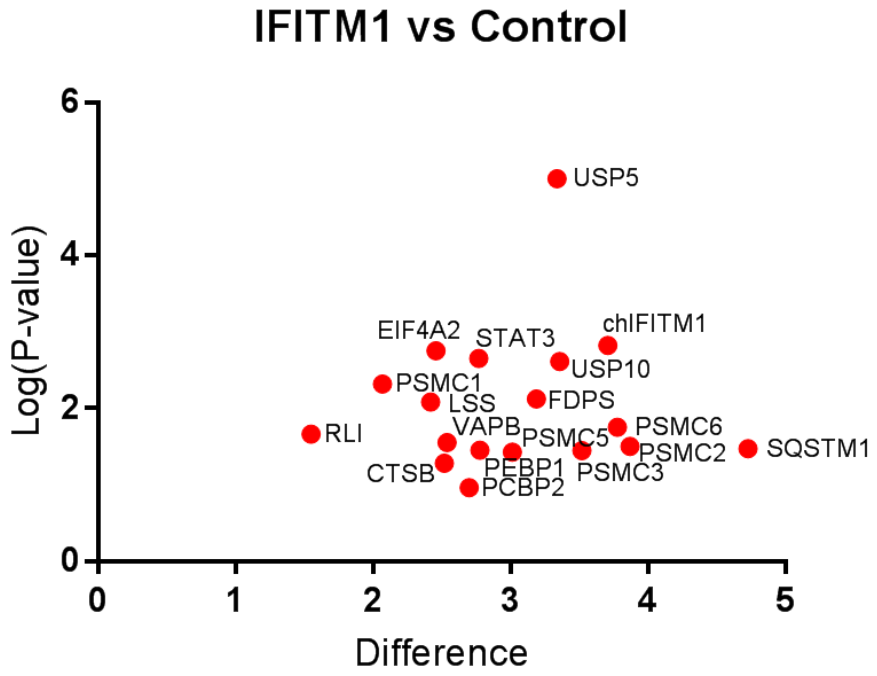
IFITM1 vs Control
Log(P-value)
Difference
USP5
EIF4A2
STAT3
chIFITM1
USP10
PSMC1
LSS
FDPS
RLI
VAPB
PSMC5
PSMC6
PSMC2
SQSTM1
CTSB
PEBP1
PSMC3
PCBP2

C

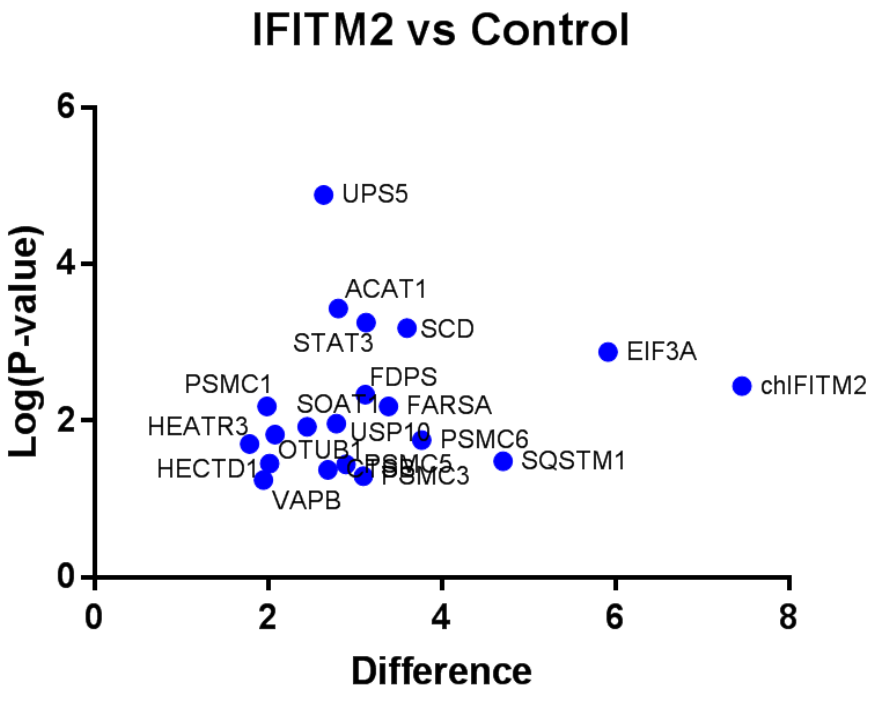
IFITM2 vs Control
Log(P-value)
Difference
UPS5
ACAT1
SCD
STAT3
EIF3A
chIFITM2
PSMC1
FDPS
SOAT1
FARSA
HEATR3
USP10
PSMC6
OTUB1
SQSTM1
HECTD1
PSMC3
VAPB

D

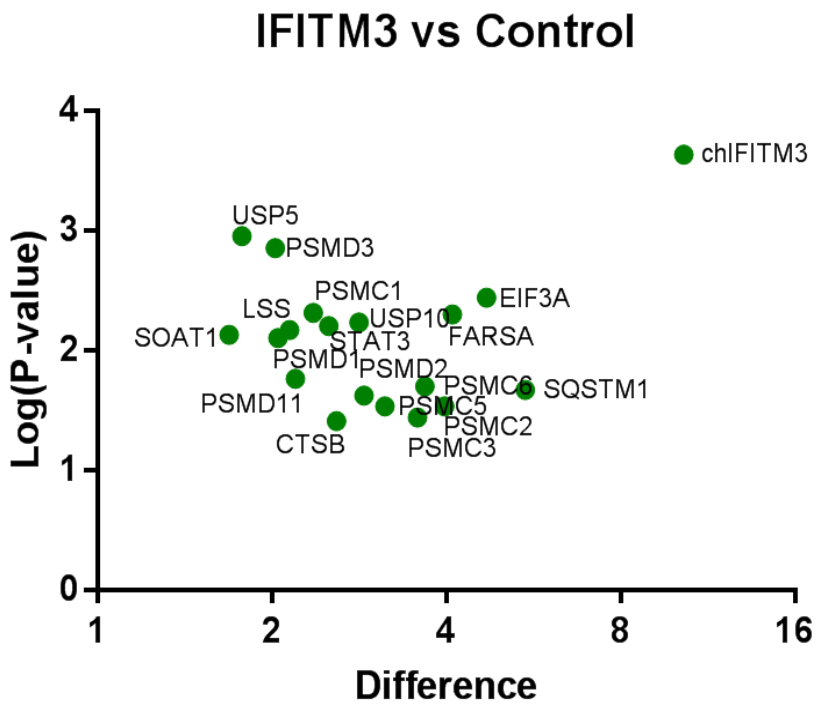

Figure 3.11 Immunoprecipitation of chicken cellular proteins after transient chIFITM-FLAG overexpression. DF-1 cells were transfected with 1µg chIFITM-FLAG or pFLAG-CMV1 expression vectors. After 24 hours, cells were lysed, and immunoprecipitations performed using FLAG 'capture' beads. (A) Eluate samples were separated by SDS-PAGE, transferred to a nitrocellulose membrane and a western blot performed using an anti-FLAG antibody. (B-D) Eluates were then sent to the University of Liverpool and were analysed by liquid chromatography mass spec/mass spec (LC-MS/MS) by Dr Stuart Armstrong. Further analysis conducted by myself, isolated peptides that were significant (as determined by a two-way ANOVA) and may be involved in chIFITM-mediated restriction as determined by prior publications. Results are from three biological replicates.

ubiquitous and have many cellular functions were discounted. For example, it is known that heat-shock proteins (HSP) are 'sticky' and are common in mass spectrometry data (Mellacheruvu et al., 2013) and therefore were excluded from any further analysis. 'Important' hits were determined by function and if they had been identified by previous publications. The final group of interacting proteins (Figure 3.11B - D) are plotted against the difference (x-axis) and Log (P-Value) (y axis). Notably, many proteins were identified that have been implicated in huIFITM-mediated restriction via modulating cholesterol/lipid biosynthesis: Stearoyl-CoA Desaturase (SCD), Sterol O-Acyltransferase (Acyl-Coenzyme A: Cholesterol Acyltransferase) (SOAT1) and Vesicle-Associated Membrane Protein-Associated Protein B/C (VAPB). Moreover, Signal Transducer And Activator Of Transcription 3 (STAT3) was identified and this acts as a transcription activator after IFN activation. As these proteins are involved in processes known to be important for huIFITM-medaited restriction, alongside their association with more than one chIFITM peptide, they were deemed suitable candidate proteins for further investigation.

3.10.2 Co-immunoprecipitations of interacting partners identified through mass spectrometry

In order to confirm if these proteins were interacting with chIFITM1, 2 and/or 3, co-immunoprecipitations were performed in DF-1 cells. Cells were transfected with the required constructs depending on whether the interacting protein has been identified by mass spectrometry. DF-1 cells were co-transfected with 1µg chIFITM-FLAG and SCD-MYC or STAT3-MYC expression vectors and after 24 hours the cells were lysed. In order to identify if the proteins of interest had expressed, the crude cell lysates were separated by SDS-PAGE, transferred to a nitrocellulose membrane and a western blot performed using an anti-FLAG or anti-MYC antibody, alongside a β-actin loading control. The western blots of the cell lysates demonstrate that each of the chIFITMs, SCD and STAT3 expressed well and this

Table 3.3 Function and localisation of proteins classified as significant interacting partners for chIFITM1, 2 and/or 3.

Protein ID	Protein Name	Function	Cellular Localisation
SCD	Stearoyl-CoA Desaturase	Enzyme involved in fatty acid biosynthesis	Endoplasmic Reticulum
SOAT1	Sterol O-Acyltransferase (Acyl-Coenzyme A: Cholesterol Acyltransferase)	Catalyzes the formation of fatty acid-cholesterol esters	Endoplasmic Reticulum
STAT3	Signal Transducer And Activator Of Transcription 3	After activation translocate to the cell nucleus where they act as transcription activators	Cytoplasm/Nucleus
VAPB	Vesicle-Associated Membrane Protein-Associated Protein B/	Involved in vesicle trafficking	plasma and intracellular vesicle membranes

is evidenced by the strength of the bands present. In contrast, in the negative control there was no protein expression in the DF-1 cell lysates and this confirms that the antibodies only bind to their specific epitopes and not to cellular proteins. (Figure 3.12). The β-actin loading control was present at equitable levels in all of the samples that were assayed.

In order to blot for interacting proteins, cell lysates underwent immunoprecipitation and were incubated with FLAG 'capture' beads overnight. These beads were separated, washed three times with co-IP wash buffer and protein-antibody complexes eluted from the beads using a 3x FLAG peptide via the process of competition elution. The eluate samples were separated by SDS-PAGE, transferred to a nitrocellulose membrane and detected with anti-FLAG and anti-MYC. Bands corresponding to the molecular weights of STAT3 and SCD were present in the elutes, which suggests that STAT3 and SCD interact with chIFITM1, 2 and 3. This is an interesting observation as SCD-chIFITM1/3 interactions were not identified in the initial mass spectrometry results. Moreover, it was not possible to clone SOAT1 or VAPB, therefore, it is not possible to draw any conclusions about the interaction of this protein

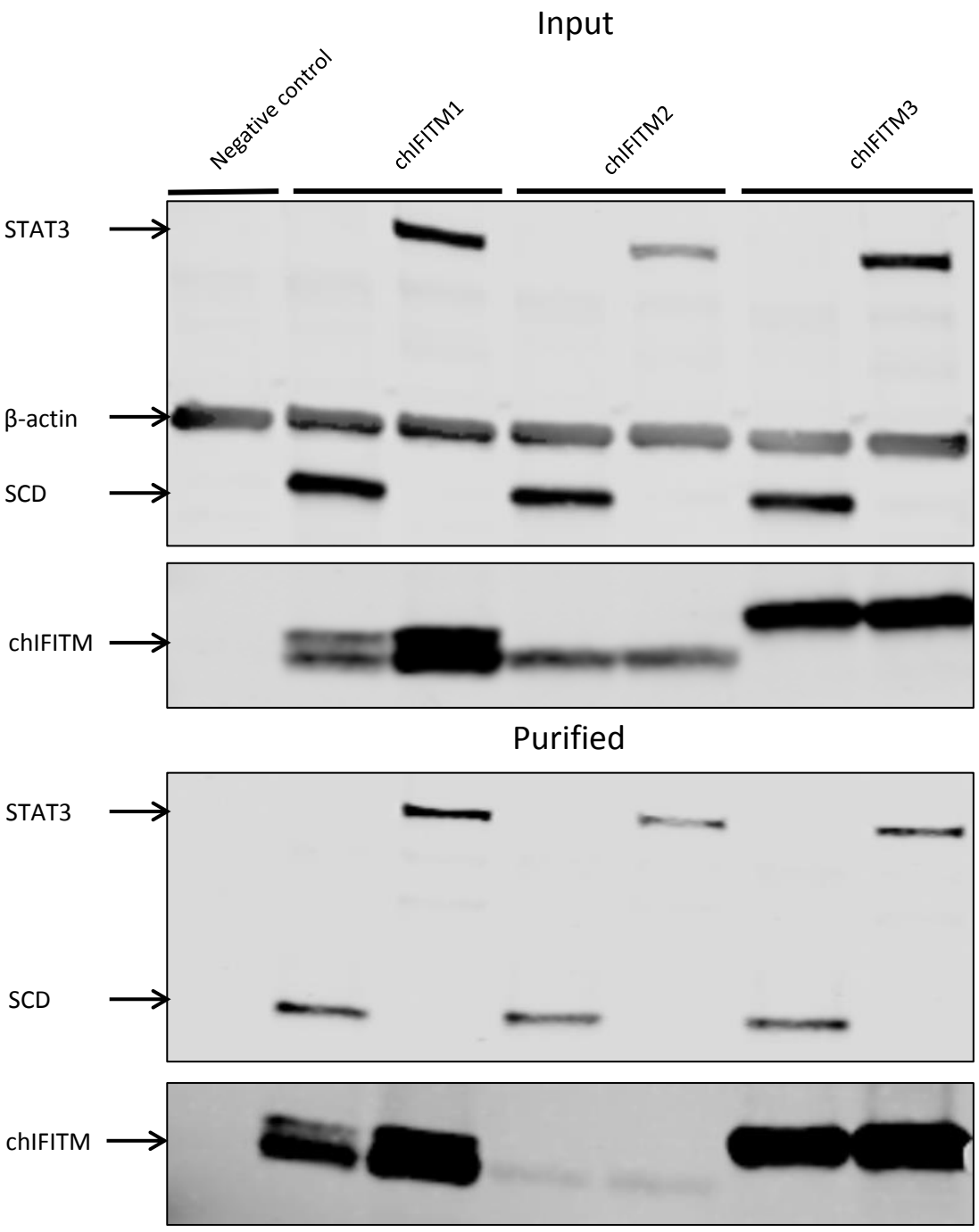

Figure 3.12 Co-Immunoprecipitation of interacting proteins with chIFITM1, 2 or 3. DF-1 cells were co-transfected with 1µg chIFITM-FLAG and SCD-MYC or STAT3-MYC expression vectors. After 24 hours, cells were lysed, and immunoprecipitations performed using FLAG 'capture' beads. (A) Crude cell lysates and eluate samples were separated by SDS-PAGE, transferred to a nitrocellulose membrane and a western blot performed using an anti-FLAG or anti-MYC antibody, alongside a β-actin loading control.

with chIFITM1 and 2. This data implies that STAT3 interacts with chIFITM1, 2 and 3 and may play a role in chIFITM-mediated restriction, especially considering that its interactions are not limited to a specific chIFITM. Moreover, this data may strengthen the mechanism postulated by Amini-Bavil-Olyaee et al as it is known that SCD is involved in lipid biosynthesis. This may imply that the recruitment of cholesterol may also be important in mediating chIFITM viral restriction although further investigation is required.

3.11 Discussion

The use of two different next generation sequencing methods, PacBio and MiSeq, significantly increased the coverage across the chIFITM locus and resulted in the generation of a contiguous sequence across this region. By utilising both PacBio and MiSeq sequencing, it was possible to generate a *de novo* assembly that was an improvement over v4 and v5 of the genome that were available at the time of publication (Bassano et al., 2017). In addition to sequencing of the IFITM locus for the reference genome (*Gallus gallus v5)*, the locus was also sequenced in three chicken cell lines using a novel pull down approach that captures and enriches the DNA within the target sequence (Figure 3.7). Using this approach, excellent coverage of the IFITM locus was obtained in each cell type, suggesting that the DNA pull down probes, developed specifically to target this region, were successful in targeting the region in different cell lines that are routinely used in the laboratory. The majority of the sequence variation that was observed in the different cell lines was found within the NCR or intergenic regions and it is not clear from our findings if this variation will have any impact on gene expression or regulation. The coding SNPs within *chIFITM1* and *3* are synonymous mutations, thus it is likely that they would not have an effect on the function of the protein. The chicken cell lines were sequenced in order to examine the effectiveness of the assays and reagents that were developed to study different aspects of

the chIFITM locus. The data presented in this chapter demonstrates that the reagents can be used across all of the cell lines that have been sequenced.

It is important to recognise that the nomenclature used for identifying the different *chIFITMs* is problematic as the sequence identity between chicken and human IFITM proteins is low (Table 3.1). However, for consistency, the nomenclature that was first described in a study published in 2013 by Smith et al has been used throughout this thesis. The genetic divergence of these genes between avian and mammalian species suggest that they are undergoing both positive selection and purifying selection due to regions of the genes that remain conserved. Smith et al also identified that the direction of transcription of chIFITM1 and 2 was opposite when compared to their mammalian counterparts. It is unknown if the chIFITM locus has undergone any further modifications including gene duplication and inversion with further research necessary. As further characterisation of the restrictive profile of each chIFITM continues, the nomenclature used to identify members of this family may be redefined. At present, the current system of naming the *chIFITMs* based on synteny with the human locus (on chromosome 11) provides the best solution to this problem; rather than re-naming them based on possible functions that have yet to be fully elucidated.

To investigate the basal levels of *chIFITM* mRNA expression, nineteen tissues from 3 RIR chickens at 3 weeks of age, 3 chicken cell lines (DF-1, HD11 and OU-2) and two *ex vivo* cell cultures (CEF and CKC) were evaluated by quantitative RT-PCR (Figures 3.4 and 5). Intriguingly the patterns of *chIFITM* mRNA expression between each tissue analysed were broadly similar. The mRNA expression of *chIFITM2* and *3* were consistently higher in comparison to *chIFITM1* and *5.* Moreover, there was greater variability in mRNA expression levels for *chIFITM1* and *5*, with higher levels of transcripts observed in the gastro intestinal tract and immune tissues such as the caecal tonsil, and lower levels in pancreas, skin and

muscle. This pattern of variable mRNA expression was also observed in each of the cell lines studied. The differential expression of the *chIFITMs* may suggest that some of the genes are more tightly regulated and this may be important in the context of viral infection and innate immunity.

The cellular localisation of huIFITM1, 2 and 3 has been postulated to have an impact on their restrictive profile, although not all studies agree on the exact localisation of these proteins (Weston et al., 2014;Narayana et al., 2015). Studies have shown that huIFITM3 localises to the endosomes and this is important for the restriction of viruses such as IAV, which enter through the acidification of late endosomes (Yoshimura et al, 1982). In this part of the chapter, the localisation of transiently overexpressed FLAG-tagged chIFITM1, 2 and 3 in DF-1 and HD11 cells was examined. This study shows that both chIFITM1 and 2 predominately localise at the plasma membrane, whereas chIFITM3 localises with Rab7, a marker for the late endosomes. It has been shown that huIFITM1 localises to the plasma membrane, whereas huIFITM2 localise at internal membrane compartments, distinct from our observations of chIFITM2 in avian cells (Figure 3.9). This finding is supported by data published in 2016 where dIFITM2 localisation was different to huIFITM2 with weak localisation within the endosomal compartments (Blyth et al., 2016). This data is also consistent with data published by Smith et al where staining of chIFITM2 is predominantly at the plasma membrane (Smith et al., 2013). Alignments of human, chicken, duck and turkey IFITM2 amino acids sequences reveals that chIFITM2 has an N-terminal truncation, lacking the YEML motif (Figure 3.6) which interacts with the μ2 subunit of AP-2 complex and targets the protein for internalisation via clathrin-mediated endocytosis (Jia et al, 2014). This truncation might explain why chIFITM2 resides primarily at the plasma membrane and may impact on the restrictive profile of chIFITM2.

Trying to identify the mechanism of action for the huIFITM proteins has been difficult and there are still many hypothesises that have yet to be definitively proven. In brief, there are two main mechanisms that have been proposed, one where the lipid composition affects the membrane rigidity of membrane-bound compartments (Amini-Bavil-Olyaee et al., 2013;Li et al., 2013;Lin et al., 2013) and another where there is a physical interaction with the membrane, independent of the lipid composition of the membrane (Desai et al., 2014). The data presented in this chapter appears to support the hypothesis of lipid metabolism and the role of cholesterol in the restriction of viruses by IFITM-mediated restriction (Figures 3.11 and 3.12). Genes encoding enzymes involved in lipid biosynthesis and metabolism, such as SCD and SOAT1, have been identified by mass spectrometry and interactions between SCD and chIFITM1, 2 and 3 have been confirmed by co-immunoprecipitation. Moreover, a protein involved in interferon signalling, STAT3, has been identified and this may suggest that the mechanisms involved are more complex than initially envisaged. In addition, VAPB was identified as interacting with chIFITM1 and 2 and this may provide further evidence that these two proteins are localised towards the plasma membrane. VAPB is known to dimerise with VAPA and both are involved in vesicular trafficking which occurs at the plasma membrane. VAPB was not identified as an interacting partner of chIFITM3, a protein found at the endosomes.

Taken together, the data presented in this chapter demonstrates a much clearer understanding of the chIFITM locus and its architecture. Moreover, details regarding chIFITM localisation, basal expression, protein topology and interacting partners have also been elucidated. This data will help inform concepts surrounding the mechanism of chIFITM-mediated restriction. Furthermore, our data demonstrates that despite low sequence identity, conserved domains, basal expression and conserved interacting partners all suggest that the function of these proteins are similar to their mammalian counterparts.

Chapter 4

Characterising *chIFITM* expression

4.1 Introduction

Viruses are dependent on host cells for a number of critical processes during the course of a productive infection. As intracellular parasites they are not capable of independent replication, thus they hijack components of the cellular machinery. Cells do not act as idle bystanders during this process and initiate an innate antiviral response. Type I and II interferons (IFNs) are critical in controlling viral infection by activating a cell-intrinsic anti-viral state (Schultz et al., 1995a;Schultz et al., 1995b;Sekellick et al., 1998). This is achieved by the transcriptional activation and modulation of over 500 genes, collectively known as interferon stimulated genes (ISGs) (Schneider et al., 2014). Invading viral pathogens are identified by specialised intracellular pattern recognition receptors (PRRs) through the detection of pathogen associated molecular patterns (PAMPs) (Mogensen, 2009). Non-host cell derived nucleic acids such as dsRNA can elicit a systemic IFN response (Weber et al., 2006), alongside other structures present on ssRNA viral genomes such as 5' triphosphate groups (Veit Hornung et al., 2006;Pichlmair et al., 2006). Mammalian IFITMs, as ISGs, are known to be highly upregulated once viral infection has been initiated (Li et al., 2017). This upregulation is a critical step in restricting viral replication, reducing the burden of disease in the host. Numerous studies have shown that human IFITM (huIFITM) and mouse ifitm (mifitm) expression can reduce viral replication by several orders of magnitude when compared to control samples (Brass et al., 2009;Foster et al., 2016;Lu et al., 2011). Currently, little is known about the expression of chIFITMs or how they are regulated. Therefore, in this project, chIFITM expression, after treatment with type I and II interferons, a synthetic dsRNA mimic poly(I:C) and lipopolysaccharide (LPS) was investigated. The effect of viral infection *in vitro, in ovo* and *in vivo* with a diverse range of avian viral pathogens on *chIFITM* and *Mx*, expression was also examined. *Mx*, a gene that is highly upregulated in response to viral infection, has been used as a positive control throughout these studies.

4.2 The modulation of *chIFITM* expression through type I and II interferons

The responsiveness of chicken cells to type I and II interferons has been well documented in the literature, but data is often limited to the particular gene of interest. Datasets from broad ranging microarrays or RNA sequencing experiments can mask genes with small induction profiles, resulting in these genes being overlooked (de Veer et al., 2001a;Schoggins et al., 2011;Giotis et al., 2016). In addition, microarrays only investigate genes present on the array and the chIFITMs were often not included due to their incorrect annotation in chicken genome. This has left a gap in the literature regarding the modulation of *chIFITM* expression through treatment with type I and II interferons. Furthermore, little has been published about specific *chIFITM* expression through any mechanism. Two studies have examined the response of chicken fibroblast cells to IFNα stimulation, with one of these studies also utilising a second type II interferon, IFNγ (Smith et al., 2013;Okuzaki et al., 2017). Smith et al examined the responsiveness of DF-1 cells to IFNα and γ and found that there was a modest induction in *chIFITM3* expression after treatment with IFNα (2.5 fold higher than mock) and no induction with IFNγ treatment (Smith et al., 2013). The second study primarily focused on *chIFITM10* induction in CEF cells but found that in the presence of IFNα, there was an increase in *chIFITM2* expression but no significant upregulation in *chIFITM10* expression (Okuzaki et al., 2017). Poly(I:C) is a synthetic analogue of dsRNA which is a potent activator of interferon production (Talal, 1971). Many viruses produce dsRNA as a replicative intermediate and this product modulates the activation of interferon during viral infection (Field et al., 1967;Colby and Duesberg, 1969;Hilleman, 1970). Poly(I:C) is therefore a useful tool for evaluating gene modulation in response to faux viral replication.

The effect of poly(I:C) stimulation (a proxy for the effects of viral infection) on *chIFITM* expression was assessed in three chicken cell lines (Figure 4.1). An aliquot of 500ng of HMW poly(I:C) was added passively to the cell culture medium and samples were harvested 6 hours later. The RNA from these samples was extracted, reverse transcribed and RT-PCR was performed to calculate the relative fold change, relative to a mock control and normalised to three optimized/stable house-keeping genes, β-actin, RPLPO and RPL13. The three cell lines induced *chIFITM* expression differentially, with OU-2 and HD11 cells appearing to be more responsive to poly(I:C) stimulation than DF-1 cells. DF-1 cells treated with poly(I:C) resulted in a significant upregulation in *chIFITM1* (4.9 fold)*, 3* (2.3 fold) and *Mx* (9.9 fold) expression (Figure 4.1A). Conversely, *chIFITM2, 5* and *10* expression was similar to, or below, the levels observed in the mock control. In contrast, much higher levels of expression were observed in HD11 and OU-2 cells, with the fold change for all genes tested being above the level of basal expression. The relative fold change for *chIFITM1* (11.7 fold), *2* (2.3 fold)*, 3* (8.1 fold)*, 10* (2.3 fold) and *Mx* (40.3 fold) were significantly higher than the mock control in HD11 cells (Figure 4.1B). Furthermore, even though *chIFITM5* expression failed to reach statistical significance there was a general trend of upregulation following poly(I:C) treatment. Similarly, a significant upregulation in *chIFITM1* (2.4 fold)*, 2* (5.2 fold) and *Mx* (11.94 fold) gene expression was observed in OU-2 cells (Figure 4.1C). Consistently higher levels of *chIFITM* gene expression in HD11 cells suggests that these cells are more sensitive to poly(I:C) treatment than the other cell lines that were tested and would be a suitable cell line to use for further characterisation.

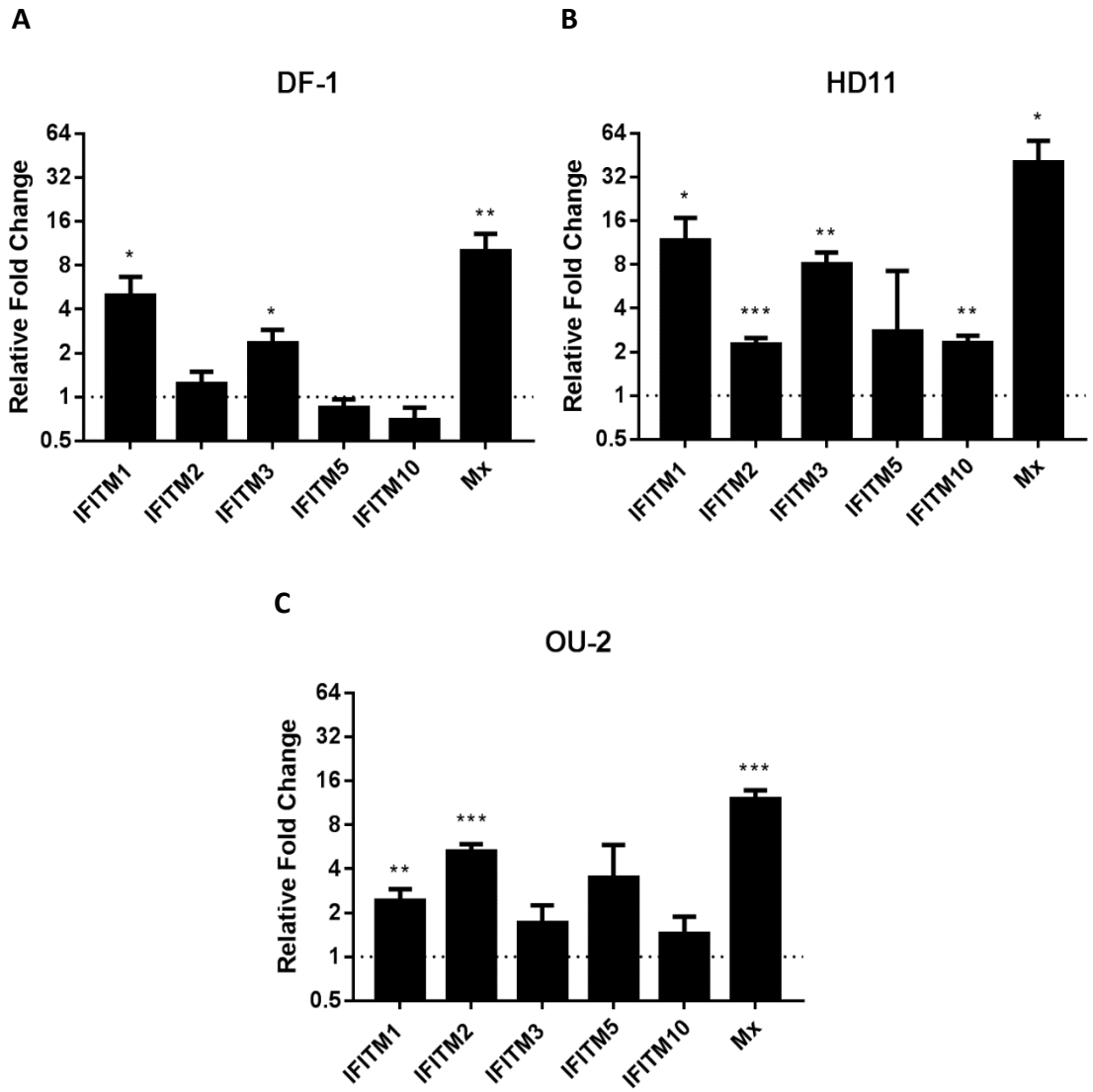

Figure 4.1 Determining responsiveness of chicken cell lines to treatment with poly(I:C). (A – C) Three chicken cell lines (DF-1, HD11 and OU-2) were treated with 500ng of poly(I:C) for 6 hours. These samples were then used in quantitative RT-PCR to assess the upregulation of *chIFITM* and *Mx* mRNA levels which were normalised to a mock control and three house-keeping genes, β-Actin, RPLPO and RPL13. Error bars show standard deviations of the means (*n* =3 biological replicates), * indicates a p-value <0.05, ** indicates a p-value <0.01, *** indicates a p-value <0.001, students t-test.

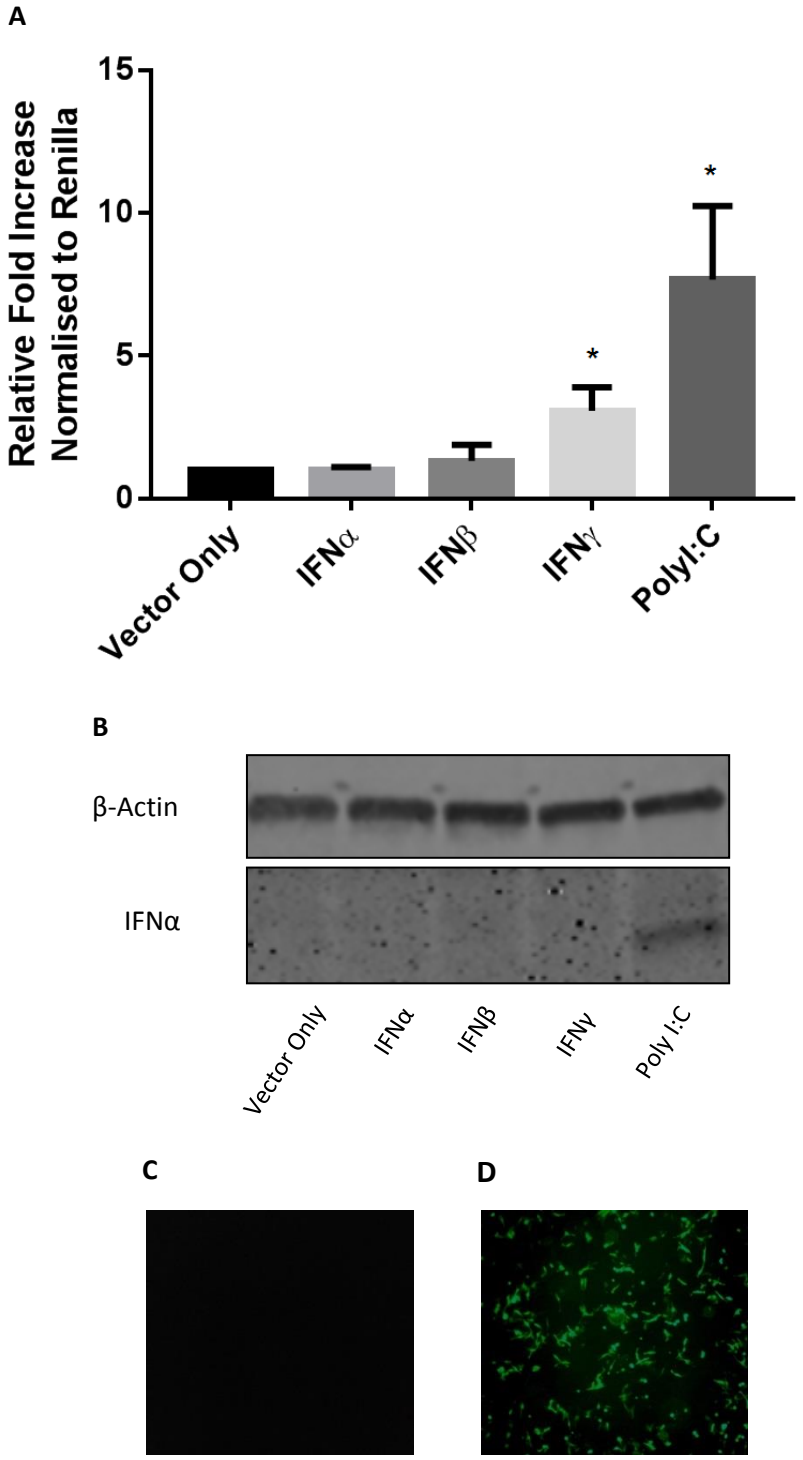

Figure 4.2 IFNβ quantification after stimulation of HD11s by IFN agonists. (A) HD11 cells were treated with IFN agonists and IFNβ promoter activity was quantified by relative luminescence from a luciferase reporter normalised to a Renilla and an empty vector control. (B) The same samples were then assayed via western blot to assess the chIFNα protein levels using an antibody specific to chIFNα as well as cellular β-actin. (C) HD11 cells were transfected with pcDNA3.1 or pEGFP-N1 (D) and were examined under a fluorescent microscope to assess cell line transfection efficiency. Error bars show standard deviations of the means (*n* =3 biological replicates), * indicates a p-value <0.05, student's t test.

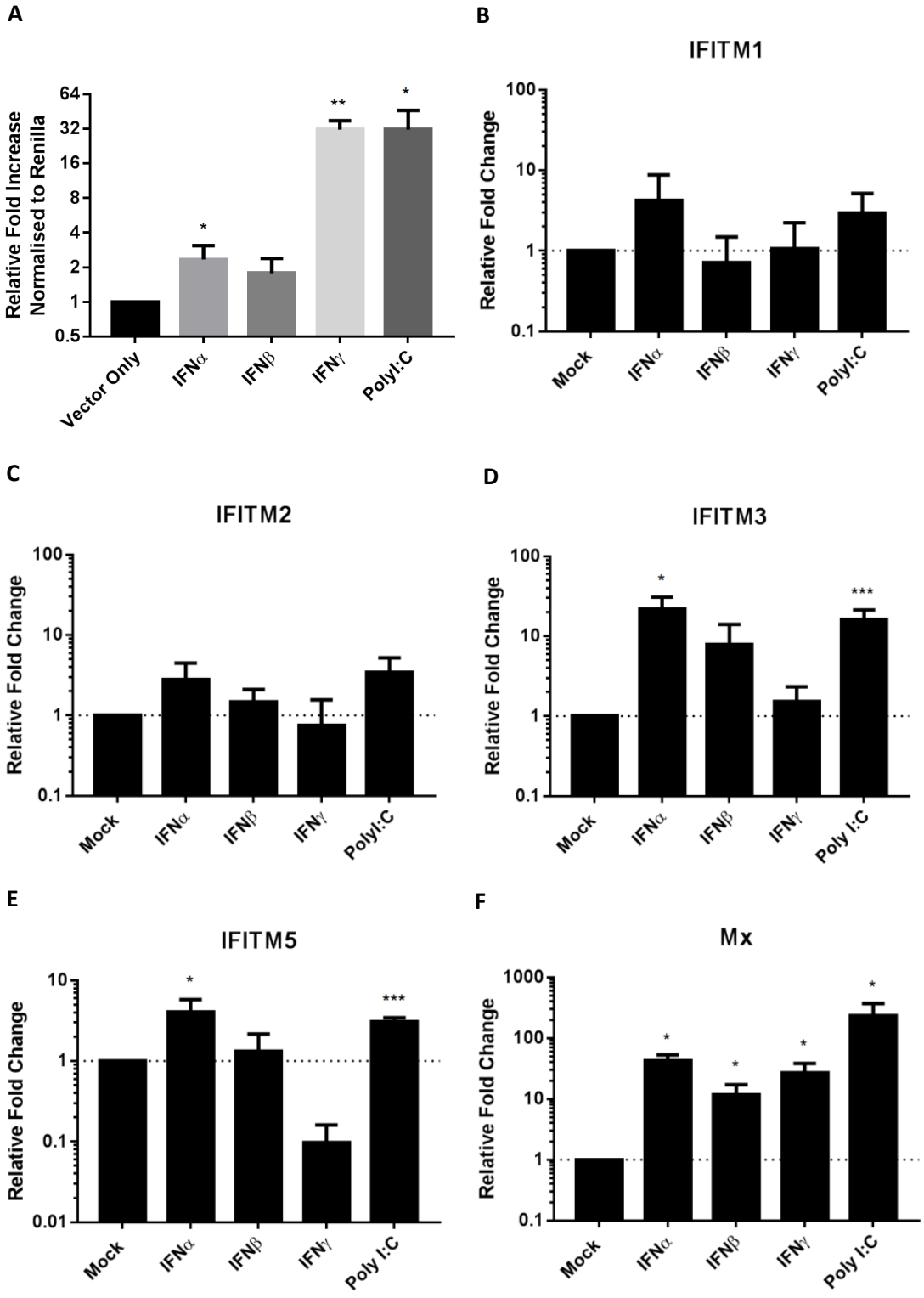

Figure 4.3 IFITM and Mx Induction in HD11s after stimulation with IFN agonists. (A) HD11 cells were treated with IFN agonists and Mx promoter activity was quantified by relative luminescence from a luciferase reporter normalised to Renilla and an empty vector control. (B-F) The same samples were then used in quantitative RT-PCR to assess the upregulation of *chIFITM* mRNA levels which where normalised to a mock control and three house-keeping genes, TBP, PLA2 and β2M. Error bars show standard deviations of the means (n =3 biological replicates), * indicates a p-value <0.05, ** indicates a p-value <0.01, *** indicates a p-value <0.001, Student's t test.

Although poly(I:C) is a good proxy for the replicative intermediates of viral replication, it is not possible to elucidate the type of interferon that is primarily responsible for *chIFITM* induction. To examine the suitability of HD11 cells for promoter reporter assays, they were co-transfected with pGL3-P-chIFN-β-luc and a plasmid constitutively expressing Renilla (internal control) for 24 hours. After 24 hours the same cells were stimulated by passively adding 2000U/ml^{-1} chicken rIFNα, 50µl of chicken IFNβ/IFNγ cell supernatants from stably-expressing COS cells or 500ng of HMW poly(I:C) to the cell culture medium. After 24 hours the cells were lysed and samples were assayed for firefly and Renilla luciferase activity. IFNβ promoter activity was highest with poly(I:C) and IFNγ stimulation and these reached statistical significance when compared to an empty vector control (Figure 4.2A). Type I IFN expression was confirmed by western blot (α-IFNα) in the poly(I:C) treated sample (Figure 4.2B). This confirms that promoter activity as well as protein levels are increased. IFNα expression was not detected in any of the other samples that were assayed, including the vector only background control. The transfection efficiency of HD11 cells was determined by transfecting equal concentrations (500ng) of either pcDNA3.1 (Figure 4.2C) or pEGFP-N1 (Figure 4.2D) and using GFP expression as a read out for total protein expression. The transfection efficiency of HD11 cells was approximately 80%, and taken together with the IFNβ promoter reporter activity and western blot, suggest that HD11 cells were a suitable cell line to continue to elucidate the mechanism of *chIFITM* upregulation.

Having confirmed that HD11s can elicit an effective IFNβ response, the effects of IFN agonists on ISG expression was assessed using an Mx reporter assay as a positive control. Previous studies have shown that Mx is upregulated upon stimulation with a range of interferon agonists, primarily poly(I:C) (Li et al., 2012;Harada et al., 2007). Treatment with 2000U/ml^{-1} rIFNα, 50µl of IFNβ/IFNγ cell supernatants from stably-expressing COS cells or 500ng of HMW poly(I:C) resulted in elevated levels of Mx promoter activity, as shown by the RLU values, normalised to a Renilla control (Figure 4.3A). The levels of Mx expression

varied, with statistically significant inductions observed with the addition of poly (I:C), IFNα and IFNγ. There was an increase in promoter activity after stimulation with IFNβ but this was not statistically significant. In order to quantify chIFITM and Mx upregulation, the same samples were analysed by quantitative RT-PCR, relative to the mock control and normalised to three selected house-keeping genes, TBP, PLA2 and β2M (Figure 4.3B – F). The data generated from this experiment suggests that there are universal up-regulators of *IFITM* expression, namely IFNα and poly(I:C). These two agonists consistently enhanced the expression of all four *chIFITMs* and the *Mx* positive control, reaching significance for chIFITM3 and chIFITM5. Furthermore, the magnitude of upregulation varied between *chIFITMs* which may be related to their function. Interestingly, IFNα elicited a greater induction of *chIFITM* expression compared with the other type I interferon, IFNβ. Many studies have examined the effect of adding exogenous type I interferon to cell cultures and in agreement with these findings, have concluded that IFNα is the more potent type I interferon (Qu et al., 2013). Previous studies have found that huIFITM5 does not act as an ISG, but is involved in bone mineralisation (Moffatt et al., 2008). Notably, this does not appear to be the case for *chIFITM5* as there is a significant upregulation in *chIFITM5* expression after treatment with IFNα and poly(I:C). *Mx* was significantly upregulated with all of the agonists that were tested. Treatment with IFNγ, a type II IFN, resulted in a relatively modest induction of *chIFITM3* and *Mx*. This suggests that type II IFNs are able to elicit *chIFITM* induction, but are not the principal activators of *chIFITM* expression.

4.3 Treatment of chicken cells with lipopolysaccharide (LPS) does not induce *chIFITM* expression

The qPCR data shown in Figure 4.3B-F demonstrates the ability of type I interferons and the synthetic dsRNA poly(I:C) to elicit an effective *chIFITM* response. The data summarising the response of human and mouse IFITMs during bacterial infection is unclear. In an ifitm3$^{-/-}$ mouse model, they find no statistical difference in the disease phenotype when mice are infected with either Salmonella typhimurium, Citrobacter rodentium, or Mycobacterium tuberculosis (MTb) when compared to a wildtype control (Everitt et al., 2013). However, work published on MTb in human monocytic and alveolar/epithelial cells suggests that not only are *huIFITM1, 2* and *3* upregulated, but they also play a role in restricting bacterial infection (Ranjbar et al., 2015). To date, there is no evidence that bacteria or the endotoxin lipopolysaccharide (LPS) induces an effective chIFITM response. The effect of LPS on *chIFITM* expression was tested in two chicken cell lines; HD11 cells that are known to be highly sensitive to LPS treatment (Qi et al., 2017) and DF-1 cells where the data is unclear as to whether LPS treatment is effective in inducing effector genes such as the proinflammatory cytokine interleukin 6 (IL-6). After treatment with 5µg/ ml^{-1} of LPS for 4 hours, DF-1 and HD11 cells were then lysed, total RNA was extracted and reverse transcribed into cDNA and analysed by quantitative RT-PCR. Treatment of DF-1 cells with LPS did not result in the upregulation of any of the genes that were tested, including the positive control, IL-6 (Figure 4.4A). In contrast, there was a significant upregulation in *IL-6* mRNA abundance in HD11 cells (Figure 4.4B). It appears that *chIFITM* and *Mx* expression in HD11 cells is actively downregulated as a result of LPS treatment. Moreover, *chIFITM5* mRNA was not detected in those samples that underwent LPS treatment.

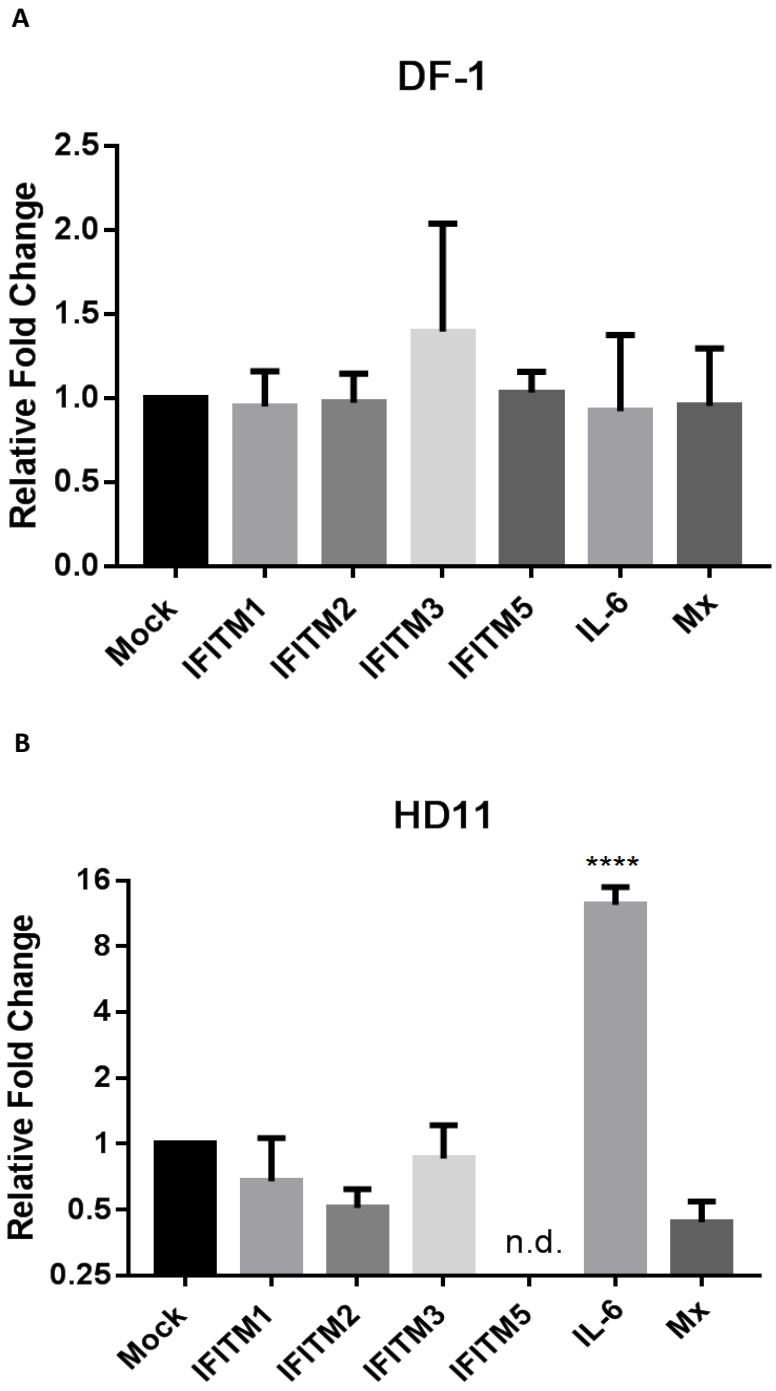

Figure 4.4 IFITM, IL-6 and Mx Induction in DF-1 and HD11 cell after LPS treatment. (A) DF-1 and (B) HD11 cells were treated with 5μg/ml^{-1} LPS for 4 hours and were then used in quantitative RT-PCR to assess the upregulation of *chIFITM, IL-6* and *Mx* mRNA levels which where normalised to a mock control and two house-keeping genes, RPLPO and β-actin. Error bars show standard deviations of the means (n =3 biological replicates), **** indicates a p-value <0.0001, student's t test. n.d. = not detected.

In order to assess the sensitivity of DF-1 cells to a variety of stimuli, an activator of protein kinase C (PKC), phorbol 12-myristate 13-acetate (PMA), was added passively to the media of DF-1 cells alongside samples treated with either LPS or poly(I:C). The aim of this experiment was to assess if DF-1 cells had an intact NF-κB signalling pathway. This was visualised by immunofluorescence using an antibody raised against P65 (an essential transcription factor complex) which, when activated, should translocate into the nucleus (Figure 4.5). The transcription factor P65 is an essential component of NF-κB signalling and has functions that include NF-κB heterodimer formation, nuclear translocation and subsequent activation of the complex. In untreated cells, P65 is located both in the cytoplasm and nucleus (Figure 4.5A) and several posttranslational modifications are required before it becomes active and is translocated into the nucleus. Treatment of DF-1 cells with PMA and LPS results in the translocalisation of P65 from the cytoplasm to the nucleus which indicates that P65 is now active (Figure 4.5B and C). Treatment of DF-1 cells with poly(I:C) did not considerably alter the cellular distribution of P65 which was predominantly located within the cytoplasm (Figure 4.5D).

To assess if the abundance of P65 was altered after treatment with either PMA, LPS or poly(I:C), DF-1 cells were treated with 1ug/ml^{-1} of the aforementioned agonists for 4 hours (or mock treated). The cells were then lysed, proteins separated by SDS-PAGE and transferred onto nitrocellulose membranes. Western blots were performed using a P65 antibody alongside β-actin. The western blot showed that levels of P65 did not change with treatment and were comparable with levels seen in the mock control. This data suggests that DF-1 cells have an active NF-κB signalling pathway, with P65 translocating into the nucleus after treatment with LPS. C*hIFITM, IL-6* and *Mx* transcript abundance did not increase after treatment with LPS in this cell type (Figure 4.4A). Therefore it is not clear as to why treatment of DF-1 cells with LPS did not increase levels of *IL-6* mRNA.

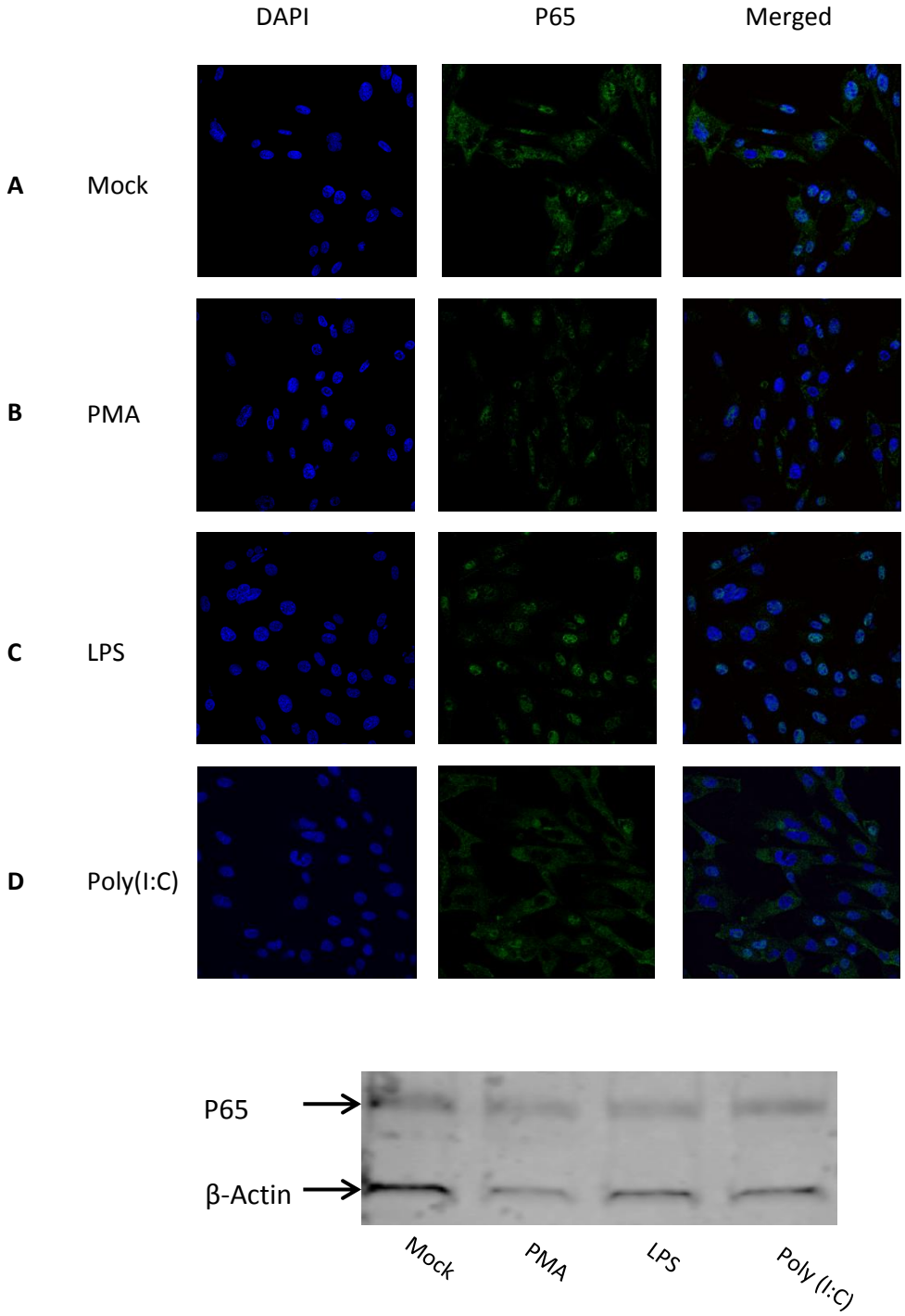

Figure 4.5 Cellular distribution and protein abundance of P65 when DF-1 cells are stimulated with PMA, LPS and poly(I:C). (A-D) Confocal microscopy of DF-1 cells treated with 1ug/ml^{-1} PMA, 1ug/ml^{-1} LPS, 1ug/ml^{-1} poly(I:C) or mock stimulated with PBS for 4 hours. Panels show nuclei stained with DAPI (4', 6-diamidino-2-phenylindole [blue]), cellular P65 stained with an antibody against P65 (green) and then merged. (E) DF-1 cells were treated with 1ug/ml^{-1} PMA, 1ug/ml^{-1} LPS, 1ug/ml^{-1} poly(I:C) or mock treated for 4 hours. Lysates were separated by SDS-PAGE and proteins were transferred to a nitrocellulose membrane and a western blot performed using an antibody specific to P65 as well as cellular β-actin.

4.4 Differential *chIFITM* expression when chicken cells are infected with a diverse range of avian viruses

4.4.1 Influenza A Virus (IAV) infection induces *chIFITM* expression in *ex vivo* cell cultures

Many studies have investigated the role that human and mouse IFITMs play in the restriction of IAV. Extensive investigations in human cell culture models and *in vivo*, utilising ifitm3$^{-/-}$ mice, have conclusively demonstrated that IAV is potently restricted (Everitt et al., 2012;Bailey et al., 2012;Desai et al., 2014). There is currently limited published data on *chIFITM* expression in IAV infected cells, both *in vitro* and *in vivo.* One publication that examined *chIFITM* and duck IFITM *(dIFITM)* expression in high pathogenicity avian influenza (HPAI) (H5N1) infected lung and ilium samples, found that the *chIFITMs* were only modestly upregulated in comparison with the corresponding *dIFITMs.* Moreover, infection with LPAI (H5N2) led to no overall changes in *chIFITM* expression (Smith et al., 2015). To examine what affect IAV infection has on *chIFITM* expression, *ex vivo* cell culture models were utilised alongside an enzootic strain of IAV (A/chicken/Pakistan/UDL-01/08 [H9N2]) and two other representative strains (A/duck/Ukraine/63 [H3N8] and A/duck/sing-Q/119/97 [H5N3]).

Chicken embryonic fibroblasts (CEFs) were infected over a 24 hour time course with H9N2 at a multiplicity of infection (MOI) of 3 and time points were taken at 2, 4, 6, 8, 12 and 24 hours post infection. The cells were lysed, RNA extracted and reverse transcribed and *chIFITM* expression levels were assessed by quantitative RT-PCR, relative to mock and normalised to two house-keeping genes, RPLPO and RPL13. Infection of CEFs with H9N2 lead to a significant upregulation in *chIFITM1* expression at 4 hours post infection and that continued until 24 hour post infection (Figure 4.6A). The upregulation of *chIFITM2*, *3* and *5*

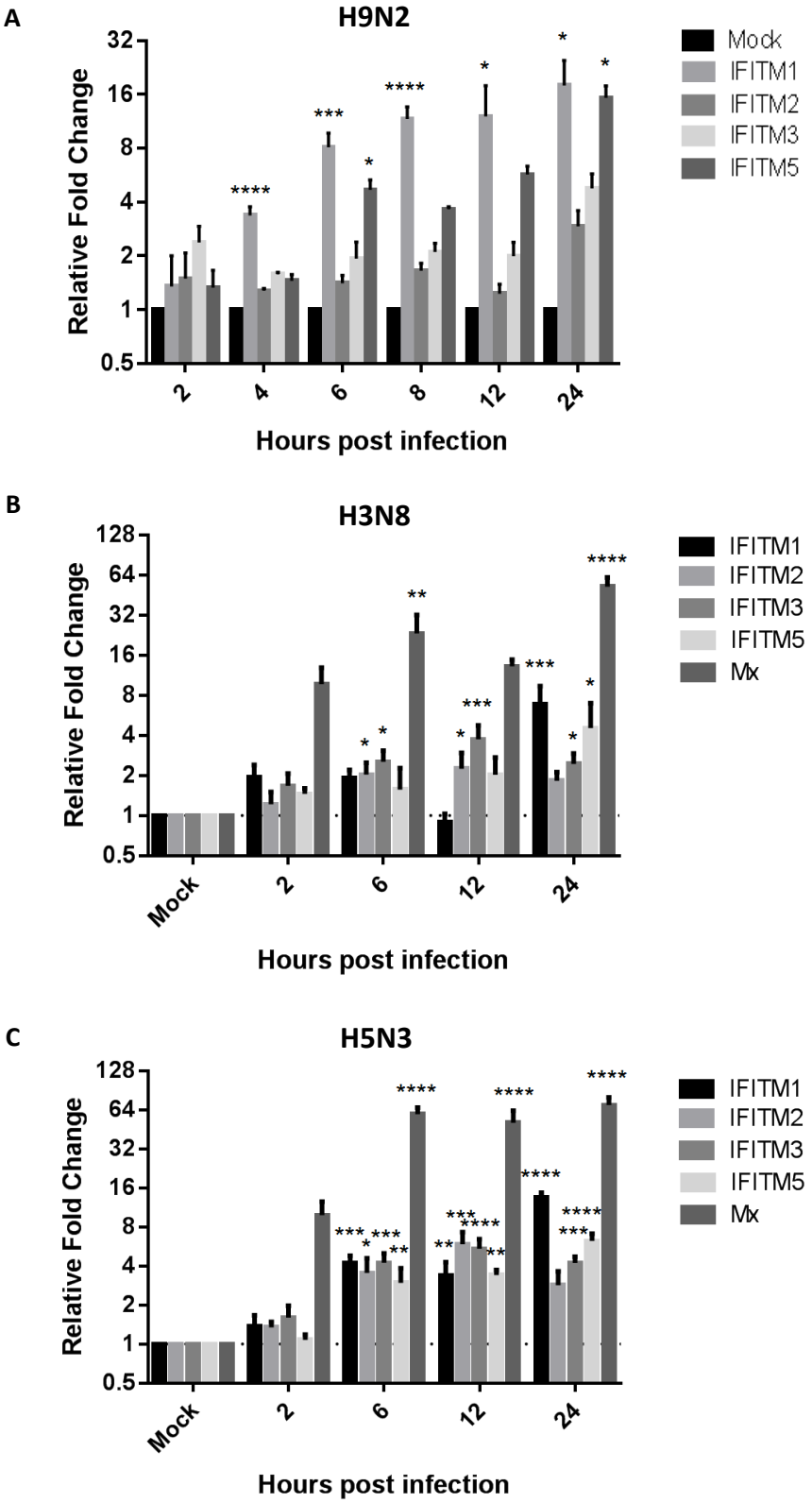

Figure 4.6 Infection of CEFs with H3N8, H5N3 and H9N2 upregulates the expression of the chIFITMs. The expression level and log fold change of *chIFITM1*, *2*, *3*, *5* and *Mx* were measured using quantitative RT-PCR after infection with H9N2 (A), H3N8 (B) or H5N3 (C) IAV (MOI 3) in CEFs, normalised to house-keeping genes, RPLPO and RPL13. Error bars show standard deviations of the means (*n* =3 biological replicates), * indicates a p-value <0.05, ** indicates a p-value<0.01, *** indicates a p-value <0.001, ****indicates a p-value <0.0001, students t test.

showed a similar, but lower level of upregulation over the time course, although upregulation of *chIFITM5* reached significance at 6 and 24 hours post infection. CEFs were also infected with two further strains of IAV (H3N8 and H5N3) at the same MOI for 24 hours. Time points were taken at 2, 6, 12 and 24 hours post infection. The cells were lysed, RNA extracted and reverse transcribed and *chIFITM* and *Mx* expression levels were assessed by quantitative RT-PCR, relative to mock and normalised to two house-keeping genes, RPLPO and RPL13. Similar to what was observed for H9N2; there are significant increases in *chIFITM* expression at each time point that was examined. After infection with H3N8 there were significant increases in *chIFITM* expression that began at 6 hours post infection for *chIFITM2, 3* and *Mx* (Figure 4.6B). At 12 hours post infection both *chIFITM2* and *3* were significantly upregulated, although there was a decrease in *Mx* expression which resulted in a loss of significance over the mock control. At 24 hours post infection *chIFITM1, 3, 5* and *Mx* were significantly upregulated. CEFs were also infected with H5N3 and quantitative RT-PCR was performed on samples that were taken at the time points indicated (Figure 4.6C). Infection with H5N3 lead to a significant upregulation in *chIFITM1, 2, 3, 5* and *Mx* expression at 6 hours post infection that continued 24 hours post infection. Mx is a well-known ISG that is highly upregulated in response to IAV, amongst other viral infections (Staeheli et al., 1986). For the purposes of these experiments, Mx was used as a positive control except for samples infected with H9N2 due to the constraints of the experimental protocol (Figure 4.6A).

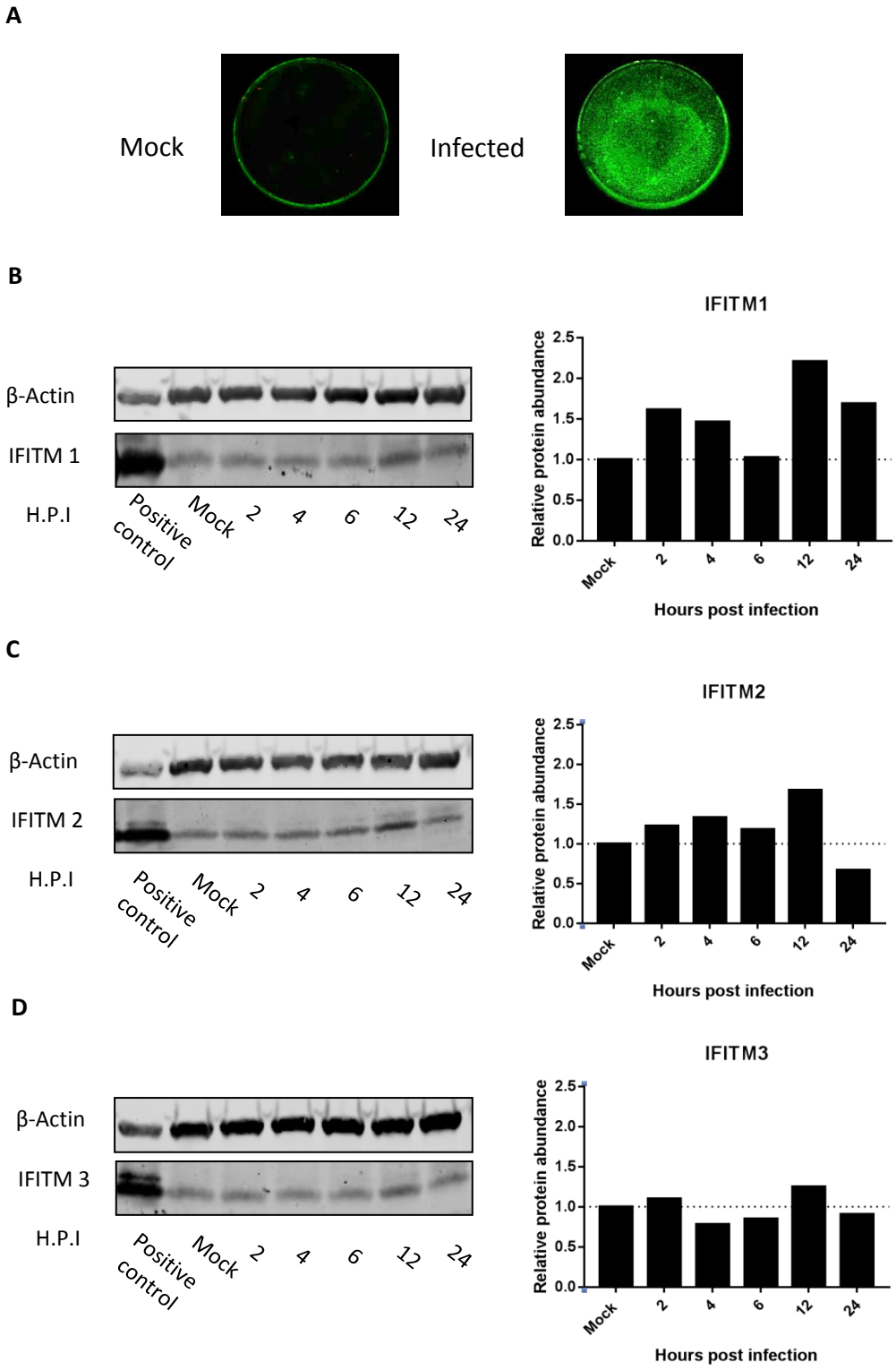

Figure 4.7 Infection of CEFs with H9N2 upregulates the expression of the chIFITMs. (A) CEFs were infected with H9N2 at an MOI 3 for 24 hours. The cells were then fixed and immunohistochemistry performed with a monoclonal antibody against NP. (B-D) CEFs were mock infected or infected with H9N2. Cells were lysed at 2, 4, 6, 12 and 24 hours post infection and lysates were separated by SDS-PAGE. Proteins were transferred to a nitrocellulose membrane and a western blot performed using specific mono or polyclonal antibodies raised against chIFITM1, 2 and 3 with β-actin as the loading control. Densitometry of relative protein expression was performed, normalised to anti-β-actin.

Using immunohistochemistry and a monoclonal antibody against the nucleoprotein (NP) of IAV (Figure 4.7A), the infection efficiency of H9N2 was determined on CEFs mock infected or infected with H9N2 for 24 hours at an MOI - 3. The infection reached 100% of the cells within the 24 hour period. No cells in the mock infected group were positive for the NP, nor was there any background fluorescence detected. In agreement with the quantitative RT-PCR data, we observed an increase in chIFITM1, 2 and 3 protein levels, with the greatest increase observed at 12 hours post infection (Figure 4.7B-D). chIFITM1, 2 and 3 protein levels were elevated at 2 hours post infection but subsequently decreased at 4 and 6 hours post infection. In a biphasic manner, protein levels increased again at 12 hours post infection before subsiding again at 24 hours post infection. Protein levels at 24 hours post infection for chIFITM2 and 3 fell below the level observed for mock infection, while protein levels for chIFITM1 remained higher. This suggests that these IFITMs are not only highly upregulated at a transcript level but protein translation is also increased as a result of infection with IAV, and appears to be tightly regulated. However, due to ongoing issues with antibody production it is not possible to repeat this experiment.

4.4.2 Infectious bronchitis virus (IBV) infection induces *chIFITM* expression in *ex vivo* cell cultures

Several studies have shown that huIFITMs potently restrict coronaviruses such as severe acute respiratory syndrome (SARS) and Middle East respiratory syndrome (MERS) (Huang et al., 2011;Zhao et al., 2018). Furthermore, as well as demonstrating restriction, studies also examine the mode of action of huIFITMs to restrict coronaviruses, concluded to be mediated via a cholesterol-independent mechanism (Wrensch et al., 2014). In contrast there are no current publications that study chIFITM in the context of coronaviruses that infect poultry, namely the prototypic gamma-coronavirus, infectious bronchitis virus (IBV). In order to fill this gap in the literature, chIFITM upregulation in the context of IBV infection

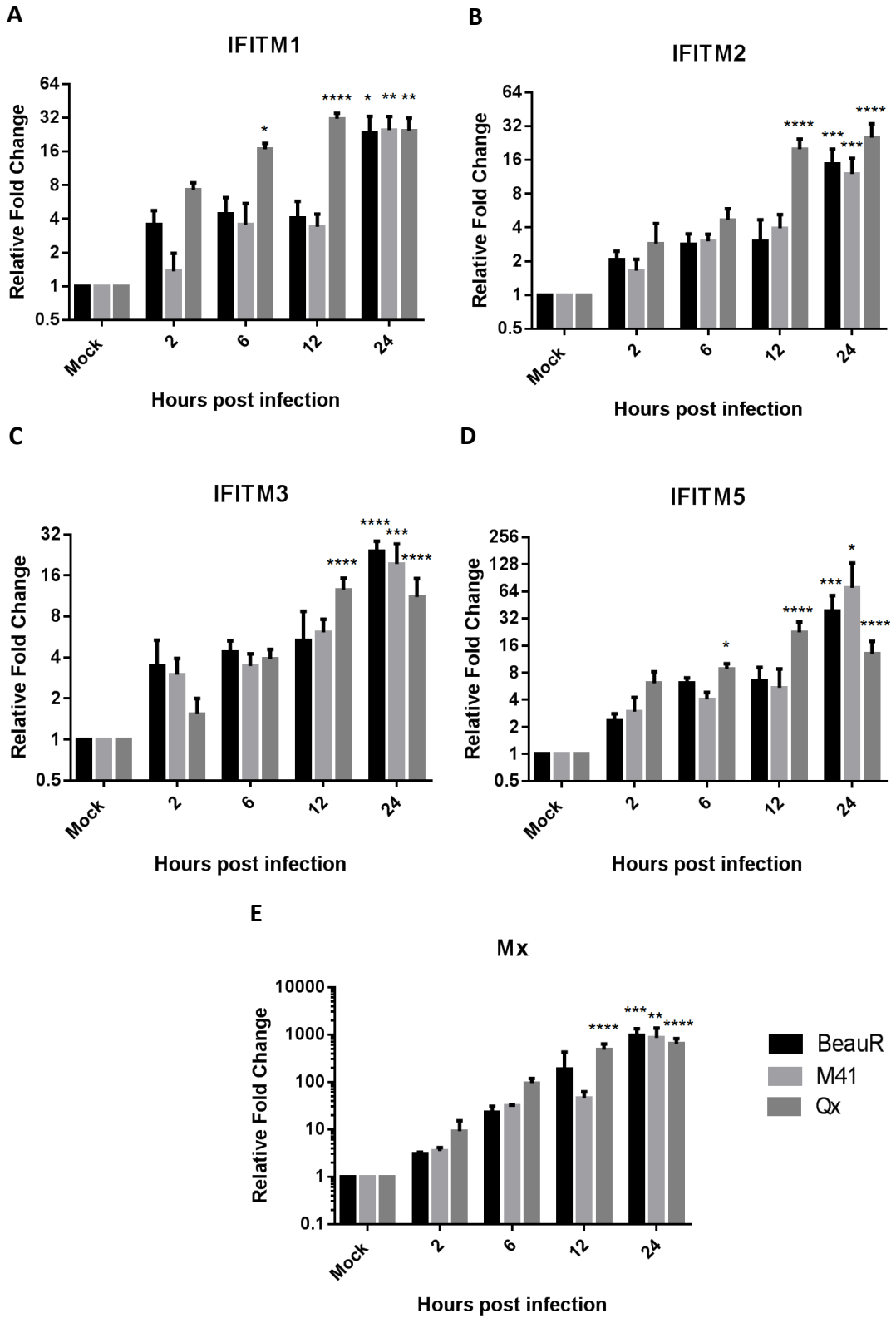

Figure 4.8 Infection of CK cells with BeauR, M41 and QX upregulates the expression of the chIFITMs. (A-E) The expression level and log fold change of *chIFITM1*, *2*, *3* , *5* and *Mx* were measured using quantitative RT-PCR after infection with BeauR, M41 and QX (MOI 1) in CK cells, normalised to house-keeping genes, RPLPO and RPL13. Error bars show standard deviations of the means (*n* =3 biological replicates), * indicates a p-value <0.05, ** indicates a p-value<0.01, *** indicates a p-value <0.001, ****indicates a p-value <0.0001, one-way ANOVA.

was studied in a primary *ex vivo* tissue culture model. Chick kidney (CK) cells were infected over a 24 hour time course with three strains of IBV that have different pathogenicities and tissue tropisms. These comprised a tissue culture attenuated strain (BeauR), a pathogenic field strain (M41) and a virulent nephropathogenic strain (QX) with time points taken at 2, 6, 12 and 24 hours post infection. The cells were lysed, RNA extracted, reverse transcribed and *chIFITM* and *Mx* mRNA expression levels were assessed by quantitative RT-PCR, relative to mock and normalised to two house-keeping genes, RPLPO and RPL13. Levels of *chIFITM1 mRNA* transcript abundance differed significantly from each other when CK cells were infected with these different strains of IBV (Figure 4.8A). At 2 hours post infection there was a large, but not significant, increase in the relative fold change in BeauR and QX infected samples, but not for cells infected with M41. This affect was lost for BeauR infected cells at 6 hours post infection and levels of *chIFITM1* expression in BeauR and M41 infected cells remained similar for all the time points that were assessed after 6 hours post infection. In comparison, levels of *chIFITM1* transcript abundance were much higher in QX infected cells and there was a significant upregulation starting at 6 hours post infection and continuing through to 24 hours post infection. *chIFITM1* expression was broadly similar for all strains at 24 hours post infection. A similar pattern of upregulation was observed across all of the chIFITMs, with a stepwise increase in *chIFITM and Mx* expression over time. In agreement with *chIFITM1,* QX infected cells had a higher level of *chIFITM* expression at earlier time points in comparison with both BeauR and M41 infected cells. Significant increases in *chIFITM2* and *3* expression were seen at 12 hours post infection when cells were infected with the QX strain. A significant upregulation of *chIFITM2* and *3* expression was observed at 24 hours post infection in all samples, irrespective of the virus used. The pattern of *chIFITM5* expression was similar to that observed for *chIFITM1* (Figure 4.8D). *chIFITM5* expression was significantly upregulated in QX infected cells, starting at 6 hours post infection and continuing throughout the time course. *chIFITM5* expression in BeauR

and M41 infected samples also reached significance at 24 hours post infection. The upregulation of *chIFITM2* and *3* in the same samples were broadly similar, with significant increases in transcript abundance typically occurring later on during infection (Figure 4.8B and C). In agreement with *chIFITM* expression, there was also a significant increase in *Mx* expression at 24 hours post infection and this was irrespective of the strain of IBV that was tested (Figure 4.8E). Interestingly there was also an increase in *Mx* expression at 12 hours post infection in the samples that had been infected with QX. This suggests that QX infection leads to an earlier onset of *chIFITM* and *Mx* expression which is significantly different to the other two strains that were tested.

4.4.3 Assessing the effect of temperature and subsequent viral assembly and egress in modulating chIFITM expression

Anecdotal evidence has suggested that BeauR is unable to replicate *in vivo* which may be significant, given the difference in temperature commonly used in cell culture (37°C) and the core temperature of birds (41°). Furthermore, research conducted by both the Genetics and Genomics and Avian Endemic Virus groups at The Pirbright Institute, have shown that live virus cannot be isolated from infected birds or from cells infected *in vitro* at 41°C. Although it has been established that cells at 41°C cannot establish a productive infection, it is still unclear as to whether the virus is able to replicate, and indeed, whether either of these would have an impact on *chIFITM* expression. In order to assess the impact temperature has on *chIFITM* expression, DF-1 cells were infected with BeauR and incubated at either 37°C or 41°C before downstream analysis was performed.

DF-1 cells were infected with BeauR at a high MOI (5) for 8 hours after which viral supernatants and cell lysates were taken for analysis via plaque assay titration and quantitative RT-PCR, respectively. Cell supernatants were harvested and serially diluted (10-fold) in 1x BES media before infecting CK cells. After 1 hour the inoculum was removed and

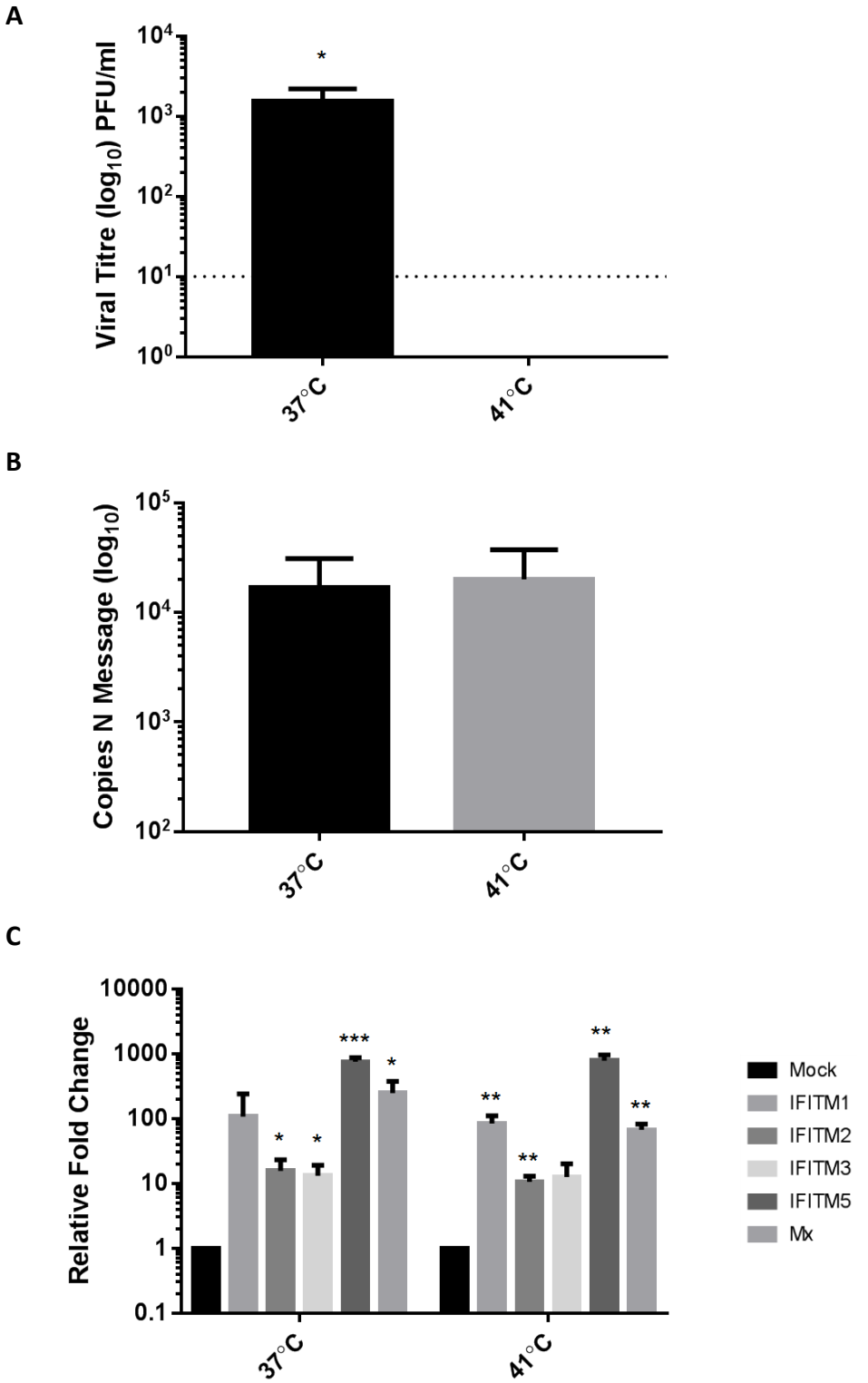

Figure 4.9 Infection of DF-1 cells with BeauR at 37°C and 41°C upregulates the expression of the chIFITMs. DF-1 cells were infected with BeauR (MOI 5). (A) Viral replication was measured by plaque assay titration in CK cells of the infected cell supernatant. (B) Viral transcription was assessed by absolute quantification of the viral N message by quantitative RT-PCR. (C) The expression level and log fold change of *chIFITM1*, *2*, *3*, *5* and *Mx* were measured using quantitative RT-PCR normalised to house-keeping genes, RPLPO and RPL13. Error bars show standard deviations of the means (*n* =3 biological replicates), * indicates a p-value <0.05, ** indicates a p-value<0.01, *** indicates a p-value <0.001, student's t-test.

the cells were overlaid with 2x BES media and 2% agar. Cells were incubated for 3 days until plaques in the cell monolayer were visible. The cells were fixed with paraformaldehyde and stained using crystal violet. In agreement with previous observations made by the Bickerton lab (The Pirbright Institute), plaque assays indicated the viral titre of BeauR when incubated at 37°C is $1x10^3$ Pfu/ml at 8 hours post infection. In comparison there were no visible plaques observed when DF-1 cells are infected and incubated at 41°C (Figure 4.9A). This suggests that a productive infection could not be established in cells placed at the higher temperature. It is still unclear as to whether the virus is unable to replicate at this temperature or whether the higher temperature interferes with viral assembly and/or egress. To address these questions the cells were lysed, RNA extracted, reverse transcribed and quantitative RT-PCR was performed on the N protein sgRNA of BeauR (Figure 4.9B). The N protein sgRNA is a product of BeauR replication, thus is a marker for active viral replication within the cell (Maier et al., 2013b). The copy number of N sgRNA was calculated from a standard curve using plasmids encoding the target sequence. There was no significant difference in the copies of N sgRNA detected with cells incubated at both temperatures containing ~$1x10^4$ copies of N sgRNA/12.5ng RNA. This data suggests that replication of the virus is not affected by temperature; therefore viral assembly or egress of the virus is likely to be impacted by the increase in temperature.

To assess whether temperature has an impact on *chIFITM* and *Mx* upregulation, quantitative RT-PCR was utilised to examine the relative fold change of the *chIFITM* and *Mx* genes, relative to a mock infected control and normalised to two house-keeping genes, RPLPO and RPL13 (Figure 4.9C). The results show that *chIFITM* and *Mx* upregulation are unaffected by temperature. The upregulation profiles are very similar, with *chIFITM1*, *2, 3* and *5* all displaying equivalent fold changes between temperatures. Although the relative fold changes were similar between temperatures, the statistics indicate that there are large

standard deviations within samples which accounts for the disparity in assigning statistically significant upregulation in gene expression.

Taken together, this data suggests that temperature does not affect viral genome replication; instead it is likely to be implicated in viral assembly, or egress of the virus. Moreover, *chIFITM* expression does not appear to be affected by this change in temperature and it is likely that chIFITM mRNA expression is dependent on the early stages of a virus life cycle, namely entry and/or replication.

4.4.4 Herpesvirus of Turkeys (HVT) infection transiently upregulates *chIFITM5* and *Mx* mRNA expression

Herpesvirus of Turkeys is the third serotype within the Marek's disease virus (MDV) group. This group contains viruses that are genetically and antigenically related lymphotropic avian herpesviruses (Afonso et al., 2001). MDV1 is the etiologic agent which manifests itself as a lymphoma-causing virus in chickens and is important because of its global distribution and the large economic effect it has on the poultry industry (Prasad, 1979). In comparison, HVT is non-pathogenic in chickens, and because of this, and the associated cross-reactive immune response due to viremia, it has been used extensively as a vaccine candidate for viruses that infect poultry (Witter, 1972;Witter et al., 1970). Vaccine candidates have been produced for protection against: Newcastle disease virus (El Khantour et al., 2017), infectious bursal disease virus (Darteil et al., 1995;Perozo et al., 2009), influenza A virus (Kapczynski et al., 2016;Rauw et al., 2012) and MDV (Gimeno et al., 2016). HVT contains a large dsDNA genome of 159kb encoding 99 functional genes (Afonso et al., 2001). HVT as a large dsDNA virus is very different to both IAV and IBV (as RNA viruses) which increases the viral diversity being assessed in the context of *chIFITM* expression. Furthermore, it is known that HVT is able to induce a protective immune response when used as a vaccine vector.

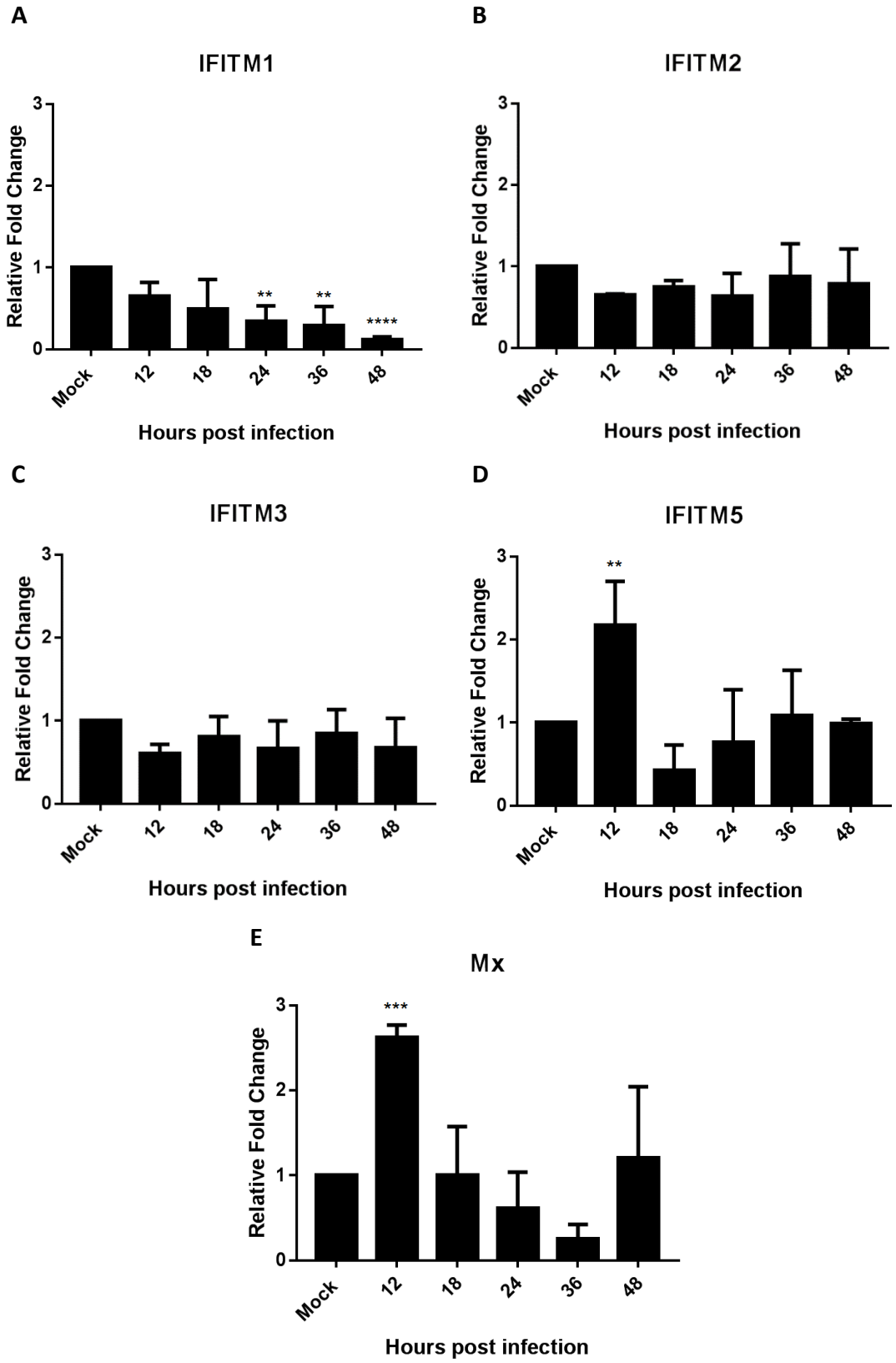

Figure 4.10 Infection of DF-1 cells with HVT transiently upregulates *chIFITM5* and *Mx* expression. (A-E) The expression level and log fold change of *chIFITM1*, *2*, *3*, *5* and *Mx* were measured using quantitative RT-PCR after infection with HVT (MOI 0.01) in DF-1 cells, normalised to house-keeping genes, RPLPO and RPL13. Error bars show standard deviations of the means (*n* =3 biological replicates), ** indicates a p-value<0.01, *** indicates a p-value <0.001, ****indicates a p-value <0.0001, one-way ANOVA.

These factors meant that it was unclear if this virus would elicit an innate immune response.

DF-1s were infected over a 48 hour time course with HVT at an MOI 0.01 (CEF:DF-1 ratio) and time points were taken at 12, 18, 24, 36 and 48 hours post infection. The cells were lysed, RNA extracted, reverse transcribed and *chIFITM* and *Mx mRNA* expression levels were measured by quantitative RT-PCR, relative to mock samples and normalised to two house-keeping genes, RPLPO and RPL13. Infection of DF-1 cells with HVT resulted in a downregulation in *chIFITM1, 2* and *3 mRNA* expression, and reaching levels of significance for *chIFITM1* mRNA expression from 24 to 48 hours post infection (Figure 4.10A – C). In contrast, *chIFITM5* mRNA expression was significantly upregulated (>2 fold) at 12 hours post infection when compared to a mock infected control. This expression decreased at 18 hours and then steadily increased again at 24 and 36 hours post infection before plateauing at 48 hours post infection with levels remaining similar to those observed in the mock infected control (Figure 4.10D). The levels of *Mx* mRNA expression were also significantly upregulated at 12 hours post infection, but again levels decreased at 18 hours post infection and continued to decrease in a stepwise manner at 24 and 36 hours post infection before reaching levels similar to those observed in the mock samples at 48 hours post infection (Figure 4.10E).

This data is markedly different to that observed for IAV and IBV infected cell cultures where a general trend of increased mRNA expression of all four *chIFITMs,* and the positive control *Mx,* was observed over the course of infection. Infection of DF-1 cells resulted in the transient upregulation of *chIFITM5* and *Mx*. This effect was not observed for any other *chIFITM,* at any other time point. This may suggest an active down regulation or suppression of *chIFITM* and *Mx* expression which may contribute to its efficiency as a possible vaccine candidate.

4.4.5 *In ovo* infection with H9N2 upregulates the expression of the chIFITMs

In addition to assessing the *in vitro* upregulation of *chIFITMs* in response to infection with IAV, IBV and HVT, the effects of *in ovo* IAV infection upon *chIFITM* gene expression was also analysed. Infection *in ovo* allows the examination of the response of the developing chick to challenge with H9N2. This has not been explored before in the context of *chIFITM* upregulation. Furthermore, as vaccines for both human and veterinary use are currently produced in embryonated hen's eggs, it will prove useful to assess the impact *in ovo* restriction may have on the vaccine yields that are currently achievable using this model of vaccine production. Ten-day old SPF Rhode Island Red embryonated chicken eggs were inoculated via injection into the allantoic cavity with $1x10^3$ pfu of H9N2 (A/chicken/Pakistan/UDL01/08) and tissue samples were taken at 24, 48 and 72 hours post infection from the lung, liver and intestine. Samples were also taken from mock (PBS) infected embryos. Samples were homogenised using the TissueLyser, total RNA was extracted and reverse transcribed into cDNA. Quantitative RT-PCR was performed, relative to three mock controls at each time point and normalised to two house-keeping genes, RPLPO and RPL13.

There was no significant upregulation of *chIFITM1* or *5* in the lung, at any time point post infection (Fig 4.11A and D) although a general trend of upregulation post infection was identified. The upregulation did not reach statistical significance because of the large standard deviation between samples. In comparison, a significant upregulation of *chIFITM2* in the lung was detected at all time points post infection, with the most significant upregulation occurring at 72 hours post infection (Fig 4.11B). Furthermore, *chIFITM3* and *Mx* were significantly upregulated at 48 and 72 and 24 and 72 hours post infection, respectively (Fig 11C and E).

Lung

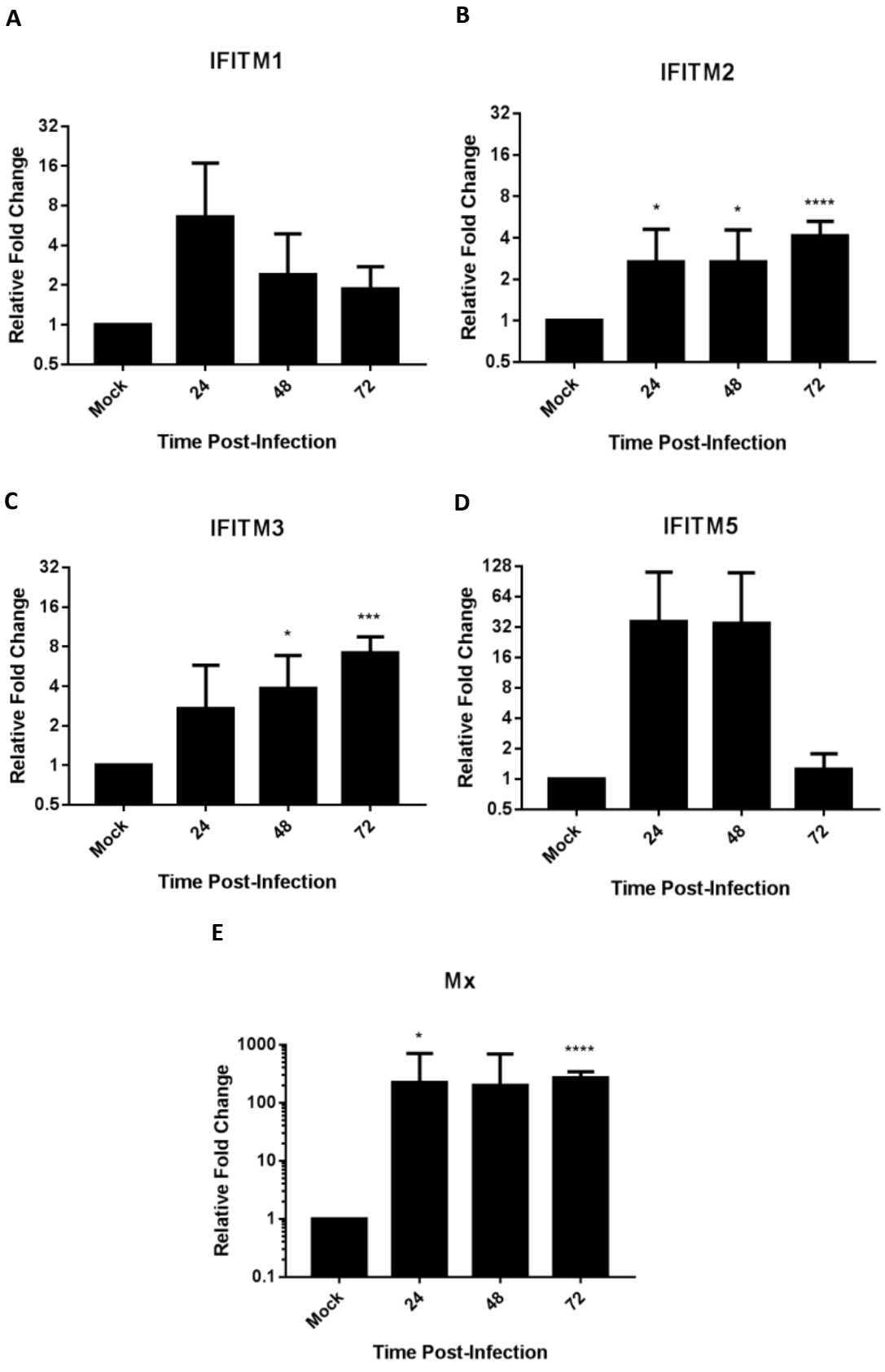
A
IFITM1
Relative Fold Change
32
16
8
4
2
1
0.5
Mock
24
48
72
Time Post-Infection
B
IFITM2
Relative Fold Change
32
16
8
4
2
1
0.5
*
*
****
Mock
24
48
72
Time Post-Infection
C
IFITM3
Relative Fold Change
32
16
8
4
2
1
0.5
*
***
Mock
24
48
72
Time Post-Infection
D
IFITM5
Relative Fold Change
128
64
32
16
8
4
2
1
0.5
Mock
24
48
72
Time Post-Infection
E
Mx
Relative Fold Change
1000
100
10
1
0.1
*
****
Mock
24
48
72
Time Post-Infection

Liver

F

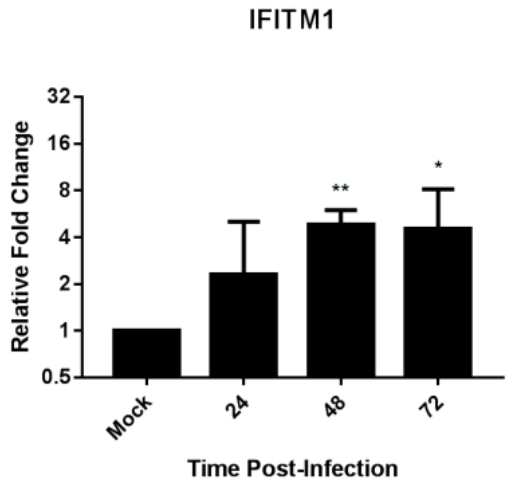
IFITM1
Relative Fold Change
32
16
8
4
2
1
0.5
**
*
Mock
24
48
72
Time Post-Infection

G

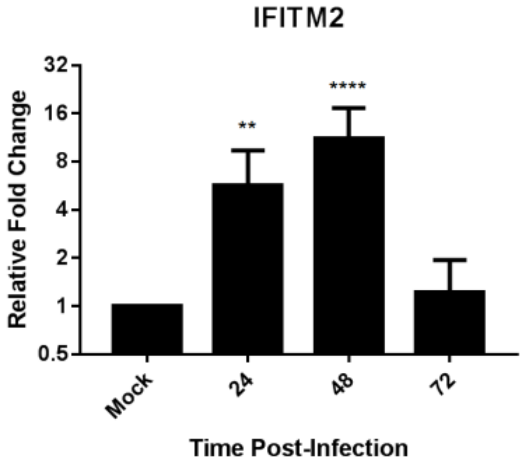
IFITM2
Relative Fold Change
32
16
8
4
2
1
0.5
**
****
Mock
24
48
72
Time Post-Infection

H

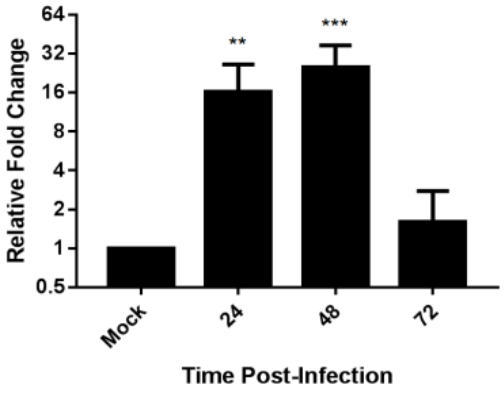
IFITM3
Relative Fold Change
64
32
16
8
4
2
1
0.5
**
***
Mock
24
48
72
Time Post-Infection

I

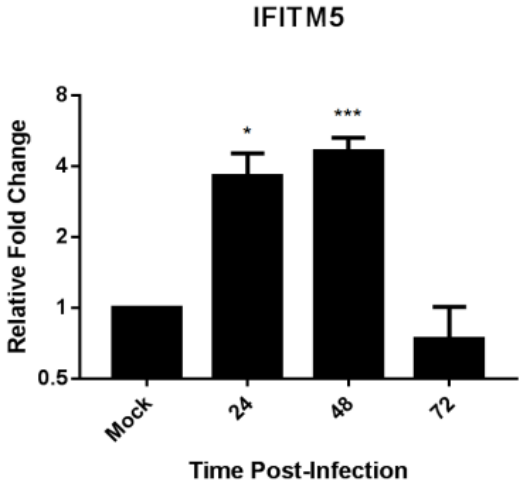
IFITM5
Relative Fold Change
8
4
2
1
0.5
*
***
Mock
24
48
72
Time Post-Infection

J

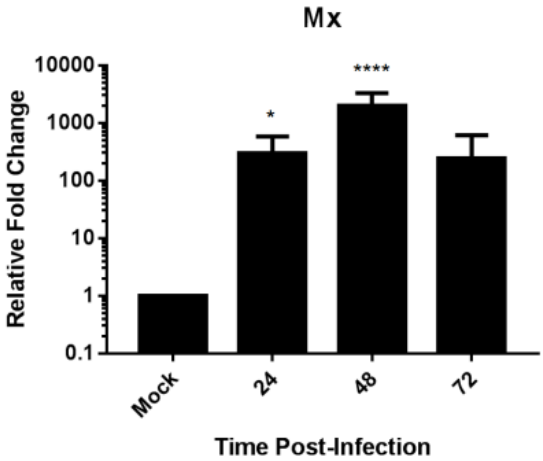
Mx
Relative Fold Change
10000
1000
100
10
1
0.1
*
****
Mock
24
48
72
Time Post-Infection

Intestine

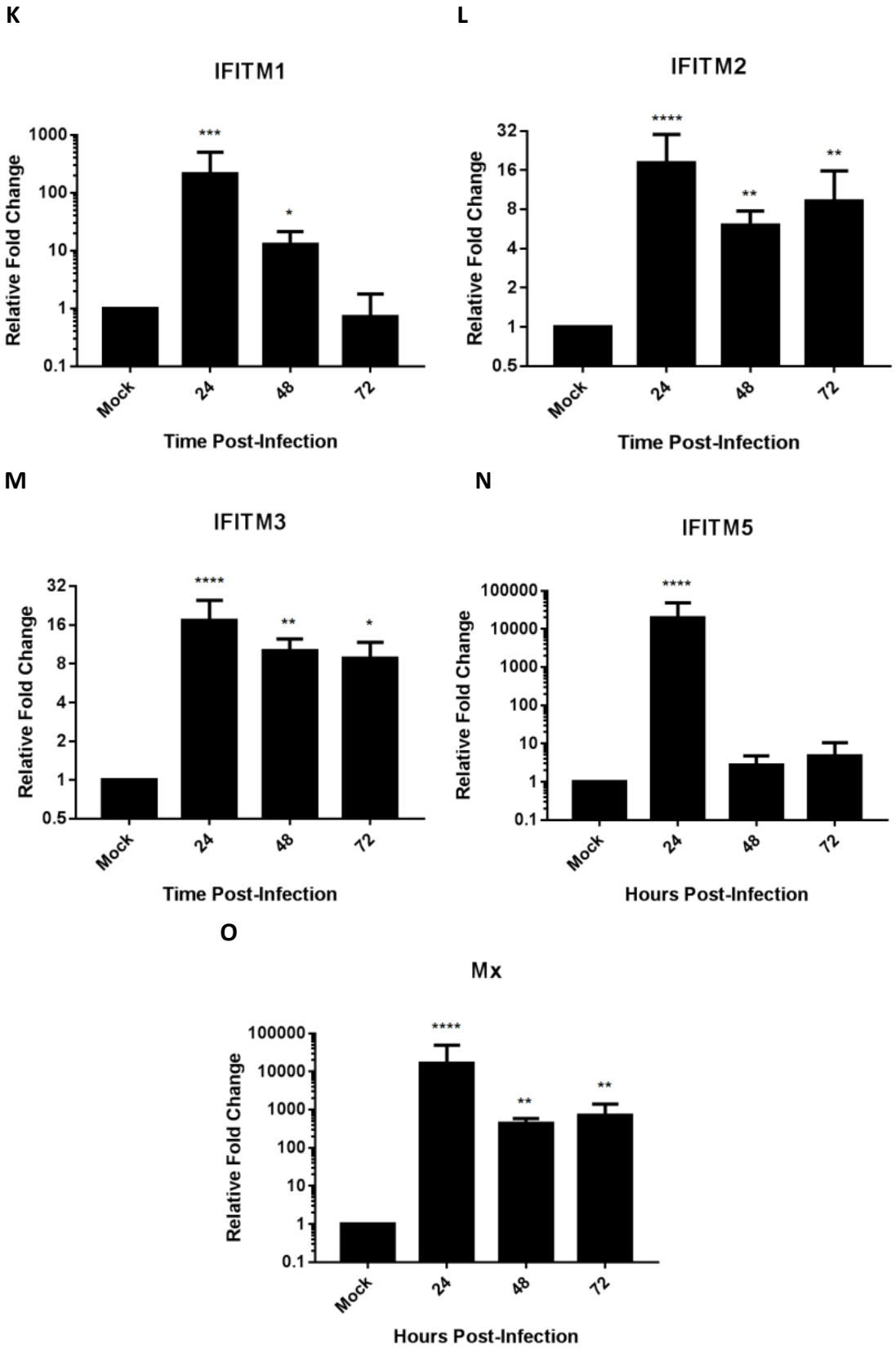
K
IFITM1
Relative Fold Change
1000
100
10
1
0.1
***
*
Mock
24
48
72
Time Post-Infection
L
IFITM2
Relative Fold Change
32
16
8
4
2
1
0.5
****
**
**
Mock
24
48
72
Time Post-Infection
M
IFITM3
Relative Fold Change
32
16
8
4
2
1
0.5
****
**
*
Mock
24
48
72
Time Post-Infection
N
IFITM5
Relative Fold Change
100000
10000
1000
100
10
1
0.1
****
Mock
24
48
72
Hours Post-Infection
O
Mx
Relative Fold Change
100000
10000
1000
100
10
1
0.1
****
**
**
Mock
24
48
72
Hours Post-Infection

P

	24 H.P.I			48 H.P.I			72 H.P.I		
Embryo	1	2	3	1	2	3	1	2	3
Lung	++	+	-	+	-	+	++	+	-
Liver	+	++	-	+	-	+	-	+	+
Intestine	+	+	+	-	-	+++	+	++	++
Embryo IAV Positive	✓	✓	✓	✓	X	✓	✓	✓	✓

Figure 4.11 *In ovo* Infection with H9N2 upregulates the expression of the chIFITMs. (A-O) The expression level and log fold change of *chIFITM1, 2, 3, 5* and *Mx* in different tissues were measured using quantitative RT-PCR (normalised to RPLPO and RPL13) after infection with H9N2 (1000 PFU) IAV in specified-pathogen-free (SPF) embryonated Rhode-Island Red hen's eggs. The presence of IAV in infected tissues was performed using end point PCR of the M gene (P) and intensity of the product summarised. Error bars show standard deviations of the means (n =3 biological replicates), * indicates a p-value <0.05, ** indicates a p-value<0.01, *** indicates a p-value <0.001, ****indicates a p-value <0.0001, one-way ANOVA.

In the liver there was a significant upregulation of all of the genes that were examined. *chIFITM1* was significantly upregulated at 48 and 72 hours post infection (Fig 11F), whereas *chIFITM2, 3, 5* and *Mx* were significantly upregulated at 24 and 48 hours post infection (Fig 11G – J). In the liver the most significant upregulation in mRNA expression was detected at 48 hours post infection for all of the *chIFITMs* and *Mx.* The mRNA expression of *chIFITM2, 3, 5* and *Mx* decreased at 72 hours post infection and this resulted in a loss of significance. The greatest level of *chIFITM* and *Mx* upregulation was found in the intestine with values represented in $\log_{10}$ format for *chIFITM1*, *5* and *Mx.* There were significant increases *in chIFITM2, 3* and *Mx* mRNA abundance at all time points post infection (Fig 4.11L, M and O). *chIFITM1* was significantly upregulated at 24 and 48 hours post infection (Fig 4.11K) and *chIFITM5* was significantly upregulated at only 24 hours post infection (Fig 4.11N), although a 10,000 fold increase (in *chIFITM5* mRNA) was observed over the mock infected embryos. There was a significant upregulation in *Mx* mRNA abundance in all tissues examined (Fig 4.11E, J and O). In order to confirm presence of the virus, end point PCR of the M gene of IAV was performed for each tissue of each embryo (Fig 4.11P). All but one embryo was found to have virus in at least one tissue and the embryo that was IAV negative was excluded from further analysis. Taken together, these data demonstrate that *chIFITM* genes are upregulated *in ovo* following IAV infection, to varying degrees in different tissues.

4.4.6 *In vivo* infection of Rhode-Island Red chicks with H9N2 modulates *chIFITM* expression

Having demonstrated *chIFITM* transcript upregulation *in vitro* and *in ovo* in response to influenza virus infection, it was evaluated if *chIFITM* transcripts were also upregulated *in vivo* following infection with IAV. Infections *in vivo* are complex as there are a multitude of factors that are at play simultaneously, such as the induction of an antiviral state which modulates the expression of over 500 genes. Moreover, environmental factors, individual genetic diversity and the health status of the animal may alter the outcome of infection. *In vivo* models are therefore less controlled in comparison to the highly controlled experiments conducted *in vitro.* Three-week-old Rhode Island Red chickens were inoculated with $1x10^5$ pfu of H9N2 (A/chicken/Pakistan/UDL01/08) intra-nasally, and tissue samples were taken at day 2 and 5 post infection from the lung, liver and colon. Samples were also taken from mock infected birds that were aged matched as controls. Samples were homogenised using the TissueLyser, RNA extracted, reverse transcribed and relative quantitative RT-PCR was performed. Copies of the *M gene* (viral), the *chIFITMs* and *Mx* were calculated from a standard curve using plasmids encoding the target sequence.

RT-PCR of the M gene was used to assess the viral burden in these tissues and relative copy numbers were determined against a known standard. Copies of IAV mRNA were detected in all of the tissues that were sampled, with IAV mRNA copies increasing in the lung from days 2 to 5 post challenge (Figure 4.12A). In all the tissues from control birds, chIFITM transcripts were detectable at comparable levels at 2 and 5 days post mock infection. In the lungs on day 5 post infection all the *chIFITM* transcripts were detected at lower levels in H9N2 infected birds with significant down regulation being observed for *chIFITM2* and *3* (Fig 4.12C).

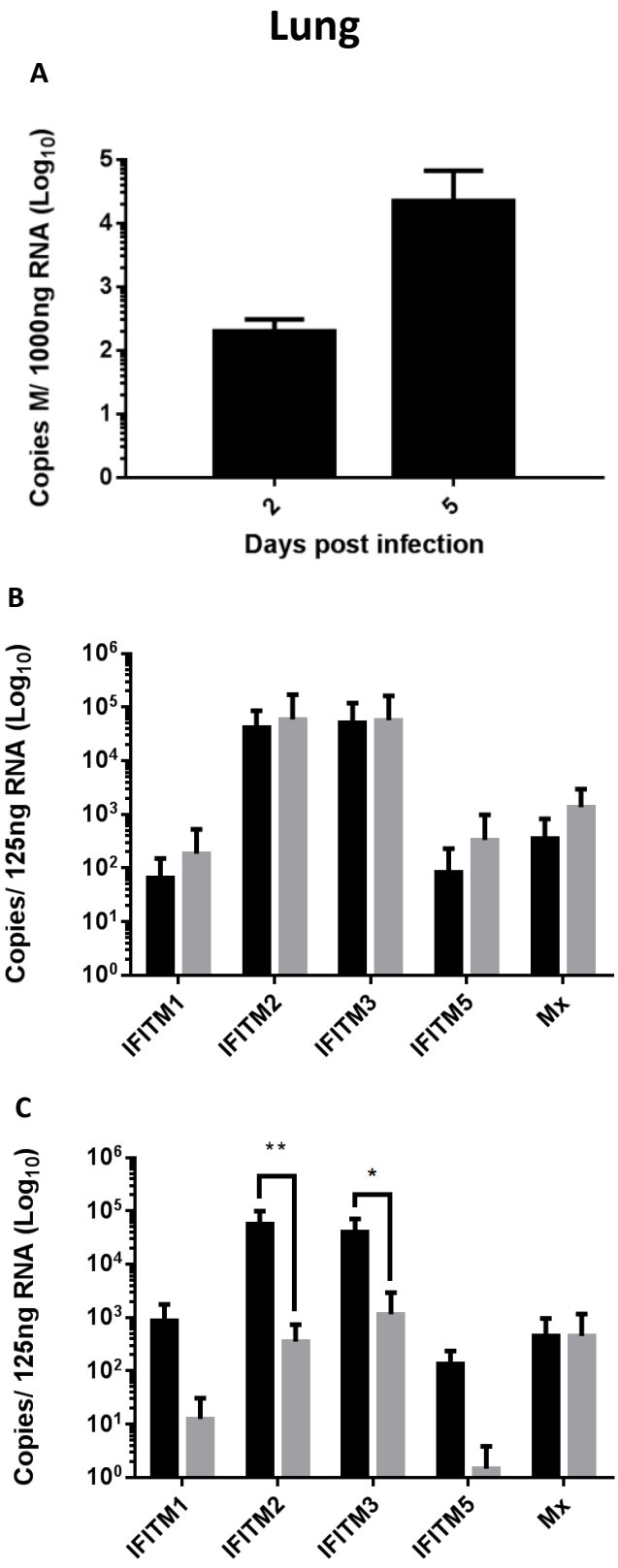
Lung
A
Copies M/ 1000ng RNA (Log10)
0
1
2
3
4
5
2
5
Days post infection
B
2 days post infection
Copies/ 125ng RNA (Log10)
10^0
10^1
10^2
10^3
10^4
10^5
10^6
IFITM1
IFITM2
IFITM3
IFITM5
Mx
C
5 days post infection
Copies/ 125ng RNA (Log10)
**
*
10^0
10^1
10^2
10^3
10^4
10^5
10^6
IFITM1
IFITM2
IFITM3
IFITM5
Mx

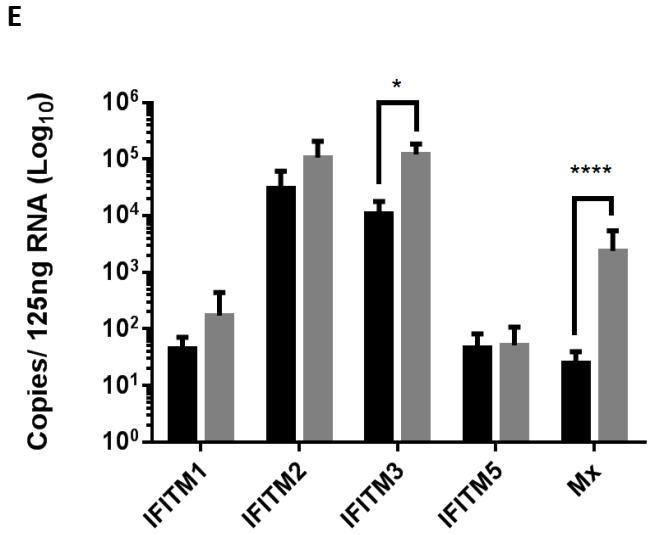

2 days post infection

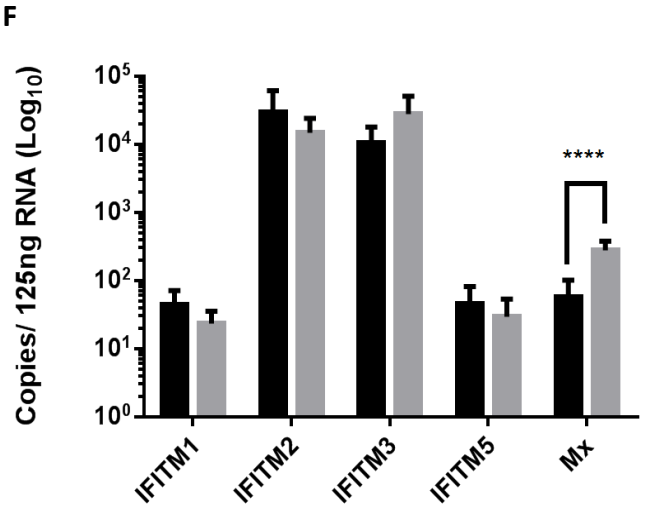

5 days post infection

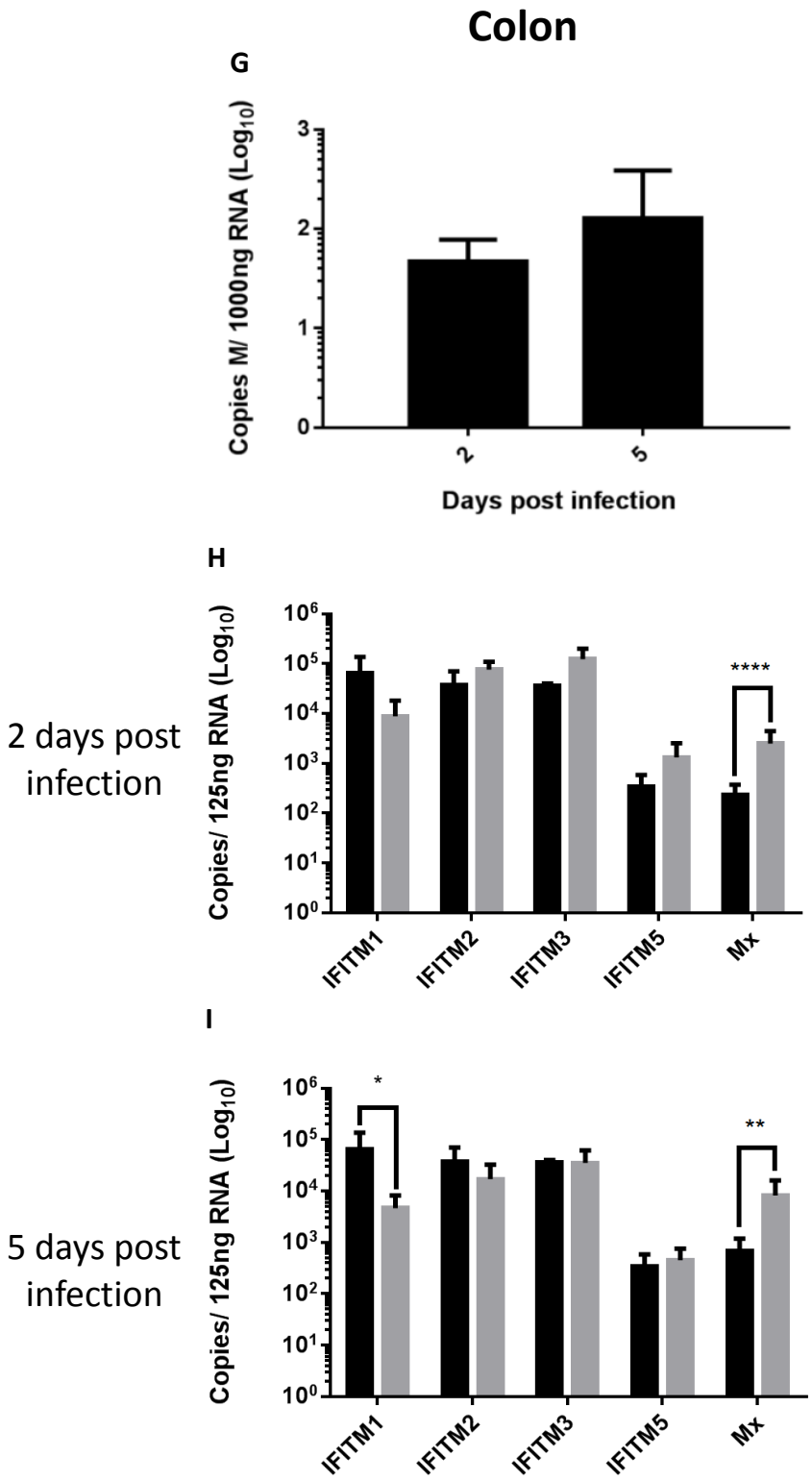

4.12 In vivo Infection with H9N2. (A, D and G) Absolute quantification of viral capsid M gene in different tissues, at 2 and 5 days post infection using quantitative RT-PCR after infection with H9N2 (1 x 10^5 PFU) IAV in specified-pathogen-free (SPF) RIR birds. (B, C, E, F, H, I) The expression level and log fold change of *chIFITM1, 2, 3, 5* and *Mx* in different tissues were measured using quantitative RT-PCR. Black bars represent mock infected birds; grey bars represent H9N2 infected birds. Error bars show standard deviations of the means (n =2 [mock infected] -4 [experimentally infected]), * indicates a p-value <0.05, ** indicates a p-value <0.01, ****indicates a p-value <0.0001, one-way ANOVA.

There were no significant differences in *chIFITM* transcript levels between mock infected and virus infected birds on day 2 post infection, although there is a general increase in transcript abundance in the IAV infected birds compared to the mock, particularly for *chIFITM1, 5* and *Mx* (Fig 4.12B). Conversely there was a decrease of M gene mRNA in the liver from days 2 to 5 post infection and this suggests that the virus is being cleared from this tissue (Fig 4.12D). Although there was a decrease in M gene expression, this did not correspond to any change in *chIFITM* transcripts abundance at 5 days post infection (Fig 4.12F). There was a significant increase in *chIFITM3* mRNA abundance at 2 days post infection in the liver (Fig 4.12E), which was not observed for any other *chIFITM*, at any other time point, in any other tissue. *Mx* expression is significantly upregulated at both time points in the liver, even though copies of the viruses decrease from 2 to 5 days post infection. There was an increase in M gene mRNA levels in the colon (Fig 4.12G) from 2 to 5 days post infection and this corresponded with a significant decrease in *chIFITM1* transcript abundance (Fig 4.12I) at 5 days post infection when compared with the mock control. At 2 days post infection there were no significant differences in the level of chIFITM transcripts, however, *chIFITM1* appear to be downregulated, whilst *chIFITM2, 3* and *5* are somewhat upregulated (Fig 4.12H). At both time points the colon contained significantly more transcripts of Mx (Figure 4.12H and I).

The data generated by the *in vivo* infection of chickens with IAV is more complex and there is not a single pattern of upregulation, unlike the *in vitro* and, to a lesser extent, the *in ovo* infection data. These data show general trends of increasing or decreasing *chIFITM* expression, although there is only a single example of significantly upregulated expression of *chIFITM3,* which is in the liver at 2 days post infection. In contrast, there are examples of significant down regulation of *chIFITM2* and *3* expression in the lung and of *chIFITM1* expression in the colon, both at 5 days post infection. *Mx* does not appear to be

downregulated at any time, nor in any tissue. This suggests a dynamic process is in operation and there may be multiple factors that control and regulate *chIFITM* expression *in vivo*.

4.5 Discussion

The results in this chapter examine the ways in which *chIFITM* expression is modulated by molecules that drive innate immune activation and from infection within a diverse range of avian pathogens. The initial investigations questioned whether commonly used avian cell lines would be a good model for exploring *chIFITM* upregulation, assessed using the synthetic dsRNA mimic poly(I:C). Figure 4.1 demonstrated that there were considerable differences in the upregulation of chIFITM transcripts in the three chicken cell lines that were examined. Treatment of DF-1 cells, with poly(I:C) gave a muted response, with only *chIFITM1* and *3* being significantly upregulated. Moreover, *chIFITM2, 5* and *10* were not upregulated at all; instead levels of transcript abundance were below mock infected levels for *chIFITM5* and *10.* In contrast, treatment of HD11 cells resulted in significant upregulation in expression for all *chIFITMs* except *chIFITM5*. Treatment of OU-2 cells fell somewhere between the other two cell lines, with a general trend of upregulation, but again only two *chIFITMs,* namely *chIFITM1* and *2,* were significantly upregulated. This led to the conclusion that HD11 cells would be the most suitable cell line for studying interferon induction and signalling in further detail.

Data published by Smith *et al.* indicated that type I, not type II interferons would lead to the activation and upregulation of *chIFITM* expression. In this study they used DF-1 cells stimulated with either IFNα or IFNγ to assess only *chIFITM3* upregulation. As is now clear, DF-1 cells may not have been the best model for these experiments and this could be

attributed to increased levels of constitutive SOCS1 expression in this cell line (Giotis et al., 2017). Utilising HD11 cells, an IFNβ promoter reporter assay and western blot demonstrated that poly(I:C) was able to activate both the IFNβ promoter and drive IFNα expression which is evident by the western blot. Analysis of samples treated with the same agonists concluded that IFNα and poly(I:C) were predominantly responsible for *chIFITM* upregulation and this appeared to be universal across all four *chIFITMs* and the positive control, *Mx*. Treatment of cells with IFNγ led to a modest, but insignificant upregulation in *chIFITM3* expression which suggests that IFNγ is not primarily involved in modulating *chIFITM* expression. These results contribute to what was already known in the literature, but also identified a novel ISG, *chIFITM5*. The role of chIFITM5 had not been examined up until now, presumably because huIFITM5 had been implicated in bone mineralisation and expression was restricted to the bone marrow. These results demonstrate that the *chIFITMs* act as classical ISGs; they are sensitive to interferon and are upregulated universally by IFNα. It has been well established that, in chickens, type I interferons differentially activate downstream effector proteins, with α/β activating different proteins to a greater or lesser extent. It is an accepted principal that IFNα is a more potent agonist of further IFNα and β activation which may contribute to an enhanced level of *chIFITM* expression (Qu et al., 2013).

The currently available evidence does not irrefutably demonstrate that bacteria are efficiently restricted by human or mouse IFITMs. Although the data in the mammalian field may be controversial, no work has currently been published elucidating the relationship between bacteria and the *chIFITMs*. In this part of the chapter, lipopolysaccharide (LPS) was used to examine this relationship in two cell lines, DF-1 and HD11 cells. LPS treatment in DF-1 cells did not lead to an upregulation of the positive control, IL-6. In order to further investigate whether DF-1 cells had an intact NF-κB signalling pathway, P65 translocation was used as a marker of NF-κB transcriptional activation. This work found that DF-1 cells

have an intact NF-κB signalling pathway and this was evidenced by the fact that P65 translocated from the cytoplasm into the nucleus which is a marker of P65 activation. As the positive control in DF-1 cells failed, no further conclusions could be confidently drawn from this data. In comparison HD11 cells responded well to LPS treatment and *IL-6* was significantly upregulated, which confirmed what was already published in the literature (Setta et al., 2012). Under the same LPS treatment *chIFITMs* were not upregulated, on the contrary, expression levels of *chIFITM2* and *5* dropped below those seen in mock treated cells. This suggests that LPS does not activate *chIFITM* expression. Moreover, *chIFITM* expression may be actively downregulated as the cell may have a preference for upregulating proinflammatory cytokines instead of ISGs, as if often the case during bacterial infection.

Understanding the molecules that are involved in ISG modulation can help to elucidate roles that the chIFITMs undertake in the context of cellular infection. In order to further understand the interplay between host cell restriction factors and invading viral pathogens, the next set of experiments examined whole avian viruses in avian cell culture and measured *chIFITM* upregulation over a time course. In Figure 4.6, primary *ex vivo* cell cultures were utilised alongside a current enzootic strain of IAV (H9N2) and two further representative strains (H3N8, H5N3). Infection with H9N2 led to a significant upregulation in *chIFITM1* and *5* expression, with *chIFITM1* being most significantly upregulated over the course of infection (Figure 4.6A). The upregulation in *chIFITM1* mRNA levels corresponds with an increase in chIFITM1 protein abundance (Figure 4.7B). Cells infected with H3N8 displayed a different and more complex expression profile (Figure 4.6B). During the course of infection *chIFITM1* displayed a biphasic regulation, initially increasing from 2 to 6 hour post infection, decreasing to mock levels at 12 hours post infection and then increasing significantly at 24 hours post infection. In contrast, *chIFITM2* was significantly upregulated at 6 and 12 hours post infection, but levels of mRNA transcript abundance were lower at 2

and 24 hours post infection. The expression of *chIFITM3* followed a similar profile to that of *chIFITM2,* although *chIFITM3* was still significantly upregulated at 24 hours post infection. *chIFITM5* was upregulated at 2 to 12 hours post infection, showing significant upregulation at 24 hours post infection. Infection with H5N3 resulted in a significant upregulation in all *chIFITMs* at 6 hours post infection and this continued throughout the time course. The only exception being *chIFITM2* which was not significantly upregulated at 24 hours post infection. These data demonstrates the complex modulation of ISGs in the context of viral infection. The differences in upregulation may reflect the virus's ability to antagonise interferon signalling, thus ISG expression. In a study examining two H1N1 viruses, the pandemic A/California/4/2009 and seasonal A/New Caledonia/20/1999, the authors report significant differences in gene expression through the Jak/Stat signalling pathway and the subsequent expression of ISGs (Fribourg et al., 2014). This study highlights the differences in interferon antagonism that are predominantly, but not solely, modulated through the activity of NS1 (Killip et al., 2017).

To investigate whether *chIFITM* expression could be upregulated by positive sense RNA viruses, the prototypic gamma coronavirus IBV was used to infect an *ex vivo* cell culture comprising chick kidney cells. Three strains of IBV were used to compare strains with different pathogenicities and tissue tropisms. These comprised a tissue culture attenuated strain (BeauR), a pathogenic field strain (M41) and a virulent nephropathogenic strain (QX). The data demonstrates that infection with QX results in earlier upregulation of *chIFITM* expression than the other two strains. Infection with QX results in a significant upregulation in *chIFITM1* and *chIFITM5* expression at 6 hours post infection, which continues to 24 hours post infection. In addition, *chIFITM2* and *3* were upregulated at 12 hours post infection and this continues throughout the duration of the time course. Conversely, infection with BeauR or M41 leads to *chIFITM* upregulation, but only at 24 hours post infection. This may suggest that tissue tropism is a factor that influences *chIFITM* expression as QX is

nephropathogenic and this strain elicits an earlier response in the CK cells. Moreover, the apathogenic strain elicits a similar level of *chIFITM* expression to the pathogenic strain. This suggests that pathogenicity does not play a significant role in *chIFITM* induction during the course of infection.

Anecdotal evidence, which is still under investigation by the avian endemic viruses group, reveals that infectious BeauR virions are not detected when DF-1 cells are incubated at 41°C. This implies that either the virus cannot replicate at this temperature or the virus is being disrupted during virus assembly or egress. In order to evaluate what step is inhibited and whether this has an impact on *chIFITM* expression, DF-1 cells were infected and then incubated at either 37°C or 41°C. Infectious virions were not detected by plaque assay titration when cells were incubated at 41°C. In comparison, replicating virus was detected by quantitative RT-PCR in both samples which suggests that viral replication is not inhibited by the increase in temperature. Quantitative RT-PCR was used to assess *chIFITM* expression. There was very little difference in the induction profiles of the *chIFITMs* and any differences in significance are likely to be attributed to the standard deviations between biological replicates. Taken together, this data suggests that temperature does not affect viral replication of IBV. Moreover, disruption of viral assembly and/or egress is not a factor that influences *chIFITM* expression during infection.

Whilst IAV and IBV represent two distinct species of viruses, their relatively small genomes (13.5kb and 27kb respectively) are similarly comprised of RNA. In contrast HVT has an expanded dsDNA genome (159kb) and utilises different mechanisms for replication, gene regulation and innate immune invasion alongside a unique method of viral entry. Investigating this viral diversity allows for a more complete characterisation of *chIFITM* expression during viral infection. Unlike infection with IAV and IBV, infection with HVT is mediated through cell to cell spread and the viral contents are released into the cell

cytoplasm in an endosomal-independent manner which may negate chIFITM-mediated restriction (Akhtar and Shukla, 2009). During the course of infection, there was a notable lack of *chIFITM* expression with the exception of *chIFITM5* and *Mx* which are significantly upregulated at 12 hours post infection. This appears to be transient and significance is lost later on during infection. Moreover, *chIFITM1* expression is significantly downregulated from 24 to 48 hours post infection. This is unique insomuch that this pattern of chIFITM modulation has not been observed for any other virus that has been studied *in vitro* thus far. The inability of the cell to upregulate *chIFITM* expression during HVT infection might be a consequence of viral entry or the mechanisms the virus exploits during gene expression and replication. It is worth noting that the MOI calculation and the method of viral entry and spread is very different to that of both IAV and IBV.

It has been known since the early 1960's that embryos are able to mount a protective interferon response from 8 days of fertilisation (Baron and Isaacs, 1961). This early interferon response is able to protect the developing chick from challenge *in ovo*. Even though an interferon response is initiated, there is still very little data available that details the magnitude of the response or the genes that are upregulated *in ovo*. The use of CEFs acts a proxy for *in ovo* responses but these models do not isolate single organs or tissues and thus it remains unclear if individual organs respond differentially to infection. In this section of the chapter, SPF RIR embryonated hen's eggs were inoculated with $1x10^3$pfu and tissues were harvested at 24, 48 and 72 hours post infection. Quantitative RT-PCR was used to examine the response of these tissues to infection with LPAI. There was a striking pattern of *chIFITM* upregulation in these tissues (Figure 4.11). The *chIFITMs* were most significantly upregulated in the lung at 72 hours post infection, in the liver at 48 hours post infection and in the intestine at 24 hours post infection. Although upregulation is most significant at the time points mentioned, there is still significant upregulation in *chIFITM* expression at other time points which appear to be in a *chIFITM* and tissue specific pattern. End point PCR of

the M gene was performed to assess the level of infection in each tissue. The results of this PCR did not correlate with *chIFITM* expression which indicates that *chIFITM* expression is not dependent on high levels of viremia. Indeed, it is still unclear if certain tissues are able to induce *chIFITM* expression to a greater or lesser extent and whether this is temporally regulated as the embryo develops. Another possible explanation is that infection leads to a systemic interferon response whereby tissues with a low viral load are primed for infection by the initiation of interferon signalling. What is clear, however, is that embryos are able to upregulate the expression of the *chIFITMs* from 11 days post infection in response to infection with H9N2.

The effect of H9N2 infection *in vivo* was used to assess *chIFITM* modulation in the host species. So far, only one study examines *chIFITM* expression *in vivo* and this was with the HPAI, H5N1 and LPAI H5N2 (Smith et al., 2015). In this study the authors noted a muted *chIFITM* response in the lungs and ilium, which was much lower in magnitude to the expression of *dIFITMs* in the same tissue. Similarly, in our experiments, the response to infection with H9N2, *chIFITMs* were not expressed to very high levels in any of the tissues that were examined. Moreover, there was only a single significant upregulation and this was in the liver at 2 days post infection with *chIFITM3* (Figure 4.12E). There was a general trend of upregulation in *chIFITM* expression in each of the tissues at 2 days post infection, notably, *chIFITM1* and *5* in the lung and *chIFITM3* and *5* in the colon, although these failed to reach statistical significance. In contrast, there was a significant downregulation of *chIFITM2* and *3* in the lung and *chIFITM1* in the colon at 5 days post infection. This may suggest that the virus is able to modulate expression of the *chIFITMs* later on during infection and this corresponds with an increase in virus in these tissues from 2 to 5 days post infection as detected by quantitative RT-PCR against the M gene. This implies that the virus is able to control the expression of *chIFITM* expression *in vivo,* likely through the actions of a global interferon antagonist.

In conclusion, the data presented in this chapter shows the dynamic regulation of the *chIFITMs in vitro, ex vivo, in ovo* and *in vivo*. It appears that *chIFITM* expression is a highly regulated process and may suggest a complex interplay between viruses and the host cell which in turn regulates the expression of this family of ISGs.

Chapter 5

ChIFITM-mediated restriction of avian viral pathogens

5.1 Introduction

The discovery of the human IFITM proteins occurred many decades ago in 1984, making them some of the first proteins to be classed as ISGs (Friedman et al., 1984). The IFITMs were initially termed 9–27(IFITM1), 1-8D (IFITM2), and 1-8U (IFITM3), a nomenclature that is very different to the one used currently. The ability to restrict viruses by the IFITM proteins was described much later on, first being reported in 1996 with the partial restriction of Vesicular stomatitis virus (VSV) by huIFITM1 (Alber and Staeheli, 1996). A further study examined the relationship between hepatitis C virus (HCV), IL-1 and 1-8U (IFITM3) and found that increased expression of 1-8U was associated with a decrease in HCV mRNA, although no specific conclusions regarding antiviral activity were made from this study (Zhu and Liu, 2003). It was not until 2009 that IAV-targeting RNA interference studies started to identify IFITM1, 2 and 3 as potential restriction factors against IAV (Brass et al., 2009;Shapira et al., 2009). Since this time, many studies have investigated the role of IFITM-mediated restriction of a diverse range of pathogens, both bacterial and viral, in a wide array of host organisms.

Human IFITM (huIFITM) proteins have been proposed to restrict the entry and replication of several highly pathogenic human viruses, although the exact mechanisms involved remain unclear. The viruses restricted by huIFITMs include: IAVs, flaviviruses (Dengue virus), filoviruses (Ebola virus and Marburg virus), coronaviruses (SARS and MERS) and HIV-1 (Brass et al., 2009;Foster et al., 2016;Lu et al., 2011;Huang et al., 2011). Murine models utilising knockout technologies have found that ifitm3$^{-/-}$ mice are more susceptible to IAV (Bailey et al., 2012;Everitt et al., 2012), respiratory syncytial virus (RSV) (Everitt et al., 2013) and West Nile virus (WNV) (Gorman et al., 2016) infection. Thus far, very little evidence is available detailing the restriction of avian viruses in avian cell culture. The chIFITMs were first characterised in 2013 by Smith et al. In this study they utilised a human cell line (A549)

stably expressing *chIFITM2* or *3* alongside DF-1 cells either transiently overexpressing *chIFITM3* or treated with a siRNA against *chIFITM3* (which ablated endogenous expression). Using lentiviral vectors pseudotyped with the Lagos bat virus (LBV), rabies virus (RABV) or influenza (H1 [human], H5 [human], H7 [bird], or H10 [bird]) glycoproteins, they assessed percentage infection by FACS or virus replication by plaque assay titration (Smith et al., 2013).

This chapter expands on previous studies and examines whether chIFITM-mediated restriction can be achieved with whole avian virus infection, rather than with pseudotyped lentiviral vectors. Furthermore, Smith et al focused only on *chIFITM2* and *3* and did not test to see if *chIFITM1* or *5* restrict viral pathogens. Therefore the scope of the investigation will be broadened to include the whole chIFITM family, alongside a diverse range of avian viral pathogens.

5.2 Transfection reagents are differentially toxic to cells

Transfection is an important process that allows for the introduction of foreign nucleic acid into cells. Transient transfection has a wide range of applications and is a commonly used laboratory technique employed for the overexpression or silencing (via siRNAs) of a gene in a concentration dependent and temporally regulated manner (Sharifi Tabar et al., 2015). During this process nucleic acids are not incorporated into the genome, thus the effect is short lived. The duration of transfection can be modulated by environmental factors such as media composition or cellular factors such as cell division (Gu et al., 2016). The purpose of transfection is to study the function or regulation of a gene or gene product in the context of whole cell expression. This may identify possible interactions that modulate the expression or function of the protein of interest (Kim and Eberwine, 2010). The most common form of transfection in mammalian tissue culture is chemical transfection with a cationic lipid. This method has relatively low levels of cytotoxicity, has an acceptable

transfection efficiency and is possible to perform in a standard laboratory (Maurisse et al., 2010;Kim and Eberwine, 2010). In this part of the chapter, the cytotoxicity's of different chemical transfection reagents were assessed in DF-1 cells. For the purpose of subsequent experiments, low cellular toxicity was required as the DF-1 cells were going to be transfected and then infected. High levels of cytotoxicity would impede the efficient infection of the transfected cells and the results would be less robust.

DF-1 cells were transfected with either 1µg of pcDNA3.1 or 20nM of scrambled siRNA according to the manufacturer's protocol for the individual transfection reagent being evaluated. Twenty four hours after transfection, the supernatant was removed, cells were trypsinised and stained with trypan blue. The ratio of living to dead cells was measured by the TC20 automated cell counter. There was a significant difference in the viability of cells transfected with siRNA using lipofectamine 2000 and HiPerfect (Figure 5.1). The lower cell viability obtained using lipofectamine 2000 suggests that this transfection reagent would not be suitable for the subsequent experiments that require viral infection. For the delivery of plasmid DNA there was no significant difference between lipofectamine 2000 and FuGene which suggests that the use of either would make little difference to cell survival. These results highlight the adverse impact that transfection can have on cell viability. The consequences of these impacts on experimental results are not fully understood.

5.3 Transient overexpression results in chIFITM-mediated restriction of avian viruses

5.3.1 Transient overexpression of chIFITM1, 2, 3 and 5 in CEFs restricts H9N2

Previous studies have demonstrated the potent restriction of IAV by huIFITM1, 2 and 3 *in vivo* and *in vitro* (Brass et al., 2009;Everitt et al., 2012;Mills et al., 2014;Williams et al., 2014;Sun et al., 2016). Similar work has shown that the murine Ifitm3

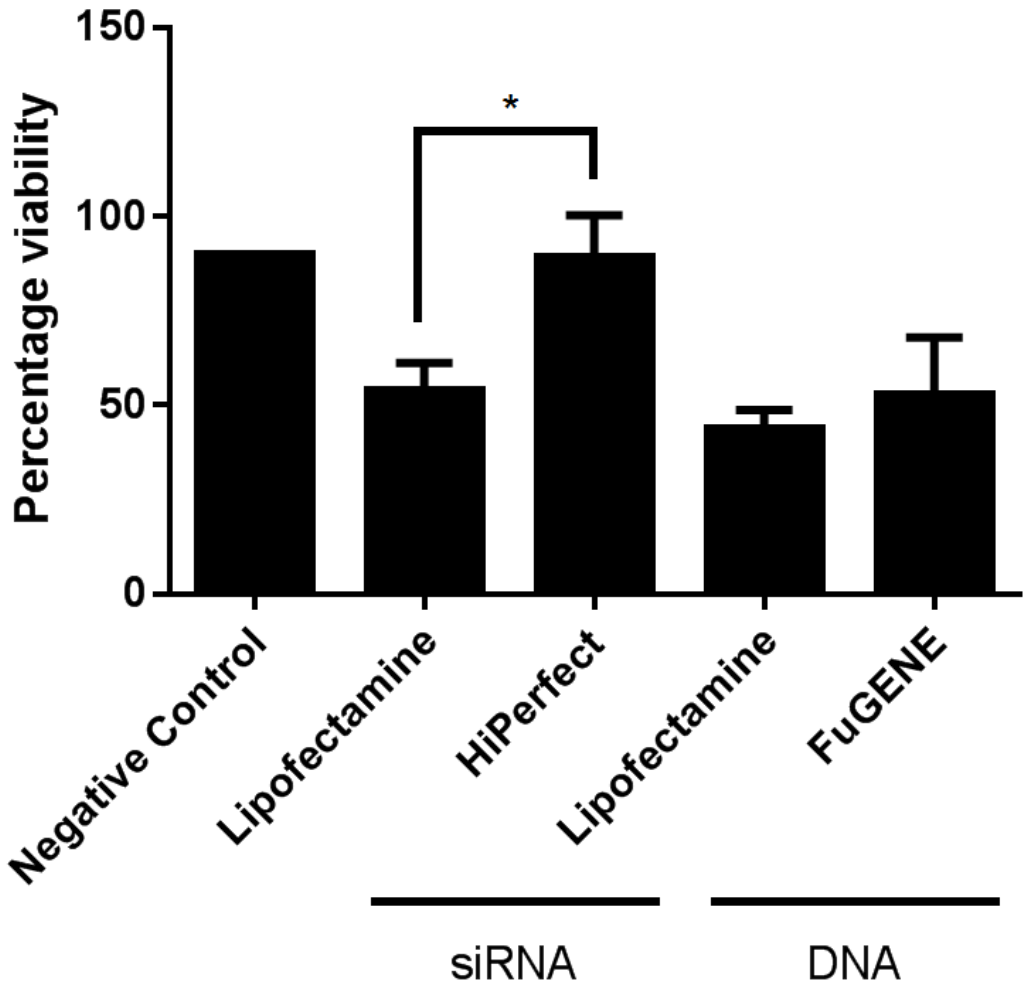

Figure 5.1 Determining the toxicity of transfection reagents in DF-1 cells. DF-1 cells were transfected with 1ug of pcDNA3.1 or 20nM of scrambled siRNA according to the manufacturer's protocol. After 24 hours cells were trypinised and stained with trypan blue. The ratio of living to dead cells was calculated by the TC20 automated cell counter (Bio Rad). Error bars show standard deviations of the means (*n* =3 biological replicates), * indicates a p-value <0.05, students t-test.

(Bailey et al., 2012;Everitt et al., 2013) and duck IFITM3 (Blyth et al., 2016) are capable of restricting the infectivity of IAV. At present, there is a lack of published data examining the expression of *chIFITMs* in the context of viral restriction of avian viruses that have not been pseudotyped onto lentiviral vectors. Furthermore, it is not clear if chIFITM5 has a role in restricting viral pathogens. In order to investigate this, chicken embryonic fibroblasts (CEFs) or DF-1 cells were transiently transfected for 24 hours and infected with IAV or IBV. Restriction was determined by a reduction in viral titres, as quantified by plaque assay titration, at 24 hours post infection. One of the major problems in avian viral research is the relatively limited host tropism that is observed affecting the ability of avian viruses to infect cells either *in vitro* or *ex* vivo. Therefore, it is not possible to perform all *in vitro* experiments in the same cells because of the limited tropism exhibited. Many viruses used in the laboratory are unable to infect commonly used chicken cell lines, and *ex vivo* cells are often used as a model of infection. This presents a problem when assessing viral restriction as these cells are often of mixed cell type, difficult to transfect and require high concentrations of DNA in order to overcome this barrier. To fully characterise the restriction of avian influenza A virus in the natural host, CEFs were transfected with 5µg of plasmids encoding either *chIFITM1*, *2*, *3* or *5* for 24 hours or were mock transfected with lipofectamine 2000 only. These cells were infected with a chicken H9N2 influenza virus at a high multiplicity of infection (MOI - 3) for 24 hours, and the supernatants were assayed for the presence of infectious virions by plaque assay. The supernatants were serially diluted in serum-free DMEM and used to infect MDCK cells in 12-well plates. After 1 hour of incubation, the inoculum was removed, and the cells were overlaid with DMEM containing 0.2% BSA, 2% agar and 1µg trypsin ml^{-1}. After 3 days, the overlay was removed, and the cells were stained with crystal violet to determine the pfu/ml. Overexpression of *chIFITM1*, 2, 3 and 5 (or a mix of all 1, 2, 3 and 5 chIFITM plasmids) significantly restricts the replication of H9N2 by 0.88, 0.6, 0.8, 0.45 and 0.75 logs respectively (Figure 5.2A). To assess

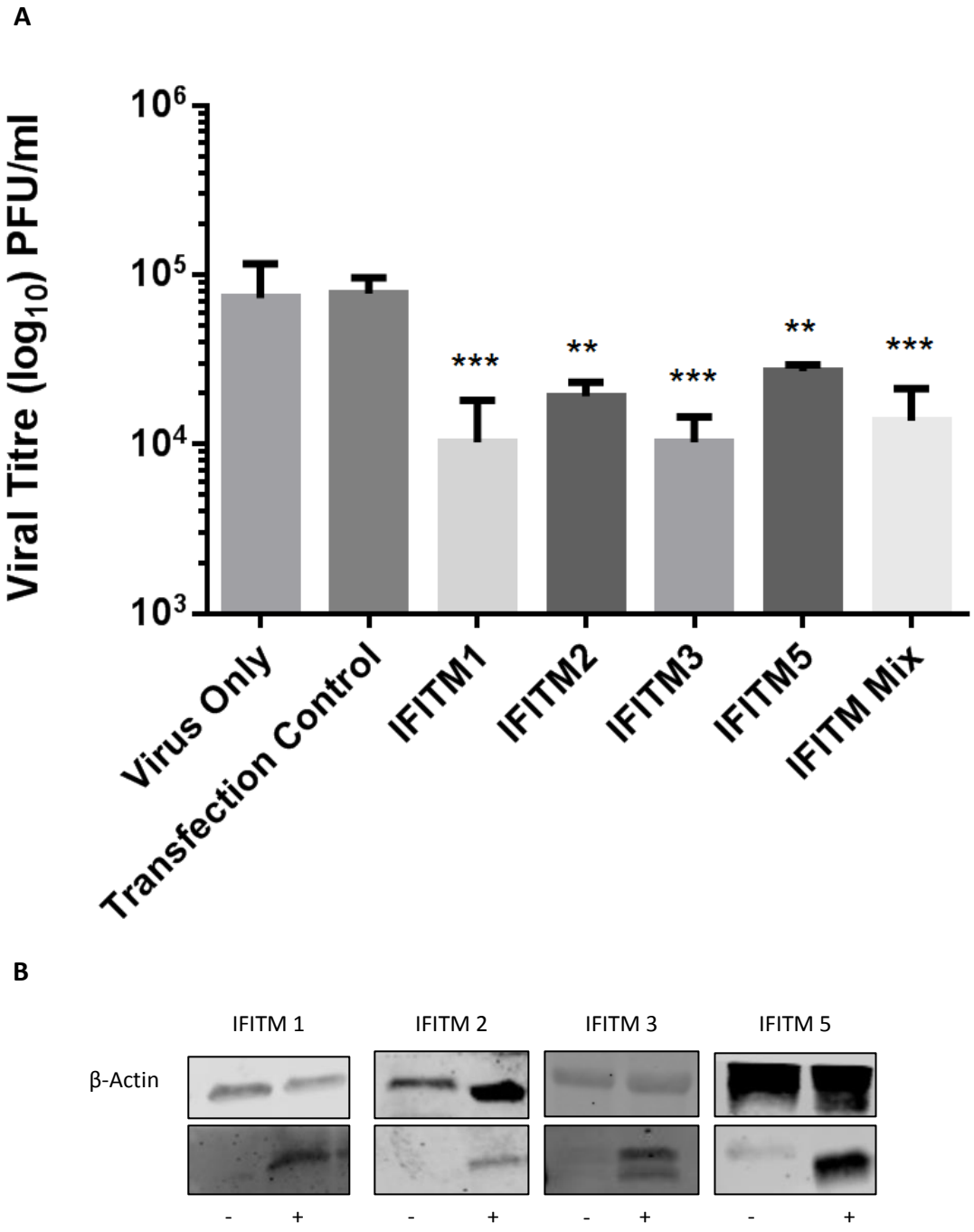

Figure 5.2 Transient overexpression of *chIFITM1, 2, 3* and *5* in CEFs significantly reduces IAV viral titres. (A) Chicken embryonic fibroblasts were transfected with 5µg of plasmid encoding chIFITM1, 2, 3 or 5 for 24 hours. These cells were then infected with H9N2 (MOI 3) for 24 hours and the supernatants harvested. Viral replication of the infected cell supernatant was measured by plaque assay titration relative to the control (cells treated with lipofectamine 2000). (B) Cells were lysed at 24 hours post infection and lysates were separated by SDS-PAGE. Proteins were transferred to a nitrocellulose membrane and a western blot performed using specific antibodies raised against a distinct epitope of each individual chIFITM protein with β-actin as the loading control. Error bars show standard deviations of the means (*n* =3 biological replicates), * indicates a p-value <0.05, students t test. (-, untransfected; +, transfected)

the level of endogenous *chIFITM* expression and overexpression by plasmid transfection in CEFs, cells were lysed at 24 hours post infection and lysates were separated by SDS-PAGE. Proteins were transferred to a nitrocellulose membrane and a western blot performed using mono- or polyclonal antibodies raised against distinct epitopes of the chIFITM proteins (Figure 5.2B). All four chIFITM exogenous proteins were separately expressed in CEFs and were readily identified. Untransfected cells showed low or absent basal endogenous *chIFITM* expression.

5.3.2 Transient overexpression of chIFITM1, 2, 3 and 5 in DF-1 cells differentially restricts H3N8, H5N3 or H9N2

The transient transfection of *ex vivo* cell cultures is problematic and requires the use of a high concentration of plasmid DNA in order to successfully blot for chIFITM protein (Figure 5.2B) in CEFs. This difficulty is not unique to CEFs and has been observed for other *ex vivo* cell culture preparations as well as *in vivo* (Kim and Eberwine, 2010). This may be due to *ex vivo* cell cultures containing a mixed cell population which change with each preparation. Continuous cell lines are easier to transfect, often requiring less DNA and transfection reagent to achieve the same result. DF-1 cells are a common chicken cell line used in many studies to assess the effects of overexpression. In order to expand the scope of this investigation, two additional strains of IAV (H3N8 and H5N3) were used.

It is known that diverse strains of IAV show different sensitivities to host cell antiviral responses, but It is currently unknown if this extends to chIFITM mediated-restriction. In order to investigate differential restriction, the *chIFITM* genes were transiently overexpressed and restriction measured by plaque assay titration. To confirm the restriction observed in CEFs Figure 5.2A, DF-1 cells were transfected with 1µg of plasmid encoding *chIFITM1*, *2*, *3* or *5.* These cells were infected with a chicken H3N8, H5N3 or H9N2

A

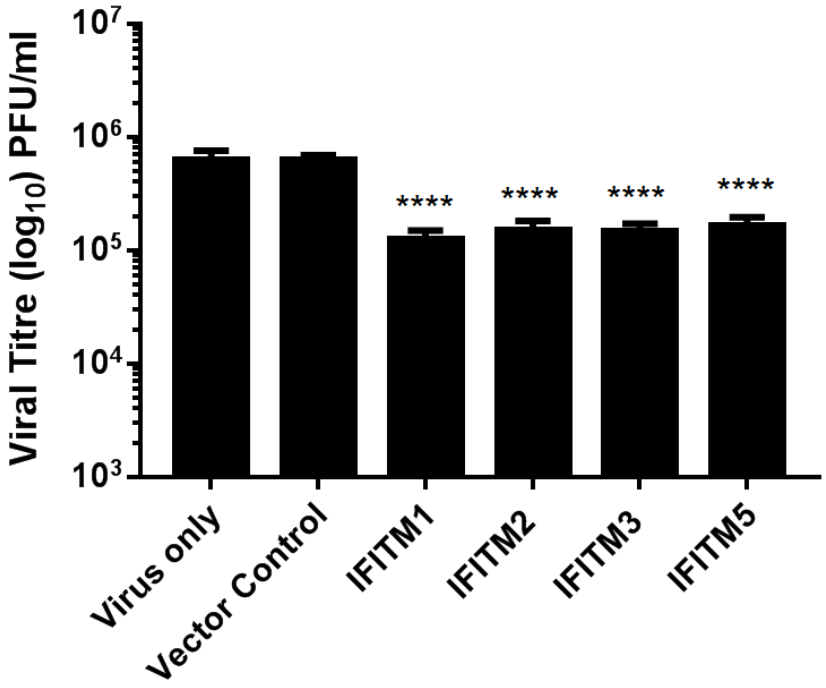
H3N8
Viral Titre (log_{10}) PFU/ml
10^7
10^6
10^5
10^4
10^3
****
****
****
****
Virus only
Vector Control
IFITM1
IFITM2
IFITM3
IFITM5

B

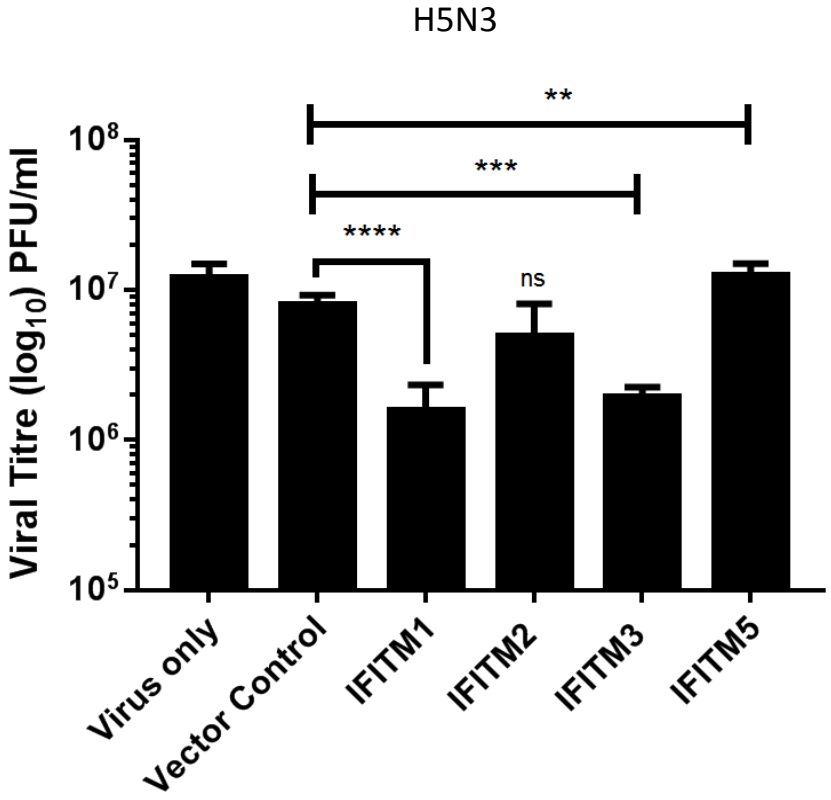
H5N3
Viral Titre (log_{10}) PFU/ml
10^8
10^7
10^6
10^5
**
***
****
ns
Virus only
Vector Control
IFITM1
IFITM2
IFITM3
IFITM5

C

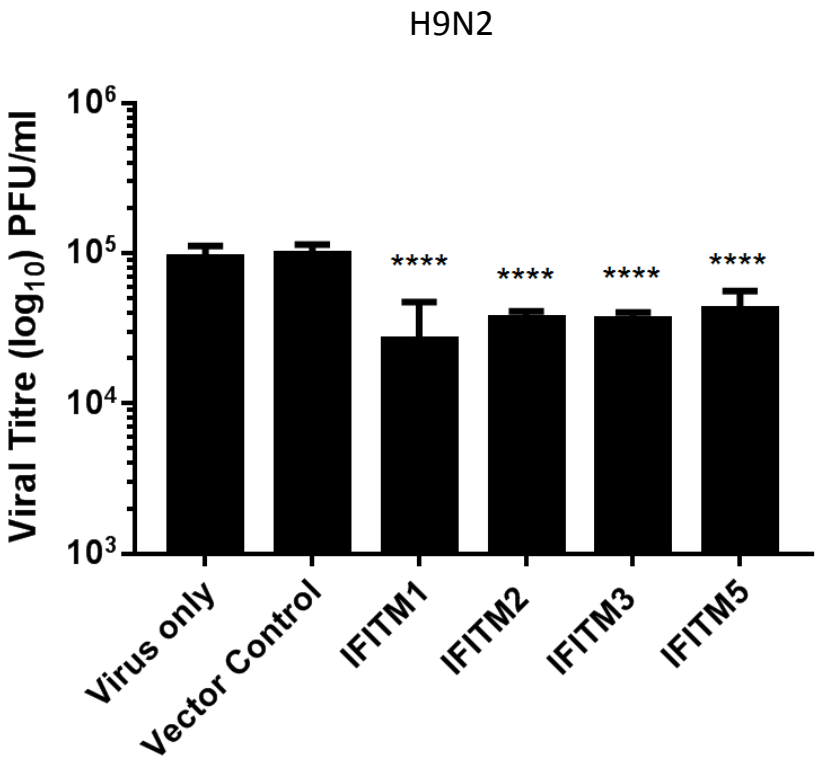

D

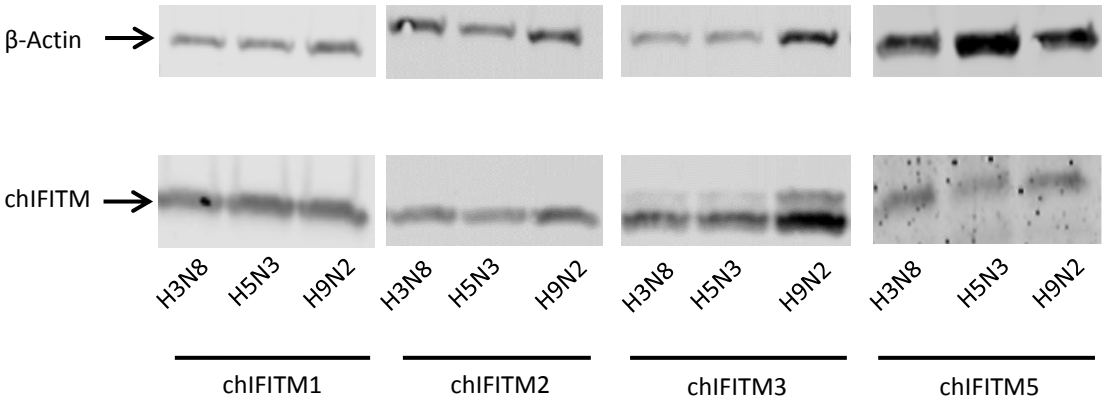

Figure 5.3 Transient overexpression of *chIFITM1, 2, 3* and *5* in DF-1 cells significantly reduces IAV viral titres. (A-C) DF-1 cells were transfected with 1µg of plasmid encoding chIFITM1, 2, 3 or 5 for 24 hours. These cells were then infected with H3N8, H5N3 or H9N2 (MOI 1) for 24 hours and the supernatants harvested. Viral replication of the infected cell supernatant was measured by plaque assay titration relative to the control (cells transfected with an empty vector). (D) Cells were lysed at 24 hours post infection and lysates were separated by SDS-PAGE. Proteins were transferred to a nitrocellulose membrane and a western blot performed using an anti-FLAG antibody against a C-terminal FLAG tag with β-actin as the loading control. Error bars show standard deviations of the means (*n* =3 biological replicates), ** indicates a p-value<0.01, *** indicates a p-value <0.001, ****indicates a p-value <0.0001, one-way ANOVA.

influenza virus (MOI - 1) for 24 hours, and the supernatants assayed for the presence of infectious virions. Material to be assayed was serially diluted in serum-free DMEM and used to infect MDCK cells in 12-well plates. After 1 hour of incubation, the inoculum was removed, and the cells were overlaid with DMEM containing 0.2% BSA, 2% agar and 1µg trypsin ml^{-1}. After 3 days, the overlay was removed, and the cells were stained with crystal violet to determine the pfu/ml. Transient overexpression of *chIFITM1*, *2*, *3* and *5* restricted the replication of H3N8 by 0.70, 0.61, 0.62, 0.58 log_{10}, respectively (Figure 5.3A), and all of these were significant when compared to the vector only control. Additionally, transient overexpression of *chIFITM1*, *2*, *3* and *5* restricted the replication of H5N3 by 0.70, 0.21, 0.61, -0.19 log_{10}, respectively (Figure 5.3B). Overexpression of *chIFITM1* and *3* resulted in a significant decrease in viral titre when compared to the vector only control. There was no significant difference in viral titre when cells overexpressing *chIFITM2* were challenged. In contrast there was a significant increase in viral titre with cells transiently overexpressing *chIFITM5*. This implies a much more complex virus-host interactome and may suggest that the chIFITMs are able to restrict viral pathogens differentially and this may be virus and/or chIFITM dependent. Transient overexpression of *chIFITM1*, *2*, *3* and *5* followed by infection with H9N2 resulted in a decrease of 0.56, 0.42, 0.43 and 0.36 log_{10} in viral titres, respectively (Figure 5.3C). This suggests that H3N8 and H9N2 have similar restrictive profiles, whereas H5N3 is sensitive only to *chIFITM1* and *3* overexpression under these experimental conditions.

Cells were lysed at 24 hours post infection and lysates were separated by SDS-PAGE. Proteins were transferred to a nitrocellulose membrane and a western blot performed using an anti-FLAG antibody against C-terminal FLAG tag or an antibody that was produced against a distinct epitope of chIFITM5 in DF-1 cells (Figure 5.3D). The expression of all four chIFITM proteins was detected in transfected DF-1 cells. The presence of a double band for

chIFITM3 has also been observed for FLAG-tagged mammalian IFITM3, for which there is no explanation (Yount et al., 2012;Chesarino et al., 2014a). The other chIFITMs have only a single band at the expected size.

5.3.3 Transient overexpression of chIFITM2 in DF-1 cells restricts IBV

Alongside influenza A, coronaviruses such as IBV also present a threat to the poultry industry. IBV is an infectious disease in countries which have an intensive poultry industry with rates of infection reaching almost 100% in many instances (Ignjatovic and Sapats, 2000). The rates of mortality associated with IBV are variable and depends on the strain of the circulating virus, with estimates ranging between 20-30%, although co- infections likely exacerbate the clinical outcome of IBV infection (Meulemans et al., 1987;Cumming, 1969b;Cumming, 1969a). There is significant morbidity associated with IBV infection, which has a costly impact on the poultry industry through loss of productivity and a reduction in the quality of meat and eggs. This loss is estimated to be between $3567.4 - $4210.8 per 1000 birds (Colvero et al., 2015).

Human coronaviruses are potently restricted by huIFITM proteins. There have been extensive studies conducted with SARS and MERS due to their pandemic potential. In 2011, a study observed preferential restriction of SARS by huIFITM1. This was assessed by analysing the effects from both the overexpression and ablated expression of huIFITM1 (Huang et al., 2011). In contrast, a more recent study focussing on SARS, MERS and two lesser known coronaviruses, NL63 and 229E (Zhao et al., 2018) found that there was no clear evidence of one huIFITM being more restrictive than another. Moreover, this study found that there was a difference in restriction between cell lines, although it is not clear if it was the cell line or the vector construct that resulted in the observed differences. At present

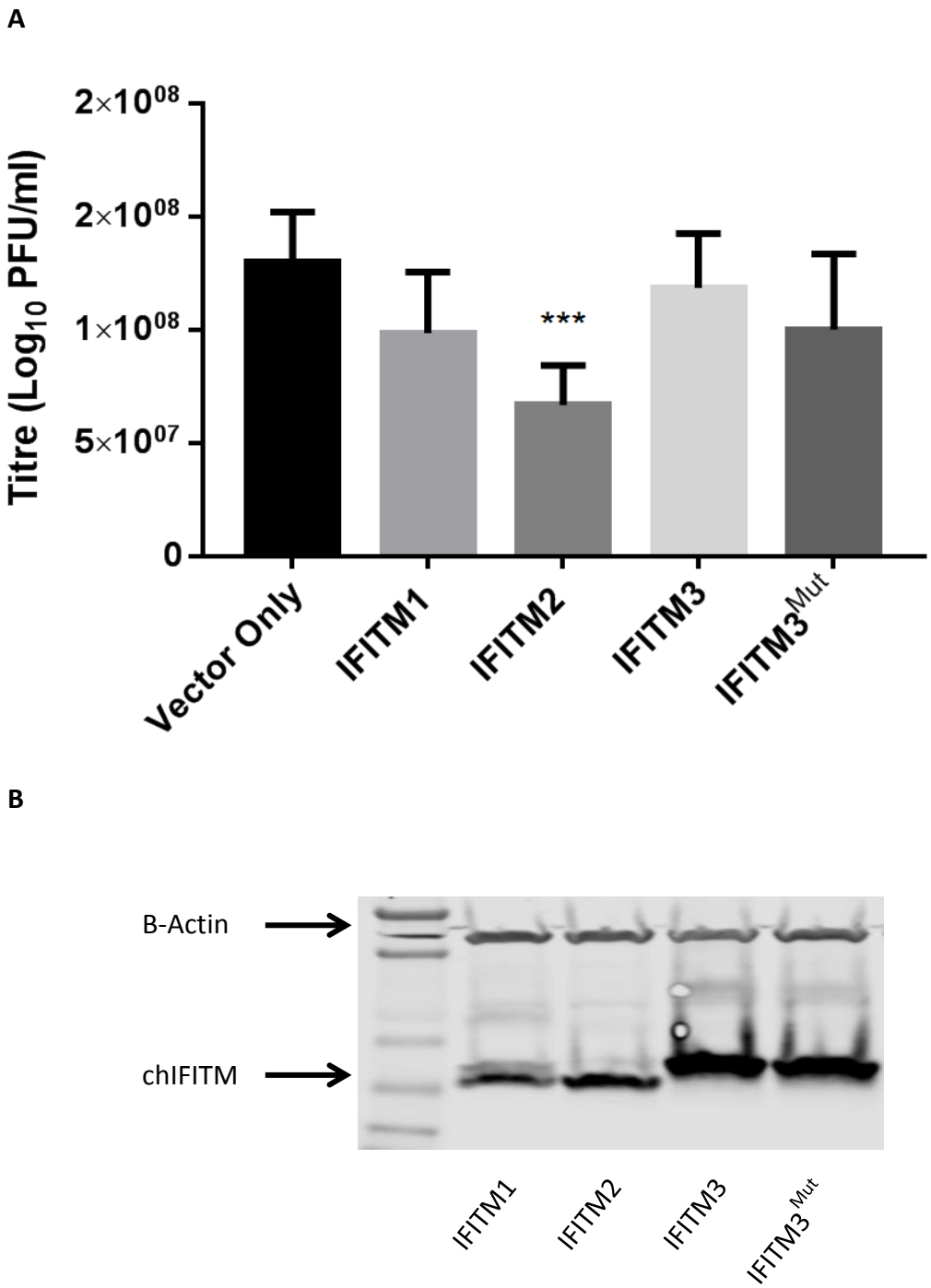

Figure 5.4 Transient overexpression of *chIFITM2* in DF-1 cells significantly reduces IBV viral titres. (A) DF-1 cells were transfected with 1µg of plasmid encoding chIFITM1, 2, 3 or 3^{MUT} for 24 hours. These cells were then infected with BeauR (MOI 1) for 24 hours and the supernatants harvested. Viral replication of the infected cell supernatant was measured by plaque assay titration relative to the control (cells transfected with an empty vector). (B) Cells were lysed at 24 hours post infection and lysates were separated by SDS-PAGE. Proteins were transferred to a nitrocellulose membrane and a western blot performed using an anti-FLAG antibody against a C-terminal FLAG tag with β-actin as the loading control. Error bars show standard deviations of the means (*n* =3 biological replicates), *** indicates a p-value <0.001, one-way ANOVA.

there is a lack of published data demonstrating whether the chIFITMs are able to restrict avian coronaviruses, namely the prototypic gammacoronavirus, IBV.

Studies have suggested that the cysteine residues at positions 71 and 72 are also important for viral restriction in human and murine IFITM3 (Yount et al., 2012;Chesarino et al., 2014b). It has been found that S-palmitoylation of cysteine residues 71, 72 and 105 of IFITM3 by the palmitoyltransferase ZDHHC20, is important for protein accumulation in cell membranes in addition to the anti-viral activity of IFITM3 against IAV (Compton et al., 2016;Yount et al., 2010;McMichael et al., 2017). It has been found that chIFITM3 contains two palmitoylated cysteine residues at position 71 and 72 (Yount et al., 2010;Yount et al., 2012) but contains a leucine residue at position 105. In all *chIFITM* genes, the palmitoylated cysteine residue found at position 105 in *huIFITM* genes, has been replaced with a leucine residue. It is unknown if the loss of a post-translationally modified amino acid at this position will have a detrimental impact on the restrictive ability of the chIFITMs. To assess the importance of the conserved residues at positions 71 and 72, both were mutated by site-directed mutagenesis (SDM) to alanine residues, thus removing two key post-translational modifications, in addition to assessing the restriction of IBV with wild-type chIFITM proteins.

To address this current lack of data, DF-1 cells were transiently transfected with 1µg of plasmid encoding chIFITM1, *2*, *3* or 3^{MUT} for 24 hours. These cells were infected with BeauR (MOI - 1) for 24 hours, and the supernatants were assayed for the presence of infectious virions. Briefly, material to be assayed was serially diluted in 1x BES and used to infect CK cells in 12-well plates. After 1 hour of incubation, the inoculum was removed, and the cells were overlaid with 2x BES and 2% agar. After 3 days the cells were fixed with 10% paraformaldehyde (PFA) in PBS which was overlaid onto the agar and incubated for 15

minutes. Agar was removed from each well and cells stained with 0.1% crystal violet (w/v) for 10 minutes and plaques counted to determine the pfu/ml.

Transient overexpression of *chIFITM2* significantly restricted the replication of BeauR by 0.45 log10 (Figure 5.4A) when compared to the vector only control. There was also a decrease in the viral titres harvested from cells that were overexpressing chIFITM1, although this was not statistically significant. Cells overexpressing either *chIFITM3* or 3^{MUT} had levels of viral titres that were comparable to each other as well as to the mock control, therefore no statistical difference was observed. The restriction of IBV is different to that of IAV (Figure 5.2A and 5.3A-C). IAV is potently restricted by *chIFITM1*, *2*, *3* and *5* expression while only the overexpression of *chIFITM2* restricts IBV. This may suggest that viral entry, and the processes that mediate this essential part of the viral lifecycle, may play a role in determining viral susceptibility to chIFITM-mediated restriction. Moreover, it is likely that chIFITM localisation plays an essential role in restricting viral infection hence further work is required in order to elucidate this relationship in more detail. It was not possible to assess the role that cysteine residues at positions 71 and 72 have in the restriction of IBV as neither the wildtype nor the mutant were able to competently restrict IBV. Therefore, it is still unclear if these residues play a critical role in the restriction of avian viruses and this will have to be assessed in the context of IAV infection.

5.4 Transient knockdown of chIFITM expression results in increased viral titres

5.4.1 Transient knockdown of *chIFITM1* renders CEFs more susceptible to IAV infection

Using siRNA as a tool to validate the role of a gene is common and was used in the study that initially found that huIFITM3 was a potent restriction factor of IAV (Brass et al., 2009) and that chIFITM3 is a restriction factor of pseudotyped lentiviral vectors (Smith et al., 2013). Synthesising and delivering siRNAs into the cell is a straightforward process that results in a good knockdown of host gene expression when the siRNAs have been designed correctly. It is more difficult to achieve a good knockdown of host innate immune genes due to their relative abundance and their subsequent reactivation upon viral infection (Malathi et al., 2007;Meng et al., 2013). These studies have shown that the innate immune system is activated by the detection of aberrant or foreign RNA, such as the introduction of siRNA, via the cytosolic receptors RIG-1, MDA-5 and LGP2 (Takeuchi and Akira, 2010). This suggests that achieving a prolonged knockdown of *chIFITM* gene expression may be difficult due to the subsequent reactivation of gene expression. In order to test this hypothesis, four individual siRNAs were designed against each chIFITM transcript alongside a single siRNA targeting chIFITM3 and a scrambled siRNA (negative control) that were originally used in the 2013 study published by Smith et al. To confirm the anti-viral effect observed with transient overexpression, transient knockdown of endogenously expressed *chIFITM* transcripts was undertaken in CEFs 24 hours prior to IAV infection. 5nM of each siRNA (20nM in total) was transfected into CEF cells using HiPerfect as per the manufacturer's protocol. After 24 hours the same cells were infected with H9N2 IAV (MOI – 3) for 24 hours after which the supernatants were harvested and viral replication was quantified by plaque assay titration. Material to be assayed was serially diluted in serum-free DMEM and used to

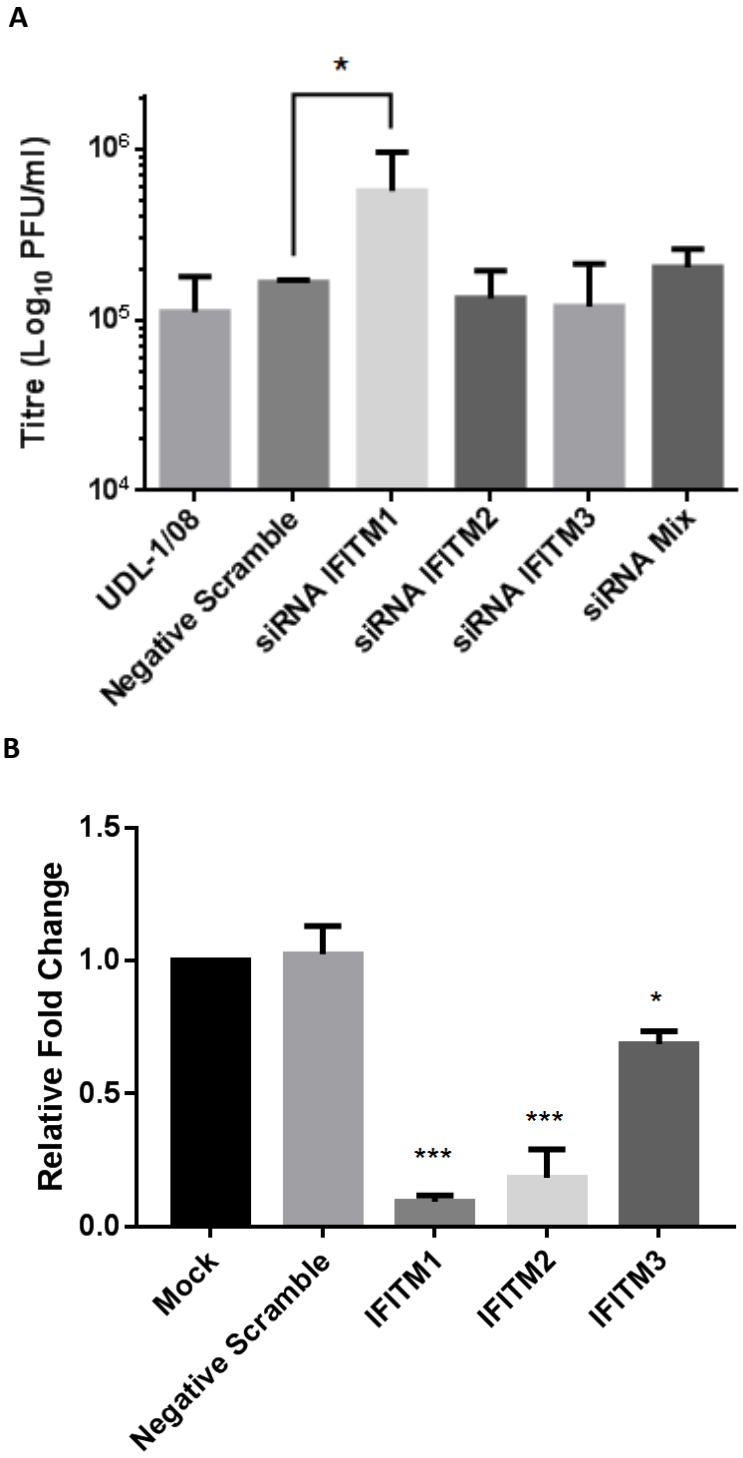

Figure 5.5 Transient knockdown of *chIFITM1* renders CEFs more susceptible to IAV infection. (A) The effect of knocking down endogenous *chIFITM1, 2 or 3* expression in CEF cells infected with H9N2. Viral replication of the infected cell supernatant was measured by plaque assay titration relative to the control (cells transfected with a scrambled siRNA). (B) The expression level and log fold change of *chIFITM1, 2 and 3* were measured using quantitative RT-PCR after pre-incubation with a non-targeting siRNA or ones specific to *chIFITM1, 2 or 3*, relative to mock and normalised by two house-keeping genes, *RPLPO* and *RPL13*. Error bars show standard deviations of the means (*n* =3 biological replicates), * indicates a p-value <0.05, *** indicates a p-value <0.001, one-way ANOVA.

infect MDCK cells in 12-well plates. After 1 hour of incubation, the inoculum was removed, and the cells were overlaid with DMEM containing 0.2% BSA, 2% agar and 1µg trypsin ml^{-1}. After 3 days, the overlay was removed, and the cells were stained with crystal violet to determine the pfu/ml. A statistically significant increase in viral supernatant titre (0.71 log_{10}) was observed with knockdown of *chIFITM1*, followed by infection with IAV (Fig 5.5A), but no statistical difference in virus titres was observed for any other chIFITM knockdown (Fig 5.5A). A combination of all of the siRNAs (5nM of each individual siRNA) at a final concentration of 20nM (siRNA mix) did not increase viral titres and this is likely to be because the most effective siRNAs, likely targeting *chIFITM1*, were further diluted in this pool when compared to targeting *chIFITM1* alone. The cells transfected with the negative scramble had similar titres to those cells that were untransfected and this was confirmed by a lack of a statistical difference between the two groups. Using the same individually designed siRNAs in unstimulated CEFs, chIFITM transcript levels were assessed by quantitative RT-PCR. CEFs were transfected with siRNAs targeting *chIFITM1, 2, 3* or a scrambled siRNA for 24 hours. Cells were harvested 24 hours post transfection, cells were lysed, RNA extracted and reverse transcribed and chIFITM expression levels were assessed by quantitative RT-PCR, relative to mock control and normalised to two house-keeping genes, *RPLPO* and *RPL13*. Although all knockdowns were significant when compared to *chIFITM* transcript abundance in the mock control, there are variances in the knockdown efficiency. Scrambled siRNA did not alter *chIFITM* transcript abundance when assessed against *chIFITM3*. Knockdown of *chIFITM1* and *2* was greater than 70% but *chIFITM3* knockdown only achieved 30% (Figure 5.5B) when compared to chIFITM levels in the mock control.Interrogating this effect in a heterogeneous cell line may allow for further analysis as transfection and infection efficiencies are different between cell lines and *ex vivo* tissue culture models.

5.4.2 Transient knockdown of *chIFITM1* and *3* renders DF-1 cells more susceptible to IAV infection

To fully characterise the effect of chIFITM gene knockdown and the impact that this has on the restriction of avian IAV, DF-1 cells were transfected with the same siRNAs as mentioned in section 5.3.1, although a higher total concentration of 80nM (20nM of each individual siRNA in a pool of four targeting each gene) was used to assess gene knockdown in this continuous cell line. Moreover, in order to expand the study and to further characterise strains we have already investigated, three strains of IAV (H3N8, H5N3 and H9N2) were used, whereas only the enzootic strain (H9N2) was used in section 5.3.1.

20nM of each siRNA (80nM in total) was transfected into DF-1 cells using HiPerfect as per the manufacturer's protocol. After 24 hours the same cells were infected with H3N8, H5N3 or H9N2 IAV (MOI – 1) for 8 and 24 hours after which the supernatants were harvested and the quantification of viral particles was performed using plaque assay titration. Material to be assayed was serially diluted in serum-free DMEM and used to infect MDCK cells in 12-well plates. After 1 hour of incubation, the inoculum was removed, and the cells were overlaid with DMEM containing 0.2% BSA, 2% agar and 1µg trypsin ml^{-1}. After 3 days, the overlay was removed, and the cells were stained with crystal violet to determine the pfu/ml. A statistically significant increase in viral supernatant titre (0.71 log_{10}) was observed with knockdown of *chIFITM3*, followed by infection with H3N8 (8 hours post infection), but no other significant increases in viral titres were observed for the other *chIFITM* knockdowns after infection with H3N8, including the samples assayed at 24 hours post infection (Figure 5.6A). Knockdown of *chIFITM3* led to an increase in viral titres of 1.3 log_{10} and 0.9 log_{10} at 8 and 24 hours post infection respectively when DF-1s were infected with H5N3 (Figure 5.6B). Although a significant knockdown using siRNAs against *chIFITM1* could not be detected by quantitative RT-PCR, there was a significant increase in viral titres

A

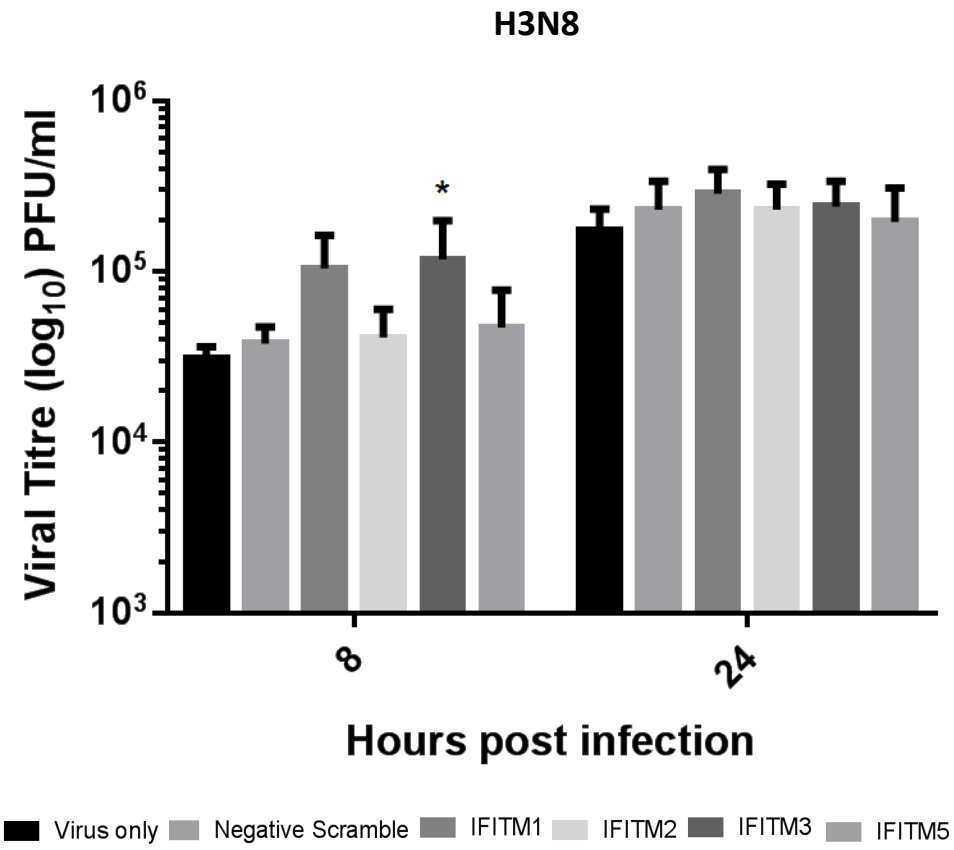
H3N8
Viral Titre (log_{10}) PFU/ml
10^6
10^5
10^4
10^3
*
8
24
Hours post infection
Virus only
Negative Scramble
IFITM1
IFITM2
IFITM3
IFITM5

B

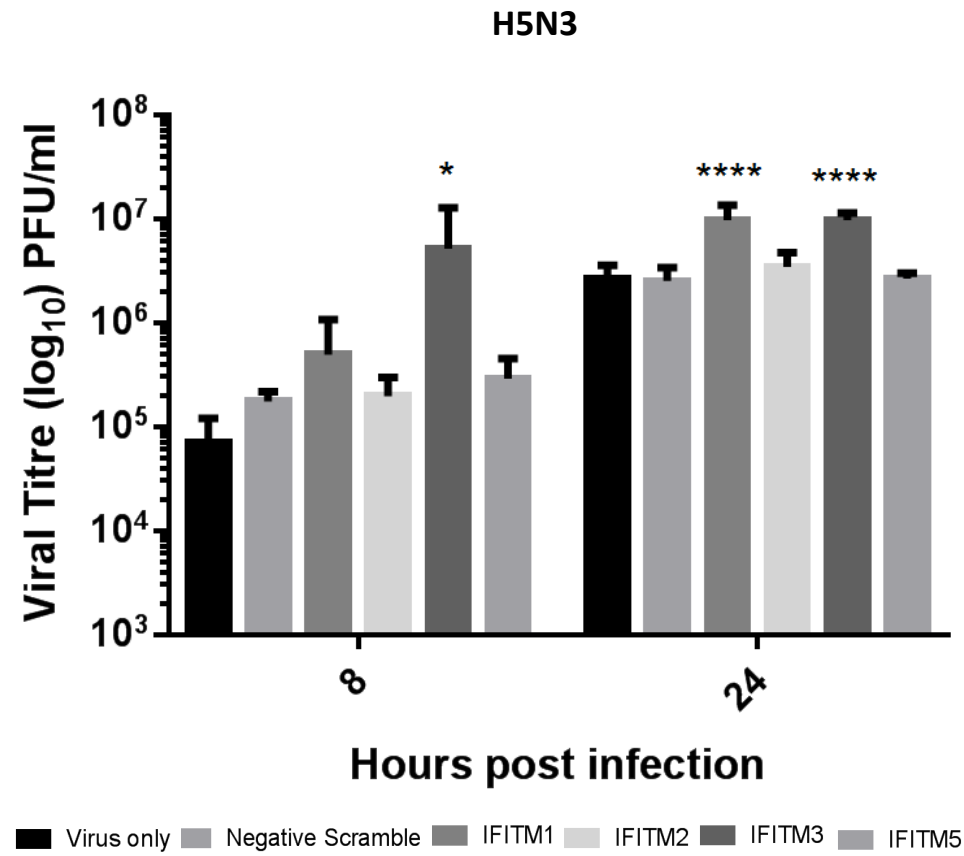
H5N3
Viral Titre (log_{10}) PFU/ml
10^8
10^7
10^6
10^5
10^4
10^3
*
****
****
8
24
Hours post infection
Virus only
Negative Scramble
IFITM1
IFITM2
IFITM3
IFITM5

C

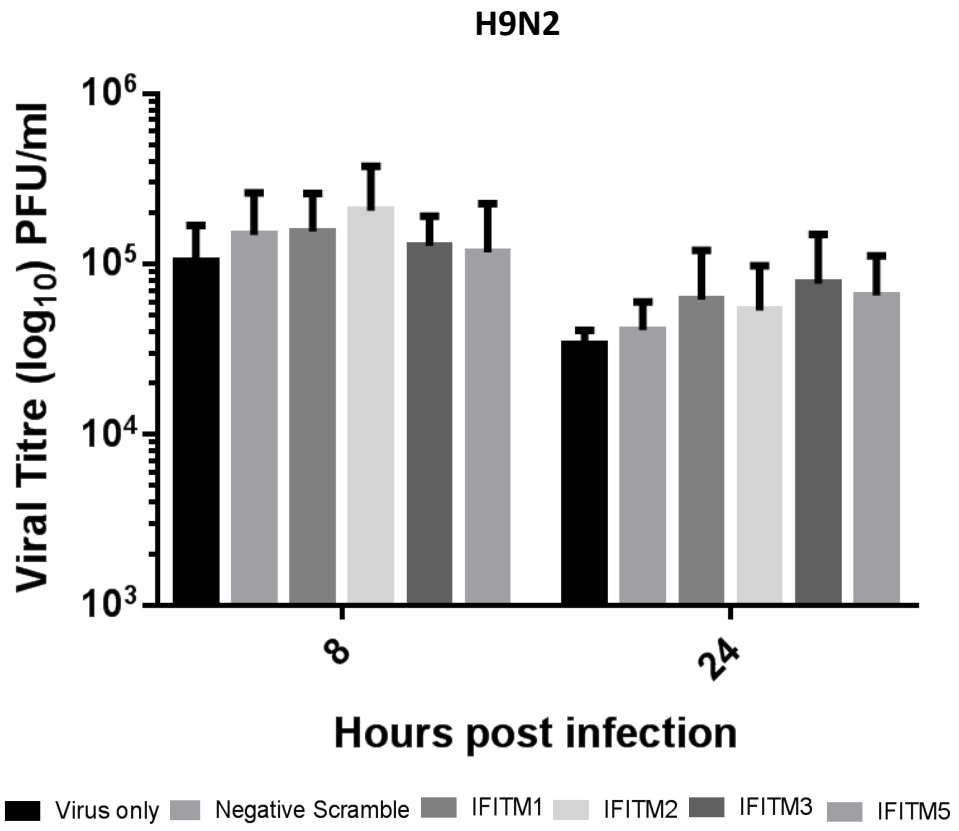
H9N2
Viral Titre (log_{10}) PFU/ml
10^6
10^5
10^4
10^3
8
24
Hours post infection
Virus only
Negative Scramble
IFITM1
IFITM2
IFITM3
IFITM5

D

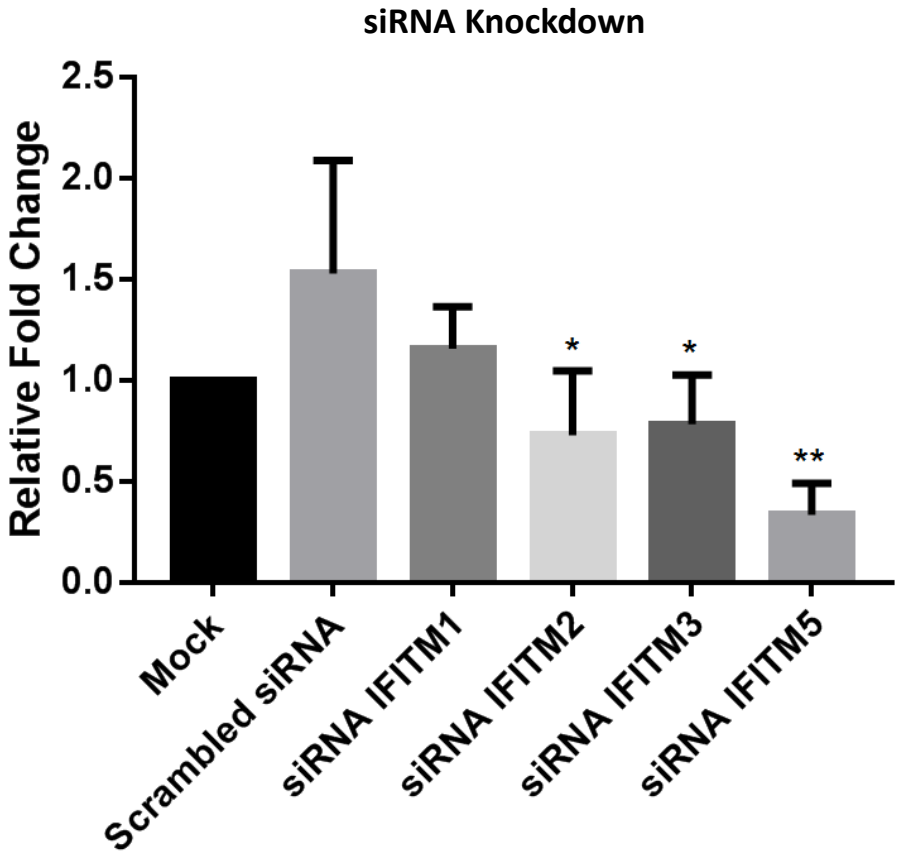
siRNA Knockdown
Relative Fold Change
2.5
2.0
1.5
1.0
0.5
0.0
*
*
**
Mock
Scrambled siRNA
siRNA IFITM1
siRNA IFITM2
siRNA IFITM3
siRNA IFITM5

E

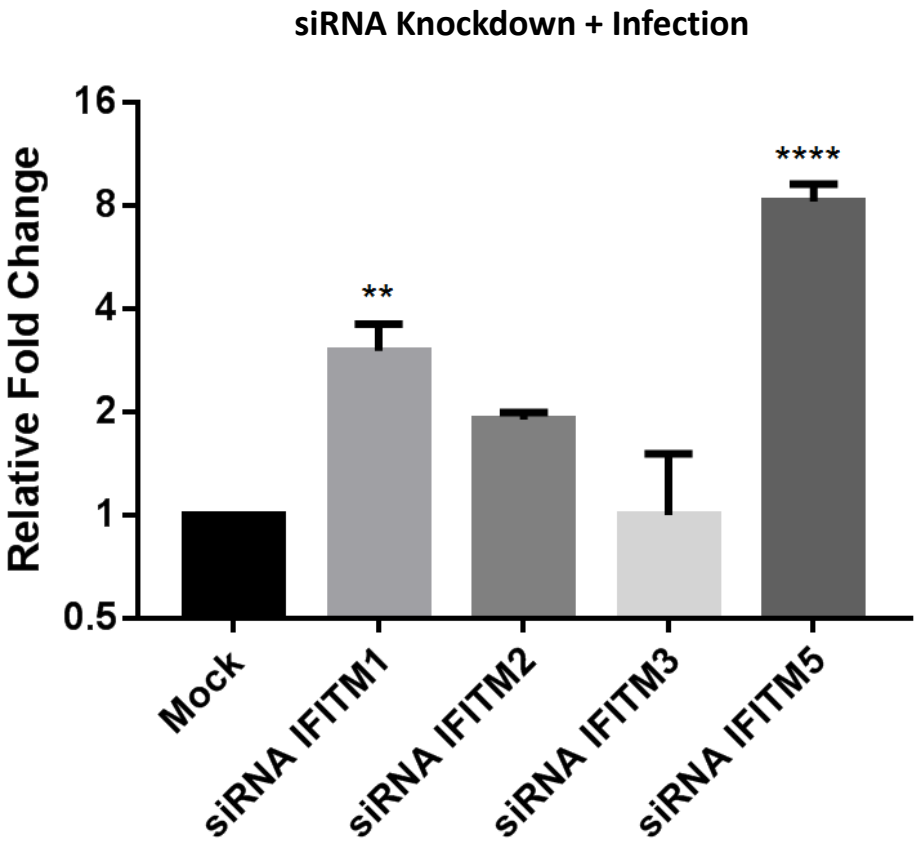
siRNA Knockdown + Infection
Relative Fold Change
16
8
4
2
1
0.5
**
****
Mock
siRNA IFITM1
siRNA IFITM2
siRNA IFITM3
siRNA IFITM5

F

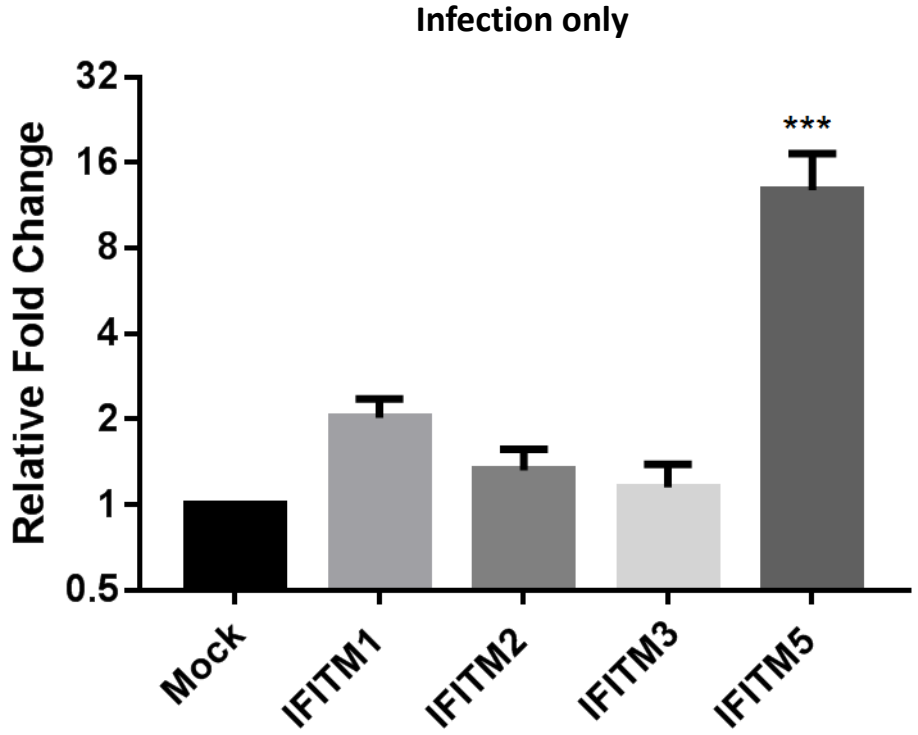
Infection only
Relative Fold Change
32
16
8
4
2
1
0.5
***
Mock
IFITM1
IFITM2
IFITM3
IFITM5

Figure 5.6 Transient knockdown of *chIFITM1* and *3* renders DF-1s more susceptible to IAV infection. (A - C) The effect of knocking down endogenous *chIFITM1*, *2*, *3* or *5* expression in DF-1 cells infected with H3N8, H5N3 or H9N2 (MOI 1, 8 and 24 hours) was measured by plaque assay titration in MDCK cells. (D) The expression level and log fold change of *chIFITM1*, *2*, *3* and *5* were measured using quantitative RT-PCR (relative to mock, normalised to RPLPO and RPL13) after pre-incubation with a non-targeting (scrambled) siRNA or siRNAs specific to *chIFITM1*, *2*, *3* or 5. (E) The effect of infection on knockdown was assessed by the expression level and log fold change of *chIFITM1*, *2*, *3* and *5* measured using quantitative RT-PCR (relative to mock, normalised to RPLPO and RPL13) 48 hours after transfection and 24 hours after infection (MOI 1). (F) The expression level and log fold change of *chIFITM1*, *2*, *3* and *5* were measured using quantitative RT-PCR (relative to mock, normalised to RPLPO and RPL13) after infection with H9N2 in DF-1 cells (MOI 1, 24 hours). Error bars show standard deviations of the means (*n* =3 biological replicates), * indicates a p-value <0.05, ** indicates a p-value<0.01, *** indicates a p-value <0.001, ****indicates a p-value <0.0001 one-way ANOVA.

(0.9 $\log_{10}$) at 24 hours post infection when chIFITM1-depleted cells were infected with H5N3 (Figure 5.6B). There were no significant differences in viral titres for chIFITM-depleted cells that were infected with H9N2 (Figure 5.6C).

Transient knockdown of endogenously expressed *chIFITM* transcripts in a continuous chicken cell line was evaluated 24 hours post transfection and before IAV infection. Using the same method as previously described, samples were harvested at 24 hours post transfection. The cells were lysed, RNA extracted and reverse transcribed and *chIFITM* expression levels were assessed by quantitative RT-PCR, relative to mock and normalised to two house-keeping genes, RPLPO and RPL13. Scrambled siRNA did not significantly alter *chIFITM* transcript abundance when assessed against an average of all four *chIFITMs* under mock conditions (Fig 5.6D). A statistically significant knockdown of *chIFITM 2* (35%)*, 3* (32%) *and 5* (75%) was achieved in this cell line. A reliable knockdown of *chIFITM1* expression could not be achieved and consequently this did not reach significance in comparison to the negative scramble. The siRNA knockdown of chIFITM expression was variable across all *chIFITMs* that were quantified (Figure 5.6D). The absence of a significant increase in viral titres for cells depleted of *chIFITM1* and infected with H9N2 may be explained by the poor, non-significant knockdown of *chIFITM1* in this cell type. It is not yet understood why *chIFITM1* knockdown was better in CEFs when compared to DF-1 cells, although the increase in H5N3 viral titres at 24 hours post infection suggest that variability may be a factor in determining which cells are susceptible to infection.

To evaluate the impact that transfection and infection has on *chIFITM* expression, the native upregulation of the *chIFITMs* were measured using samples without transfection of the negative scramble (80nM). Samples were taken 24 and 48 hours post infection with H9N2 (MOI – 1) and were analysed using quantitative RT-PCR. The cells were lysed, RNA extracted and reverse transcribed and chIFITM expression levels were assessed by

quantitative RT-PCR, relative to mock and normalised to two house-keeping genes, RPLPO and RPL13. Transfection of the negative scramble, followed by infection with H9N2 led to significant upregulation in both *chIFITM1* and *chIFITM5* mRNA expression, when compared to the mock control. The transcript abundance of *chIFITM2* was upregulated 2 fold, whilst *chIFITM3* was not upregulated and levels of mRNA were comparable to those of the mock-infected control. In contrast, in the untransfected cells, only *chIFITM5* was significantly upregulated upon infection with H9N2. Moreover, although levels of *chIFITM1* and *2* were scarcely upregulated, these failed to reach the levels observed in the pre-transfected sample and were not significant. As described previously, levels of *chIFITM3* remained comparable to mock-infected levels. This data suggests that siRNA treatment may increase *chIFITM* transcript abundance which may be a result of further innate immune activation driven by siRNA transfection. This implies that siRNA treatment for the purposes of knocking down ISG expression may not be the most preferable method of choice as the knockdown appears to be inefficient. In order to reduce cellular stress, the activation of innate immune pathways and the subsequent induction of ISG expression, other methods of gene silencing, such as CRISPR/CAS9 may allow for better silencing without reactivation.

5.4.3 Transient knockdown of chIFITM2 renders DF-1s more susceptible to IBV infection

As has previously been mentioned in chapter 4, the cellular tropism of both M41 and QX is constrained and they are only able to infect primary chick kidney cultures which are not suitable for transfection experiments. Due to these constraints, BeauR is utilised as a model strain of IBV as it can infect DF-1 cells, a cell line that can also be transfected. The data has demonstrated that the *chIFITMs* are transcriptionally upregulated in response to viral challenge (Figure 4.7) and this was investigated using quantitative RT-PCR and this was significant for all four chIFITM genes at 24 hours post infection. Furthermore, DF-1 cells

transiently transfected with the *chIFITM* expression constructs resulted in a significant decrease in viral titres for *chIFITM2* overexpressing cells. The data implies that the *chIFITMs* play a functional role in the restriction of IBV, although there is currently a lack of data demonstrating if knockdown of *chIFITM* expression results in increased viral titres.

In order to address these challenges and gaps in our current understanding, DF-1 cells were transiently transfected with 20nM of each siRNA (80nM in total) using HiPerfect as per the manufacturer's protocol. These cells were infected with BeauR (MOI - 1) for 24 hours, and the supernatants assayed for the presence of infectious virions. Briefly, material to be assayed was serially diluted in 1x BES and used to infect CK cells in 12-well plates. After 1 hour of incubation, the inoculum was removed, and the cells were overlaid with 2x BES and 2% agar. After 3 days the cells were fixed with 10% paraformaldehyde (PFA) in PBS which was overlaid onto to the agar and incubated for 15 minutes. Agar was removed from each well and cells stained with 0.1% crystal violet (w/v) for 10 minutes and plaques counted to determine the pfu/ml. A statistically significant increase in viral supernatant titre (1.1 $\log_{10}$) was observed with knockdown of *chIFITM2*, followed by infection with BeauR (24 hours post infection, MOI – 1), but no other significant increases in viral titres were observed for any of the other *chIFITMs* that were targeted (Figure 5.7A). The viral titres between infected cells and cells that were treated with scrambled siRNA before infection are not significantly different. Transient knockdown of endogenously expressed *chIFITM* transcripts was assessed by quantitative RT-PCR with samples that were harvested at 24 hours post transfection. The cells were lysed, RNA extracted and reverse transcribed and *chIFITM* expression levels were assessed by quantitative RT-PCR, relative to mock and normalised to two house-keeping genes, *RPLPO* and *RPL13*. Scrambled siRNA did not significantly alter *chIFITM* transcript abundance when assessed against an average of all four *chIFITMs* at basal levels (Figure 5.7B). The knockdown of all four *chIFITM* genes was significant when

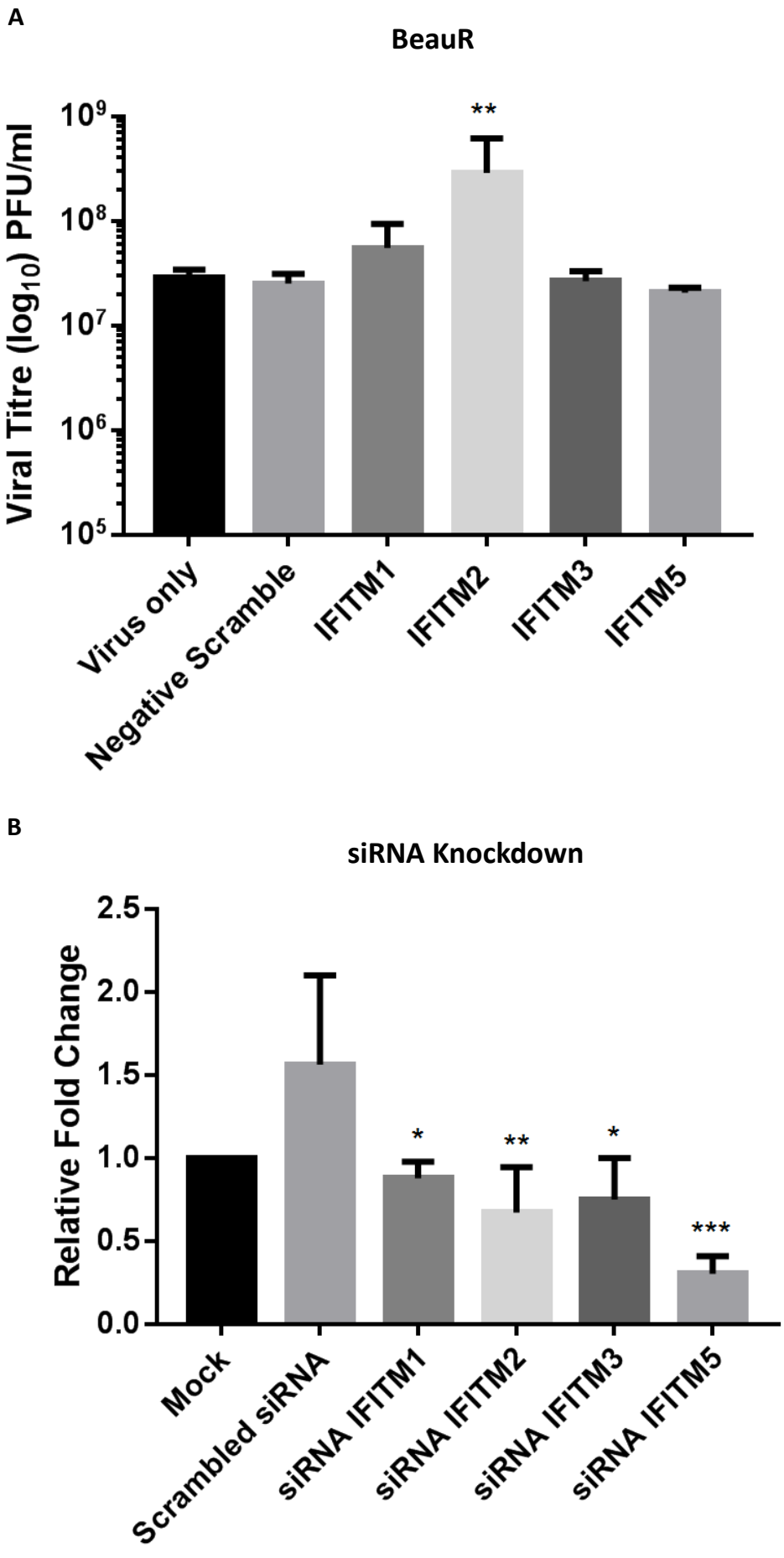
A
BeauR
Viral Titre (log10) PFU/ml
10^9
10^8
10^7
10^6
10^5
**
Virus only
Negative Scramble
IFITM1
IFITM2
IFITM3
IFITM5
B
siRNA Knockdown
Relative Fold Change
2.5
2.0
1.5
1.0
0.5
0.0
*
**
*
***
Mock
Scrambled siRNA
siRNA IFITM1
siRNA IFITM2
siRNA IFITM3
siRNA IFITM5

C

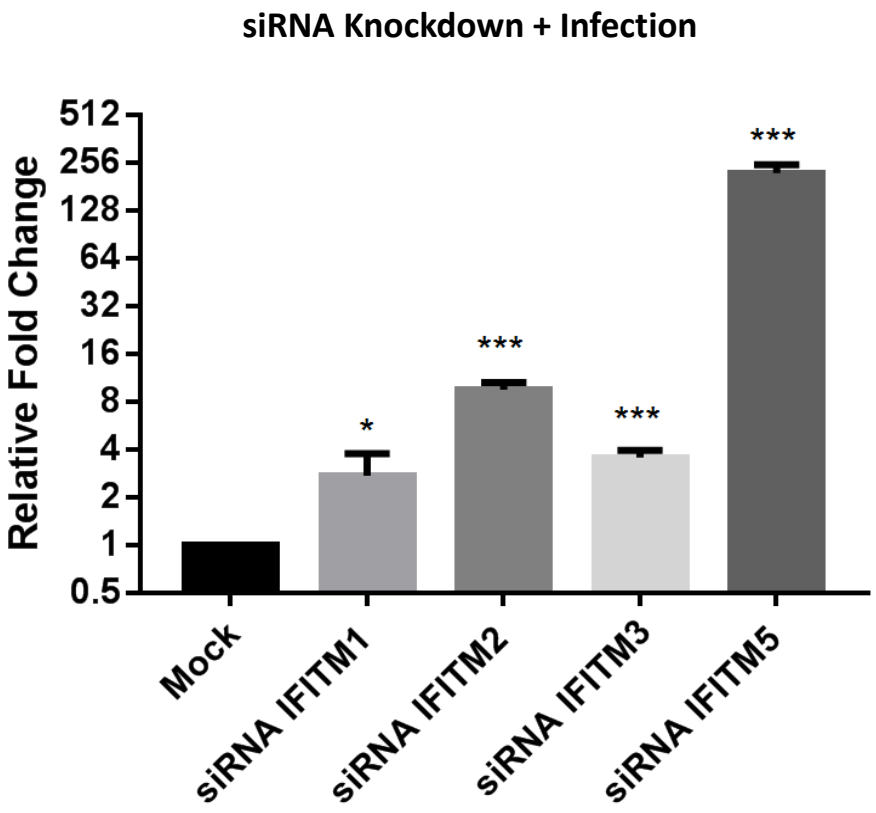
siRNA Knockdown + Infection
Relative Fold Change
512
256
128
64
32
16
8
4
2
1
0.5
*
***
***
***
Mock
siRNA IFITM1
siRNA IFITM2
siRNA IFITM3
siRNA IFITM5

D

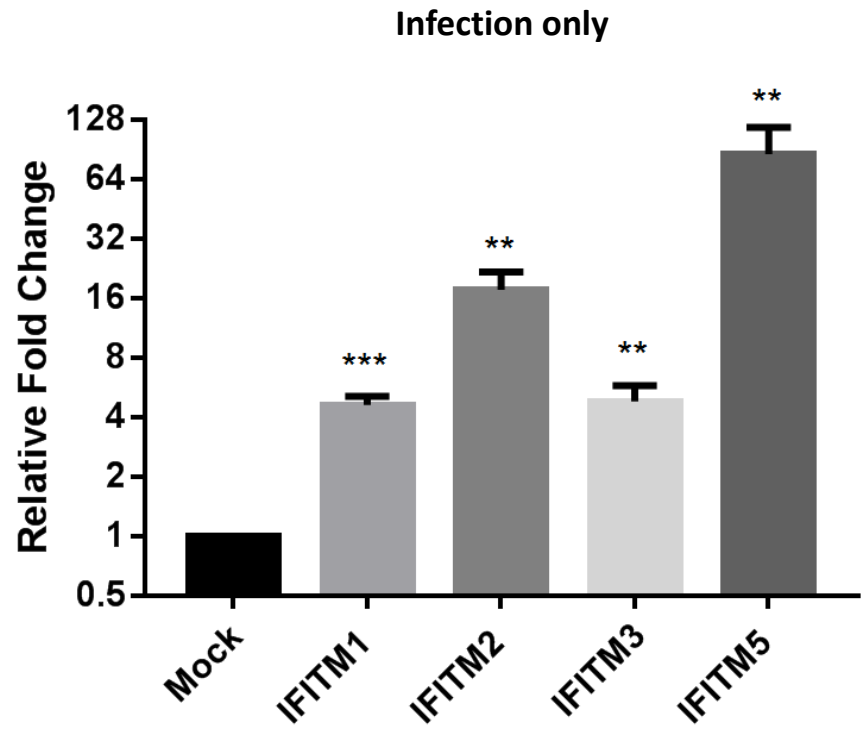
Infection only
Relative Fold Change
128
64
32
16
8
4
2
1
0.5
***
**
**
**
Mock
IFITM1
IFITM2
IFITM3
IFITM5

Figure 5.7 Transient knockdown of *chIFITM2* renders DF-1s more susceptible to IBV infection. (A) The effect of knocking down endogenous *chIFITM1*, *2*, *3* or *5* expression in DF-1 cells infected with BeauR (MOI 1, 24 hours) was measured by plaque assay titration in CK cells. (B) The expression level and log fold change of *chIFITM1*, *2*, *3* and *5* were measured using quantitative RT-PCR (relative to mock, normalised to RPLPO and RPL13) after pre-incubation with a non-targeting (scrambled) siRNA or siRNAs specific to *chIFITM1*, *2*, *3* or 5. (C) The effect of infection on knockdown was assessed by the expression level and log fold change of *chIFITM1*, *2*, *3* and *5* measured using quantitative RT-PCR (relative to mock, normalised to *RPLPO* and *RPL13*) 48 hours after transfection and 24 hours after infection (MOI 1). (D) The expression level and log fold change of *chIFITM1*, *2*, *3* and *5* were measured using quantitative RT-PCR (relative to mock, normalised to RPLPO and RPL13) after infection with BeauR in DF-1 cells (MOI 1, 24 hours). Error bars show standard deviations of the means (*n* =3 biological replicates), * indicates a p-value <0.05, ** indicates a p-value<0.01, *** indicates a p-value <0.001, ****indicates a p-value <0.0001 one-way ANOVA.

compared to the scrambled siRNA control, similar to what was observed in the IAV study (Figure 5.6D). In agreement with data shown earlier in this chapter, transfection with siRNA prior to infection appears to prime the cell for an enhanced response as the *chIFITMs* are transcriptionally upregulated when compared to the infection only control and normalised to the mock infection control. There is a significant increase in the mRNA expression for all four *chIFITMs*, and only *chIFITM1* has a less significant increase in gene expression compared to the infection only control (Figure 5.7C and D). Furthermore, the pattern of *chIFITM* gene expression is similar between the two conditions, with *chIFITM5* having the greatest increase in mRNA expression followed by *chIFITM2*. Although the Y axis on both figures is in a $\log_2$ format, it is important to note that the scales are different. For example the Y axis is significantly higher for the samples treated with scrambled siRNA prior to infection than for the samples that were only infected with BeauR.

Taken together with the transient overexpression data (Figure 5.4), these observations suggest that chIFITM2 is the primary restriction factor of IBV in DF-1 cells. The other chIFITMs, either when ablated or overexpressed, do not appear to play a significant role in the restriction of IBV. This may imply that viral entry and/or replication is a determining factor in restriction, although the mechanisms underpinning this are unclear. The specific antiviral activities of chIFITM-mediated restriction may be important in the context of viral infection as chIFITMs differentially restrict viral pathogens and this may be dependent on the cell line used.

5.5 DF-1 cells stably-expressing chIFITM1, 2, 3 or 3^{MUT} result in the restriction of avian viruses

5.5.1 DF-1 cells stably-expressing chIFITM1, 2, 3 or 3^{MUT} differentially restrict H3N8, H5N3 or H9N2

Stable transfection allows for the expansion of cells that are stably expressing a gene of interest under the selection of a reporter gene or antibiotic. Stably transfected nucleic acid can either be delivered into the cells for incorporation into the host genome or it can be transfected into the target cell where it remains as an expression vector without incorporation.

Transient transfection delivers nucleic acid, such as dsDNA plasmids, into cells in a copy number independent manner. Cells will therefore express one or more copies of the exogenous gene, resulting in differential expression levels of the gene of interest. After stable transfection, it is possible to select clonal populations that can be expanded so that the expression profile of each cell is comparable. In this study, DF-1 cells were transfected with expression vectors that had the *chIFITM* gene sequences cloned into them with a FLAG tag on the C-terminus immediately following the chIFITM protein. Synthetic copies of *chIFITM1, 2, 3* and 3^{MUT} gene strings were cloned into the *BamHI* and *NotI* sites of the vector pcDNA4myc/HIS B and sequences and junctions confirmed by Sanger sequencing. Stably transfected cells were generated by transfecting DF-1 cells with 1µg of plasmid and 4µl of Lipofectamine 2000 in one well of a 12 well plate, as per the manufacturers protocol. After 24 hours the medium was removed from the cells and replaced with DMEM containing 10% fetal bovine serum (FBS) and 100µg/ml zeocin. To determine the incorporation of the pcDNA4 plasmids into the target cells, untransfected DF-1 cells were treated with the same concentration of zeocin and cell death was used as a marker for

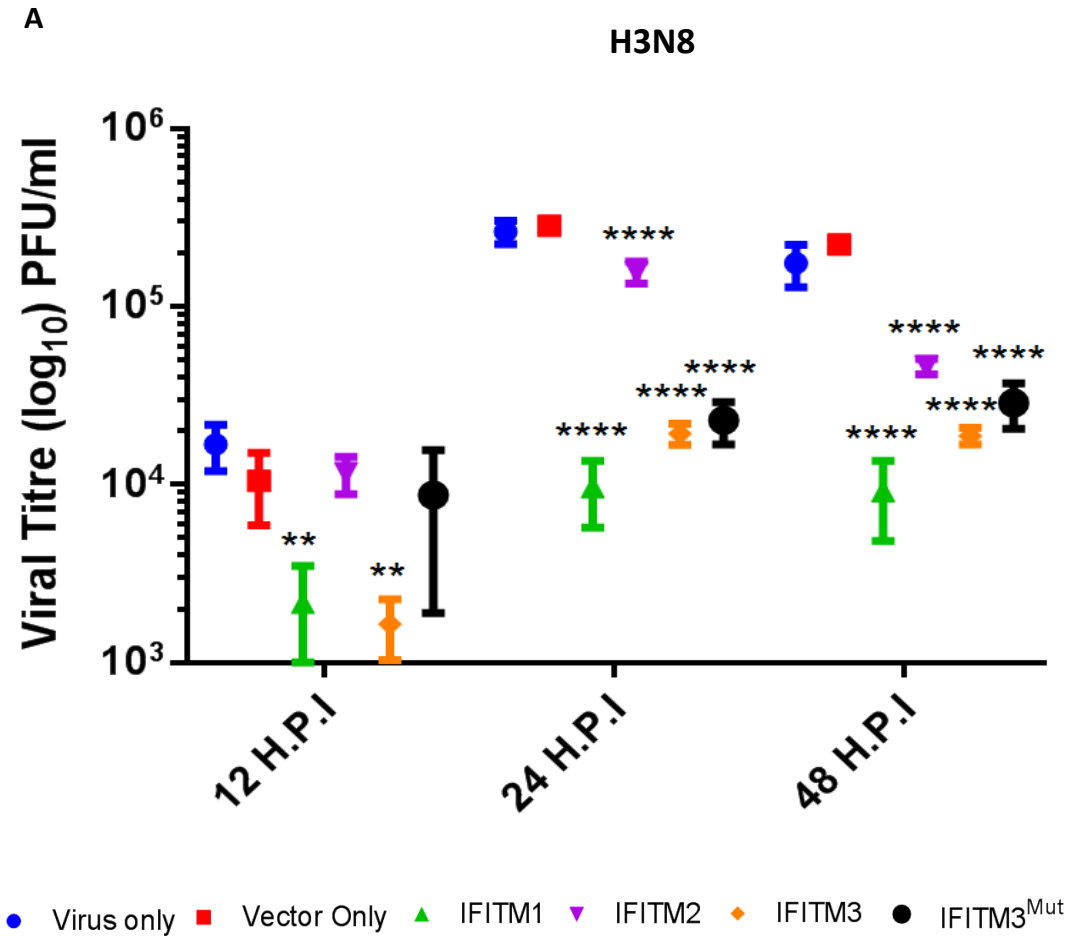
A
H3N8
Viral Titre (log10) PFU/ml
10^6
10^5
10^4
10^3
12 H.P.I
24 H.P.I
48 H.P.I
Virus only
Vector Only
IFITM1
IFITM2
IFITM3
IFITM3Mut

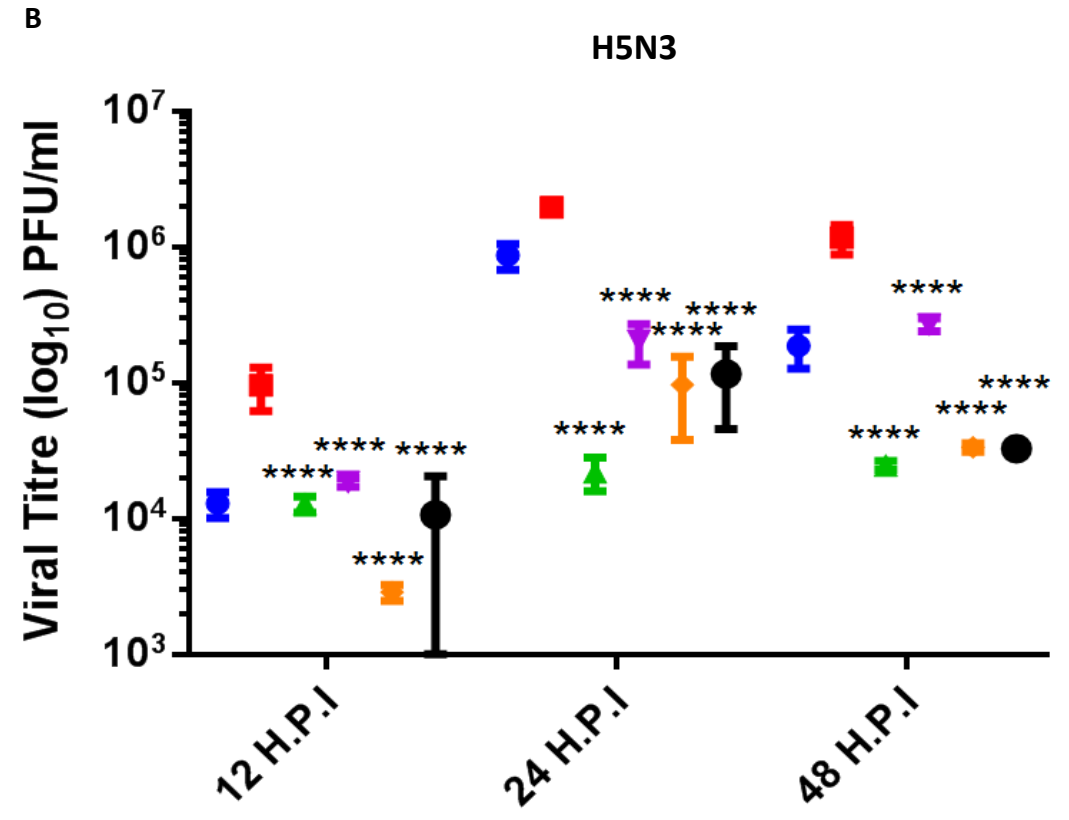
B
H5N3
Viral Titre (log10) PFU/ml
10^7
10^6
10^5
10^4
10^3
12 H.P.I
24 H.P.I
48 H.P.I

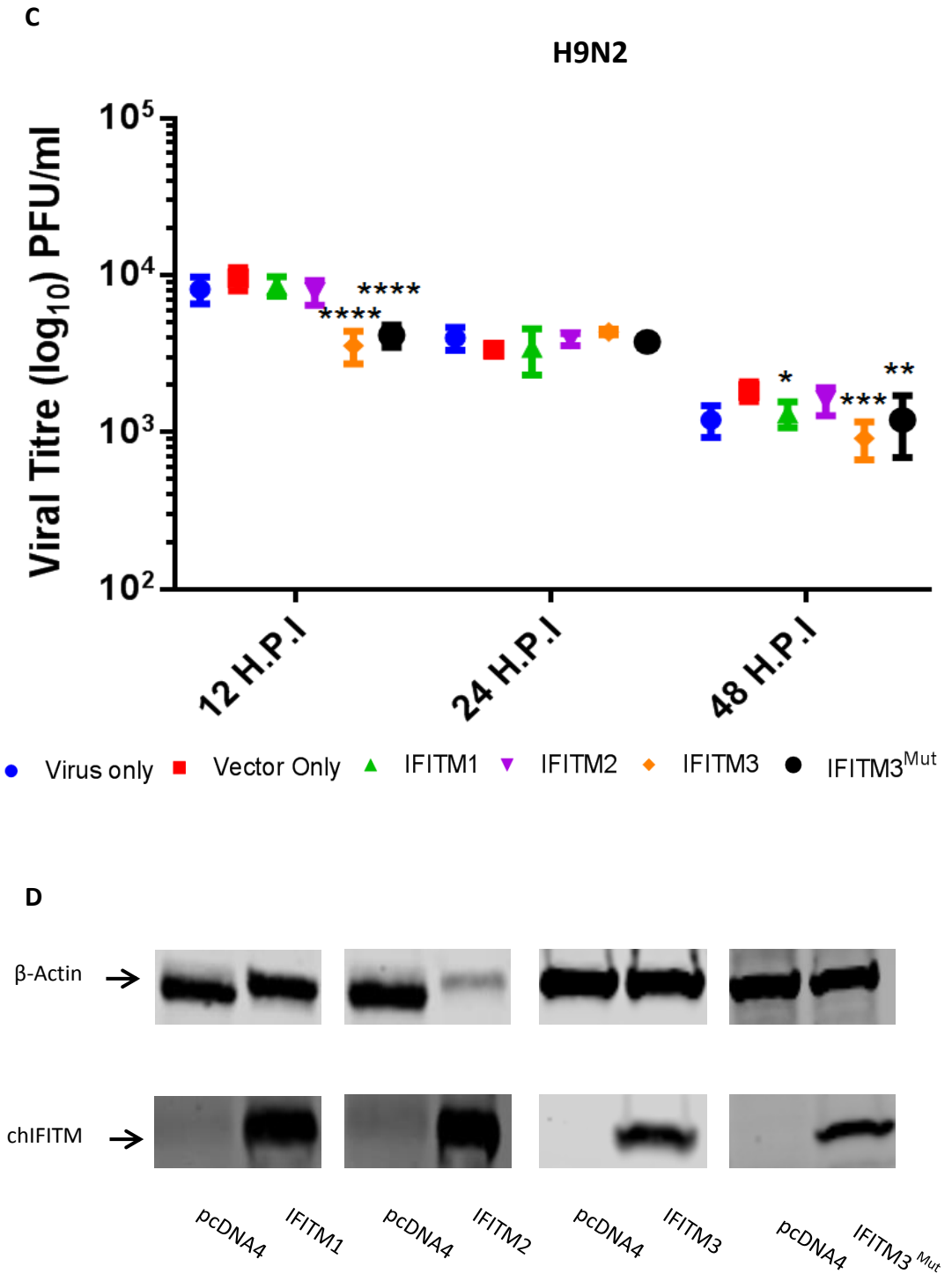

Figure 5.8 DF-1 cells stably-overexpressing *chIFITM1*, 2, 3 and 3^{MUT} restrict IAV infection. (A – C) DF-1 cells stably-expressing chIFITM1, 2, 3 or 3^{MUT} were infected with IAV (H3N8, H5N3 or H9N2, respectively, MOI 0.1) for 12, 24 or 48 hours. Viral replication was measured by plaque assay titration in MDCK cells of the infected cell supernatant relative to the control (empty vector). (D) Lysates were separated by SDS-PAGE and proteins were transferred to a nitrocellulose membrane and a western blot performed using a monoclonal antibody against the FLAG tag. Error bars show standard deviations of the means (n =3 biological replicates), * indicates a p-value <0.05, ** indicates a p-value<0.01, *** indicates a p-value <0.001 ****indicates a p-value <0.0001, one-way ANOVA.

vector incorporation. To verify the observations achieved with either transient knockdown or transient overexpression, DF-1 cells that stably express *chIFITM1, 2, 3* or *3^{MUT}* were generated. The chIFITM3^{MUT} cell line was been engineered so that the cysteine residues at positions 71 and 72 were mutated to alanine residues, which we hypothesise would alter the antiviral properties of chIFITM3.

The stably-expressing DF-1 cells, alongside a vector only control and untransfected DF-1 cells, were infected with the aforementioned strains of IAV (H3N8, H5N3 or H9N2) at an MOI of 0.1 for 12, 24 or 48 hours. The supernatants from infected cells were harvested and the quantification of viral particles was performed using plaque assay titration. Material to be assayed was serially diluted in serum-free DMEM and used to infect MDCK cells in 12-well plates. After 1 hour of incubation, the inoculum was removed, and the cells were overlaid with DMEM containing 0.2% BSA, 2% agar and 1µg trypsin ml^{-1}. After 3 days, the overlay was removed, and the cells were stained with crystal violet to determine the pfu/ml. Under these experimental conditions a statistically significant difference in the restriction of these viruses by the chIFITMs was observed. H3N8 and H5N3 were restricted by all of the chIFITMs that were tested (Figure 5.8A and B). The only significant difference between these two strains was observed at 12 hours post infection (Figure 5.8A). In these samples chIFITM2 and chIFITM3^{MUT} were not able to restrict H3N8, although this effect was not observed at the later time points. A 1 $\log_{10}$ reduction in viral titres was consistently observed in those cells that were stable-expressing *chIFITM1, 3* and *3^{MUT}.* Smaller but still significant reductions in viral titres were observed with cells stably-overexpressing *chIFITM2*. Infection with H9N2 led to a smaller, but still significant, decrease in viral titres with chIFITM3 and 3^{MUT} at 12 hours post infection and with chIFITM1, 3 and 3^{MUT} at 48 hours post infection. No significant differences in viral titres were observed at 24 hours post infection when these cells were challenged with H9N2. Moreover, there was no significant

decrease in viral titres for cells stably-expressing *chIFITM2* and infected with H9N2. This may suggest preferential restriction of IAV by *chIFITM1* and *3.*

The level of chIFITM protein expression was assessed using western blot against the C-terminal FLAG tag (Figure 5.8D). Samples of stably expressing cell lysate were taken at 0 hours post infection to assess protein expression at the start of infection. The cells were lysed, the proteins were separated by SDS-PAGE and transferred onto a nitrocellulose membrane. Western blots were performed using a FLAG antibody alongside β-actin loading control. All of the chIFITM proteins were expressed when compared to the vector only control. Levels of β-actin were relatively stable across all of the samples, with the exception of the chIFITM2 overexpressing cell lysate where the level of β-actin was lower than the corresponding control.

These data suggest that chIFITMs are potent restriction factors of IAV. In particular, H3N8 and H5N3 viral titres are significantly reduced by chIFITM1, 2, 3 and 3^{MUT} overexpression, although nuances in the data suggest that not all chIFITMs are equally as potent in restricting IAV. Moreover, the data suggests that *chIFITM2* is less able to restrict IAV as the differences in viral titres, although significant, are lower than those observed with *chIFITM1* and 3 overexpression. This implies that chIFITM1 and 3 preferentially restrict IAV *in vitro*. In addition, this study aimed to determine the importance of the cysteine residues at positions 71 and 72 in chIFITM-mediated restriction. It appears that there is little difference in the restrictive profile between the native and the mutated chIFITM3 proteins. There was a greater degree of variation in the $chIFITM3^{MUT}$ viral titres early on post infection, but these effects were transient and viral titres were comparable at later time points, across all three strains of IAV that were tested. It is therefore proposed that mutations at these positions have little impact on restriction, which is in contrast to data published in the mammalian field.

5.5.2 Stably-expressing DF-1 cells differentially restrict IAV when infected at a high MOI

The ability of a virus to colonise a host is critical in ensuring its maintenance in the viral population (Caron et al., 2017). Viral infections are able to propagate with relatively few virions. This makes seasonal cases of influenza prevalent in the community as well as other viral infections. In section 5.4.2 a relatively low MOI was used to assess chIFITM mediated restriction and this simulates a more realistic model of infection, especially when transmission is mediated through liquid droplets produced from coughing and/or sneezing. These data demonstrate that three strains of IAV are potently restricted by chIFITM overexpression, although differences between both viral restriction and the chIFITMs mediating this effect suggest that restriction is not universal. Moreover, chIFITM1 and 3 may preferentially restrict influenza. In agreement with other data presented in this chapter, H9N2 appears to be less sensitive to chIFITM-mediated restriction than the other two avian influenza A viruses that have been examined. Although the mechanism underlying this is currently unknown, it is possible that one of the viral interferon agonists, NS1 or PB1-F2, is mediating this effect.

Stably-expressing DF-1 cells were infected with chicken H3N8, H5N3 or H9N2 influenza virus (MOI - 5) for 12 or 24 hours, and the supernatants were assayed for the presence of infectious virions. Material to be assayed was serially diluted in serum-free DMEM and used to infect MDCK cells in 12-well plates. After 1 hour of incubation, the inoculum was removed, and the cells were overlaid with DMEM containing 0.2% BSA, 2% agar and 1µg trypsin ml^{-1}. After 3 days, the overlay was removed, and the cells were stained with crystal violet to determine the pfu/ml. Cells overexpressing any of the *chIFITMs* at 12 hours post infection and infected with H3N8 were not able to restrict viral infection as evidenced by non-significant differences in viral titres (Figure 5.9A). At 24 hours post infection there was

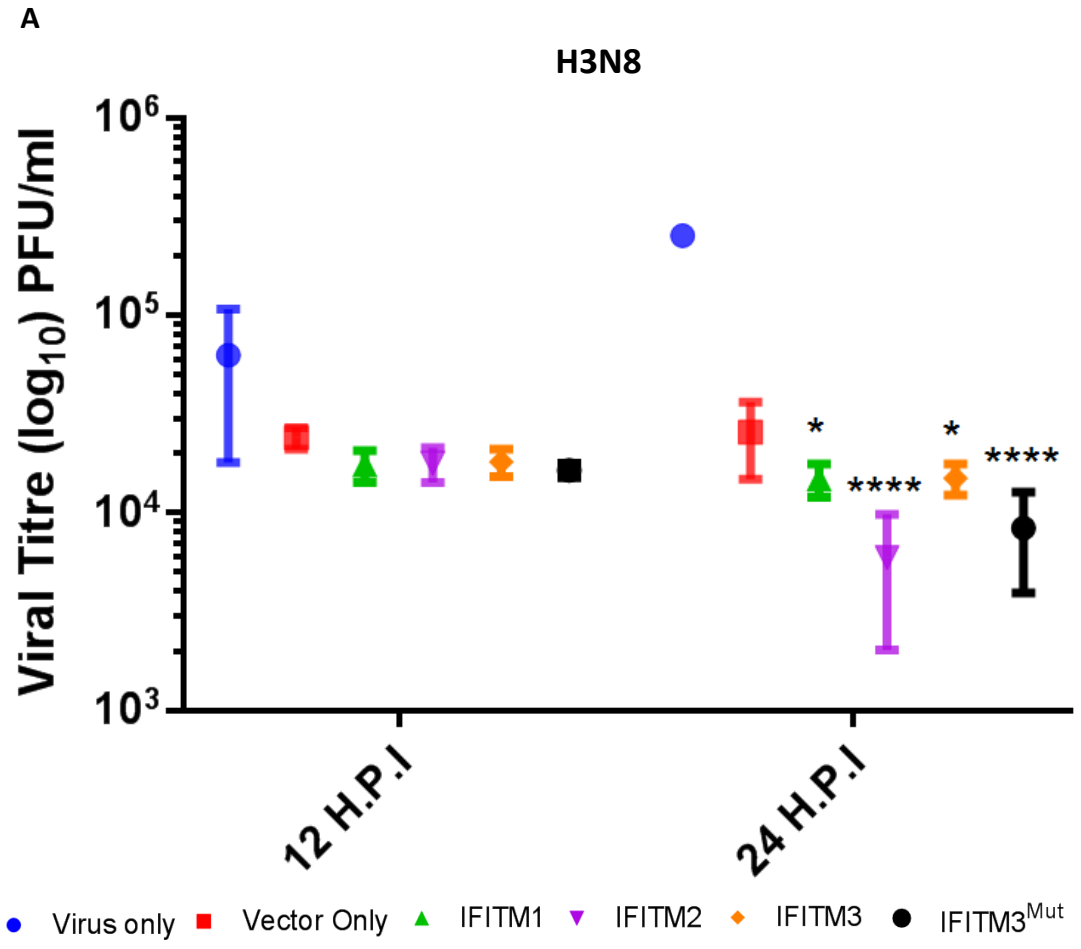
A
H3N8
Viral Titre (log_{10}) PFU/ml
10^6
10^5
10^4
10^3
*
****
*
****
12 H.P.I
24 H.P.I
Virus only
Vector Only
IFITM1
IFITM2
IFITM3
IFITM3Mut

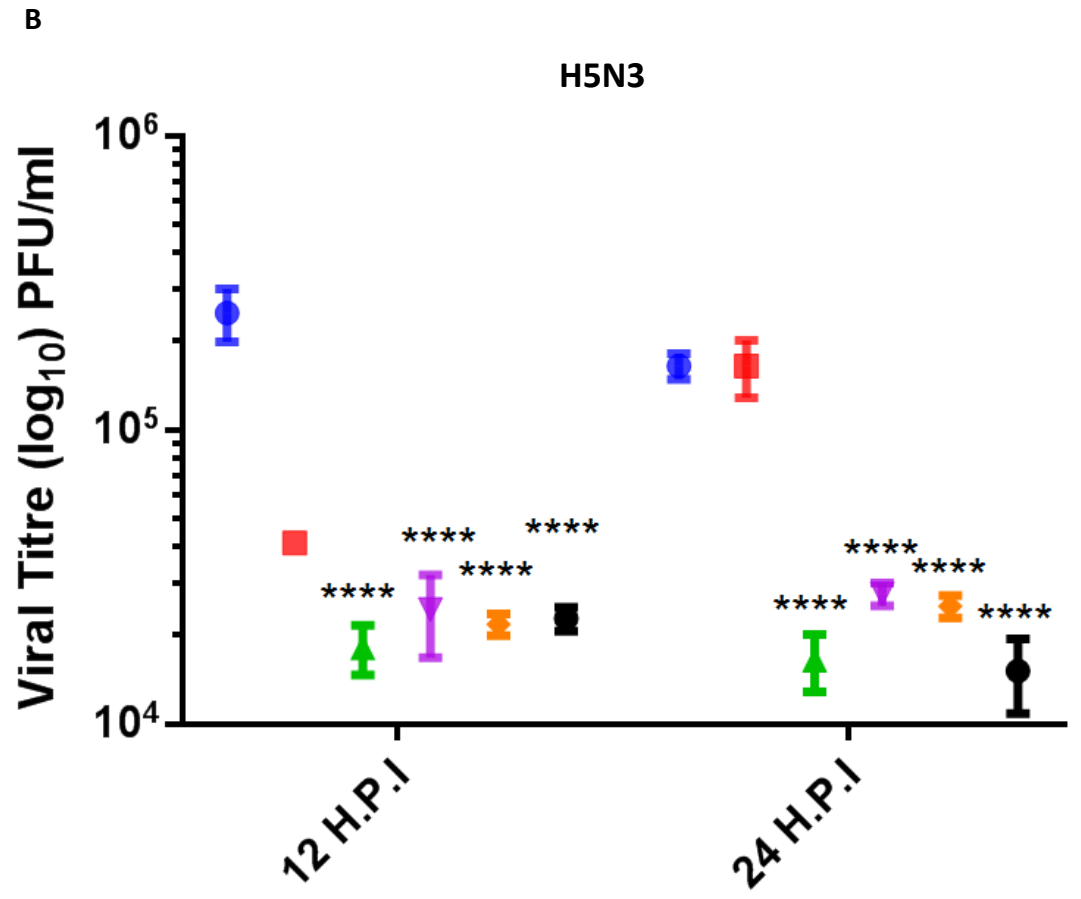
B
H5N3
Viral Titre (log_{10}) PFU/ml
10^6
10^5
10^4
****
****
****
****
****
****
****
12 H.P.I
24 H.P.I

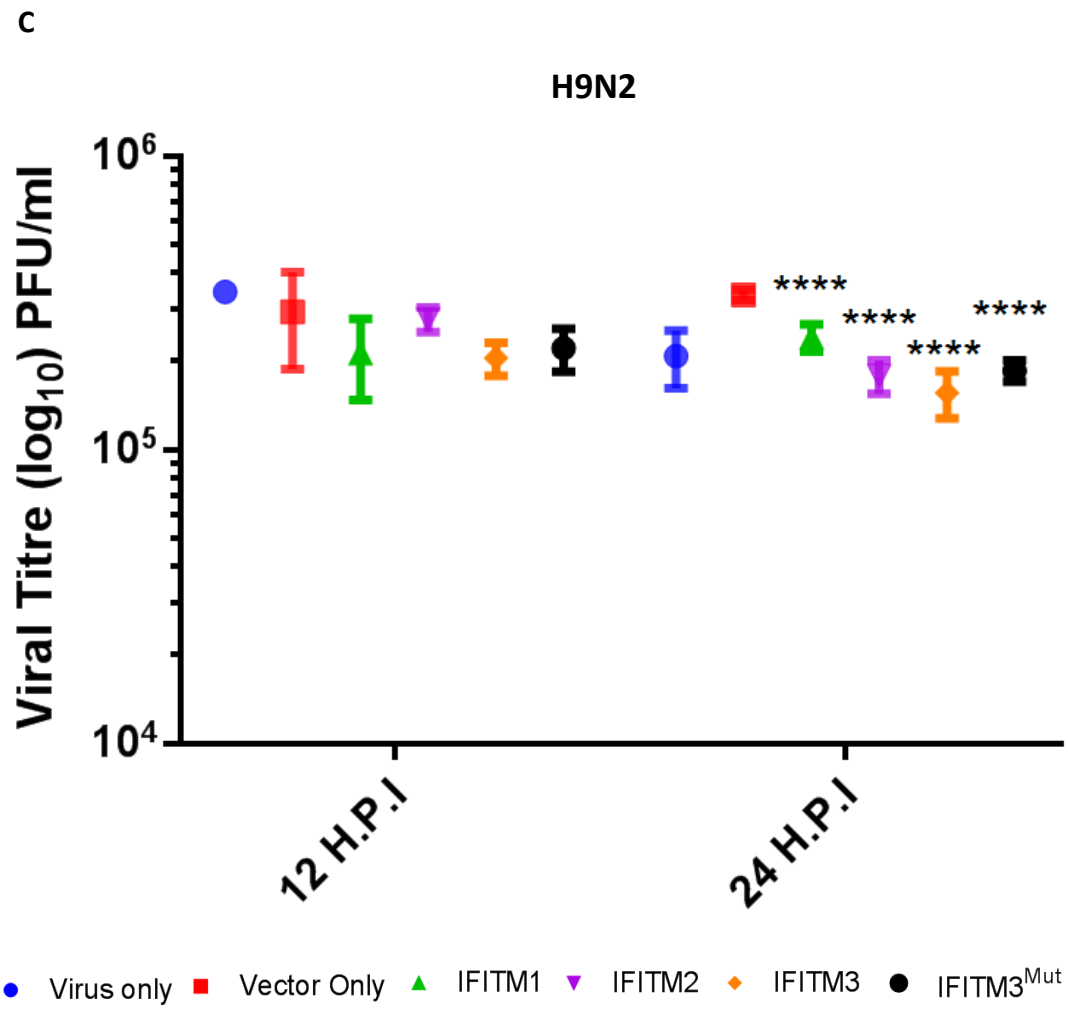

Figure 5.9 DF-1 cells stably-overexpressing chIFITM1, 2, 3 and 3^{MUT} restrict IAV infection. (A – C) DF-1 cells stably-expressing chIFITM1, 2, 3 or 3^{MUT} were infected with IAV (MOI 5) for 24 or 48 hours. Viral replication was measured by plaque assay titration in MDCK cells of the infected cell supernatant relative to the control (empty vector). Error bars show standard deviations of the means (n =3 biological replicates), * indicates a p-value <0.05, ****indicates a p-value <0.0001, one-way ANOVA.

a significant decrease in viral titres in cells overexpressing chIFITM1, 2, 3 or 3^{MUT}. The most significant decrease in viral titres was observed with chIFITM2 and 3^{MUT} which is in contrast with the data presented in figure 5.8A. It is unknown whether an increase in the number of viral particles added during infection alters the restrictive nature of the chIFITM proteins but these data highlights a difference under these experimental conditions. Infection with H5N3 resulted in a significant decrease in viral titres at both 12 and 24 hours post infection. The viral titres of both the infection and vector only controls increased over time unlike the chIFITM stably-expressing samples that remained at comparable levels between time points (Figure 5.9B). In agreement with data shown in figure 5.8B, chIFITM1 and $3/3^{MUT}$ appear to restrict IAV preferentially, with cells overexpressing chIFITM2 having higher viral titres in comparison to either chIFITM1 or $3/3^{MUT}$. These data presented in figure 5.9C is similar to the data in figure 5.8C in regards to the difference in viral titres, although smaller in magnitude and restriction occurring later during infection. Overexpression of all the chIFITM proteins enables restriction of H9N2, although chIFITM3 appears to preferentially restrict this virus at a high MOI. The differences in the restrictive capabilities of chIFITM3 and 3^{MUT} appear to be small and this data does not suggest a loss of function when the cysteine residues are mutated to alanine residues. Moreover, it could be suggested that the alanine substitutions confer an advantage to chIFITM3 when these cells are challenged at a high MOI. There appears to be a further reduction in viral titres in comparison to the wild-type chIFITM3 after cells are challenged with either H3N8 and or H5N3.

Taken together, these data suggests that the chIFITM proteins are able to potently restrict a current enzootic strain of avian influenza virus (H9N2) alongside two further strains (H3N8, H5N3) of IAV at a low and a high MOI. This suggests a functional role for the chIFITM proteins in the restriction of viral infections with strains of low pathogenicity avian influenza virus.

5.5.3 DF-1 cells stably-expressing chIFITM2 restrict IBV when cells are challenged at a high MOI

Data presented in this chapter demonstrates that the overexpression of chIFITM2 renders the cells more refractory to infection with IBV. Conversely, knocking down chIFITM2 expression makes cells more susceptible to infection with BeauR. Although the exact mechanism for this remains unclear, it may be because of the relocalisation of IFITM2 from intracellular compartments in mammalian cells to the plasma membrane in chicken cells. In order to examine this in further detail, the stably-expressing DF-1 cells were used to characterise the restriction of IBV when these cells are challenged with a high MOI as opposed to the lower MOI (1) that was used in both the transient overexpression (figure 5.4) and knockdown (figure 5.7) experiments.

Stably-expressing DF-1 cells were infected with BeauR (MOI - 5) for 8 hours, and the supernatants assayed for the presence of infectious virions. Briefly, material to be assayed was serially diluted in 1x BES and used to infect CK cells in 12-well plates. After 1 hour of incubation, the inoculum was removed, and the cells were overlaid with 2x BES and 2% agar. After 3 days the cells were fixed with 10% paraformaldehyde (PFA) in PBS which was overlaid onto to the agar and incubated for 15 minutes. Agar was removed from each well and cells stained with 0.1% crystal violet (w/v) for 10 minutes and plaques counted to determine the pfu/ml. In agreement with the previous data presented in this chapter, the only significant decrease in virus titre was observed in cells overexpressing chIFITM2. There was no statistical difference between the virus titres of any of the other overexpressing cell lines when compared to the vector only control. This suggests that chIFITM2 is the only restriction factor of the non-pathogenic strain of IBV, BeauR *in vitro*, although it is unclear if chIFITM2 is a restriction factor of other strains within the IBV viral family. As previously

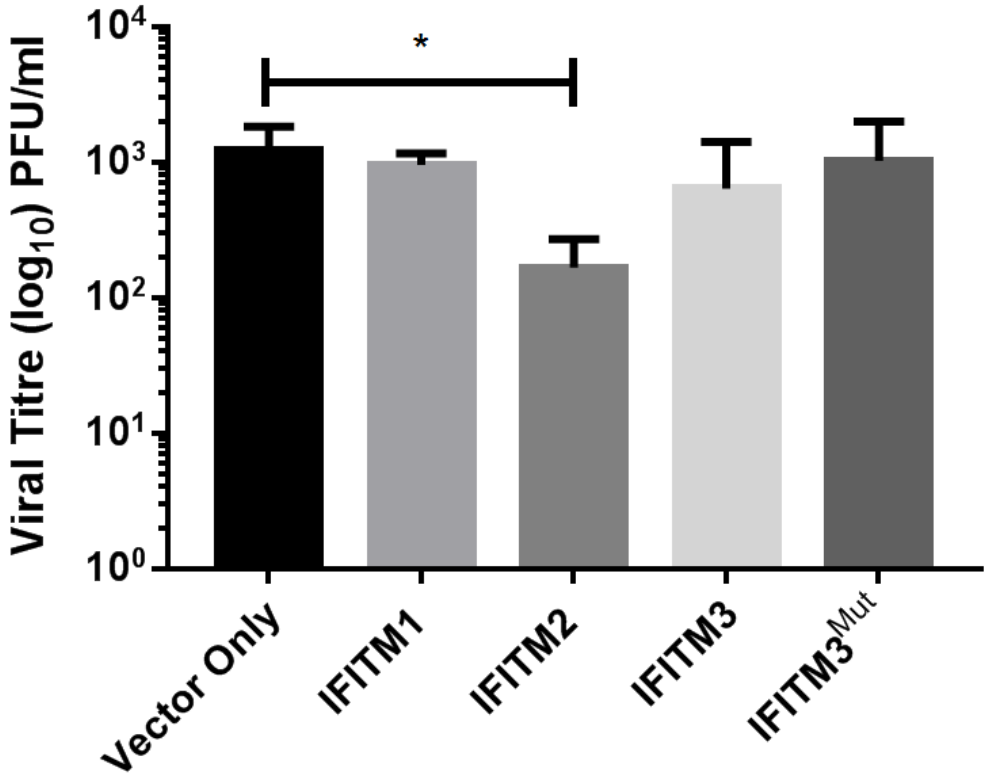

Figure 5.10 DF-1 cells stably-overexpressing chIFITM2 restrict IBV infection. DF-1 cells stably-expressing chIFITM1, 2, 3 or 3^{MUT} were infected with IBV (MOI 5) for 8 hours. Viral replication was measured by plaque assay titration in CKC cells of the infected cell supernatant relative to the control (empty vector). Error bars show standard deviations of the means (n =3 biological replicates), * indicates a p-value <0.05, one-way ANOVA.

described, the other strains are not able to infect continuous cell lines as their cellular tropism is restricted.

5.6 Mutational analysis of chIFITM3 suggests that conserved domains may be important in determining antiviral activity against IAV

It has been determined that the IFITM proteins are post-translationally modified and that these modifications have an impact on viral restriction if mutated (Chesarino et al., 2014a;Chesarino et al., 2014b;Compton et al., 2016). These modifications include: palmitoylation (Cys71, 72 and 105), phosphorylation (Tyr20 and 99), ubiquitination (Lys24, 83, 88, 104) and methylation (Lys88). In 2014, Jia *et al.* described a motif that is critical for endosomal localisation (YEML motif) which is important for the cellular distribution and restriction of IFITM3 (Jia et al., 2014). It has been hypothesised that two specific residues (F75 and 78) may be important for dimerization which in turn may be essential for the correct structure required for restriction (John et al., 2013). This study examined the importance of these residues in mammalian IFITM3 and described how these residues facilitate a physical association between IFITM proteins. It has been found that the palmitoylation of cysteine residues is necessary for the restrictive activity of IFITM3 (Chesarino et al., 2014b;Yount et al., 2012;Yount et al., 2010). Moreover, the palmitoylation of Cys72 may play a critical part in modulating IFITM3 antiviral activity. The three palmitoyl groups found on huIFITM3 have been shown to confer stability, are necessary for the correct cellular localisation and for their association with lipid rafts (Yount et al., 2012;Yount et al., 2010). It has been hypothesised that the ubiquitination of the IFITM proteins regulates their expression and stabilises the protein *in vitro*, with ubiquitinated IFITM3 localising to the endosomes compared to IFITM3 which mislocalises when ubiquitination is perturbed (Chesarino et al., 2014a). Although it has been found that ubiquitination of these residues in essential for a multitude of functions, mutating these

residues to alanine residues does not significantly alter the restriction of enveloped viruses (Shan et al., 2013). A study published in 2013 showed that the methylation of huIFITM3 is increased through IAV infection and decreased with IFNα treatment. This may suggest that IAV actively promotes IFITM3 methylation as this perturbs the antiviral function and may act as a strategy for innate immune evasion (Shan et al., 2013). Phosphorylation of the Tyr20 residue has been shown to regulate subcellular localization and restriction activity of IFITM3 (Chesarino et al., 2014a). In addition, mutating Tyr99 to Ala99 differentially reduces the restrictive capabilities of IFITM3 in regards to IAV infection, but not for DENV (Jia et al., 2012;John et al., 2013).

In this study we aimed to assess whether the residues identified as being important or essential for the restrictive capabilities of huIFITM3 are necessary for chIFITM-mediated restriction, and whether the loss of these residues through mutation would alter the restrictive profile of chIFITM3. In order to investigate this, wildtype amino acids were sequentially mutated to alanine residues in blocks of ten. Starting from the second residue immediately after the start methionine, ten alanine residues were incorporated into the backbone of chIFITM3 with sequential mutagenesis across the whole protein, ending at the stop codon which was not mutated (Figure 5.11A). It was hypothesised that if residues within the alanine scanning mutant were important, then the restriction of IAV would be detrimentally affected and that this would be assessed through increased viral titres compared to the wildtype chIFITM3 positive control. Restoration of IAV viral titres would be assessed as a comparison to an empty vector control.

It has already been established that the mutation of two palmitoylated cysteine residues at position 71 and 72 does not appear to have any detrimental impact on chIFITM3 viral restriction (Figures 5, 6, 7 and 8). It is not clear if this is due to them being non-essential in the avian host or whether there are compensatory residues which are differentially post-

translationally modified and assume a similar role of those missing residues in chickens. To confirm whether the aforementioned residues/motifs are essential, DF-1 cells were transfected with 1µg of plasmid encoding the wildtype *chIFITM3* or an alanine scanning mutant (Figure 5.11A). These cells were then infected with H9N2 influenza virus (MOI - 1) for 24 hours, and the supernatants assayed for the presence of infectious virions.

Material to be assayed was serially diluted in serum-free DMEM and used to infect MDCK cells in 12-well plates. After 1 hour of incubation, the inoculum was removed, and the cells were overlaid with DMEM containing 0.2% BSA, 2% agar and 1µg trypsin ml^{-1}. The virus only and vector only controls showed comparable titres at 24 hours post infection (Figure 5.11B). Transfection of any of the alanine scanning constructs prior to infection with IAV resulted in a significant decrease in viral titre compared to the vector only control (Figure 5.11B and C). The average decrease in viral titre across all 14 alanine scanning mutants and the wildtype chIFITM3 control was 0.63 log_{10}. However, variations in viral titres were observed with the lowest level of restriction seen with IFITM3.11 (0.4 log_{10}) and the greatest level of restriction with IFITM3.2 (0.81 log_{10}), which was superior to the restriction observed with wildtype chIFITM3. The large variation within the alanine scanning mutants suggests that specific regions of the chIFITM3 protein are important in mediating restriction. Mutant 3.11, located within the C-terminus, appears to be significantly less able to restrict IAV and these reductions in viral restriction are significant when compared to wildtype chIFITM3. In particular, mutants 3.11, 3.12 and 3.13 have viral titres that are, on average, 0.2 log_{10} more than the average of the mutants across the entire protein. This suggests that this region is important in mediating restriction, although they do not restore viral titres to the levels seen in the vector only control, implying partial but not complete ablation of function. The level of chIFITM3 protein expression was assessed using western blot against the C-terminal FLAG tag (Figure 5.11D). Samples of transiently transfected cell lysates were taken at 24 hours post transfection to assess protein expression at the start of

infection. The cells were lysed, proteins separated by SDS-PAGE and transferred onto nitrocellulose membranes. Western blots were performed using a FLAG antibody alongside a β-actin loading control. All of the chIFITM3 mutants were expressed when compared to the wildtype chIFITM3 protein levels. A decrease in protein abundance when compared to wild type chIFITM3 protein levels was detected in mutants 3.9, 3.12 and 3.14 although bands were detected in the corresponding lanes. Levels of β-actin were detected in all samples at equitable levels, even in those samples where chIFITM3 expression was lower than expected.

The impact of mutating residues that are post-translationally modified on the restrictive capabilities of human IFITMs has been well studied, focussing particularly on huIFITM3. The data presented in those studies has suggested that altering certain essential residues, such as Cys72, has a profound impact on restriction, whereas other residues (Lys88) can be readily mutated without a loss of function (Yount et al., 2012). The data presented in this section sought to address whether any residues or regions within chIFITM3 were essential for restriction. It appears that no specific region of chIFITM3 is absolutely essential for restriction. There are notable and significant differences in the viral titres obtained from cells that have been transfected with alanine scanning mutants, but all of these proteins were able to restrict IAV when compared to a vector only control. This may imply that the C-terminus is important in mediating restriction, as there are significant increases in viral titres in cells expressing constructs 3.11 – 3.14, but the increases observed are not large enough to suggest that these regions are critical. A study published in 2013 suggested that the N-terminus is essential in huIFITM3 for the restriction of IAV, but no such evidence presented here suggests that this is the case with chIFITM3 (Bailey et al., 2013). Moreover, Bailey *et al*. suggest that the C-terminus does not play a significant role is huIFITM3 restriction of IAV, whereas the data presented here appears to suggest that this region may play a minor role in determining restriction of IAV by chIFITM3. It was already known that

A

IFITM3:
MERVRASGPGVPPYEPLMDGMDMEGKTRSTVVTVETPLVPPPRDHLAWSLCTTLYANVCCLGFLALVFSVKSRDRKVLGDYSGALSYGSTAKYLNITAHLINVFLIILIIALVASGTIMVANIFNHQQQHPEFIGPT

IFITM3_1:
MAAAAAAAAAAPPYEPLMDGMDMEGKTRSTVVTVETPLVPPPRDHLAWSLCTTLYANVCCLGFLALVFSVKSRDRKVLGDYSGALSYGSTAKYLNITAHLINVFLIILIIALVASGTIMVANIFNHQQQHPEFIGPT

IFITM3_2
MERVRASGPGVAAAAAAAAAADMEGKTRSTVVTVETPLVPPPRDHLAWSLCTTLYANVCCLGFLALVFSVKSRDRKVLGDYSGALSYGSTAKYLNITAHLINVFLIILIIALVASGTIMVANIFNHQQQHPEFIGPT

IFITM3_3:
MERVRASGPGVPPYEPLMDGMAAAAAAAAAAVTVETPLVPPPRDHLAWSLCTTLYANVCCLGFLALVFSVKSRDRKVLGDYSGALSYGSTAKYLNITAHLINVFLIILIIALVASGTIMVANIFNHQQQHPEFIGPT

IFITM3_4:
MERVRASGPGVPPYEPLMDGMDMEGKTRSTVAAAAAAAAAAPRDHLAWSLCTTLYANVCCLGFLALVFSVKSRDRKVLGDYSGALSYGSTAKYLNITAHLINVFLIILIIALVASGTIMVANIFNHQQQHPEFIGPT

IFITM3_5:
MAAAAAAAAAAPPYEPLMDGMDMEGKTRSTVVTVETPLVPPAAAAAAAAAATTLYANVCCLGFLALVFSVKSRDRKVLGDYSGALSYGSTAKYLNITAHLINVFLIILIIALVASGTIMVANIFNHQQQHPEFIGPT

IFITM3_6:
MERVRASGPGVAAAAAAAAAADMEGKTRSTVVTVETPLVPPPRDHLAWSLCAAAAAAAAAAGFLALVFSVKSRDRKVLGDYSGALSYGSTAKYLNITAHLINVFLIILIIALVASGTIMVANIFNHQQQHPEFIGPT

IFITM3_7:
MERVRASGPGVPPYEPLMDGMDMEGKTRSTVVTVETPLVPPPRDHLAWSLCTTLYANVCCLAAAAAAAAAASRDRKVLGDYSGALSYGSTAKYLNITAHLINVFLIILIIALVASGTIMVANIFNHQQQHPEFIGPT

IFITM3_8:
MERVRASGPGVPPYEPLMDGMDMEGKTRSTVVTVETPLVPPPRDHLAWSLCTTLYANVCCLGFLALVFSVKAAAAAAAAAASGALSYGSTAKYLNITAHLINVFLIILIIALVASGTIMVANIFNHQQQHPEFIGPT

IFITM3_9:
MAAAAAAAAAAPPYEPLMDGMDMEGKTRSTVVTVETPLVPPPRDHLAWSLCTTLYANVCCLGFLALVFSVKSRDRKVLGDYAAAAAAAAAAKYLNITAHLINVFLIILIIALVASGTIMVANIFNHQQQHPEFIGPT

IFITM_10:
MERVRASGPGVAAAAAAAAAADMEGKTRSTVVTVETPLVPPPRDHLAWSLCTTLYANVCCLGFLALVFSVKSRDRKVLGDYSGALSYGSTAAAAAAAAAANVFLIILIIALVASGTIMVANIFNHQQQHPEFIGPT

IFITM3_11:
MERVRASGPGVPPYEPLMDGMDMEGKTRSTVVTVETPLVPPPRDHLAWSLCTTLYANVCCLGFLALVFSVKSRDRKVLGDYSGALSYGSTAKYLNITAHLIAAAAAAAAAALVASGTIMVANIFNHQQQHPEFIGPT

IFITM3_12:
MERVRASGPGVPPYEPLMDGMDMEGKTRSTVVTVETPLVPPPRDHLAWSLCTTLYANVCCLGFLALVFSVKSRDRKVLGDYSGALSYGSTAKYLNITAHLINVFLIILIIAAAAAAAAAANIFNHQQQHPEFIGPT

IFITM3_13:
MAAAAAAAAAAPPYEPLMDGMDMEGKTRSTVVTVETPLVPPPRDHLAWSLCTTLYANVCCLGFLALVFSVKSRDRKVLGDYSGALSYGSTAKYLNITAHLINVFLIILIIALVASGTIMVAAAAAAAAAAEFIGPT

IFITM3_14:
MERVRASGPGVAAAAAAAAAADMEGKTRSTVVTVETPLVPPPRDHLAWSLCTTLYANVCCLGFLALVFSVKSRDRKVLGDYSGALSYGSTAKYLNITAHLINVFLIILIIALVASGTIMVANIFNHQQQHPAAAAAA

B

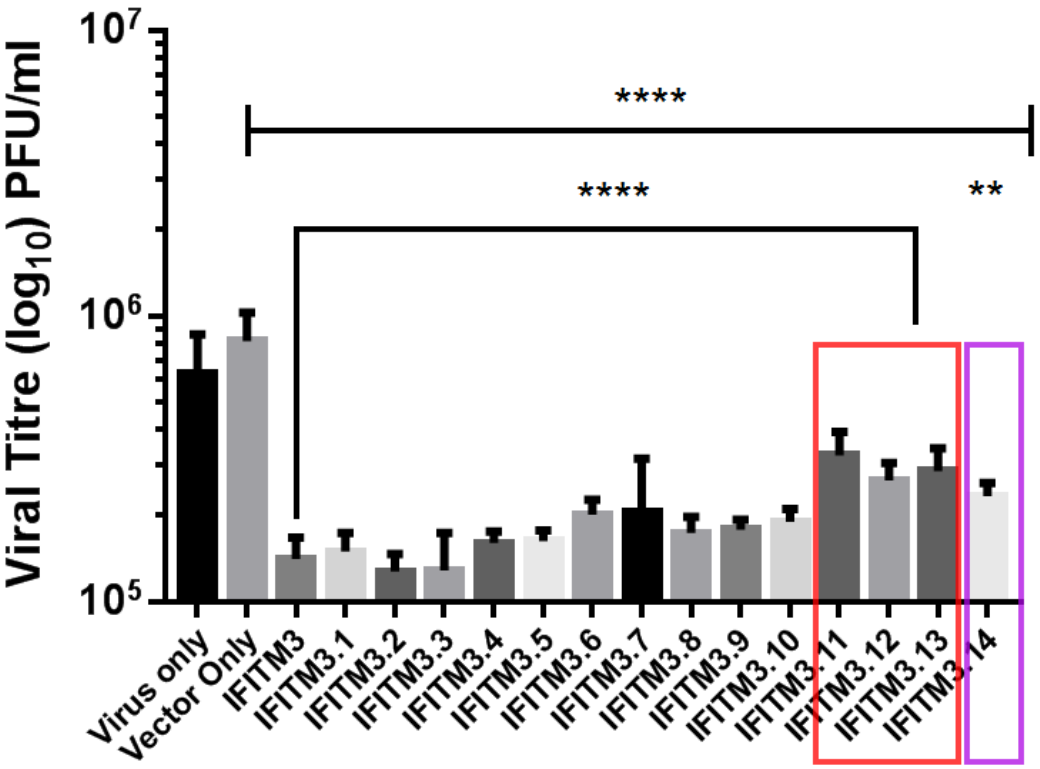

C

Construct ID	Viral titre (log_{10})	Difference (log_{10})
Vector control	5.912045007	
IFITM3	5.148704431	0.76
IFITM3.1	5.176091259	0.74
IFITM3.2	5.105510185	0.81
IFITM3.3	5.108338347	0.8
IFITM3.4	5.206375163	0.71
IFITM3.5	5.213073939	0.7
IFITM3.6	5.304634838	0.61
IFITM3.7	5.312107508	0.6
IFITM3.8	5.240965871	0.67
IFITM3.9	5.253258022	0.66
IFITM3.10	5.278753601	0.63
IFITM3.11	5.511883361	0.4
IFITM3.12	5.424608892	0.49
IFITM3.13	5.457377702	0.45
IFITM3.14	5.369525692	0.54

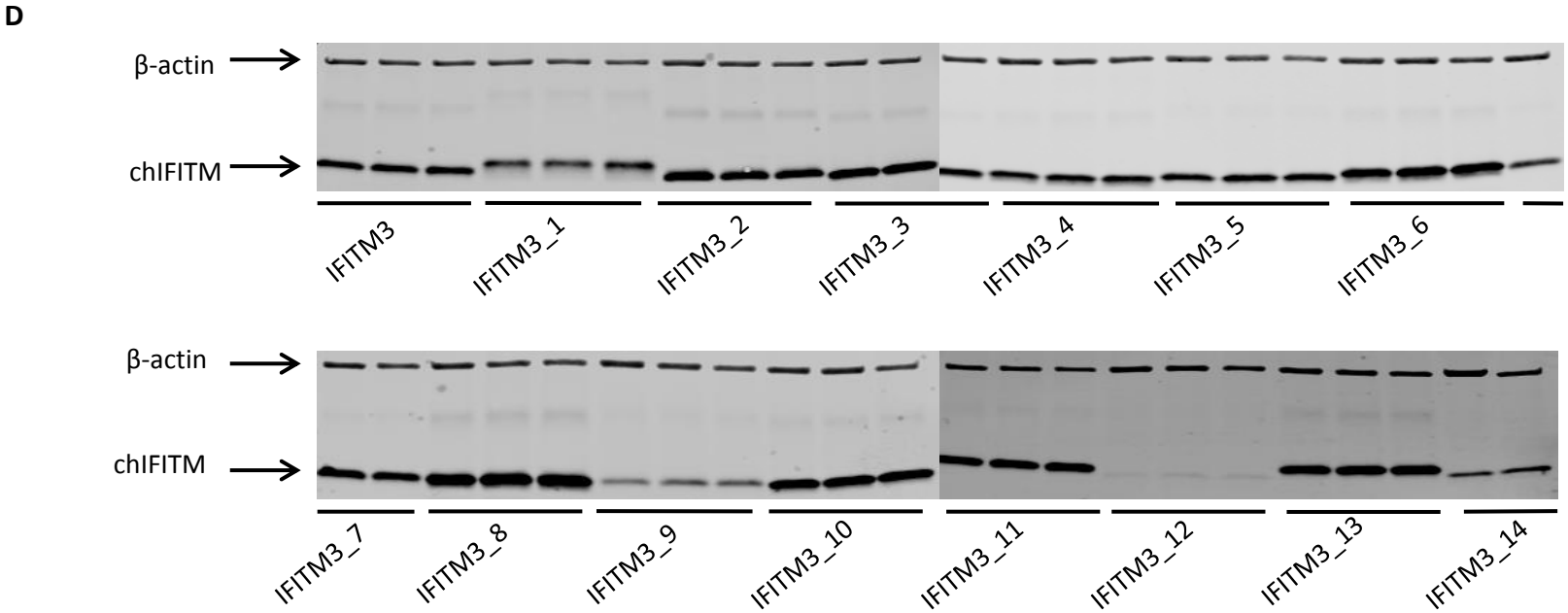

Figure 5.11 Mutational analysis of chIFITM3 suggests that certain domains may be important in determining antiviral activity against IAV. (A) A schematic representation of the alanine scanning substitutions that have been made within each construct. Sequentially ten wild-type residues were mutated to alanine residues in order to assess the impact these substitutions have on restriction of IAV. (B) DF-1 cells were transfected with 1µg of plasmid encoding chIFITM3 or an alanine scanning mutant for 24 hours. These cells were then infected with H9N2 (MOI 1) for 24 hours and the supernatants harvested. Viral replication of the infected cell supernatant was measured by plaque assay titration relative to the control (cells transfected with an empty vector). (C) A table of H9N2 viral titres and the differences in viral titres in comparison to the vector only control. (D) Cells were lysed at 24 hours post infection and lysates were separated by SDS-PAGE. Proteins were transferred to a nitrocellulose membrane and a western blot performed using an anti-FLAG antibody against a C-terminal FLAG tag with β-actin as the loading control. Error bars show standard deviations of the means (*n* =3 biological replicates), ** indicates a p-value<0.01, ****indicates a p-value <0.0001, one-way ANOVA.

the amino acid sequence homology between human and chicken IFITM3 was low at 36%. However, data published thus far had not been established if these conserved residues were important in mediating chIFITM antiviral activity. This data suggest that this is not the case. Mutations incorporated into the protein do not appear to be detrimental to restriction, even if viral titres are increased when mutations are introduced near to or incorporating the C-terminus.

5.7 Discussion

It has been established that mammalian IFITM proteins act as potent restriction factors, specifically of IAV and other enveloped viruses that enter the cell through the acidification of the endosomes (Desai et al., 2014). To complement the early characterisation of these proteins, there have been a tremendous number of studies that have sought to uncover the mechanisms underpinning this activity (Desai et al., 2014;Li et al., 2013). Current evidence is still unclear and in some instances conflicted, although several hypothesise has been suggested. The most favoured current hypothesis is that the IFITMs are able to recruit cholesterol which modifies the rigidity of the membranes surrounding the endosomal compartment. This process traps the virus which is then degraded through the lysosomal pathway (Amini-Bavil-Olyaee et al., 2013). Studies utilising mass spectroscopy have identified a number of interacting partners that are involved in cholesterol biosynthesis and the recruitment of cholesterol. Additionally, the membrane topology of the huIFITMs is also unclear with the most robust evidence coming from studies using NMR and EPR to suggest a type 2 membrane topology (Ling et al., 2016). Further research is required in order to make more detailed claims into their antiviral activity and the mechanisms that modulate this.

In contrast, very little is currently known about the antiviral role that the chIFITMs play in restricting avian viruses in the avian host. Initial work was undertaken in 2013 which

suggested that chIFITMs were restriction factors, however, this work was fragmented as each study focussed only on a particular member of the chIFITM gene family and chIFITM1 was not investigated at all (Smith et al., 2013). In addition, the authors did not use whole avian viruses, instead using pseudo-typed lentiviral vectors, making it difficult to draw accurate conclusions. This results in a gap in our understanding of the restrictive ability of chIFITMs as a whole. When one considers that the amino acid homology between human and chicken IFITM3 is only 36%, it is not surprising that certain residues and motifs, such as the cysteine residues at position 71, 72 and 105 are absent in some chIFITM protein sequences. It is unclear if compensatory residues assume the role of those missing residues or whether they are dispensable for their antiviral activity in chickens. To investigate the restrictive profile of the chIFITMs in further detail, siRNA knockdown, transient overexpression and stable overexpression was used in continuous avian cells alongside strains of pathogenic IAV and non-pathogenic, lab attenuated IBV.

To investigate the role that the chIFITMs play in restricting viral replication, the chIFITMs were transiently overexpressed in both primary *ex vivo* tissue cultures and in a continuous avian cell line that is routinely used in the laboratory. Whilst these are useful tools for studying gene function, it is important to consider that transfection and the reagents used can place the cell under extreme stress. This in turn can lead to the activation of an antiviral state or, under extreme circumstances, can culminate to the cell undergoing apoptosis (Wenzel et al., 2012;Li et al., 1999). In experiments where the cells are to be transfected as well as infected, it is important that the cells remain viable for the duration of the experiment. Experimental and anecdotal evidence suggest that different chemical transfection reagents place the cells under different amounts of stress. Furthermore, the transfection of different nucleic acids also exert differential adverse effects on the cell. The results in Figure 5.1 demonstrate that different transfection reagents are differentially cytotoxic to the cell, demonstrating the importance of using the most optimal transfection

reagents as a high proportion of dead cells after transfection may adversely affect the outcome of the infection experiment. Also, it is clear that different nucleic acids, such as siRNA and dsDNA plasmids, can impact on cellular health and maintenance (Li et al., 1999).

As previously discussed, primary cells are more difficult to transfect and this often results in using a higher concentration of plasmid and transfection reagent in order to achieve comparable results. In this specific example, 5µg of DNA was required in CEFs in comparison to 1µg in DF-1 cells in order to demonstrate a good level of chIFITM protein expression. When CEFs were challenged with H9N2 after transfection there was a significant decrease in viral titres for all the chIFITM expressing cells, which suggests that they all have an antiviral function when overexpressed in avian cells. When DF-1 cells are transfected with the same chIFITM gene sequences and infected at a lower MOI (1) with different strains of influenza there is a more nuanced outcome. DF-1 cells transfected with plasmids encoding the chIFITM sequences and then infected with H3N8 and H9N2 resulted in a significant decrease in viral titres, similar to that observed with CEFs. Interestingly, infection with H5N3 does not show a uniform pattern of restriction. The pan restriction observed with both H3N8 and H9N2 does not appear to be the case for cells infected with H5N3. In these samples only cells overexpressing *chIFITM1* and *chIFITM3* were able to restrict H5N3, although the magnitude of restriction was larger than that observed for both H3N8 and H9N2. The viral titres for cells overexpressing *chIFITM2* and infected with H5N3 was not significantly different to the empty vector control. Moreover, cells overexpressing *chIFITM5* had significantly higher viral titres than the vector only control, thus this implies that *chIFITM5* is pro-viral and results in more progeny virus being made over the 24 hour time course. When DF-1 cells were transfected *with chIFITM1*, 2, 3 and 3^{MUT} and then infected with BeauR (IBV), only those cells expressing *chIFITM2* had reduced viral titres compared to a vector only control as measured by plaque assay titration. This suggests that only chIFITM2 is able to restrict BeauR which is in contrast to infection with IAV. IAV is able

to be restricted by more than one of the chIFITM proteins and this may imply a dual level of control in IAV infected cells.

Having established that the chIFITMs are able to restrict viral replication when overexpressed in both primary *ex vivo* and *in vitro* cell cultures, we then sought to test whether reduced *chIFITM* expression would result in increased viral titres. Four siRNAs were designed against each *chIFITM* transcripts (except *chIFITM3* where a single published siRNA was used) and these were transfected into CEFs and DF-1s. Knockdown of *chIFITM* expression was variable (Figures 5.5B, 5.6D and 5.7B) and this could be attributed to innate immune activation due to the transfection protocol. The knockdown of *chIFITM1* in CEFs resulted in a significant increase in viral titres at 24 hours post infection when these cells were infected with H9N2. Similarly, studies conducted in DF-1 cells, increases viral titres were observed in cells with diminished *chIFITM3* expression at 8 hours post infection when infected with H3N8 (Figure 5.6A) and H5N3 (Figure 5.6B). In addition, cells with reduced chIFITM1 and 3 expression had increased viral titres at 24 hours post infection when infected with H5N3 (Figure 5.6B). There were no significant differences with cells that underwent the same knockdown protocol and were then infected with H9N2. This may suggest that different viruses display different sensitivities to chIFITM restriction and of those cells that are sensitive; chIFITM1 and 3 may preferentially restrict IAV. In contrast, DF-1 cells with diminished *chIFITM2* expression had increased BeauR viral titres when assessed against cells that had been transfected with a scrambled siRNA control. Taken together with the overexpression data, this implies that BeauR is preferentially restricted by chIFITM2, although the mechanisms behind this remain unclear. Quantitative RT-PCR data suggests that knockdown by siRNAs followed by infection with either H9N2 or BeauR resulted in more significant chIFITM upregulation when compared to the virus only, no transfection control (Figures 5.6E and F, 5.7C and D). This may suggest that knockdown

prior to infection activates an innate immune response thus increasing chIFITM expression above levels observed with infection alone.

To remove the need for prior transfection, stably-expressing DF-1 cells were created that each express *chIFITM1, 2, 3* or 3^{MUT}. It has been known that chemically transfecting cells prior to infection can perturb cell membranes and this may have consequences for downstream analysis including assessing virus replication by plaque assay titration. These cells were challenged with the aforementioned strains of IAV at two MOIs (0.1 and 5) in order to assess whether these cells could competently restrict IAV under two different conditions. In agreement with data previously described, when stably-expressing cells are infected at a low MOI, chIFITM1 and 3 were able to restrict infection by H3N8, H5N3 and H9N2, although the magnitude of restriction was different between the strains of IAV used. Overexpression of *chIFITM2* was also able to restrict infection with H3N8 and H5N3, although the viral titres were higher than those cells expressing either chIFITM1 or 3. When the same cells were infected at a high MOI a similar pattern of restriction was observed. One notable difference was an increase in restriction by chIFITM2. When challenged at a high MOI the same cells appear to be more refractory to infection in comparison to cells that were infected with a lower MOI (Figure 5.8A, B and C). Moreover, reductions in viral titres are observed later on in infection at 24 hours when these cells are challenged with H3N8 and H9N2. Significant reductions in viral titres are observed at 12 hours post infection for cells infected with H5N3. In contrast to what is known in the mammalian IFITM literature (Yount et al., 2012;Yount et al., 2010), mutation of both Cys71 and 72 did not lead to any detrimental impacts on chIFITM-mediated restriction. At earlier time points there was a greater degree of variation in the chIFITM3^{MUT} viral titres but these effects were transient and viral titres were comparable at later time points, across all three strains of IAV tested. The differences in the restrictive capabilities between chIFITM3 and 3^{MUT} appear to

be small, and this data does not suggest a loss of function when these 'critical' cysteine residues are mutated to alanine residues.

The stably-expressing DF-1 cells were also infected at a high MOI (5) for 8 hours with BeauR. Consistent with data already presented in this chapter, chIFITM2 expressing DF-1 cells were able to significantly restrict BeauR. Viral tires for the other chIFITM-overexpressing cells were comparable to the vector only control. This suggests that under the conditions tested, only chIFITM2 is able to restrict infection with BeauR, although only one strain of IBV was used due to the restricted cellular tropism of the more pathogenic strains.

Many studies have identified important residues in huIFITM3 that modulate its antiviral activities. Studies have described the many ways in which residues are post-translationally modified, and studies utilising mutagenesis have demonstrated that antiviral activity can be lost if these residues are substituted with alanine residues. Particular emphasis has been placed on three palmitoylated cysteine residues at positions 71, 72 and 105 which are important for protein stability, cellular localisation and association of chIFITM3 with lipid rafts (Narayana et al., 2015). Other residues undergo phosphorylation (Tyr20 and 99), ubiquitination (Lys24, 83, 88, 104) (Yount et al., 2012) and methylation (Lys88) (Shan et al., 2013) although not all of these residues are essential for restriction and can be mutated to alanine residues without a loss of function. In the data presented here, sequential mutations were made across the whole chIFITM3 protein except for the start methionine and stop codon. The viral titres obtained from this experiment suggest that the cysteine residues at position 71 and 72 are not essential for restriction, which is in agreement with the data generated utilising the stably-expressing cell lines. There were increases in viral titres when cells were expressing chIFITM3.11 – 3.14 which suggests that the C-terminus has a role in determining antiviral activity. Although viral titres were increased when

mutations were made in this region, there was not a complete ablation of function, with levels below that observed with the vector only control. It remains unclear if this is virus specific and whether there are specific residues that modulate this effect specifically.

To conclude, it has been demonstrated that chIFITMs are potent restriction factors and are able to restrict a diverse range of strains of IAV and the laboratory attenuated strain of IBV, BeauR. Taken together this data demonstrates that chIFITM1 and 3 preferentially restrict IAV, although at high MOIs it appears that chIFITM2 is able to restrict IAV to levels which are not seen at low MOIs. In contrast, only chIFITM2 is able to restrict IBV and this has been investigated through transient overexpression, knockdown and stable overexpression. It is unclear what mechanism is driving restriction, although it could be hypothesised that the cellular relocalisation of chIFITM2 may be partially responsible for this phenotype. Further research is required to examine this relationship in more detail and it would be useful to investigate whether pathogenic strains of IBV are also restricted by chIFITM2. The data presented in Figure 5.11A-D also suggests that specific regions of chIFITM3 are not absolutely essential for restriction. When blocks of 10 amino acids were mutated to alanine residues there was not a complete loss of restriction and all chIFITM3 variants were able to restrict IAV, when compared to a vector only control. This work suggests that the C-terminus may influence restriction, although the individual residues involved are yet to be identified.

Chapter 6

Discussion

6.1 Concluding remarks

The main aims of this project were to investigate the architecture of the chIFITM locus, determine the expression of the *chIFITM* genes and to elucidate which viruses are restricted by *chIFITM* expression.

The chIFITM locus is present in the genome of the ancestor (*Gallus gallus)* as well as in avian cell lines used in research. Re-sequencing this locus now means that a high quality, contiguous sequence is available and will aid further research. It also allows for greater interrogation of this locus by comparative genomics, something that has not been possible up until now. Moreover, it has now been shown that these genes are constitutively expressed in all tissues and cell lines.

It is now clear that the *chIFITMs* are robustly upregulated in response to either IAV and IBV viral challenge, stimulation with the dsRNA analogue poly(I:C) or after treatment with exogenous type I interferon. Notably, infection with HVT does not induce *chIFITM* expression although the reasons for this remain unclear. Moreover, the data presented in this thesis using pull-down assays provides evidence that the chIFITMs are able to restrict enveloped viral pathogens via the possible modulation of lipid biosynthesis which may prevent viral entry into the cytoplasm. Targeted mutations of the cysteine residues at positions 71 and 72 do not appear to abolish or diminish the restrictive ability of the chIFITMs, unlike mammalian IFITMs. Mutagenesis across the entire polypeptide of chIFITM3 has failed to identify any regions of the protein that are essential for chIFITM-mediated restriction.

Taken together, this demonstrates that chIFITMs are part of the wider ISG family and suggests that they have a functional role in restricting enveloped viral pathogens. In addition, the findings of this thesis establish that *chIFITM5* is a novel ISG as it is potently

upregulated upon viral infection and its expression is found in every cell line, *ex vivo* cell culture and tissue that was investigated.

6.1 Future work and directions

The work outlined in this thesis advances our knowledge of chIFITMs and their restriction of avian viral pathogens. However, there are still a number of areas where further research would enhance our knowledge of these genes and may broaden our insights into chIFITM-mediated viral restriction. The sequence diversity within the chIFITM locus has not been extensively examined in outbred chicken populations. There are a diverse range of chickens that occupy distinct geographical niches which may have a greater degree of variation within the chIFITM locus. Chickens in these environments are often unvaccinated and encounter a wide range of viral pathogens. This places additional selection pressures on the animals, which may result in chIFITM genes that have more potent antiviral activity. To do this, it would be possible to use the DNA sequencing technology outlined in chapter 3 to assess the chIFITM locus from a variety of different chickens, worldwide. This would allow for further investigations into SNPs that confer a protective advantage against emerging avian viral pathogens. Moreover, any SNPs identified could be used in commercial breeding programmes, ensuring the welfare of chickens and enhancing the resistant of commercial poultry to viruses.

Although potential protein-chIFITM interactions have been identified in this study by mass spectrometry, and preliminary research undertaken to confirm these interactions, it has not been possible to investigate any possible mechanisms of action. Further investigations could be undertaken utilising yeast-2-hybrid screens and high resolution microscopy. In order to examine the functional relevance of these interactions, molecular techniques such as CRISPR/Cas9 could be used, as it may be possible to perturb these interactions, therefore reducing the functional activity of the chIFITM proteins. This would provide useful insights

into the mechanism mediating viral restriction and it may be possible to elucidate how viruses are able to evade chIFITM-mediated restriction. Furthermore, many studies have shown that the IFITM proteins are found within the plasma and intracellular membranes and this has been hypothesised to be necessary for restriction. However, it is still not clear if the IFITM proteins reside in only one location or whether they are trafficked around the cell in response to viral infection. These studies have been frustrated by a lack of reagents, namely antibodies that cross-react and detect more than one IFITM protein simultaneously. To examine this in further detail it may be necessary to design and make further sets of custom antibodies or it may be possible to genetically alter a cell line in such a way that the *chIFITM/IFITM* genes are tagged within the germline. This would somewhat alleviate the problems associated with transient overexpression as the wildtype gene could be stimulated and the localisation examined without the need for prior transfection.

Data presented in this thesis has demonstrated that *in vivo* modulation of *chIFITM* expression is complex. Only one example of *chIFITM* upregulation was found at 2 days post infection, whereas there were multiple examples of downregulation of *chIFITM* expression at day 5 post infection. Currently, there are very few studies that have examined the *in vivo* regulation of *chIFITM* expression in response to viral infection. Upregulation of *chIFITM* expression occurs very quickly after the virus has established infection in the host cell. Therefore, it would be beneficial if tissues were harvested earlier during infection to ensure a more robust assessment of chIFITM expression can be made. Although only a single significant increase in chIFITM expression was found in the IAV study (chapter 4), it may be that tissues were harvested too late in infection. In addition, there are currently no data that examines the *in vivo* effects of infection with a diverse range of avian viruses. Conducting a larger scale experiment with a number of different viruses would be expensive and time consuming, so it may be more practical to combine studies with groups already undertaking *in vivo* experimentation.

Although the findings in this thesis demonstrate that enveloped viruses can be restricted by one or more chIFITM *in vitro*, it is still unclear if there are avian viruses that are insensitive to restriction. With stably expressing cell lines it would be possible to investigate this, using both plaque assay titrations and FACs to determine viral entry and replication. With new advances in CRISPR/Cas9 technology it may also be possible to generate a number of avian cell lines that have one or more of the *chIFITM* genes knocked out from the genome. Using these cells, it may be possible to determine which chIFITMs are essential for viral restriction and could provide further insights into viral specificity.

The chIFITM gene family is known to encode five genes, although this project has primarily focused on *chIFITM1, 2, 3* and *5* and only preliminary investigations into *chIFITM10* have been undertaken. The function(s) of huIFITM10 are currently unknown, although it has not been implicated in viral restriction to date. It is clear by data produced by others in the Genetics and Genomics groop and by (Okuzaki et al., 2017), that chIFITM10 has some antiviral function and it is upregulated in response to treatment with poly(I:C). Additional investigations would further elucidate its function, although it appears that chickens have five antiviral *IFITM* genes, in comparison to humans who appears to have only have three (clade I).

Finally, vaccines are the main tool used to counter endemic and emerging viral pathogens, both in humans and domesticated livestock. Vaccines are predominantly produced in cell culture or embryonated chicken eggs and it has been proposed that host immune responses are a significant bottleneck in production, thereby reducing viral yields. It may be possible to employ CRISPR/Cas9 gene editing technology to stably knock-out individual *chIFITM* genes, or the entire chIFITM locus. Enabling the vaccine virus to replicate more efficiently, thus increasing vaccine yields. An increase in vaccine yields would mean that the same number of embryonated hens eggs would produce more vaccine antigen, therefore,

the price per vaccine would decrease and the availability of the vaccine would increase. This technology would be instrumental for enhancing availability of vaccines for a wide range of human and livestock diseases, particularly for countries where these viruses are currently endemic.

Appendix

Table 7.1: Cellular proteins identified through LC-MS/MS that have a significant interaction with chIFITM1-FLAG

Protein ID	Unique peptides	Confidence	p Value (-log10)	Fold change (Log2) chIFITM-FLAG/FLAG
HSP25	13	323.31	4.305603414	6.834736506
DYNC1H1	68	323.31	2.835969155	5.421052933
CCT8	3	99.631	5.141197079	5.26325798
EIF3A	6	323.31	2.585348053	5.074971517
NCAPG2	11	49.391	4.270305368	4.937030792
LDHA	19	323.31	2.518098041	4.813216527
SQSTM1	15	323.31	1.470419201	4.731942495
CCT3	24	305.37	1.880163207	4.702330271
CANX	20	157.95	1.257145499	4.494015376
IPO7	10	232	3.280602704	4.39438502
CDK1	8	35.88	1.223571466	4.281110764
ATP1A1	15	139.5	2.62818604	4.224599202
Gga.29531	6	47.091	2.147919477	4.162239075
CCT2	20	145.55	2.068429602	4.157755534
TCP1	22	323.31	2.265824833	4.130930583
SF3B1	13	225.89	2.108254562	4.118561427
TLN1	34	174.23	2.523705007	4.078789393
PHB2	6	96.297	2.572913722	3.913258235
SCD	4	37.377	3.254485621	3.893405914
PSMC2	15	144.7	1.501915552	3.8703626
ITGAV	8	46.996	5.122413932	3.79074351
PSMC6	13	144.67	1.759887094	3.787675858
ASNS	10	33.647	1.533082583	3.73182869
THBS1	13	66.292	1.819960634	3.726994832
VDAC2	8	74.109	1.606765662	3.725519816
IMMT	11	41.53	3.039864163	3.722098668
LOC422993	3	23.29	2.819725271	3.715384165
HSPD1	32	323.31	2.041430986	3.693489075
ATP5A1	22	237.25	2.169944784	3.68871816
FASN	19	134.74	1.557370524	3.664454778
CCT5	31	323.31	2.032462167	3.660306295
PHB	12	113.93	1.581966882	3.650803884
CKAP5	14	43.292	3.589406719	3.638519923
CCT7	24	317.94	2.431943039	3.637254715
EPRS	42	323.31	1.668972189	3.581262589
ACTG1	3	153.56	1.267821947	3.551416397
P4HA1	9	26.705	2.795478247	3.533287684
PSMC3	19	206.76	1.447710318	3.527540207
CCT6A	8	76.084	1.933596484	3.527329127
SLC25A6	8	323.31	2.46148202	3.487776438
HADHA	12	61.348	3.520863473	3.457870483

SEC16A	6	52.355	2.352883693	3.450616837
STIM1	9	70.254	2.745501458	3.42634201
TUBA4B	5	66.675	1.99495939	3.382062276
RARS	16	70.115	2.192744878	3.373652776
ATP2B4	8	34.53	3.658400427	3.363090515
USP10	6	23.566	2.614748908	3.362263362
USP5	17	220.37	5.016576333	3.348976771
GNAI2	8	66.375	3.25124411	3.307685852
CDC5L	5	12.866	4.785674639	3.267774582
ATP2A2	10	37.284	2.652855517	3.255442301
CSPG4	19	250.35	2.119175017	3.218390783
FDPS	9	94.391	2.129536124	3.19761912
CDC42	9	98.625	1.425154204	3.19547526
EIF3J	4	31.952	2.42980925	3.150187174
MYO1C	5	17.606	2.375271122	3.142530441
IARS	31	221.35	1.142744362	3.133894602
FARSA	7	98.578	3.12503711	3.133508046
SDR16C5	6	105.5	2.103298843	3.127801895
PSMD11	7	17.25	2.401419822	3.093861262
FAP	7	28.318	3.772544743	3.088174184
DNAJA2	8	87.09	1.439065443	3.087294896
PPFIBP1	11	150.82	2.307074908	3.060188929
CMPK	5	13.041	1.558977479	3.056732178
CCT4	17	269.31	1.274252171	3.050540924
PSMC5	9	98.398	1.429098755	3.016515732
FUBP3	3	12.631	3.343757074	2.982807795
IDH1	7	20.494	3.003159615	2.915957133
RPN1	15	113.75	0.894955971	2.914335251
PFKP	12	103.4	1.208276847	2.894284566
CLTC	15	55.967	2.420110117	2.893357595
ERLIN2	4	25.402	2.773810015	2.886475881
DCTN1	19	177.17	4.124129402	2.884970983
PDCD6IP	7	35.052	2.833244977	2.863434474
ASPH	9	32.303	1.745605023	2.837875366
CSE1L	13	148.96	1.456381008	2.824026108
THBD	6	78.016	1.733421265	2.807112376
SPARC	2	5.6287	2.314068436	2.803776423
HSP90AB1	17	189.11	1.774212827	2.803049723
ANO5	7	64.922	3.467850015	2.788849513
CCDC47	10	30.393	1.844698043	2.787649155
PEBP1	2	16.19	1.459741425	2.786532084
RACK1	9	89.626	0.918557514	2.781419754
AIMP2	6	51.175	1.508468518	2.777436574
STAT3	15	211.23	2.64815975	2.776613235
PSMD3	6	118.71	2.024544988	2.760412852
AACS	5	12.064	1.741834717	2.739242554

GLG1	9	33.482	1.551758626	2.716735204
TMX3	6	48.607	2.623314275	2.704293569
LOC426023	2	157.16	0.961344933	2.703414917
PSMD2	13	153.17	1.501737941	2.698867798
ENDOD1	6	22.892	3.529420587	2.683257421
RPS19	9	46.62	1.084119756	2.673265457
U2AF1	7	49.804	1.853636133	2.673015594
RPN2	7	19.119	3.397314714	2.63639768
FAM129A	7	61.942	2.356880002	2.630837123
NDUFA13	2	5.8809	1.060605641	2.628943761
GAPDH	23	323.31	2.929298554	2.624592463
EHD3	6	14.311	2.07677479	2.620141347
chPKCI	3	8.3655	1.944439407	2.608301163
RPS27	3	6.4858	3.495934757	2.594365438
AARS	12	66.434	1.67803325	2.59357516
SNRPA1	7	37.593	2.014927908	2.587144852
TUBA3E	8	161.67	2.294180078	2.586465836
SFXN1	5	21.707	2.676637603	2.586369832
PITPNB	7	91.343	1.121468219	2.575382868
ACAT1	14	170.81	3.058768422	2.568665187
HMGCS1	13	232.38	0.944311687	2.566100438
YWHAQ	8	323.31	0.967804325	2.560787837
Gga.8044	6	35.601	2.760698487	2.559461594
PSMD1	3	13.45	2.333457727	2.557753881
HMOX1	4	76.834	1.479380276	2.54686292
VAPB	5	14.111	1.553510606	2.543721517
DDX1	10	53.472	1.593217418	2.542738597
CNN2	7	54.582	1.233704488	2.536920547
CTSB	8	100.36	1.281013919	2.521387736
ACTC1	2	323.31	2.196103426	2.510709763
FKBP10	11	63.753	1.183137794	2.508864085
RPRD2	26	175.01	1.304629494	2.498984019
CAPZA2	3	34.656	1.146767094	2.497057597
GCN1	8	18.537	2.097475145	2.495181402
UTRN	13	41.284	2.823791563	2.470219294
EIF4A2	16	323.31	2.756572828	2.468886693
ACTR2	4	67.241	1.468417717	2.46795845
AHCY	12	48.978	0.913343492	2.46537145
NSF	7	38.856	1.920549436	2.459726969
C8H1ORF27	4	48.942	0.891287095	2.452457428
TMEM43	6	17.45	3.145093585	2.43120575
SNRNP200	5	24.904	4.304018846	2.429847717
LSS	5	9.7567	2.086062129	2.420662562
ITGB1	10	123.8	1.697889508	2.400142034
RAN	8	39.098	2.91438789	2.399489085
PGK1	25	323.31	3.439503246	2.388788859

TMED10	3	8.393	2.011539633	2.384888331
YWHAH	2	6.4754	0.907783324	2.384681702
DDOST	6	25.592	2.102387326	2.37872378
PSME3	5	17.173	2.203478537	2.377358119
SSR1	4	36.772	0.951832008	2.37128067
ACTR3	9	99.696	1.924622382	2.356495539
rbf	3	9.5799	2.022676364	2.346045812
VAC14	4	62.707	2.173292958	2.338926315
MAP2K1	4	59.022	2.875290313	2.32945315
SOD1	3	75.467	0.950012703	2.313290278
PSMD7	5	19.446	1.427790875	2.291647593
Gga.6352	7	21.881	2.349628297	2.289354324
PYCR2	7	25.084	2.96821938	2.285896937
LRPPRC	8	31.999	1.709519104	2.284812291
NOP58	6	26.616	1.854223541	2.278680801
Gga.13539	4	13.612	2.129574379	2.272961299
NOTCH2	8	59.641	1.177802415	2.265687943
TNPO2	5	13.978	2.19825106	2.264511744
RAB1A	5	51.725	1.444960092	2.263924917
LOC107050681	2	7.833	1.194780348	2.24335289
COPA	22	98.863	2.079152769	2.213364919
ITGA4	5	19.631	2.085949564	2.196920395
ATP6V1A	5	31.195	1.498944796	2.188772202
ATAD3A	3	26.098	2.12806293	2.175035477
PLXNB2	4	27.007	2.573939939	2.167338689
NAP1L1	14	289.48	2.293023899	2.14788119
BTF3	3	64.365	3.572391935	2.143585841
RHOA	4	20.506	2.203238275	2.126673381
EIF3I	10	51.11	1.815638114	2.120548884
API5	3	59.919	2.969269337	2.114971797
IDH2	10	57.949	4.298106925	2.114658356
CTNNB1	6	25.752	1.577592526	2.112138112
DHRS7	4	15.398	2.533973309	2.100897471
MOCS3	5	17.321	2.331300359	2.084353765
PSMC1	9	69.023	2.317540965	2.076733271
NUP93	7	25.174	3.086492511	2.068166097
UQCRC2	7	22.2	1.242487267	2.065335592
SDPR	4	36.328	2.045241942	2.063906988
ATOX1	2	4.999	1.780900457	2.05995814
ALG14	2	22.474	1.431153376	2.040431341
EIF1AY	3	10.252	2.321634934	2.030502955
COPB1	6	20.925	2.116842505	2.026149114
HSP90B1	23	323.31	1.058872729	2.025220871
GBF1	4	14.251	4.164874977	2.010924021
LDHB	8	37.561	1.56694683	2.009641647
CTNNA1	5	29.523	2.016348127	2.009197871

SLK	3	16.265	2.231857144	2.006470362
RPL36A	2	8.4456	1.411720515	1.986380259
ALDH18A1	11	25.153	2.006606749	1.973993937
COX4I1	2	5.2368	2.299689399	1.970929464
PDLIM5	10	137.62	2.44801124	1.915373484
UBAP2L	5	17.46	2.486885322	1.89474233
MCM3	7	45.438	1.227478824	1.892674128
HP1BP3	4	24.102	2.793816016	1.88903745
PSPC1	5	69.157	2.556588234	1.884175618
SLC25A3	6	35.115	1.903750275	1.881043116
SERPINH1	18	194.12	1.187668326	1.877236048
SEC24D	2	28.262	2.77314512	1.873903275
XPO5	4	50.792	1.302642628	1.870145798
MCM5	6	29.08	1.435611573	1.866726557
TM9SF2	4	20.586	2.620409504	1.850023905
PPP4R1	3	46.071	1.702153525	1.837327957
DARS	15	89.271	2.648201797	1.8364652
cRac1A	4	8.3718	2.584680817	1.827336629
PFDN5	2	15.575	3.119213542	1.825728734
IQGAP1	36	323.31	1.625705284	1.81727155
MMP2	4	41.839	2.262808234	1.779094696
ATP5B	13	216.4	2.689281965	1.767122269
ACAD9	3	17.126	1.307210951	1.736946742
ITGA3	8	43.677	1.572075141	1.686815262
GARS	14	76.71	3.093960841	1.646132787
HSPA4L	15	108.95	1.438531838	1.640161514
ST13	4	9.9389	1.505745967	1.599136988
KTN1	4	111.4	2.261345946	1.590699514
RAB5C	4	18.734	1.803799774	1.58764712
EIF4G1	21	184.79	2.308550044	1.585198085
SEPT2	2	5.2564	1.721428045	1.545096715
RLI	4	11.786	1.66293744	1.544646581
CHMP4B	2	7.9591	3.46332992	1.540771484
NDUFA5	3	17.596	2.326935183	1.536884308
RPS7	13	84.611	1.643951874	1.53361702
LOC107049501	4	72.957	1.804135718	1.518319448
C1H21ORF33	3	12.642	2.367531411	1.478792826
ALG12	2	5.528	1.773801761	1.464152018
HEATR1	5	28.313	2.405157671	1.453435262
EEF1A	24	323.31	1.843960831	1.435681025
TUFM	8	23.213	2.047409639	1.377058029
DYNC1LI1	5	233.81	2.304305619	1.330360413
ABCF2	3	6.4771	2.662077272	1.306410472
HSPA8	43	323.31	2.225863201	-1.542245229
PPM1B	24	323.31	2.505344328	-1.570994695
NT5C2	8	41.665	1.671545303	-1.576644262

YBX1	4	62.589	1.95898217	-1.607637405
BOD1L1	49	323.31	3.022677205	-1.748095194
NCL	32	323.31	1.470378971	-1.761480967
SPATA2L	2	8.6975	1.333498196	-1.933946609
HSPA5	60	323.31	2.565852157	-1.957557678
NDUFAF7	12	101.58	2.452812561	-1.966108958
S100A6	5	15.419	2.982895828	-1.986438115
HSPH1	89	323.31	2.629169436	-2.089324951
ROCK1	8	48.623	1.151578878	-2.095235189
SPTBN1	110	323.31	2.21435941	-2.103445689
IMPDH2	4	323.31	2.387622173	-2.1088473
SPINW	9	33.674	2.292014507	-2.213559469
SPTAN1	5	323.31	2.16577041	-2.222287496
HNRNPH3	8	130.99	2.11451382	-2.334253311
ATXN3	6	77.165	2.508016568	-2.389877955
vcp	2	323.31	1.586693911	-2.619759242
TRA2A	4	13.521	1.535457001	-2.692606608
SPTAN1	2	14.628	1.718737045	-2.902865092
TRA2B	4	20.807	1.966623003	-4.002351761

Table 7.2: Cellular proteins identified through LC-MS/MS that have a significant interaction with chIFITM2-FLAG

Protein ID	Unique peptides	Confidence	p Value (-log10)	Fold change (Log2) chIFITM-FLAG/FLAG
chIFITM2	8	49.593	2.445076959	7.469003677
HSP25	13	323.31	4.326174743	7.363372167
DYNC1H1	68	323.31	3.087061802	6.315587997
EIF3A	6	323.31	2.877993257	5.918581645
CCT3	24	305.37	2.202832132	5.674060186
CCT8	3	99.631	5.646946062	5.670385361
SDR16C5	6	105.5	3.115409114	5.200796127
SF3B1	13	225.89	2.427561743	4.876956304
SQSTM1	15	323.31	1.481708979	4.710184097
IPO7	10	232	3.724051702	4.545094808
IARS	31	221.35	1.69521349	4.48835055
LDHA	19	323.31	2.369464322	4.442468643
CDK1	8	35.88	1.22976687	4.332385381
NCAPG2	11	49.391	2.653844397	4.252642949
EPRS	42	323.31	1.915573275	4.242449443
CSE1L	13	148.96	3.033449365	4.212331136
CANX	20	157.95	1.182678703	4.207326253
ATP1A1	15	139.5	2.673207375	4.180628459
CCT7	24	317.94	2.788449422	4.156349182
Gga.29531	6	47.091	2.302121127	4.137016932
STIM1	9	70.254	3.15435794	4.014463425
STAG2	16	177.78	3.438425849	3.996290207
FAM129A	7	61.942	2.599629678	3.930781047
TCP1	22	323.31	2.173285664	3.9271698
CCT2	20	145.55	1.921301166	3.896890004
ASNS	10	33.647	1.592795141	3.876338323
TLN1	34	174.23	2.124380342	3.844771067
PSMC6	13	144.67	1.753329829	3.778470993
CCT5	31	323.31	2.071155924	3.768192291
PSMC2	15	144.7	1.464661699	3.750332514
AIMP2	6	51.175	1.959364534	3.742291133
FASN	19	134.74	1.569717909	3.738395055
TNPO1	6	20.847	2.773956048	3.705701828
RARS	16	70.115	2.310301802	3.673597972
IMMT	11	41.53	3.042550972	3.670180003
SCD	4	37.377	3.184947219	3.603063583
DCTN1	19	177.17	3.527874568	3.530180613
HADHA	12	61.348	3.589676138	3.502772649
ATP5A1	22	237.25	2.079727631	3.477888743
HSPD1	32	323.31	2.03957805	3.402423223
TMX4	3	11.002	3.560774855	3.38886706
FARSA	7	98.578	2.178199862	3.385704676

PHB	12	113.93	1.430900091	3.373878479
RPS27	3	6.4858	2.848336909	3.3373305
CCT8	2	7.5913	2.568147928	3.328855515
VDAC2	8	74.109	1.65354084	3.327263514
PHB2	6	96.297	2.182346833	3.305337906
EIF3J	4	31.952	2.068944969	3.275941849
CCT6A	8	76.084	1.701558527	3.274384181
THBS1	13	66.292	1.874612898	3.261089325
SLC25A6	8	323.31	2.425711778	3.236560822
VAC14	4	62.707	2.207904651	3.20622317
GNAI2	8	66.375	3.334751828	3.193691254
POLR2B	9	19.278	3.15837681	3.174894969
MYO1C	5	17.606	2.078571365	3.172915141
U2AF1	7	49.804	1.669443595	3.157801946
FDPS	9	94.391	2.336276036	3.152849833
CKAP5	14	43.292	2.782566784	3.146830877
TNPO2	5	13.978	2.75640114	3.142286936
RPS19	9	46.62	1.39274428	3.140827815
RPN2	7	19.119	1.559585966	3.138600032
STAT3	15	211.23	3.253114784	3.137093226
P4HA1	9	26.705	2.597993725	3.119019826
CCDC47	10	30.393	2.187215393	3.119002024
PSMC3	19	206.76	1.29274579	3.101836522
EHD3	6	14.311	2.075124468	3.100144068
XPO1	11	92.471	2.21486258	3.095006307
TUBA4B	5	66.675	1.704561631	3.082262675
CLTC	15	55.967	3.295478158	3.046436946
EIF3K	8	63.536	1.162587029	3.018058141
PSMD3	6	118.71	2.11284867	3.013111115
NDUFA13	2	5.8809	1.188381765	2.9940389
PSMC5	9	98.398	1.442907793	2.909222921
CCT4	17	269.31	1.202932268	2.902838389
CMPK	5	13.041	1.500558835	2.89503479
CSPG4	19	250.35	1.839671256	2.892531077
ACTG1	3	153.56	1.021841036	2.863100052
YWHAQ	8	323.31	1.166970481	2.846311569
SDPR	4	36.328	2.091962443	2.845929464
CDC42	9	98.625	1.2677994	2.824139913
chPKCI	3	8.3655	2.035773364	2.816921234
ACAT1	14	170.81	3.343049678	2.806132634
USP10	6	23.566	1.964289597	2.7915109
PSMD2	13	153.17	1.549901919	2.769669851
PFKP	12	103.4	1.138503569	2.749342601
IDH1	7	20.494	3.095953473	2.743671417
TMEM43	6	17.45	2.856196409	2.738091151
DDX1	10	53.472	1.580641185	2.736730576

GCN1	8	18.537	2.419450625	2.716710409
MOCS3	5	17.321	2.590021774	2.709089915
RHOA	4	20.506	2.647159908	2.707740148
HSP90AB1	17	189.11	1.733848243	2.702168783
CTSB	8	100.36	1.376642342	2.696722031
ATP2A2	10	37.284	2.790578061	2.683575312
NSF	7	38.856	1.923326078	2.67626826
ATP2B4	8	34.53	1.087421815	2.67515564
PPFIBP1	11	150.82	1.849545044	2.674128215
UTRN	13	41.284	2.003754865	2.651385625
COPG1	6	66.787	1.945678963	2.649789174
USP5	17	220.37	4.88746192	2.649095535
ENDOD1	6	22.892	3.40595702	2.634342194
AHCY	12	48.978	0.991467659	2.630637487
ALDH18A1	11	25.153	2.192563401	2.607969284
Gga.8044	6	35.601	2.035424533	2.58783404
PLXNB2	4	27.007	2.930530676	2.545332591
EIF3I	10	51.11	1.929255832	2.540725072
EDC4	4	13.804	1.440294548	2.539190292
GBF1	4	14.251	4.242959724	2.522668839
RAN	8	39.098	2.291259128	2.517677307
GAPDH	23	323.31	2.517200415	2.505799611
ATAD3A	3	26.098	2.054974092	2.479478836
RPRD2	26	175.01	1.262749462	2.466138204
SOAT1	2	18.005	1.929849629	2.453660329
SFXN1	5	21.707	3.995052514	2.450597763
ITGB1	10	123.8	1.568793014	2.438363393
NOTCH2	8	59.641	1.257267175	2.434970856
PITPNB	7	91.343	1.075769867	2.434462229
SPARC	2	5.6287	2.499294348	2.432851156
GLG1	9	33.482	1.134580148	2.415925344
DNAJC1	4	10.751	1.327652289	2.390054703
ACTC1	2	323.31	1.917813454	2.379570643
CNN2	7	54.582	1.375774375	2.378480911
NUP93	7	25.174	2.738056578	2.377450307
EEF1E1	3	17.328	1.636046975	2.375113805
PSMD1	3	13.45	1.916109624	2.36824735
ITGAV	8	46.996	1.511563258	2.353199641
COPB1	6	20.925	2.248721538	2.337599436
PPP2R5E	2	2.1576	1.169149278	2.336082458
RAB1A	5	51.725	1.304254284	2.332671483
XPO5	4	50.792	1.752807287	2.317404429
EIF3B	10	78.999	1.074088508	2.312555313
ERLIN2	4	25.402	3.761337636	2.31069692
TMX3	6	48.607	4.468018685	2.28552564
PSME3	5	17.173	2.862764768	2.281152725

HEATR1	5	28.313	2.725178487	2.273145676
PSMD11	7	17.25	1.998459688	2.272556941
TPD52L2	4	55.373	1.936268512	2.266269684
TUBA3E	8	161.67	1.99339852	2.257233938
PGK1	25	323.31	4.012831993	2.246002197
DCTN3	5	38.743	1.609935437	2.20492808
COPA	22	98.863	2.101759404	2.195163091
DARS	15	89.271	3.163852173	2.167094549
ASPH	9	32.303	1.329528784	2.165141424
HMOX1	4	76.834	1.831881513	2.156843185
API5	3	59.919	1.336446884	2.150719961
KTN1	4	111.4	2.430243023	2.150167465
VCL	7	119.78	1.106810367	2.144846598
EIF4A2	16	323.31	2.517714032	2.14086469
DYNC1LI1	5	233.81	2.828902861	2.138638179
RPL15	7	29.814	1.631813014	2.132679621
SLC25A3	6	35.115	2.053256381	2.118378321
ALG14	2	22.474	1.410899491	2.113187154
ANO5	7	64.922	3.111842095	2.088412603
OTUB1	13	173.11	1.819916747	2.087624232
VIM	24	184.76	1.77520025	2.086383184
NOP58	6	26.616	1.468047372	2.05809466
PYCR2	7	25.084	3.299878345	2.055835724
DNM1	2	20.948	1.359274639	2.037164052
BTF3	3	64.365	3.776356396	2.035149256
ACTR3	9	99.696	1.676200702	2.030383428
HECTD1	5	13.916	1.452998213	2.019544601
cRac1A	4	8.3718	2.371487155	2.009869893
PSMC1	9	69.023	2.187439075	1.999320984
ITGA4	5	19.631	1.741431953	1.986832937
SNRNP200	5	24.904	4.203478592	1.979991277
LRPPRC	8	31.999	1.54016619	1.977901459
MAP2K1	4	59.022	2.589000326	1.972227732
CTNNB1	6	25.752	1.313219265	1.954692841
VAPB	5	14.111	1.241655034	1.95451355
IDH2	10	57.949	2.055378598	1.940518061
rbf	3	9.5799	2.205205921	1.847288132
HP1BP3	4	24.102	2.925596402	1.809938431
NAA25	12	56.679	2.206889853	1.799413045
NAP1L1	14	289.48	1.935406173	1.79881986
HEATR3	2	23.072	1.707934755	1.792274475
EIF4G1	21	184.79	2.451553611	1.792161306
DHRS7	4	15.398	2.524164254	1.768868764
IQGAP1	36	323.31	1.54661529	1.729729335
UQCRH	2	15.468	1.863087647	1.703221003
UBAP2L	5	17.46	3.075062166	1.687862396

PSPC1	5	69.157	1.757423804	1.678568522
PAK1	2	8.0648	1.822117097	1.654495875
ATP6V1B2	5	14.039	1.958081339	1.623662949
AIMP1	10	98.839	2.104155018	1.616096497
LARS	5	20.747	1.905938539	1.507425308
PLXNA1	2	2.4045	3.1704939	1.384658178
RPS3	19	192.75	2.517771255	1.368536631
HDX	5	14.986	2.30542369	-1.480677923
BOD1L1	49	323.31	1.994677676	-1.652287165
CTGF	12	109.18	1.773437219	-1.726145426
NCL	32	323.31	1.468261448	-1.734089533
LOC107049323	2	128.52	1.589549929	-1.851186117
SPTBN1	110	323.31	1.974706753	-1.892238617
DEK	2	1.7474	1.917386635	-1.984127045
TRA2A	4	13.521	1.42866799	-2.014672597
SPTAN1	5	323.31	1.851981086	-2.079819361
HSPA5	60	323.31	2.875608695	-2.081845601
NDUFAF7	12	101.58	2.514862995	-2.089780807
NT5C2	8	41.665	1.952556557	-2.119684855
ATXN3	6	77.165	2.249910735	-2.282540003
IMPDH2	4	323.31	2.785973109	-2.284492493
HNRNPH3	8	130.99	2.242230366	-2.294961929
HSPH1	89	323.31	3.382627134	-2.300445557
vcp	2	323.31	1.460722495	-2.396660487
ERH	6	88.804	2.464682059	-2.59946696
SPINW	9	33.674	3.383617848	-2.784644445
S100A6	5	15.419	2.142808292	-2.987522125
TRA2B	4	20.807	1.776776852	-3.08575503
SPTAN1	2	14.628	1.75086118	-3.134355545

Table 7.3: Cellular proteins identified through LC-MS/MS that have a significant interaction with chIFITM3-FLAG

Protein ID	Unique peptides	Confidence	p Value (-log10)	Fold change (Log2) chIFITM-FLAG/FLAG
LOC770612	7	104.65	3.630419145	10.29512533
HSP25	13	323.31	4.363101183	7.070083618
CANX	20	157.95	1.580599825	5.756710052
SQSTM1	15	323.31	1.667569334	5.47755305
DYNC1H1	68	323.31	2.818217715	5.227775574
NCAPG2	11	49.391	3.856420356	5.020467122
CCT8	3	99.631	5.253041713	4.807755152
EIF3A	6	323.31	2.447108438	4.704882304
ATP1A1	15	139.5	2.838708768	4.623772939
THBS1	13	66.292	2.406049554	4.605814616
ITGAV	8	46.996	4.826042316	4.600322088
CDK1	8	35.88	1.276132774	4.48836263
CCT3	24	305.37	1.716308328	4.130586624
ATP2A2	10	37.284	2.570121093	4.088137309
CCT2	20	145.55	2.003683254	4.085613887
SCD	4	37.377	3.359428192	4.081071854
FARSA	7	98.578	2.304696861	4.08078448
IMMT	11	41.53	3.036923864	4.011659622
PSMC2	15	144.7	1.537516983	3.980131149
ACTG1	3	153.56	1.251361668	3.947575251
IPO7	10	232	3.085629834	3.775609334
STIM1	9	70.254	3.03844791	3.77339681
CYR61	2	14.44	2.999902365	3.764981588
PHB	12	113.93	1.615315907	3.750914256
LDHA	19	323.31	1.859074064	3.738895416
PHB2	6	96.297	2.360877934	3.710563024
TMEM43	6	17.45	2.700800181	3.691612244
ATP5A1	22	237.25	2.130403853	3.688059489
PSMC6	13	144.67	1.704122697	3.687732061
TCP1	22	323.31	2.055135774	3.626918157
NOTCH2	8	59.641	2.191827677	3.611919403
HADHA	12	61.348	3.168827339	3.599042257
SLC25A6	8	323.31	2.524756661	3.582530975
PSMC3	19	206.76	1.448062762	3.576231003
CKAP5	14	43.292	3.191180412	3.495733897
VDAC2	8	74.109	1.72076105	3.486772537
P4HA1	9	26.705	2.838202836	3.463476817
SF3B1	13	225.89	1.909343675	3.457794825
DNAJA2	8	87.09	1.662178633	3.451449712
CSE1L	13	148.96	2.397118543	3.371655782
SDR16C5	6	105.5	2.015931289	3.371075312
CCT5	31	323.31	1.824752823	3.362906138

GNAI2	8	66.375	2.946411855	3.331900279
RPN2	7	19.119	2.616228518	3.277194341
MYO1C	5	17.606	2.499839688	3.275560379
RARS	16	70.115	2.155700426	3.267416636
FASN	19	134.74	1.390022188	3.236302694
U2AF1	7	49.804	2.718207812	3.223299026
POLR2B	9	19.278	2.52044985	3.212713242
TUBA4B	5	66.675	1.825230428	3.171902339
PSMC5	9	98.398	1.535975837	3.140721003
TLN1	34	174.23	2.202330253	3.130899429
SSR1	4	36.772	2.567321682	3.121081034
EPRS	42	323.31	1.443976356	3.116552989
ERLIN2	4	25.402	2.447678652	3.082304637
GLG1	9	33.482	1.538048547	3.023597717
Gga.29531	6	47.091	1.710323425	3.014978409
CCT6A	8	76.084	1.585401196	3.007674535
HSPD1	32	323.31	1.867353318	2.995848974
HMOX1	4	76.834	2.958081115	2.958384832
SFXN1	5	21.707	3.117408207	2.910378774
TUBA3E	8	161.67	2.301732918	2.899048487
PSMD2	13	153.17	1.61735499	2.889470418
FAP	7	28.318	3.343122045	2.879177729
DCTN1	19	177.17	3.296528472	2.870218913
PSMD3	6	118.71	2.03873117	2.854577382
ATP2B4	8	34.53	1.077305789	2.834074656
USP10	6	23.566	2.233138151	2.830677032
DDOST	6	25.592	2.047615449	2.821216583
AP2M1	6	38.937	1.913654624	2.818874359
CSPG4	19	250.35	1.852461453	2.770407995
RPS27	3	6.4858	1.876748494	2.758853277
ACTC1	2	323.31	2.163619022	2.734042486
CCDC47	10	30.393	1.982588088	2.697664261
CLTC	15	55.967	2.600831902	2.679939906
SLC25A3	6	35.115	2.294947555	2.672269185
SLC25A13	3	8.3486	1.854762227	2.62946256
ACAT1	14	170.81	3.445964044	2.624891917
CTSB	8	100.36	1.409661889	2.59772555
KTN1	4	111.4	2.139658459	2.593623479
CCT7	24	317.94	1.880483298	2.588375092
ATP5C1	8	44.925	1.926817115	2.586951574
RAN	8	39.098	2.443365293	2.585869471
PPFIBP1	11	150.82	2.050195045	2.58391126
ANO5	7	64.922	3.624847559	2.57084465
Gga.13539	4	13.612	2.417575186	2.526112874
APLP2	5	24.719	1.500355612	2.517800013
RPRD2	26	175.01	1.20259298	2.516488393

STAT3	15	211.23	2.208806802	2.508850098
FUBP3	3	12.631	2.534501024	2.504039764
ITGA4	5	19.631	2.213135992	2.494370778
EHD3	6	14.311	2.006874987	2.492059072
ASPH	9	32.303	1.387204197	2.4868927
EIF3J	4	31.952	2.034913949	2.446747462
GCN1	8	18.537	2.235974076	2.417862574
PSMC1	9	69.023	2.310755002	2.36905543
VAC14	4	62.707	2.408947437	2.355473836
TMX3	6	48.607	3.400009938	2.345234553
SNRNP200	5	24.904	3.342706877	2.326904933
THBD	6	78.016	1.325099924	2.304016113
NSF	7	38.856	1.874121466	2.278828303
MMP2	4	41.839	2.479936824	2.258871714
NUP93	7	25.174	2.722212028	2.25872167
MAP2K1	4	59.022	2.901282265	2.208045959
PSMD11	7	17.25	1.769480054	2.205809275
RAB5C	4	18.734	1.407370142	2.189044317
LSS	5	9.7567	2.174658748	2.154309591
SPARC	2	5.6287	1.816069601	2.153369268
CTNNA1	5	29.523	1.566157168	2.139104843
UTRN	13	41.284	2.551315918	2.136250178
EIF3I	10	51.11	1.594381025	2.11662674
GAPDH	23	323.31	2.610707212	2.079033534
Gga.6352	7	21.881	2.235736161	2.070884069
PSMD1	3	13.45	2.105053158	2.056708654
FAM129A	7	61.942	3.412036058	2.053544998
MCM5	6	29.08	1.646871779	2.025832494
RPL15	7	29.814	1.574807581	2.014740626
PLXNB2	4	27.007	2.972082723	2.012008667
COPA	22	98.863	1.989875709	2.011975606
PSME3	5	17.173	2.686152341	2.000639598
COPB1	6	20.925	1.997127405	1.892422358
RUVBL1	7	29.977	2.25725563	1.874531428
ATP6V1B2	5	14.039	1.824879551	1.865509669
TM9SF2	4	20.586	1.823669904	1.83956782
UBAP2L	5	17.46	2.445918997	1.801150004
USP5	17	220.37	2.950680161	1.788431168
SLK	3	16.265	1.955582593	1.773825328
GBF1	4	14.251	2.346721719	1.732352575
RPS3	19	192.75	3.10433856	1.727890015
SOAT1	2	18.005	2.10342566	1.699886322
EIF4G1	21	184.79	2.468801552	1.628341675
CNDP2	5	9.4043	1.833866252	-2.038715998
FUS	3	29.89	1.77693538	-2.194421132

References

Abdel-Moneim, A. S., Zlotowski, P., Veits, J., Keil, G. M. & Teifke, J. P. 2009. Immunohistochemistry for detection of avian infectious bronchitis virus strain m41 in the proventriculus and nervous system of experimentally infected chicken embryos. *Virol J,* 6**,** 15.

Abdul-Careem, M. F., Haq, K., Shanmuganathan, S., Read, L. R., Schat, K. A., Heidari, M. & Sharif, S. 2009. Induction of innate host responses in the lungs of chickens following infection with a very virulent strain of marek's disease virus. *Virology,* 393**,** 250-257.

Addinger, H. K. & Calnek, B. W. 1973. Pathogenesis of marek's disease: Early distribution of virus and viral antigens in infected chickens. *J Natl Cancer Inst,* 50**,** 1287-98.

Afonso, C. L., Tulman, E. R., Lu, Z., Zsak, L., Rock, D. L. & Kutish, G. F. 2001. The genome of turkey herpesvirus. *J Virol,* 75**,** 971-8.

Akhtar, J. & Shukla, D. 2009. Viral entry mechanisms: Cellular and viral mediators of herpes simplex virus entry. *FEBS J,* 276**,** 7228-36.

Alber, D. & Staeheli, P. 1996. Partial inhibition of vesicular stomatitis virus by the interferon-induced human 9-27 protein. *J Interferon Cytokine Res,* 16**,** 375-80.

Alonso-Caplen, F. V., Nemeroff, M. E., Qiu, Y. & Krug, R. M. 1992. Nucleocytoplasmic transport: The influenza virus ns1 protein regulates the transport of spliced ns2 mrna and its precursor ns1 mrna. *Genes Dev,* 6**,** 255-67.

Ambali, A. G. & Jones, R. C. 1990. Early pathogenesis in chicks of infection with an enterotropic strain of infectious bronchitis virus. *Avian Dis,* 34**,** 809-17.

Amini-Bavil-Olyaee, S., Choi, Y. J., Lee, J. H., Shi, M., Huang, I. C., Farzan, M. & Jung, J. U. 2013. The antiviral effector ifitm3 disrupts intracellular cholesterol homeostasis to block viral entry. *Cell Host Microbe,* 13**,** 452-64.

Anafu, A. A., Bowen, C. H., Chin, C. R., Brass, A. L. & Holm, G. H. 2013. Interferon-inducible transmembrane protein 3 (ifitm3) restricts reovirus cell entry. *J Biol Chem,* 288**,** 17261-71.

Anna, A. & Monika, G. 2018. Splicing mutations in human genetic disorders: Examples, detection, and confirmation. *J Appl Genet*.

Au, K. F., Underwood, J. G., Lee, L. & Wong, W. H. 2012. Improving pacbio long read accuracy by short read alignment. *PLoS One,* 7**,** e46679.

Bailey, C. C., Huang, I. C., Kam, C. & Farzan, M. 2012. Ifitm3 limits the severity of acute influenza in mice. *PLoS Pathog,* 8**,** e1002909.

Bailey, C. C., Kondur, H. R., Huang, I. C. & Farzan, M. 2013. Interferon-induced transmembrane protein 3 is a type ii transmembrane protein. *J Biol Chem,* 288**,** 32184-93.

Bailey, C. C., Zhong, G., Huang, I. C. & Farzan, M. 2014. Ifitm-family proteins: The cell's first line of antiviral defense. *Annu Rev Virol,* 1**,** 261-283.

Baron, S. & Isaacs, A. 1961. Mechanism of recovery from viral infection in the chick embryo. *Nature,* 191**,** 97-8.

Bassano, I., Ong, S. H., Lawless, N., Whitehead, T., Fife, M. & Kellam, P. 2017. Accurate characterization of the ifitm locus using miseq and pacbio sequencing shows genetic variation in galliformes. *BMC Genomics,* 18**,** 419.

Beasley, J. N., Patterson, L. T. & Mcwade, D. H. 1970. Transmission of marek's disease by poultry house dust and chicken dander. *Am J Vet Res,* 31**,** 339-44.

Belouzard, S., Millet, J. K., Licitra, B. N. & Whittaker, G. R. 2012. Mechanisms of coronavirus cell entry mediated by the viral spike protein. *Viruses,* 4**,** 1011-33.

Benitez, A. A., Panis, M., Xue, J., Varble, A., Shim, J. V., Frick, A. L., Lopez, C. B., Sachs, D. & Tenoever, B. R. 2015. In vivo rnai screening identifies mda5 as a significant

contributor to the cellular defense against influenza a virus. *Cell Reports,* 11**,** 1714-1726.
Benyeda, Z., Mato, T., Suveges, T., Szabo, E., Kardi, V., Abonyi-Toth, Z., Rusvai, M. & Palya, V. 2009. Comparison of the pathogenicity of qx-like, m41 and 793/b infectious bronchitis strains from different pathological conditions. *Avian Pathology,* 38**,** 449-456.
Bercovich-Kinori, A., Tai, J., Gelbart, I. A., Shitrit, A., Ben-Moshe, S., Drori, Y., Itzkovitz, S., Mandelboim, M. & Stern-Ginossar, N. 2016. A systematic view on influenza induced host shutoff. *Elife,* 5.
Bhardwaj, K., Liu, P., Leibowitz, J. L. & Kao, C. C. 2012. The coronavirus endoribonuclease nsp15 interacts with retinoblastoma tumor suppressor protein. *J Virol,* 86**,** 4294-304.
Blaas, D., Patzelt, E. & Kuechler, E. 1982. Identification of the cap binding protein of influenza virus. *Nucleic Acids Res,* 10**,** 4803-12.
Blyth, G. A., Chan, W. F., Webster, R. G. & Magor, K. E. 2016. Duck interferon-inducible transmembrane protein 3 mediates restriction of influenza viruses. *J Virol,* 90**,** 103-16.
Bosch, B. J., Van Der Zee, R., De Haan, C. a. M. & Rottier, P. J. M. 2003. The coronavirus spike protein is a class i virus fusion protein: Structural and functional characterization of the fusion core complex. *Journal of Virology,* 77**,** 8801-8811.
Bowles, N. E., Arrington, C. B., Hirono, K., Nakamura, T., Ngo, L., Wee, Y. S., Ichida, F. & Weis, J. H. 2014. Kawasaki disease patients homozygous for the rs12252-c variant of interferon-induced transmembrane protein-3 are significantly more likely to develop coronary artery lesions. *Mol Genet Genomic Med,* 2**,** 356-61.
Braam, J., Ulmanen, I. & Krug, R. M. 1983. Molecular model of a eucaryotic transcription complex: Functions and movements of influenza p proteins during capped rna-primed transcription. *Cell,* 34**,** 609-18.
Brass, A. L., Huang, I. C., Benita, Y., John, S. P., Krishnan, M. N., Feeley, E. M., Ryan, B. J., Weyer, J. L., Van Der Weyden, L., Fikrig, E., Adams, D. J., Xavier, R. J., Farzan, M. & Elledge, S. J. 2009. The ifitm proteins mediate cellular resistance to influenza a h1n1 virus, west nile virus, and dengue virus. *Cell,* 139**,** 1243-54.
Brian, D. A. & Baric, R. S. 2005. Coronavirus genome structure and replication. *Curr Top Microbiol Immunol,* 287**,** 1-30.
Brierley, I., Boursnell, M. E. G., Binns, M. M., Bilimoria, B., Blok, V. C., Brown, T. D. K. & Inglis, S. C. 1987. An efficient ribosomal frame-shifting signal in the polymerase-encoding region of the coronavirus ibv. *Embo Journal,* 6**,** 3779-3785.
British Poultry Council. 2016. *About the poultry industry* [Online]. Available: http://www.britishpoultry.org.uk/how-the-sector-works [Accessed 1st June 2018].
Bui, C. M., Gardner, L., Macintyre, C. R. & Sarkar, S. 2017. Influenza a h5n1 and h7n9 in china: A spatial risk analysis. *Plos One,* 12.
Bui, M., Whittaker, G. & Helenius, A. 1996. Effect of m1 protein and low ph on nuclear transport of influenza virus ribonucleoproteins. *J Virol,* 70**,** 8391-401.
Burt, D. W., Bruley, C., Dunn, I. C., Jones, C. T., Ramage, A., Law, A. S., Morrice, D. R., Paton, I. R., Smith, J., Windsor, D., Sazanov, A., Fries, R. & Waddington, D. 1999. The dynamics of chromosome evolution in birds and mammals. *Nature,* 402**,** 411-413.
Calnek, B. W. 2001. Pathogenesis of marek's disease virus infection. *Curr Top Microbiol Immunol,* 255**,** 25-55.
Caron, A., Cappelle, J. & Gaidet, N. 2017. Challenging the conceptual framework of maintenance hosts for influenza a viruses in wild birds. *Journal of Applied Ecology,* 54**,** 681-690.

Casais, R., Dove, B., Cavanagh, D. & Britton, P. 2003. Recombinant avian infectious bronchitis virus expressing a heterologous spike gene demonstrates that the spike protein is a determinant of cell tropism. *Journal of Virology,* 77**,** 9084-9089.

Casais, R., Thiel, V., Siddell, S. G., Cavanagh, D. & Britton, P. 2001. Reverse genetics system for the avian coronavirus infectious bronchitis virus. *J Virol,* 75**,** 12359-69.

Chandran, K. & Nibert, M. L. 1998. Protease cleavage of reovirus capsid protein mu 1/mu 1c is blocked by alkyl sulfate detergents, yielding a new type of infectious subvirion particle. *Journal of Virology,* 72**,** 467-475.

Chandran, K., Sullivan, N. J., Felbor, U., Whelan, S. P. & Cunningham, J. M. 2005. Endosomal proteolysis of the ebola virus glycoprotein is necessary for infection. *Science,* 308**,** 1643-1645.

Chen, B., Fang, S. G., Tam, J. P. & Liu, D. X. 2009. Formation of stable homodimer via the c-terminal alpha-helical domain of coronavirus nonstructural protein 9 is critical for its function in viral replication. *Virology,* 383**,** 328-337.

Chen, S. L., Wang, L., Chen, J. Y., Zhang, L. L., Wang, S., Goraya, M. U., Chi, X. J., Na, Y., Shao, W. H., Yang, Z., Zeng, X. C., Chen, S. Y. & Chen, J. L. 2017. Avian interferon-inducible transmembrane protein family effectively restricts avian tembusu virus infection. *Frontiers in Microbiology,* 8.

Chesarino, N. M., Mcmichael, T. M., Hach, J. C. & Yount, J. S. 2014a. Phosphorylation of the antiviral protein interferon-inducible transmembrane protein 3 (ifitm3) dually regulates its endocytosis and ubiquitination. *J Biol Chem,* 289**,** 11986-92.

Chesarino, N. M., Mcmichael, T. M. & Yount, J. S. 2014b. Regulation of the trafficking and antiviral activity of ifitm3 by post-translational modifications. *Future Microbiol,* 9**,** 1151-63.

Churchill, A. E. & Biggs, P. M. 1967. Agent of marek's disease in tissue culture. *Nature,* 215**,** 528-30.

Chutiwitoonchai, N., Hiyoshi, M., Hiyoshi-Yoshidomi, Y., Hashimoto, M., Tokunaga, K. & Suzu, S. 2013. Characteristics of ifitm, the newly identified ifn-inducible anti-hiv-1 family proteins. *Microbes Infect,* 15**,** 280-90.

Colby, C. & Duesberg, P. H. 1969. Double-stranded rna in vaccinia virus infected cells. *Nature,* 222**,** 940-4.

Colvero, L. P., Villarreal, L. Y., Torres, C. A. & Brando, P. E. 2015. Assessing the economic burden of avian infectious bronchitis on poultry farms in brazil. *Rev Sci Tech,* 34**,** 993-9.

Compton, A. A., Bruel, T., Porrot, F., Mallet, A., Sachse, M., Euvrard, M., Liang, C., Casartelli, N. & Schwartz, O. 2014. Ifitm proteins incorporated into hiv-1 virions impair viral fusion and spread. *Cell Host Microbe,* 16**,** 736-47.

Compton, A. A., Roy, N., Porrot, F., Billet, A., Casartelli, N., Yount, J. S., Liang, C. & Schwartz, O. 2016. Natural mutations in ifitm3 modulate post-translational regulation and toggle antiviral specificity. *EMBO Rep,* 17**,** 1657-1671.

Cook, J. K., Jackwood, M. & Jones, R. C. 2012. The long view: 40 years of infectious bronchitis research. *Avian Pathol,* 41**,** 239-50.

Corse, E. & Machamer, C. E. 2003. The cytoplasmic tails of infectious bronchitis virus e and m proteins mediate their interaction. *Virology,* 312**,** 25-34.

Cox, J., Hein, M. Y., Luber, C. A., Paron, I., Nagaraj, N. & Mann, M. 2014. Accurate proteome-wide label-free quantification by delayed normalization and maximal peptide ratio extraction, termed maxlfq. *Molecular & Cellular Proteomics,* 13**,** 2513-2526.

Cumming, R. B. 1969a. Studies on avian infectious bronchitis virus. 2. Incidence of the virus in broiler and layer flocks, by isolation and serological methods. *Aust Vet J,* 45**,** 309-11.

Cumming, R. B. 1969b. Studies on avian infectious bronchitis virus. I. Distribution and survival of the virus in tissues of affected chickens and studies on the carrier status. *Aust Vet J,* 45**,** 305-8.
Darteil, R., Bublot, M., Laplace, E., Bouquet, J. F., Audonnet, J. C. & Riviere, M. 1995. Herpesvirus of turkey recombinant viruses expressing infectious bursal disease virus (ibdv) vp2 immunogen induce protection against an ibdv virulent challenge in chickens. *Virology,* 211**,** 481-90.
David, S., Correia, V., Antunes, L., Faria, R., Ferrao, J., Faustino, P., Nunes, B., Maltez, F., Lavinha, J. & Rebelo De Andrade, H. 2018. Population genetics of ifitm3 in portugal and central africa reveals a potential modifier of influenza severity. *Immunogenetics,* 70**,** 169-177.
De Jonge, J. & Van Trijp, H. C. M. 2013. The impact of broiler production system practices on consumer perceptions of animal welfare. *Poultry Science,* 92**,** 3080-3095.
De Veer, M. J., Holko, M., Frevel, M., Walker, E., Der, S., Paranjape, J. M., Silverman, R. H. & Williams, B. R. 2001a. Functional classification of interferon-stimulated genes identified using microarrays. *J Leukoc Biol,* 69**,** 912-20.
De Veer, M. J., Holko, M., Frevel, M., Walker, E., Der, S., Paranjape, J. M., Silverman, R. H. & Williams, B. R. G. 2001b. Functional classification of interferon-stimulated genes identified using microarrays. *Journal of Leukocyte Biology,* 69**,** 912-920.
Decker, T., Lew, D. J., Mirkovitch, J. & Darnell, J. E., Jr. 1991. Cytoplasmic activation of gaf, an ifn-gamma-regulated DNA-binding factor. *EMBO J,* 10**,** 927-32.
Decroly, E., Imbert, I., Coutard, B., Bouvet, M. L., Selisko, B., Alvarez, K., Gorbalenya, A. E., Snijder, E. J. & Canard, B. 2008. Coronavirus nonstructural protein 16 is a cap-0 binding enzyme possessing (nucleoside-2'o)-methyltransferase activity. *Journal of Virology,* 82**,** 8071-8084.
Defra. 2018. *Poultry and poultry meat statistics* [Online]. Available: https://www.gov.uk/government/collections/poultry-and-poultry-meat-statistics [Accessed 1st June 2018].
Deng, T., Vreede, F. T. & Brownlee, G. G. 2006. Different de novo initiation strategies are used by influenza virus rna polymerase on its crna and viral rna promoters during viral rna replication. *J Virol,* 80**,** 2337-48.
Desai, T. M., Marin, M., Chin, C. R., Savidis, G., Brass, A. L. & Melikyan, G. B. 2014. Ifitm3 restricts influenza a virus entry by blocking the formation of fusion pores following virus-endosome hemifusion. *PLoS Pathog,* 10**,** e1004048.
Desai, T. M., Marin, M., Mason, C. & Melikyan, G. B. 2017. Ph regulation in early endosomes and interferon-inducible transmembrane proteins control avian retrovirus fusion. *Journal of Biological Chemistry,* 292**,** 7817-+.
Diamond, J. M. 1991. Distribution and taxonomy of birds of the world - sibley,cg, monroe,bl. *Nature,* 350**,** 537-538.
Diamond, M. S. & Farzan, M. 2013. The broad-spectrum antiviral functions of ifit and ifitm proteins. *Nat Rev Immunol,* 13**,** 46-57.
Dias, A., Bouvier, D., Crepin, T., Mccarthy, A. A., Hart, D. J., Baudin, F., Cusack, S. & Ruigrok, R. W. 2009. The cap-snatching endonuclease of influenza virus polymerase resides in the pa subunit. *Nature,* 458**,** 914-8.
Ding, S., Pan, Q., Liu, S. L. & Liang, C. 2014. Hiv-1 mutates to evade ifitm1 restriction. *Virology,* 454-455**,** 11-24.
Ebert, D. H., Deussing, J., Peters, C. & Dermody, T. S. 2002. Cathepsin l and cathepsin b mediate reovirus disassembly in murine fibroblast cells. *Journal of Biological Chemistry,* 277**,** 24609-24617.
Eid, J., Fehr, A., Gray, J., Luong, K., Lyle, J., Otto, G., Peluso, P., Rank, D., Baybayan, P., Bettman, B., Bibillo, A., Bjornson, K., Chaudhuri, B., Christians, F., Cicero, R., Clark, S., Dalal, R., Dewinter, A., Dixon, J., Foquet, M., Gaertner, A., Hardenbol, P., Heiner,

C., Hester, K., Holden, D., Kearns, G., Kong, X., Kuse, R., Lacroix, Y., Lin, S., Lundquist, P., Ma, C., Marks, P., Maxham, M., Murphy, D., Park, I., Pham, T., Phillips, M., Roy, J., Sebra, R., Shen, G., Sorenson, J., Tomaney, A., Travers, K., Trulson, M., Vieceli, J., Wegener, J., Wu, D., Yang, A., Zaccarin, D., Zhao, P., Zhong, F., Korlach, J. & Turner, S. 2009. Real-time DNA sequencing from single polymerase molecules. *Science,* 323**,** 133-8.

Eierhoff, T., Hrincius, E. R., Rescher, U., Ludwig, S. & Ehrhardt, C. 2010. The epidermal growth factor receptor (egfr) promotes uptake of influenza a viruses (iav) into host cells. *Plos Pathogens,* 6.

El Khantour, A., Darkaoui, S., Tatar-Kis, T., Mato, T., Essalah-Bennani, A., Cazaban, C. & Palya, V. 2017. Immunity elicited by a turkey herpesvirus-vectored newcastle disease vaccine in turkey against challenge with a recent genotype iv newcastle disease virus field strain. *Avian Dis,* 61**,** 378-386.

Engelhardt, O. G., Smith, M. & Fodor, E. 2005. Association of the influenza a virus rna-dependent rna polymerase with cellular rna polymerase ii. *J Virol,* 79**,** 5812-8.

Enjuanes, L., Almazan, F., Sola, I. & Zuniga, S. 2006. Biochemical aspects of coronavirus replication and virus-host interaction. *Annu Rev Microbiol,* 60**,** 211-30.

Everitt, A. R., Clare, S., Mcdonald, J. U., Kane, L., Harcourt, K., Ahras, M., Lall, A., Hale, C., Rodgers, A., Young, D. B., Haque, A., Billker, O., Tregoning, J. S., Dougan, G. & Kellam, P. 2013. Defining the range of pathogens susceptible to ifitm3 restriction using a knockout mouse model. *PLoS One,* 8**,** e80723.

Everitt, A. R., Clare, S., Pertel, T., John, S. P., Wash, R. S., Smith, S. E., Chin, C. R., Feeley, E. M., Sims, J. S., Adams, D. J., Wise, H. M., Kane, L., Goulding, D., Digard, P., Anttila, V., Baillie, J. K., Walsh, T. S., Hume, D. A., Palotie, A., Xue, Y., Colonna, V., Tyler-Smith, C., Dunning, J., Gordon, S. B., Gen, I. I., Investigators, M., Smyth, R. L., Openshaw, P. J., Dougan, G., Brass, A. L. & Kellam, P. 2012. Ifitm3 restricts the morbidity and mortality associated with influenza. *Nature,* 484**,** 519-23.

Fang, S., Shen, H., Wang, J., Tay, F. P. & Liu, D. X. 2010. Functional and genetic studies of the substrate specificity of coronavirus infectious bronchitis virus 3c-like proteinase. *J Virol,* 84**,** 7325-36.

Fang, S. G., Shen, H. Y., Wang, J. B., Tay, F. P. L. & Liu, D. X. 2008. Proteolytic processing of polyproteins 1a and 1ab between non-structural proteins 10 and 11/12 of coronavirus infectious bronchitis virus is dispensable for viral replication in cultured cells. *Virology,* 379**,** 175-180.

Faostat. 2011. *Animals slaughtered worldwide* [Online]. Available: www.fao.org/faostat/en/#data [Accessed 1st June 2018].

Farber, C. R., Reich, A., Barnes, A. M., Becerra, P., Rauch, F., Cabral, W. A., Bae, A., Quinlan, A., Glorieux, F. H., Clemens, T. L. & Marini, J. C. 2014. A novel ifitm5 mutation in severe atypical osteogenesis imperfecta type vi impairs osteoblast production of pigment epithelium-derived factor. *J Bone Miner Res,* 29**,** 1402-11.

Farrar, M. A. & Schreiber, R. D. 1993. The molecular cell biology of interferon-gamma and its receptor. *Annual Review of Immunology,* 11**,** 571-611.

Field, A. K., Tytell, A. A., Lampson, G. P. & Hilleman, M. R. 1967. Inducers of interferon and host resistance. Ii. Multistranded synthetic polynucleotide complexes. *Proc Natl Acad Sci U S A,* 58**,** 1004-10.

Firth, A. E., Jagger, B. W., Wise, H. M., Nelson, C. C., Parsawar, K., Wills, N. M., Napthine, S., Taubenberger, J. K., Digard, P. & Atkins, J. F. 2012. Ribosomal frameshifting used in influenza a virus expression occurs within the sequence ucc_uuu_cgu and is in the+1 direction. *Open Biology,* 2.

Flick, R., Neumann, G., Hoffmann, E., Neumeier, E. & Hobom, G. 1996. Promoter elements in the influenza vrna terminal structure. *RNA,* 2**,** 1046-57.

Fodor, E. 2013. The rna polymerase of influenza a virus: Mechanisms of viral transcription and replication. *Acta Virol,* 57**,** 113-22.
Foster, G. R. 1997. Interferons in host defense. *Semin Liver Dis,* 17**,** 287-95.
Foster, T. L., Wilson, H., Iyer, S. S., Coss, K., Doores, K., Smith, S., Kellam, P., Finzi, A., Borrow, P., Hahn, B. H. & Neil, S. J. D. 2016. Resistance of transmitted founder hiv-1 to ifitm-mediated restriction. *Cell Host Microbe,* 20**,** 429-442.
Fribourg, M., Hartmann, B., Schmolke, M., Marjanovic, N., Albrecht, R. A., Garcia-Sastre, A., Sealfon, S. C., Jayaprakash, C. & Hayot, F. 2014. Model of influenza a virus infection: Dynamics of viral antagonism and innate immune response. *J Theor Biol,* 351**,** 47-57.
Friedman, R. L., Manly, S. P., Mcmahon, M., Kerr, I. M. & Stark, G. R. 1984. Transcriptional and posttranscriptional regulation of interferon-induced gene expression in human cells. *Cell,* 38**,** 745-55.
Fu, B., Wang, L., Li, S. & Dorf, M. E. 2017. Zmpste24 defends against influenza and other pathogenic viruses. *J Exp Med,* 214**,** 919-929.
Fu, X. Y., Kessler, D. S., Veals, S. A., Levy, D. E. & Darnell, J. E. 1990. Isgf3, the transcriptional activator induced by interferon-alpha, consists of multiple interacting polypeptide-chains. *Proceedings of the National Academy of Sciences of the United States of America,* 87**,** 8555-8559.
Fumihito, A., Miyake, T., Takada, M., Shingu, R., Endo, T., Gojobori, T., Kondo, N. & Ohno, S. 1996. Monophyletic origin and unique dispersal patterns of domestic fowls. *Proc Natl Acad Sci U S A,* 93**,** 6792-5.
Gack, M. U., Albrecht, R. A., Urano, T., Inn, K. S., Huang, I. C., Carnero, E., Farzan, M., Inoue, S., Jung, J. U. & Garcia-Sastre, A. 2009. Influenza a virus ns1 targets the ubiquitin ligase trim25 to evade recognition by the host viral rna sensor rig-i. *Cell Host & Microbe,* 5**,** 439-449.
Gack, M. U., Shin, Y. C., Joo, C. H., Urano, T., Liang, C., Sun, L. J., Takeuchi, O., Akira, S., Chen, Z. J., Inoue, S. S. & Jung, J. U. 2007. Trim25 ring-finger e3 ubiquitin ligase is essential for rig-i-mediated antiviral activity. *Nature,* 446**,** 916-U2.
Ghebrehewet, S., Macpherson, P. & Ho, A. 2016. Influenza. *Bmj-British Medical Journal,* 355.
Gibbert, K., Schlaak, J. F., Yang, D. & Dittmer, U. 2013. Ifn-alpha subtypes: Distinct biological activities in anti-viral therapy. *Br J Pharmacol,* 168**,** 1048-58.
Gimeno, I. M., Cortes, A. L., Faiz, N., Villalobos, T., Badillo, H. & Barbosa, T. 2016. Efficacy of various hvt vaccines (conventional and recombinant) against marek's disease in broiler chickens: Effect of dose and age of vaccination. *Avian Dis,* 60**,** 662-8.
Giotis, E. S., Robey, R. C., Skinner, N. G., Tomlinson, C. D., Goodbourn, S. & Skinner, M. A. 2016. Chicken interferome: Avian interferon-stimulated genes identified by microarray and rna-seq of primary chick embryo fibroblasts treated with a chicken type i interferon (ifn-alpha). *Vet Res,* 47**,** 75.
Giotis, E. S., Ross, C. S., Robey, R. C., Nohturfft, A., Goodbourn, S. & Skinner, M. A. 2017. Constitutively elevated levels of socs1 suppress innate responses in df-1 immortalised chicken fibroblast cells. *Sci Rep,* 7**,** 17485.
Gomez-Puertas, P., Albo, C., Perez-Pastrana, E., Vivo, A. & Portela, A. 2000. Influenza virus matrix protein is the major driving force in virus budding. *Journal of Virology,* 74**,** 11538-11547.
Gorman, M. J., Poddar, S., Farzan, M. & Diamond, M. S. 2016. The interferon-stimulated gene ifitm3 restricts west nile virus infection and pathogenesis. *J Virol,* 90**,** 8212-25.
Graham, A. C., Hilmer, K. M., Zickovich, J. M. & Obar, J. J. 2013. Inflammatory response of mast cells during influenza a virus infection is mediated by active infection and rig-i signaling. *Journal of Immunology,* 190**,** 4676-4684.

Gu, J., Hao, J., Fang, X. & Sha, X. 2016. Factors influencing the transfection efficiency and cellular uptake mechanisms of pluronic p123-modified polypropyleneimine/pdna polyplexes in multidrug resistant breast cancer cells. *Colloids Surf B Biointerfaces,* 140**,** 83-93.

Hach, J. C., Mcmichael, T., Chesarino, N. M. & Yount, J. S. 2013a. Palmitoylation on conserved and nonconserved cysteines of murine ifitm1 regulates its stability and anti-influenza a virus activity. *J Virol,* 87**,** 9923-7.

Hach, J. C., Mcmichael, T., Chesarino, N. M. & Yount, J. S. 2013b. Palmitoylation on conserved and nonconserved cysteines of murine ifitm1 regulates its stability and anti-influenza a virus activity. *Journal of Virology,* 87**,** 9923-9927.

Hale, B. G., Randall, R. E., Ortin, J. & Jackson, D. 2008. The multifunctional ns1 protein of influenza a viruses. *J Gen Virol,* 89**,** 2359-76.

Hara, K., Schmidt, F. I., Crow, M. & Brownlee, G. G. 2006. Amino acid residues in the n-terminal region of the pa subunit of influenza a virus rna polymerase play a critical role in protein stability, endonuclease activity, cap binding, and virion rna promoter binding. *J Virol,* 80**,** 7789-98.

Harada, K., Sato, Y., Itatsu, K., Isse, K., Ikeda, H., Yasoshima, M., Zen, Y., Matsui, A. & Nakanuma, Y. 2007. Innate immune response to double-stranded rna in biliary epithelial cells is associated with the pathogenesis of biliary atresia. *Hepatology,* 46**,** 1146-54.

Harris, A., Cardone, G., Winkler, D. C., Heymann, J. B., Brecher, M., White, J. M. & Steven, A. C. 2006. Influenza virus pleiomorphy characterized by cryoelectron tomography. *Proc Natl Acad Sci U S A,* 103**,** 19123-7.

Hayashi, T., Watanabe, C., Suzuki, Y., Tanikawa, T., Uchida, Y. & Saito, T. 2014. Chicken mda5 senses short double-stranded rna with implications for antiviral response against avian influenza viruses in chicken. *Journal of Innate Immunity,* 6**,** 58-71.

Hilleman, M. R. 1970. Double-stranded rnas (poly i:C) in the prevention of viral infections. *Arch Intern Med,* 126**,** 109-24.

Hillier, L. W., Miller, W., Birney, E., Warren, W., Hardison, R. C., Ponting, C. P., Bork, P., Burt, D. W., Groenen, M. a. M., Delany, M. E., Dodgson, J. B., Chinwalla, A. T., Cliften, P. F., Clifton, S. W., Delehaunty, K. D., Fronick, C., Fulton, R. S., Graves, T. A., Kremitzki, C., Layman, D., Magrini, V., Mcpherson, J. D., Miner, T. L., Minx, P., Nash, W. E., Nhan, M. N., Nelson, J. O., Oddy, L. G., Pohl, C. S., Randall-Maher, J., Smith, S. M., Wallis, J. W., Yang, S. P., Romanov, M. N., Rondelli, C. M., Paton, B., Smith, J., Morrice, D., Daniels, L., Tempest, H. G., Robertson, L., Masabanda, J. S., Griffin, D. K., Vignal, A., Fillon, V., Jacobbson, L., Kerje, S., Andersson, L., Crooijmans, R. P. M., Aerts, J., Van Der Poel, J. J., Ellegren, H., Caldwell, R. B., Hubbard, S. J., Grafham, D. V., Kierzek, A. M., Mclaren, S. R., Overton, I. M., Arakawa, H., Beattie, K. J., Bezzubov, Y., Boardman, P. E., Bonfield, J. K., Croning, M. D. R., Davies, R. M., Francis, M. D., Humphray, S. J., Scott, C. E., Taylor, R. G., Tickle, C., Brown, W. R. A., Rogers, J., Buerstedde, J. M., Wilson, S. A., Stubbs, L., Ovcharenko, I., Gordon, L., Lucas, S., Miller, M. M., Inoko, H., Shiina, T., Kaufman, J., Salomonsen, J., Skjoedt, K., Wong, G. K. S., Wang, J., Liu, B., Wang, J., Yu, J., Yang, H. M., Nefedov, M., Koriabine, M., Dejong, P. J., Goodstadt, L., Webber, C., Dickens, N. J., Letunic, I., Suyama, M., Torrents, D., Von Mering, C., et al. 2004. Sequence and comparative analysis of the chicken genome provide unique perspectives on vertebrate evolution. *Nature,* 432**,** 695-716.

Hofstad, M. S. & Yoder, H. W., Jr. 1966. Avian infectious bronchitis--virus distribution in tissues of chicks. *Avian Dis,* 10**,** 230-9.

Horimoto, T. & Kawaoka, Y. 2005. Influenza: Lessons from past pandemics, warnings from current incidents. *Nat Rev Microbiol,* 3**,** 591-600.

Hornung, V., Ellegast, J., Kim, S., Brzózka, K., Jung, A., Kato, H., Poeck, H., Akira, S., Conzelmann, K.-K., Schlee, M., Endres, S. & Hartmann, G. 2006. 5'-triphosphate rna is the ligand for rig-i. *Science,* 314**,** 994-997.

Hoyo, J. D., Elliott, A., Sargatal, J. & Cabot, J. 1992. *Handbook of the birds of the world,* Barcelona, Lynx Edicions.

Hu, Y., Li, W., Gao, T., Cui, Y., Jin, Y. W., Li, P., Ma, Q. J., Liu, X. & Cao, C. 2017. The severe acute respiratory syndrome coronavirus nucleocapsid inhibits type i interferon production by interfering with trim25-mediated rig-i ubiquitination. *Journal of Virology,* 91.

Huang, I. C., Bailey, C. C., Weyer, J. L., Radoshitzky, S. R., Becker, M. M., Chiang, J. J., Brass, A. L., Ahmed, A. A., Chi, X., Dong, L., Longobardi, L. E., Boltz, D., Kuhn, J. H., Elledge, S. J., Bavari, S., Denison, M. R., Choe, H. & Farzan, M. 2011. Distinct patterns of ifitm-mediated restriction of filoviruses, sars coronavirus, and influenza a virus. *PLoS Pathog,* 7**,** e1001258.

Huang, I. C., Bosch, B. J., Li, W. H., Farzan, M., Rottier, P. M. & Choe, H. 2006. Sars-cov, but not hcov-nl63, utilizes cathepsins to infect cells - viral entry. *Nidoviruses: Toward Control of Sars and Other Nidovirus Diseases,* 581**,** 335-338.

Ignjatovic, J. & Sapats, S. 2000. Avian infectious bronchitis virus. *Rev Sci Tech,* 19**,** 493-508.

Inglis, S. C., Rolley, N. & Brierley, I. 1990. A ribosomal frameshift signal in the polymerase-encoding region of the ibv genome. *Adv Exp Med Biol,* 276**,** 269-73.

International Human Genome Sequencing, C. 2004. Finishing the euchromatic sequence of the human genome. *Nature,* 431**,** 931-45.

Isaacs, A. & Lindenmann, J. 1957. Virus interference. I. The interferon. *Proc R Soc Lond B Biol Sci,* 147**,** 258-67.

Ivashkiv, L. B. & Donlin, L. T. 2014. Regulation of type i interferon responses. *Nature Reviews Immunology,* 14**,** 36-49.

Jagger, B. W., Wise, H. M., Kash, J. C., Walters, K. A., Wills, N. M., Xiao, Y. L., Dunfee, R. L., Schwartzman, L. M., Ozinsky, A., Bell, G. L., Dalton, R. M., Lo, A., Efstathiou, S., Atkins, J. F., Firth, A. E., Taubenberger, J. K. & Digard, P. 2012. An overlapping protein-coding region in influenza a virus segment 3 modulates the host response. *Science,* 337**,** 199-204.

Jardetzky, T. S. & Lamb, R. A. 2004. Virology: A class act. *Nature,* 427**,** 307-8.

Jia, R., Pan, Q., Ding, S., Rong, L., Liu, S. L., Geng, Y., Qiao, W. & Liang, C. 2012. The n-terminal region of ifitm3 modulates its antiviral activity by regulating ifitm3 cellular localization. *J Virol,* 86**,** 13697-707.

Jia, R., Xu, F., Qian, J., Yao, Y., Miao, C., Zheng, Y. M., Liu, S. L., Guo, F., Geng, Y., Qiao, W. & Liang, C. 2014. Identification of an endocytic signal essential for the antiviral action of ifitm3. *Cell Microbiol,* 16**,** 1080-93.

Jiang, D., Weidner, J. M., Qing, M., Pan, X. B., Guo, H. T., Xu, C. X., Zhang, X. C., Birk, A., Chang, J. H., Shi, P. Y., Block, T. M. & Guo, J. T. 2010. Identification of five interferon-induced cellular proteins that inhibit west nile virus and dengue virus infections. *Journal of Virology,* 84**,** 8332-8341.

Jiang, X., Kinch, L. N., Brautigam, C. A., Chen, X., Du, F., Grishin, N. V. & Chen, Z. J. 2012. Ubiquitin-induced oligomerization of the rna sensors rig-i and mda5 activates antiviral innate immune response. *Immunity,* 36**,** 959-73.

John, S. P., Chin, C. R., Perreira, J. M., Feeley, E. M., Aker, A. M., Savidis, G., Smith, S. E., Elia, A. E., Everitt, A. R., Vora, M., Pertel, T., Elledge, S. J., Kellam, P. & Brass, A. L. 2013. The cd225 domain of ifitm3 is required for both ifitm protein association and inhibition of influenza a virus and dengue virus replication. *J Virol,* 87**,** 7837-52.

Johnson, C. A., Pekas, D. J. & Winzler, R. J. 1964. Neuraminidases and influenza virus infection in embryonated eggs. *Science,* 143**,** 1051-2.

Kamitani, W., Narayanan, K., Huang, C., Lokugamage, K., Ikegami, T., Ito, N., Kubo, H. & Makino, S. 2006. Severe acute respiratory syndrome coronavirus nsp1 protein suppresses host gene expression by promoting host mrna degradation. *Proceedings of the National Academy of Sciences of the United States of America,* 103**,** 12885-12890.

Kan, X. Z., Yang, J. K., Li, X. F., Chen, L., Lei, Z. P., Wang, M., Qian, C. J., Gao, H. & Yang, Z. Y. 2010. Phylogeny of major lineages of galliform birds (aves: Galliformes) based on complete mitochondrial genomes. *Genet Mol Res,* 9**,** 1625-33.

Kapczynski, D. R., Dorsey, K., Chrzastek, K., Moraes, M., Jackwood, M., Hilt, D. & Gardin, Y. 2016. Vaccine protection of turkeys against h5n1 highly pathogenic avian influenza virus with a recombinant turkey herpesvirus expressing the hemagglutinin gene of avian influenza. *Avian Dis,* 60**,** 413-7.

Karpala, A. J., Stewart, C., Mckay, J., Lowenthal, J. W. & Bean, A. G. D. 2011. Characterization of chicken mda5 activity: Regulation of ifn-beta in the absence of rig-i functionality. *Journal of Immunology,* 186**,** 5397-5405.

Kasaai, B., Gaumond, M. H. & Moffatt, P. 2013. Regulation of the bone-restricted ifitm-like (bril) gene transcription by sp and gli family members and cpg methylation. *J Biol Chem,* 288**,** 13278-94.

Kawai, T. & Akira, S. 2009. The roles of tlrs, rlrs and nlrs in pathogen recognition. *Int Immunol,* 21**,** 317-37.

Killip, M. J., Jackson, D., Perez-Cidoncha, M., Fodor, E. & Randall, R. E. 2017. Single-cell studies of ifn-beta promoter activation by wild-type and ns1-defective influenza a viruses. *J Gen Virol,* 98**,** 357-363.

Kim, T. K. & Eberwine, J. H. 2010. Mammalian cell transfection: The present and the future. *Anal Bioanal Chem,* 397**,** 3173-8.

Kint, J., Dickhout, A., Kutter, J., Maier, H. J., Britton, P., Koumans, J., Pijlman, G. P., Fros, J. J., Wiegertjes, G. F. & Forlenza, M. 2015. Infectious bronchitis coronavirus inhibits stat1 signaling and requires accessory proteins for resistance to type i interferon activity. *Journal of Virology,* 89**,** 12047-12057.

Kint, J., Langereis, M. A., Maier, H. J., Britton, P., Van Kuppeveld, F. J., Koumans, J., Wiegertjes, G. F. & Forlenza, M. 2016. Infectious bronchitis coronavirus limits interferon production by inducing a host shutoff that requires accessory protein 5b. *J Virol,* 90**,** 7519-7528.

Klumperman, J., Locker, J. K., Meijer, A., Horzinek, M. C., Geuze, H. J. & Rottier, P. J. 1994. Coronavirus m proteins accumulate in the golgi complex beyond the site of virion budding. *J Virol,* 68**,** 6523-34.

Kotenko, S. V., Gallagher, G., Baurin, V. V., Lewis-Antes, A., Shen, M. L., Shah, N. K., Langer, J. A., Sheikh, F., Dickensheets, H. & Donnelly, R. P. 2003. Ifn-lambda s mediate antiviral protection through a distinct class ii cytokine receptor complex. *Nature Immunology,* 4**,** 69-77.

Kuniyoshi, K., Takeuchi, O., Pandey, S., Satoh, T., Iwasaki, H., Akira, S. & Kawai, T. 2014. Pivotal role of rna-binding e3 ubiquitin ligase mex3c in rig-i-mediated antiviral innate immunity. *Proceedings of the National Academy of Sciences of the United States of America,* 111**,** 5646-5651.

Lai, M. M. & Cavanagh, D. 1997. The molecular biology of coronaviruses. *Adv Virus Res,* 48**,** 1-100.

Lamb, R. A. & Choppin, P. W. 1981. Identification of a second protein (m2) encoded by rna segment 7 of influenza virus. *Virology,* 112**,** 729-37.

Lamb, R. A. & Lai, C. J. 1980. Sequence of interrupted and uninterrupted mrnas and cloned DNA coding for the two overlapping nonstructural proteins of influenza virus. *Cell,* 21**,** 475-85.

Lange, U. C., Adams, D. J., Lee, C., Barton, S., Schneider, R., Bradley, A. & Surani, M. A. 2008. Normal germ line establishment in mice carrying a deletion of the ifitm/fragilis gene family cluster. *Mol Cell Biol,* 28**,** 4688-96.

Laver, W. G. & Valentine, R. C. 1969. Morphology of the isolated hemagglutinin and neuraminidase subunits of influenza virus. *Virology,* 38**,** 105-19.

Lee, C. W., Brown, C. & Jackwood, M. W. 2002. Tissue distribution of avian infectious bronchitis virus following in ovo inoculation of chicken embryos examined by in situ hybridization with antisense digoxigenin-labeled universal riboprobe. *J Vet Diagn Invest,* 14**,** 377-81.

Levy, D., Larner, A., Chaudhuri, A., Babiss, L. E. & Darnell, J. E., Jr. 1986. Interferon-stimulated transcription: Isolation of an inducible gene and identification of its regulatory region. *Proc Natl Acad Sci U S A,* 83**,** 8929-33.

Li, K., Markosyan, R. M., Zheng, Y. M., Golfetto, O., Bungart, B., Li, M., Ding, S., He, Y., Liang, C., Lee, J. C., Gratton, E., Cohen, F. S. & Liu, S. L. 2013. Ifitm proteins restrict viral membrane hemifusion. *PLoS Pathog,* 9**,** e1003124.

Li, L. H., Sen, A., Murphy, S. P., Jahreis, G. P., Fuji, H. & Hui, S. W. 1999. Apoptosis induced by DNA uptake limits transfection efficiency. *Exp Cell Res,* 253**,** 541-50.

Li, P., Shi, M. L., Shen, W. L., Zhang, Z., Xie, D. J., Zhang, X. Y., He, C., Zhang, Y. & Zhao, Z. H. 2017. Coordinated regulation of ifitm1, 2 and 3 genes by an ifn-responsive enhancer through long-range chromatin interactions. *Biochim Biophys Acta,* 1860**,** 885-893.

Li, Y. G., Siripanyaphinyo, U., Tumkosit, U., Noranate, N., A, A. N., Pan, Y., Kameoka, M., Kurosu, T., Ikuta, K., Takeda, N. & Anantapreecha, S. 2012. Poly (i:C), an agonist of toll-like receptor-3, inhibits replication of the chikungunya virus in beas-2b cells. *Virol J,* 9**,** 114.

Lim, K. P. & Liu, D. X. 1998. Characterization of the two overlapping papain-like proteinase domains encoded in gene 1 of the coronavirus infectious bronchitis virus and determination of the c-terminal cleavage site of an 87-kda protein. *Virology,* 245**,** 303-12.

Lim, K. P. & Liu, D. X. 2001. The missing link in coronavirus assembly - retention of the avian coronavirus infectious bronchitis virus envelope protein in the pre-golgi compartments and physical interaction between the envelope and membrane proteins. *Journal of Biological Chemistry,* 276**,** 17515-17523.

Lin, T. Y., Chin, C. R., Everitt, A. R., Clare, S., Perreira, J. M., Savidis, G., Aker, A. M., John, S. P., Sarlah, D., Carreira, E. M., Elledge, S. J., Kellam, P. & Brass, A. L. 2013. Amphotericin b increases influenza a virus infection by preventing ifitm3-mediated restriction. *Cell Rep,* 5**,** 895-908.

Ling, S., Zhang, C., Wang, W., Cai, X., Yu, L., Wu, F., Zhang, L. & Tian, C. 2016. Combined approaches of epr and nmr illustrate only one transmembrane helix in the human ifitm3. *Sci Rep,* 6**,** 24029.

Liu, Y., Liu, H., Titus, L. & Boden, S. D. 2012. Natural antisense transcripts enhance bone formation by increasing sense ifitm5 transcription. *Bone,* 51**,** 933-8.

Loo, Y. M. & Gale, M., Jr. 2011. Immune signaling by rig-i-like receptors. *Immunity,* 34**,** 680-92.

Lopez-Rodriguez, M., Herrera-Ramos, E., Sole-Violan, J., Ruiz-Hernandez, J. J., Borderias, L., Horcajada, J. P., Lerma-Chippirraz, E., Rajas, O., Briones, M., Perez-Gonzalez, M. C., Garcia-Bello, M. A., Lopez-Granados, E., Rodriguez De Castro, F. & Rodriguez-Gallego, C. 2016. Ifitm3 and severe influenza virus infection. No evidence of genetic association. *Eur J Clin Microbiol Infect Dis,* 35**,** 1811-1817.

Lu, J., Pan, Q., Rong, L., He, W., Liu, S. L. & Liang, C. 2011. The ifitm proteins inhibit hiv-1 infection. *J Virol,* 85**,** 2126-37.

Lu, Y., Zuo, Q., Zhang, Y., Wang, Y., Li, T. & Han, J. 2017. The expression profile of ifitm family gene in rats. *Intractable Rare Dis Res,* 6**,** 274-280.

Ludwig, S., Pleschka, S. & Wolff, T. 1999. A fatal relationship--influenza virus interactions with the host cell. *Viral Immunol,* 12**,** 175-96.

Ludwig, S., Wang, X. Y., Ehrhardt, C., Zheng, H. Y., Donelan, N., Planz, O., Pleschka, S., Garcia-Sastre, A., Heins, G. & Wolff, T. 2002. The influenza a virus ns1 protein inhibits activation of jun n-terminal kinase and ap-1 transcription factors. *Journal of Virology,* 76**,** 11166-11171.

Luytjes, W., Krystal, M., Enami, M., Parvin, J. D. & Palese, P. 1989. Amplification, expression, and packaging of foreign gene by influenza virus. *Cell,* 59**,** 1107-13.

Lv, J., Wei, L., Yang, Y., Wang, B., Liang, W., Gao, Y., Xia, X., Gao, L., Cai, Y., Hou, P., Yang, H., Wang, A., Huang, R., Gao, J. & Chai, T. 2015. Amino acid substitutions in the neuraminidase protein of an h9n2 avian influenza virus affect its airborne transmission in chickens. *Vet Res,* 46**,** 44.

Maier, H. J., Cottam, E. M., Stevenson-Leggett, P., Wilkinson, J. A., Harte, C. J., Wileman, T. & Britton, P. 2013a. Visualizing the autophagy pathway in avian cells and its application to studying infectious bronchitis virus. *Autophagy,* 9**,** 496-509.

Maier, H. J., Hawes, P. C., Cottam, E. M., Mantell, J., Verkade, P., Monaghan, P., Wileman, T. & Britton, P. 2013b. Infectious bronchitis virus generates spherules from zippered endoplasmic reticulum membranes. *MBio,* 4**,** e00801-13.

Makino, S., Joo, M. & Makino, J. K. 1991. A system for study of coronavirus mrna synthesis: A regulated, expressed subgenomic defective interfering rna results from intergenic site insertion. *J Virol,* 65**,** 6031-41.

Makvandi-Nejad, S., Laurenson-Schafer, H., Wang, L., Wellington, D., Zhao, Y., Jin, B., Qin, L., Kite, K., Moghadam, H. K., Song, C., Clark, K., Hublitz, P., Townsend, A. R., Wu, H., Mcmichael, A. J., Zhang, Y. & Dong, T. 2018. Lack of truncated ifitm3 transcripts in cells homozygous for the rs12252-c variant that is associated with severe influenza infection. *J Infect Dis,* 217**,** 257-262.

Malathi, K., Dong, B., Gale, M., Jr. & Silverman, R. H. 2007. Small self-rna generated by rnase l amplifies antiviral innate immunity. *Nature,* 448**,** 816-9.

Marini, J. C., Reich, A. & Smith, S. M. 2014. Osteogenesis imperfecta due to mutations in non-collagenous genes: Lessons in the biology of bone formation. *Curr Opin Pediatr,* 26**,** 500-7.

Masters, P. S. 2006. The molecular biology of coronaviruses. *Advances in Virus Research, Vol 66,* 66**,** 193-292.

Maurisse, R., De Semir, D., Emamekhoo, H., Bedayat, B., Abdolmohammadi, A., Parsi, H. & Gruenert, D. C. 2010. Comparative transfection of DNA into primary and transformed mammalian cells from different lineages. *BMC Biotechnol,* 10**,** 9.

Mcgeoch, D., Fellner, P. & Newton, C. 1976. Influenza virus genome consists of eight distinct rna species. *Proc Natl Acad Sci U S A,* 73**,** 3045-9.

Mcmichael, T. M., Zhang, L., Chemudupati, M., Hach, J. C., Kenney, A. D., Hang, H. C. & Yount, J. S. 2017. The palmitoyltransferase zdhhc20 enhances interferon-induced transmembrane protein 3 (ifitm3) palmitoylation and antiviral activity. *J Biol Chem,* 292**,** 21517-21526.

Mehrbod, P., Eybpoosh, S., Fotouhi, F., Shokouhi Targhi, H., Mazaheri, V. & Farahmand, B. 2017. Association of ifitm3 rs12252 polymorphisms, bmi, diabetes, and hypercholesterolemia with mild flu in an iranian population. *Virol J,* 14**,** 218.

Meir, R., Rosenblut, E., Perl, S., Kass, N., Ayali, G., Perk, S. & Hemsani, E. 2004. Identification of a novel nephropathogenic infectious bronchitis virus in israel. *Avian Dis,* 48**,** 635-41.

Mellacheruvu, D., Wright, Z., Couzens, A. L., Lambert, J. P., St-Denis, N. A., Li, T., Miteva, Y. V., Hauri, S., Sardiu, M. E., Low, T. Y., Halim, V. A., Bagshaw, R. D., Hubner, N. C., Al-

Hakim, A., Bouchard, A., Faubert, D., Fermin, D., Dunham, W. H., Goudreault, M., Lin, Z. Y., Badillo, B. G., Pawson, T., Durocher, D., Coulombe, B., Aebersold, R., Superti-Furga, G., Colinge, J., Heck, A. J., Choi, H., Gstaiger, M., Mohammed, S., Cristea, I. M., Bennett, K. L., Washburn, M. P., Raught, B., Ewing, R. M., Gingras, A. C. & Nesvizhskii, A. I. 2013. The crapome: A contaminant repository for affinity purification-mass spectrometry data. *Nat Methods,* 10**,** 730-6.

Meng, Z., Zhang, X., Wu, J., Pei, R., Xu, Y., Yang, D., Roggendorf, M. & Lu, M. 2013. Rnai induces innate immunity through multiple cellular signaling pathways. *PLoS One,* 8**,** e64708.

Meulemans, G., Carlier, M. C., Gonze, M., Petit, P. & Vandenbroeck, M. 1987. Incidence, characterisation and prophylaxis of nephropathogenic avian infectious bronchitis viruses. *Vet Rec,* 120**,** 205-6.

Mibayashi, M., Martinez-Sobrido, L., Loo, Y. M., Cardenas, W. B., Gale, M. & Garcia-Sastre, A. 2007. Inhibition of retinoic acid-inducible gene i-mediated induction of beta interferon by the ns1 protein of influenza a virus. *Journal of Virology,* 81**,** 514-524.

Mills, T. C., Rautanen, A., Elliott, K. S., Parks, T., Naranbhai, V., Ieven, M. M., Butler, C. C., Little, P., Verheij, T., Garrard, C. S., Hinds, C., Goossens, H., Chapman, S. & Hill, A. V. 2014. Ifitm3 and susceptibility to respiratory viral infections in the community. *J Infect Dis,* 209**,** 1028-31.

Moeller, A., Kirchdoerfer, R. N., Potter, C. S., Carragher, B. & Wilson, I. A. 2012. Organization of the influenza virus replication machinery. *Science,* 338**,** 1631-4.

Moffatt, P., Gaumond, M. H., Salois, P., Sellin, K., Bessette, M. C., Godin, E., De Oliveira, P. T., Atkins, G. J., Nanci, A. & Thomas, G. 2008. Bril: A novel bone-specific modulator of mineralization. *J Bone Miner Res,* 23**,** 1497-508.

Mogensen, T. H. 2009. Pathogen recognition and inflammatory signaling in innate immune defenses. *Clin Microbiol Rev,* 22**,** 240-73, Table of Contents.

Mosley, V. M. & Wyckoff, R. W. 1946. Electron micrography of the virus of influenza. *Nature,* 157**,** 263.

Mudhasani, R., Tran, J. P., Retterer, C., Radoshitzky, S. R., Kota, K. P., Altamura, L. A., Smith, J. M., Packard, B. Z., Kuhn, J. H., Costantino, J., Garrison, A. R., Schmaljohn, C. S., Huang, I. C., Farzan, M. & Bavari, S. 2013. Ifitm-2 and ifitm-3 but not ifitm-1 restrict rift valley fever virus. *J Virol,* 87**,** 8451-64.

Murray, J. 2016. On the 150(th) anniversary of darwin's submission of one of his "five great books", the variation of animals and plants under domestication. 12.

Nan, Y., Nan, G. & Zhang, Y. J. 2014. Interferon induction by rna viruses and antagonism by viral pathogens. *Viruses,* 6**,** 4999-5027.

Narayana, S. K., Helbig, K. J., Mccartney, E. M., Eyre, N. S., Bull, R. A., Eltahla, A., Lloyd, A. R. & Beard, M. R. 2015. The interferon-induced transmembrane proteins, ifitm1, ifitm2, and ifitm3 inhibit hepatitis c virus entry. *J Biol Chem,* 290**,** 25946-59.

Narayanan, K., Maeda, A., Maeda, J. & Makino, S. 2000. Characterization of the coronavirus m protein and nucleocapsid interaction in infected cells. *Journal of Virology,* 74**,** 8127-8134.

Neuman, B. W., Kiss, G., Kunding, A. H., Bhella, D., Baksh, M. F., Connelly, S., Droese, B., Klaus, J. P., Makino, S., Sawicki, S. G., Siddell, S. G., Stamou, D. G., Wilson, I. A., Kuhn, P. & Buchmeier, M. J. 2011. A structural analysis of m protein in coronavirus assembly and morphology. *Journal of Structural Biology,* 174**,** 11-22.

O'neill, R. E., Talon, J. & Palese, P. 1998. The influenza virus nep (ns2 protein) mediates the nuclear export of viral ribonucleoproteins. *EMBO J,* 17**,** 288-96.

Okuzaki, Y., Kidani, S., Kaneoka, H., Iijima, S. & Nishijima, K. I. 2017. Characterization of chicken interferon-inducible transmembrane protein-10. *Biosci Biotechnol Biochem,* 81**,** 914-921.

Oostra, M., Te Lintelo, E. G., Deijs, M., Verheije, M. H., Rottier, P. J. & De Haan, C. A. 2007. Localization and membrane topology of coronavirus nonstructural protein 4: Involvement of the early secretory pathway in replication. *J Virol,* 81**,** 12323-36.

Oshiumi, H., Matsumoto, M., Hatakeyama, S. & Seya, T. 2009. Riplet/rnf135, a ring finger protein, ubiquitinates rig-i to promote interferon-beta induction during the early phase of viral infection. *Journal of Biological Chemistry,* 284**,** 807-817.

Pan, Y., Yang, P., Dong, T., Zhang, Y., Shi, W., Peng, X., Cui, S., Zhang, D., Lu, G., Liu, Y., Wu, S. & Wang, Q. 2017. Ifitm3 rs12252-c variant increases potential risk for severe influenza virus infection in chinese population. *Front Cell Infect Microbiol,* 7**,** 294.

Perlman, S. & Netland, J. 2009. Coronaviruses post-sars: Update on replication and pathogenesis. *Nat Rev Microbiol,* 7**,** 439-50.

Perozo, F., Villegas, A. P., Fernandez, R., Cruz, J. & Pritchard, N. 2009. Efficacy of single dose recombinant herpesvirus of turkey infectious bursal disease virus (ibdv) vaccination against a variant ibdv strain. *Avian Dis,* 53**,** 624-8.

Pichlmair, A., Schulz, O., Tan, C. P., Näslund, T. I., Liljeström, P., Weber, F. & Reis E Sousa, C. 2006. Rig-i-mediated antiviral responses to single-stranded rna bearing 5'-phosphates. *Science,* 314**,** 997-1001.

Pielak, R. M. & Chou, J. J. 2011. Influenza m2 proton channels. *Biochim Biophys Acta,* 1808**,** 522-9.

Platanias, L. C. 2005. Mechanisms of type-i- and type-ii-interferon-mediated signalling. *Nat Rev Immunol,* 5**,** 375-86.

Pleschka, S. 2013. Overview of influenza viruses. *Swine Influenza,* 370**,** 1-20.

Poddar, S., Hyde, J. L., Gorman, M. J., Farzan, M. & Diamond, M. S. 2016. The interferon-stimulated gene ifitm3 restricts infection and pathogenesis of arthritogenic and encephalitic alphaviruses. *Journal of Virology,* 90**,** 8780-8794.

Poon, L. L., Pritlove, D. C., Sharps, J. & Brownlee, G. G. 1998. The rna polymerase of influenza virus, bound to the 5' end of virion rna, acts in cis to polyadenylate mrna. *J Virol,* 72**,** 8214-9.

Portela, A. & Digard, P. 2002. The influenza virus nucleoprotein: A multifunctional rna-binding protein pivotal to virus replication. *J Gen Virol,* 83**,** 723-34.

Prasad, L. B. 1979. Turkey herpesvirus and marek's disease virus. A comparative appraisal. *Comp Immunol Microbiol Infect Dis,* 2**,** 335-58.

Promkuntod, N., Van Eijndhoven, R. E., De Vrieze, G., Grone, A. & Verheije, M. H. 2014. Mapping of the receptor-binding domain and amino acids critical for attachment in the spike protein of avian coronavirus infectious bronchitis virus. *Virology,* 448**,** 26-32.

Qi, X., Liu, C., Li, R., Zhang, H., Xu, X. & Wang, J. 2017. Modulation of the innate immune-related genes expression in h9n2 avian influenza virus-infected chicken macrophage-like cells (hd11) in response to escherichia coli lps stimulation. *Res Vet Sci,* 111**,** 36-42.

Qu, H., Yang, L., Meng, S., Xu, L., Bi, Y., Jia, X., Li, J., Sun, L. & Liu, W. 2013. The differential antiviral activities of chicken interferon alpha (chifn-alpha) and chifn-beta are related to distinct interferon-stimulated gene expression. *PLoS One,* 8**,** e59307.

Rajsbaum, R., Albrecht, R. A., Wang, M. K., Maharaj, N. P., Versteeg, G. A., Nistal-Villan, E., Garcia-Sastre, A. & Gack, M. U. 2012. Species-specific inhibition of rig-i ubiquitination and ifn induction by the influenza a virus ns1 protein. *Plos Pathogens,* 8.

Randall, R. E. & Goodbourn, S. 2008. Interferons and viruses: An interplay between induction, signalling, antiviral responses and virus countermeasures. *Journal of General Virology,* 89**,** 1-47.

Ranjbar, S., Haridas, V., Jasenosky, L. D., Falvo, J. V. & Goldfeld, A. E. 2015. A role for ifitm proteins in restriction of mycobacterium tuberculosis infection. *Cell Rep,* 13**,** 874-83.

Rauw, F., Palya, V., Gardin, Y., Tatar-Kis, T., Dorsey, K. M., Lambrecht, B. & Van Den Berg, T. 2012. Efficacy of rhvt-ai vector vaccine in broilers with passive immunity against challenge with two antigenically divergent egyptian clade 2.2.1 hpai h5n1 strains. *Avian Dis,* 56**,** 913-22.

Rehwinkel, J., Tan, C. P., Goubau, D., Schulz, O., Pichlmair, A., Bier, K., Robb, N., Vreede, F., Barclay, W., Fodor, E. & Sousa, C. R. E. 2010. Rig-i detects viral genomic rna during negative-strand rna virus infection. *Cell,* 140**,** 397-U143.

Robb, N. C., Smith, M., Vreede, F. T. & Fodor, E. 2009. Ns2/nep protein regulates transcription and replication of the influenza virus rna genome. *J Gen Virol,* 90**,** 1398-407.

Roberts, A., Maclean, G. L., Newman, K., Lockwood, G. & Roberts, A. 1985. *Roberts' birds of southern africa,* Cape Town, Trustees of the J. Voelcker Bird Book Fund.

Robertson, J. S., Schubert, M. & Lazzarini, R. A. 1981. Polyadenylation sites for influenza virus mrna. *J Virol,* 38**,** 157-63.

Rohde, F., Schusser, B., Hron, T., Farkasova, H., Plachy, J., Hartle, S., Hejnar, J., Elleder, D. & Kaspers, B. 2018. Characterization of chicken tumor necrosis factor-alpha, a long missed cytokine in birds. *Front Immunol,* 9**,** 605.

Romanov, M. N., Tuttle, E. M., Houck, M. L., Modi, W. S., Chemnick, L. G., Korody, M. L., Mork, E. M. S., Otten, C. A., Renner, T., Jones, K. C., Dandekar, S., Papp, J. C., Da, Y., Green, E. D., Magrini, V., Hickenbotham, M. T., Glasscock, J., Mcgrath, S., Mardis, E. R., Ryder, O. A. & Progra, N. C. S. 2009. The value of avian genomics to the conservation of wildlife. *Bmc Genomics,* 10.

Rossman, J. S., Leser, G. P. & Lamb, R. A. 2012. Filamentous influenza virus enters cells via macropinocytosis. *J Virol,* 86**,** 10950-60.

Ruch, T. R. & Machamer, C. E. 2011. The hydrophobic domain of infectious bronchitis virus e protein alters the host secretory pathway and is important for release of infectious virus. *Journal of Virology,* 85**,** 675-685.

Ruch, T. R. & Machamer, C. E. 2012. The coronavirus e protein: Assembly and beyond. *Viruses-Basel,* 4**,** 363-382.

Salmon Farm Science. 2012. *Efficient use of limited resources* [Online]. Available: https://salmonfarmscience.wordpress.com/2012/03/04/efficient-use-of-limited-resources/ [Accessed 1st June 2018].

Santhakumar, D., Rubbenstroth, D., Martinez-Sobrido, L. & Munir, M. 2017. Avian interferons and their antiviral effectors. *Frontiers in Immunology,* 8.

Satoh, T., Kato, H., Kumagai, Y., Yoneyama, M., Sato, S., Matsushita, K., Tsujimura, T., Fujita, T., Akira, S. & Takeuchi, O. 2010. Lgp2 is a positive regulator of rig-i- and mda5-mediated antiviral responses. *Proceedings of the National Academy of Sciences of the United States of America,* 107**,** 1512-1517.

Sawai, H., Kim, H. L., Kuno, K., Suzuki, S., Gotoh, H., Takada, M., Takahata, N., Satta, Y. & Akishinonomiya, F. 2010. The origin and genetic variation of domestic chickens with special reference to junglefowls gallus g. Gallus and g. Varius. *PLoS One,* 5**,** e10639.

Sawicki, S. G., Sawicki, D. L. & Siddell, S. G. 2007. A contemporary view of coronavirus transcription. *J Virol,* 81**,** 20-9.

Schindler, C., Fu, X. Y., Improta, T., Aebersold, R. & Darnell, J. E. 1992. Proteins of transcription factor isgf-3 - one gene encodes the 91-kda and 84-kda isgf-3 proteins that are activated by interferon-alpha. *Proceedings of the National Academy of Sciences of the United States of America,* 89**,** 7836-7839.

Schirmer, M., Ijaz, U. Z., D'amore, R., Hall, N., Sloan, W. T. & Quince, C. 2015. Insight into biases and sequencing errors for amplicon sequencing with the illumina miseq platform. *Nucleic Acids Research,* 43.

Schneider, W. M., Chevillotte, M. D. & Rice, C. M. 2014. Interferon-stimulated genes: A complex web of host defenses. *Annu Rev Immunol,* 32**,** 513-45.

Schoenborn, J. R. & Wilson, C. B. 2007. Regulation of interferon-gamma during innate and adaptive immune responses. *Adv Immunol,* 96**,** 41-101.

Schoggins, J. W., Wilson, S. J., Panis, M., Murphy, M. Y., Jones, C. T., Bieniasz, P. & Rice, C. M. 2011. A diverse range of gene products are effectors of the type i interferon antiviral response. *Nature,* 472**,** 481-5.

Schrauwen, E. J. & Fouchier, R. A. 2014. Host adaptation and transmission of influenza a viruses in mammals. *Emerg Microbes Infect,* 3**,** e9.

Schultz, U., Kaspers, B., Rinderle, C., Sekellick, M. J., Marcus, P. I. & Staeheli, P. 1995a. Recombinant chicken interferon: A potent antiviral agent that lacks intrinsic macrophage activating factor activity. *Eur J Immunol,* 25**,** 847-51.

Schultz, U., Rinderle, C., Sekellick, M. J., Marcus, P. I. & Staeheli, P. 1995b. Recombinant chicken interferon from escherichia coli and transfected cos cells is biologically active. *Eur J Biochem,* 229**,** 73-6.

Schultze, B., Cavanagh, D. & Herrler, G. 1992. Neuraminidase treatment of avian infectious-bronchitis coronavirus reveals a hemagglutinating activity that is dependent on sialic acid-containing receptors on erythrocytes. *Virology,* 189**,** 792-794.

Sekellick, M. J., Lowenthal, J. W., O'neil, T. E. & Marcus, P. I. 1998. Chicken interferon types i and ii enhance synergistically the antiviral state and nitric oxide secretion. *J Interferon Cytokine Res,* 18**,** 407-14.

Selman, M., Dankar, S. K., Forbes, N. E., Jia, J. J. & Brown, E. G. 2012. Adaptive mutation in influenza a virus non-structural gene is linked to host switching and induces a novel protein by alternative splicing. *Emerg Microbes Infect,* 1**,** e42.

Setta, A., Barrow, P. A., Kaiser, P. & Jones, M. A. 2012. Immune dynamics following infection of avian macrophages and epithelial cells with typhoidal and non-typhoidal salmonella enterica serovars; bacterial invasion and persistence, nitric oxide and oxygen production, differential host gene expression, nf-kappab signalling and cell cytotoxicity. *Vet Immunol Immunopathol,* 146**,** 212-24.

Seybert, A., Posthuma, C. C., Van Dinten, L. C., Snijder, E. J., Gorbalenya, A. E. & Ziebuhr, J. 2005. A complex zinc finger controls the enzymatic activities of nidovirus helicases. *J Virol,* 79**,** 696-704.

Shan, Z., Han, Q., Nie, J., Cao, X., Chen, Z., Yin, S., Gao, Y., Lin, F., Zhou, X., Xu, K., Fan, H., Qian, Z., Sun, B., Zhong, J., Li, B. & Tsun, A. 2013. Negative regulation of interferon-induced transmembrane protein 3 by set7-mediated lysine monomethylation. *J Biol Chem,* 288**,** 35093-103.

Shapira, S. D., Gat-Viks, I., Shum, B. O., Dricot, A., De Grace, M. M., Wu, L., Gupta, P. B., Hao, T., Silver, S. J., Root, D. E., Hill, D. E., Regev, A. & Hacohen, N. 2009. A physical and regulatory map of host-influenza interactions reveals pathways in h1n1 infection. *Cell,* 139**,** 1255-67.

Sharifi Tabar, M., Hesaraki, M., Esfandiari, F., Sahraneshin Samani, F., Vakilian, H. & Baharvand, H. 2015. Evaluating electroporation and lipofectamine approaches for transient and stable transgene expressions in human fibroblasts and embryonic stem cells. *Cell J,* 17**,** 438-50.

Shih, S. R., Suen, P. C., Chen, Y. S. & Chang, S. C. 1998. A novel spliced transcript of influenza a/wsn/33 virus. *Virus Genes,* 17**,** 179-83.

Shtyrya, Y. A., Mochalova, L. V. & Bovin, N. V. 2009. Influenza virus neuraminidase: Structure and function. *Acta Naturae,* 1**,** 26-32.

Shuai, K., Schindler, C., Prezioso, V. R. & Darnell, J. E., Jr. 1992. Activation of transcription by ifn-gamma: Tyrosine phosphorylation of a 91-kd DNA binding protein. *Science,* 258**,** 1808-12.

Siegrist, F., Ebeling, M. & Certa, U. 2011. The small interferon-induced transmembrane genes and proteins. *J Interferon Cytokine Res,* 31**,** 183-97.

Skehel, J. J. & Wiley, D. C. 2000. Receptor binding and membrane fusion in virus entry: The influenza hemagglutinin. *Annu Rev Biochem,* 69**,** 531-69.

Smith, J., Smith, N., Yu, L., Paton, I. R., Gutowska, M. W., Forrest, H. L., Danner, A. F., Seiler, J. P., Digard, P., Webster, R. G. & Burt, D. W. 2015. A comparative analysis of host responses to avian influenza infection in ducks and chickens highlights a role for the interferon-induced transmembrane proteins in viral resistance. *BMC Genomics,* 16**,** 574.

Smith, S. E., Gibson, M. S., Wash, R. S., Ferrara, F., Wright, E., Temperton, N., Kellam, P. & Fife, M. 2013. Chicken interferon-inducible transmembrane protein 3 restricts influenza viruses and lyssaviruses in vitro. *J Virol,* 87**,** 12957-66.

Snijder, E. J. & Meulenberg, J. J. 1998. The molecular biology of arteriviruses. *J Gen Virol,* 79 (Pt 5)**,** 961-79.

Staeheli, P., Danielson, P., Haller, O. & Sutcliffe, J. G. 1986. Transcriptional activation of the mouse mx gene by type i interferon. *Mol Cell Biol,* 6**,** 4770-4.

Stetson, D. B. & Medzhitov, R. 2006. Type i interferons in host defense. *Immunity,* 25**,** 373-81.

Strobel, M. C. & Abelson, J. 1986. Effect of intron mutations on processing and function of saccharomyces cerevisiae sup53 trna in vitro and in vivo. *Mol Cell Biol,* 6**,** 2663-73.

Sun, X., Zeng, H., Kumar, A., Belser, J. A., Maines, T. R. & Tumpey, T. M. 2016. Constitutively expressed ifitm3 protein in human endothelial cells poses an early infection block to human influenza viruses. *J Virol,* 90**,** 11157-11167.

Takahasi, K., Yoneyama, M., Nishihori, T., Hirai, R., Kumeta, H., Narita, R., Gale, M., Inagaki, F. & Fujita, T. 2008. Nonself rna-sensing mechanism of rig-i helicase and activation of antiviral immune responses. *Molecular Cell,* 29**,** 428-440.

Takeuchi, O. & Akira, S. 2010. Pattern recognition receptors and inflammation. *Cell,* 140**,** 805-20.

Talal, N. 1971. The diverse biological effects of polyinosinic-polycytidylic acid. *Agents Actions,* 2**,** 45-9.

Talon, J., Horvath, C. M., Polley, R., Basler, C. F., Muster, T., Palese, P. & Garcia-Sastre, A. 2000. Activation of interferon regulatory factor 3 is inhibited by the influenza a virus ns1 protein. *Journal of Virology,* 74**,** 7989-7996.

Tan, Y. W., Fung, T. S., Shen, H., Huang, M. & Liu, D. X. 2018. Coronavirus infectious bronchitis virus non-structural proteins 8 and 12 form stable complex independent of the non-translated regions of viral rna and other viral proteins. *Virology,* 513**,** 75-84.

Tanaka, S. S., Yamaguchi, Y. L., Tsoi, B., Lickert, H. & Tam, P. P. 2005. Ifitm/mil/fragilis family proteins ifitm1 and ifitm3 play distinct roles in mouse primordial germ cell homing and repulsion. *Dev Cell,* 9**,** 745-56.

Tartour, K., Appourchaux, R., Gaillard, J., Nguyen, X. N., Durand, S., Turpin, J., Beaumont, E., Roch, E., Berger, G., Mahieux, R., Brand, D., Roingeard, P. & Cimarelli, A. 2014. Ifitm proteins are incorporated onto hiv-1 virion particles and negatively imprint their infectivity. *Retrovirology,* 11**,** 103.

Tenoever, B. R. 2016. The evolution of antiviral defense systems. *Cell Host & Microbe,* 19**,** 142-149.

Terregino, C., Toffan, A., Beato, M. S., De Nardi, R., Vascellari, M., Meini, A., Ortali, G., Mancin, M. & Capua, I. 2008. Pathogenicity of a qx strain of infectious bronchitis virus in specific pathogen free and commercial broiler chickens, and evaluation of

protection induced by a vaccination programme based on the ma5 and 4/91 serotypes. *Avian Pathol,* 37**,** 487-93.
Thiel, V. 2007. *Coronaviruses : Molecular and cellular biology*.
Tong, S., Li, Y., Rivailler, P., Conrardy, C., Castillo, D. A., Chen, L. M., Recuenco, S., Ellison, J. A., Davis, C. T., York, I. A., Turmelle, A. S., Moran, D., Rogers, S., Shi, M., Tao, Y., Weil, M. R., Tang, K., Rowe, L. A., Sammons, S., Xu, X., Frace, M., Lindblade, K. A., Cox, N. J., Anderson, L. J., Rupprecht, C. E. & Donis, R. O. 2012. A distinct lineage of influenza a virus from bats. *Proc Natl Acad Sci U S A,* 109**,** 4269-74.
Tong, S., Zhu, X., Li, Y., Shi, M., Zhang, J., Bourgeois, M., Yang, H., Chen, X., Recuenco, S., Gomez, J., Chen, L. M., Johnson, A., Tao, Y., Dreyfus, C., Yu, W., Mcbride, R., Carney, P. J., Gilbert, A. T., Chang, J., Guo, Z., Davis, C. T., Paulson, J. C., Stevens, J., Rupprecht, C. E., Holmes, E. C., Wilson, I. A. & Donis, R. O. 2013. New world bats harbor diverse influenza a viruses. *PLoS Pathog,* 9**,** e1003657.
Tsukamoto, T., Li, X., Morita, H., Minowa, T., Aizawa, T., Hanagata, N. & Demura, M. 2013. Role of s-palmitoylation on ifitm5 for the interaction with fkbp11 in osteoblast cells. *PLoS One,* 8**,** e75831.
Tyanova, S., Temu, T., Sinitcyn, P., Carlson, A., Hein, M. Y., Geiger, T., Mann, M. & Cox, J. 2016. The perseus computational platform for comprehensive analysis of (prote)omics data. *Nature Methods,* 13**,** 731-740.
Uchikawa, E., Lethier, M., Malet, H., Brunel, J., Gerlier, D. & Cusack, S. 2016. Structural analysis of dsrna binding to anti-viral pattern recognition receptors lgp2 and mda5. *Mol Cell,* 62**,** 586-602.
United Nations. 2015. *World population projected to reach 9.7 billion by 2050* [Online]. Available: http://www.un.org/en/development/desa/news/population/2015-report.html [Accessed 1st June 2018].
Van Marle, G., Dobbe, J. C., Gultyaev, A. P., Luytjes, W., Spaan, W. J. M. & Snijder, E. J. 1999. Arterivirus discontinuous mrna transcription is guided by base pairing between sense and antisense transcription-regulating sequences. *Proceedings of the National Academy of Sciences of the United States of America,* 96**,** 12056-12061.
Van Vliet, A. L., Smits, S. L., Rottier, P. J. & De Groot, R. J. 2002. Discontinuous and non-discontinuous subgenomic rna transcription in a nidovirus. *EMBO J,* 21**,** 6571-80.
Vandermost, R. G., Degroot, R. J., Luytjes, W. & Spaan, W. J. M. 1993. Coronavirus di rnas - a tool to study replication, transcription and recombination. *Journal of Cellular Biochemistry***,** 4-4.
Vandesompele, J., De Preter, K., Pattyn, F., Poppe, B., Van Roy, N., De Paepe, A. & Speleman, F. 2002. Accurate normalization of real-time quantitative rt-pcr data by geometric averaging of multiple internal control genes. *Genome Biology,* 3.
Varga, Z. T., Grant, A., Manicassamy, B. & Palese, P. 2012. Influenza virus protein pb1-f2 inhibits the induction of type i interferon by binding to mavs and decreasing mitochondrial membrane potential. *Journal of Virology,* 86**,** 8359-8366.
Veit Hornung, J. E., Sarah Kim, Krzysztof Brzózka, Andreas Jung,, Hiroki Kato, H. P., Shizuo Akira, Karl-Klaus Conzelmann, Martin Schlee,, Stefan Endres, G. H. & * 2006. 5'-triphosphate rna is the ligand for rig-i. *Science,* 314.
Wack, A., Terczynska-Dyla, E. & Hartmann, R. 2015. Guarding the frontiers: The biology of type iii interferons. *Nature Immunology,* 16**,** 802-809.
Wang, X. Y., Li, M., Zheng, H. Y., Muster, T., Palese, P., Beg, A. A. & Garcia-Sastre, A. 2000. Influenza a virus ns1 protein prevents activation of nf-kappa b and induction of alpha/beta interferon. *Journal of Virology,* 74**,** 11566-11573.
Wang, Z., Zhang, A., Wan, Y., Liu, X., Qiu, C., Xi, X., Ren, Y., Wang, J., Dong, Y., Bao, M., Li, L., Zhou, M., Yuan, S., Sun, J., Zhu, Z., Chen, L., Li, Q., Zhang, Z., Zhang, X., Lu, S., Doherty, P. C., Kedzierska, K. & Xu, J. 2014a. Early hypercytokinemia is associated

with interferon-induced transmembrane protein-3 dysfunction and predictive of fatal h7n9 infection. *Proc Natl Acad Sci U S A,* 111**,** 769-74.

Wang, Z. F., Zhang, A. L., Wan, Y. M., Liu, X. N., Qiu, C., Xi, X. H., Ren, Y. Q., Wang, J., Dong, Y., Bao, M. J., Li, L. Z., Zhou, M. Z., Yuan, S. H., Sun, J., Zhu, Z. Q., Chen, L., Li, Q. S., Zhang, Z. Y., Zhang, X. Y., Lu, S. H., Doherty, P. C., Kedzierska, K. & Xu, J. Q. 2014b. Early hypercytokinemia is associated with interferon-induced transmembrane protein-3 dysfunction and predictive of fatal h7n9 infection. *Proceedings of the National Academy of Sciences of the United States of America,* 111**,** 769-774.

Warren, C. J., Griffin, L. M., Little, A. S., Huang, I. C., Farzan, M. & Pyeon, D. 2014. The antiviral restriction factors ifitm1, 2 and 3 do not inhibit infection of human papillomavirus, cytomegalovirus and adenovirus. *PLoS One,* 9**,** e96579.

Warren, W. C., Hillier, L. W., Tomlinson, C., Minx, P., Kremitzki, M., Graves, T., Markovic, C., Bouk, N., Pruitt, K. D., Thibaud-Nissen, F., Schneider, V., Mansour, T. A., Brown, C. T., Zimin, A., Hawken, R., Abrahamsen, M., Pyrkosz, A. B., Morisson, M., Fillon, V., Vignal, A., Chow, W., Howe, K., Fulton, J. E., Miller, M. M., Lovell, P., Mello, C. V., Wirthlin, M., Mason, A. S., Kuo, R., Burt, D. W., Dodgson, J. B. & Cheng, H. H. 2017. A new chicken genome assembly provides insight into avian genome structure. *G3-Genes Genomes Genetics,* 7**,** 109-117.

Webb, A. E., Gerek, Z. N., Morgan, C. C., Walsh, T. A., Loscher, C. E., Edwards, S. V. & O'connell, M. J. 2015. Adaptive evolution as a predictor of species-specific innate immune response. *Molecular Biology and Evolution,* 32**,** 1717-1729.

Weber, F., Wagner, V., Rasmussen, S. B., Hartmann, R. & Paludan, S. R. 2006. Double-stranded rna is produced by positive-strand rna viruses and DNA viruses but not in detectable amounts by negative-strand rna viruses. *J Virol,* 80**,** 5059-64.

Webster, R. G., Bean, W. J., Gorman, O. T., Chambers, T. M. & Kawaoka, Y. 1992. Evolution and ecology of influenza a viruses. *Microbiol Rev,* 56**,** 152-79.

Weidner, J. M., Jiang, D., Pan, X. B., Chang, J., Block, T. M. & Guo, J. T. 2010a. Interferon-induced cell membrane proteins, ifitm3 and tetherin, inhibit vesicular stomatitis virus infection via distinct mechanisms. *J Virol,* 84**,** 12646-57.

Weidner, J. M., Jiang, D., Pan, X. B., Chang, J. H., Block, T. M. & Guo, J. T. 2010b. Interferon-induced cell membrane proteins, ifitm3 and tetherin, inhibit vesicular stomatitis virus infection via distinct mechanisms. *Journal of Virology,* 84**,** 12646-12657.

Wenzel, M., Wunderlich, M., Besch, R., Poeck, H., Willms, S., Schwantes, A., Kremer, M., Sutter, G., Endres, S., Schmidt, A. & Rothenfusser, S. 2012. Cytosolic DNA triggers mitochondrial apoptosis via DNA damage signaling proteins independently of aim2 and rna polymerase iii. *J Immunol,* 188**,** 394-403.

Weston, S., Czieso, S., White, I. J., Smith, S. E., Kellam, P. & Marsh, M. 2014. A membrane topology model for human interferon inducible transmembrane protein 1. *PLoS One,* 9**,** e104341.

Weston, S., Czieso, S., White, I. J., Smith, S. E., Wash, R. S., Diaz-Soria, C., Kellam, P. & Marsh, M. 2016. Alphavirus restriction by ifitm proteins. *Traffic,* 17**,** 997-1013.

Williams, D. E., Wu, W. L., Grotefend, C. R., Radic, V., Chung, C., Chung, Y. H., Farzan, M. & Huang, I. C. 2014. Ifitm3 polymorphism rs12252-c restricts influenza a viruses. *PLoS One,* 9**,** e110096.

Winter, C., Schwegmann-Wessels, C., Cavanagh, D., Neumann, U. & Herrler, G. 2006. Sialic acid is a receptor determinant for infection of cells by avian infectious bronchitis virus. *Journal of General Virology,* 87**,** 1209-1216.

Witter, R. L. 1972. Turkey herpesvirus: Lack of oncogenicity for turkeys. *Avian Dis,* 16**,** 666-70.

Witter, R. L., Nazerian, K., Purchase, H. G. & Burgoyne, G. H. 1970. Isolation from turkeys of a cell-associated herpesvirus antigenically related to marek's disease virus. *Am J Vet Res,* 31**,** 525-38.

Wrensch, F., Karsten, C. B., Gnirss, K., Hoffmann, M., Lu, K., Takada, A., Winkler, M., Simmons, G. & Pohlmann, S. 2015. Interferon-induced transmembrane protein-mediated inhibition of host cell entry of ebolaviruses. *J Infect Dis,* 212 Suppl 2**,** S210-8.

Wrensch, F., Winkler, M. & Pohlmann, S. 2014. Ifitm proteins inhibit entry driven by the mers-coronavirus spike protein: Evidence for cholesterol-independent mechanisms. *Viruses,* 6**,** 3683-98.

Xia, C., Vijayan, M., Pritzl, C. J., Fuchs, S. Y., Mcdermott, A. B. & Hahm, B. 2016. Hemagglutinin of influenza a virus antagonizes type i interferon (ifn) responses by inducing degradation of type i ifn receptor 1. *Journal of Virology,* 90**,** 2403-2417.

Xu, L., Khadijah, S., Fang, S., Wang, L., Tay, F. P. & Liu, D. X. 2010. The cellular rna helicase ddx1 interacts with coronavirus nonstructural protein 14 and enhances viral replication. *J Virol,* 84**,** 8571-83.

Yamada, Y. & Liu, D. X. 2009. Proteolytic activation of the spike protein at a novel rrrr/s motif is implicated in furin-dependent entry, syncytium formation, and infectivity of coronavirus infectious bronchitis virus in cultured cells. *Journal of Virology,* 83**,** 8744-8758.

Yamayoshi, S., Watanabe, M., Goto, H. & Kawaoka, Y. 2016. Identification of a novel viral protein expressed from the pb2 segment of influenza a virus. *J Virol,* 90**,** 444-56.

Yang, X., Tan, B., Zhou, X., Xue, J., Zhang, X., Wang, P., Shao, C., Li, Y., Li, C., Xia, H. & Qiu, J. 2015. Interferon-inducible transmembrane protein 3 genetic variant rs12252 and influenza susceptibility and severity: A meta-analysis. *PLoS One,* 10**,** e0124985.

Yoneyama, M., Kikuchi, M., Matsumoto, K., Imaizumi, T., Miyagishi, M., Taira, K., Foy, E., Loo, Y. M., Gale, M., Akira, S., Yonehara, S., Kato, A. & Fujita, T. 2005. Shared and unique functions of the dexd/h-box helicases rig-i, mda5, and lgp2 in antiviral innate immunity. *Journal of Immunology,* 175**,** 2851-2858.

Yoshimura, A., Kuroda, K., Kawasaki, K., Yamashina, S., Maeda, T. & Ohnishi, S. 1982. Infectious cell entry mechanism of influenza virus. *J Virol,* 43**,** 284-93.

Yount, J. S., Karssemeijer, R. A. & Hang, H. C. 2012. S-palmitoylation and ubiquitination differentially regulate interferon-induced transmembrane protein 3 (ifitm3)-mediated resistance to influenza virus. *J Biol Chem,* 287**,** 19631-41.

Yount, J. S., Moltedo, B., Yang, Y. Y., Charron, G., Moran, T. M., Lopez, C. B. & Hang, H. C. 2010. Palmitoylome profiling reveals s-palmitoylation-dependent antiviral activity of ifitm3. *Nat Chem Biol,* 6**,** 610-4.

Yu, J., Li, M., Wilkins, J., Ding, S., Swartz, T. H., Esposito, A. M., Zheng, Y. M., Freed, E. O., Liang, C., Chen, B. K. & Liu, S. L. 2015. Ifitm proteins restrict hiv-1 infection by antagonizing the envelope glycoprotein. *Cell Rep,* 13**,** 145-56.

Yu, X., Bi, W. Z., Weiss, S. R. & Leibowitz, J. L. 1994. Mouse hepatitis-virus gene 5b protein is a new virion envelope protein. *Virology,* 202**,** 1018-1023.

Yuan, P., Bartlam, M., Lou, Z., Chen, S., Zhou, J., He, X., Lv, Z., Ge, R., Li, X., Deng, T., Fodor, E., Rao, Z. & Liu, Y. 2009. Crystal structure of an avian influenza polymerase pa(n) reveals an endonuclease active site. *Nature,* 458**,** 909-13.

Yunis, R., Ben-David, A., Heller, E. D. & Cahaner, A. 2002. Antibody responses and morbidity following infection with infectious bronchitis virus and challenge with escherichia coli, in lines divergently selected on antibody response. *Poult Sci,* 81**,** 149-59.

Zebedee, S. L. & Lamb, R. A. 1988. Influenza a virus m2 protein: Monoclonal antibody restriction of virus growth and detection of m2 in virions. *J Virol,* 62**,** 2762-72.

Zhang, Y., Makvandi-Nejad, S., Qin, L., Zhao, Y., Zhang, T., Wang, L., Repapi, E., Taylor, S., Mcmichael, A., Li, N., Dong, T. & Wu, H. 2015. Interferon-induced transmembrane protein-3 rs12252-c is associated with rapid progression of acute hiv-1 infection in chinese msm cohort. *AIDS,* 29**,** 889-94.

Zhang, Y. H., Zhao, Y., Li, N., Peng, Y. C., Giannoulatou, E., Jin, R. H., Yan, H. P., Wu, H., Liu, J. H., Liu, N., Wang, D. Y., Shu, Y. L., Ho, L. P., Kellam, P., Mcmichael, A. & Dong, T. 2013. Interferon-induced transmembrane protein-3 genetic variant rs12252-c is associated with severe influenza in chinese individuals. *Nat Commun,* 4**,** 1418.

Zhang, Z., Liu, J., Li, M., Yang, H. & Zhang, C. Y. 2012. Evolutionary dynamics of the interferon-induced transmembrane gene family in vertebrates. *Plos One,* 7.

Zhao, X., Guo, F., Liu, F., Cuconati, A., Chang, J., Block, T. M. & Guo, J. T. 2014. Interferon induction of ifitm proteins promotes infection by human coronavirus oc43. *Proc Natl Acad Sci U S A,* 111**,** 6756-61.

Zhao, X., Sehgal, M., Hou, Z., Cheng, J., Shu, S., Wu, S., Guo, F., Le Marchand, S. J., Lin, H., Chang, J. & Guo, J. T. 2018. Identification of residues controlling restriction versus enhancing activities of ifitm proteins on entry of human coronaviruses. *J Virol,* 92.

Zhou, Z. L., Hamming, O. J., Ank, N., Paludan, S. R., Nielsen, A. L. & Hartmann, R. 2007. Type iii interferon (ifn) induces a type iifn-like response in a restricted subset of cells through signaling pathways involving both the jak-stat pathway and the mtogen-activated protein kinases. *Journal of Virology,* 81**,** 7749-7758.

Zhu, H. & Liu, C. 2003. Interleukin-1 inhibits hepatitis c virus subgenomic rna replication by activation of extracellular regulated kinase pathway. *J Virol,* 77**,** 5493-8.

Ziebuhr, J., Snijder, E. J. & Gorbalenya, A. E. 2000. Virus-encoded proteinases and proteolytic processing in the nidovirales. *J Gen Virol,* 81**,** 853-79.

Zuniga, S., Cruz, J. L., Sola, I., Mateos-Gomez, P. A., Palacio, L. & Enjuanes, L. 2010. Coronavirus nucleocapsid protein facilitates template switching and is required for efficient transcription. *J Virol,* 84**,** 2169-75.